Development of software tools for simulation and design of jointless track circuits

Berova, Marinna Lubomirova

Award date:
1997

Awarding institution:
University of Bath

DEVELOPMENT OF SOFTWARE TOOLS FOR SIMULATION AND DESIGN OF JOINTLESS TRACK CIRCUITS

submitted by Marinna Lubomirova Berova
for the degree of PhD
of the University of Bath

December 1997

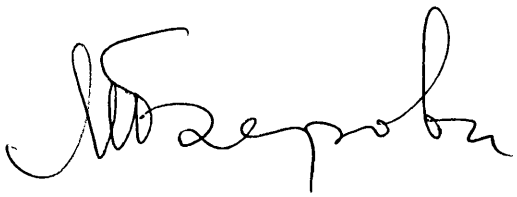

ProQuest LLC
789 East Eisenhower Parkway
P.O. Box 1346
Ann Arbor, MI 48106-1346

To my parents

ACKNOWLEDGEMENTS

The author sincerely thanks her supervisor Dr R J Hill for his constant guidance, advice and encouragement during the course of the work and the preparation of the thesis.

The author is also grateful to the Department of Electrical and Electronic engineering of the University of Bath for the provision of facilities for research work.

The author expresses her gratitude to the Bulgarian State and Bulgarian State Railways for the provision of financial support.

The author would like to acknowledge as well Mr G J Meecham and Mr T Clegg of Westinghouse Brake and Signal Ltd at Chippenham for the helpful discussions and the provision of data which enabled a rational verification of the track circuit model.

Thanks are extended as well to Kennedy and Donkin Ltd for the provision of facilities during the preparation of the thesis.

SYNOPSIS

This thesis is concerned with modern audio frequency jointless track circuits (AF JTCs) for railway signalling and control systems. It describes the development of a methodology and computer based design tools for a systematic investigation, design and optimisation of this, most widespread modern train detection system.

The traditional method of track circuit design is by continuous development, based on good engineering judgement and the trial-and-error technique, complemented by experimental measurements. In view of the increased complexity of AF JTCs the traditional methods of design do not necessarily lead to an optimum design.

An efficient and economic alternative is to use modern computer based simulation methods which is the subject of the present research work. Analysing the facilities provided by the professional electric circuit simulation software it was considered more appropriate to develop a specialised computer track circuit simulation program. This enabled to implement a more efficient and precise track circuit model, as well as specific facilities for systematic track circuit investigation and optimisation.

The software tool has been applied for the simulation and investigation of an established track circuit. The results from the simulations have confirmed the validity and usefulness of the program and have justified the possibility for its further development and extension towards a universal user friendly CAE tool for solving various track circuit related problems.

'It is the mark of an instructed mind to rest satisfied with the degree of precision which the nature of the subject admits and not to seek exactness where only an approximation of the truth is possible.'

Aristotle

CONTENTS

Chapter 0

Chapter 1

Chapter 2

Chapter 3

Chapter 6

Chapter 7

Chapter 0

ABBREVIATIONS AND NOTATION

0.1 LIST OF ABBREVIATIONS

AC	Alternating Current
AF	Audio Frequency
ASK	Amplitude Shift Keying
AT	Autotransformer
BARTD	Bay Area Rapid Transit System (San Francisco)
BH	Bull Head (Rail)
CAE	Computer Aided Engineering
DC	Direct Current
ESJ	Electrical Separating Joint
EMI	Electro Magnetic Interference
EMTDC	Electromagnetic Transient Simulation Program for DC Transmission Systems
ext	External
FB	Flat Bottom (Rail)
FEM	Finite Element Modelling
FDM	Finite Difference Modelling
FSK	Frequency Shift Keying
GMD	Geometric Mean Distance
hf	High Frequency
IBJ	Insulated Block Joint
int	Internal
JTC	Jointless Track Circuit
lf	Low Frequency
MARTA	Metropolitan Atlanta Rapid Transit Authority
MTL	Multiconductor Transmission Line
SABER	Professional Software for Simulation of Electric Circuits
TB	Termination Bond

TC	Track Circuit
TCADP	Computer Program for Track Circuit Analysis and Design
TCT	Track Circuit Termination
TL	Transmission Line
TE	Transverse Electric
TEM	Transverse Electro-Magnetic
TM	Transverse Magnetic
TU	Tuning Unit
Tx	Transmitter
Rx	Receiver
WMATA	Washington Metropolitan Area Transit Authority System
WELCO	Westinghouse Electric Corporation

0.2 NOTATION

0.2.1 General

The notation is based on the following convention:

- Phasor quantities and other complex quantities representing derivatives of phasors are represented in bold typeface.
- Matrix quantities are represented in square brackets
- Superscript 'T' denotes the transposed of a matrix
- Superscript '-1' denotes the inverse of a matrix
- Superscript '*' denotes the transposed of the complex conjugate of a matrix
- Superscripts 'm' and 'p' denote 'modal' and 'phase' quantities
- Subscript 'TL' stands for 'Transmission Line'
- Subscript 'D' stands for 'Discontinuity'
- Subscripts 'T' and 'π' refer to 'T-' and 'π-' lumped parameter networks
- Subscripts '1', '2', . . . 'i', . .'j', . .'n', 'ij', etc. designate elements of a matrix
- Subscripts '(1)', '(2)', . . . '(i)', . .'(j), . '(n)' designate transmission line section number or discontinuity number.

0.2.2 Notation used in Chapter 3

$\mathbf{D}$	Region of existence of a track circuit
$\mathbf{D_D}$	Region of definition of TC design parameters
$\mathbf{D_o}$	Region of definition of the specified design parameters
$\mathbf{d} = (d_1, d_2, \cdots d_i \cdots d_l)$	Vector of TC design parameters
$\mathbf{d_o}$	Vector of the specified TC design parameters
$\bar{\mathbf{d}}_o$	Vector of the specified design parameters
$\Delta\bar{\mathbf{d}}_o$	Vector of the specified design tolerances
$\mathbf{F}$	TC function
$\mathbf{F}_{br}(x_{br})$	Reaction to broken rail
$\mathbf{F}_{sh}(R_{sh}, x_{sh})$	Reaction to train shunt
$\mathbf{f}$	TC response function
$\mathbf{h}$	Function of TC output decision element
$I^{\uparrow}, I_{\downarrow}$	Actual levels of energisation and de-energisation of TC receiver
$\underline{I}^{\uparrow}, \underline{I}_{\downarrow}$	Specified (designed) levels of energisation and de-energisation of TC receiver
$+\Delta I^{\uparrow}, -\Delta I_{\downarrow}$	Safety margins necessary to account for the instability of TC receiver levels of energisation and de-energisation
I_{Rx}, I_{Rx}^{sh}, I_{Rx}^{br} I_{Rx}^{b}, $I_{Rx}^{sh.b}$, $I_{Rx}^{br.b}$ I_{Rx}^{w}, $I_{Rx}^{sh.w}$, $I_{Rx}^{br.w}$	Current in TC receiver (relay) specifically defined with the superscripts as follows: First superscript refers to TC operating mode: none - TC unoccupied, no broken rail sh - TC occupied br - Broken rail Second superscript refers to TC performance scenario: b - best scenario w - worst scenario and underscore: No inderscored symbols refer to actual values Underscored symbols refer to values specified in the design
λI_{Rx}	Summary destabilising effect of the value of track circuit operating parameter as result of TC input effects
I_{Tx}	Current in TC transmitter
κ	Coefficient of energisation - TC performance criteria in 'Unoccupied, no broken rail' operating mode

K_{br}	Coefficient of broken rail sensitivity
K_{sh}	Coefficient of train shunt sensitivity
K_{ft}	Coefficient of longitudinal leakage (feedthrough)
K_{ij}	Transfer function from port i to port j of ESJ model (Fig.3.4)
$\mathbf{R}$	Region of definition of TC input operating effects
$\mathbf{R}_o$	Region of definition of safety critical input operating effects
$\mathbf{r} = (r_1, r_2, \cdots r_j \cdots r_m)$	Vector of TC input operating effects
Δr_j	Definition interval of the j-th component of vector $\mathbf{r}$
R_{sh}	Actual value of train shunt resistance
$\underline{R_{sh.min}}$	Minimum value of train shunt resistance which can be detected by a TC under the worst case scenario of shunted operation (specified in the design)
$\mathbf{S}$	Region of definition of the TC environmental conditions
$\mathbf{s} = (s_1, s_2, \cdots s_k \cdots s_n)$	Vector of TC environmental effects
Δs_k	Definition interval of the k-th component of vector $\mathbf{s}$
$\mathbf{U}$	Region of definition of vector $\mathbf{u}$
$\mathbf{u}$	Vector of TC input operating signal
$\mathbf{X}$	Region of definition of TC status
$\mathbf{X}_o$	Region of definition of TC safety critical status
$\mathbf{x}$	Vector of TC input status
$\mathbf{x}_b$, $\mathbf{x}_w$	'Worst case' TC status vector
$\mathbf{V}$	Region of definition of TC response vector $\mathbf{v}$
$\mathbf{V}_o$	Subset of $\mathbf{V}$ including those values of $\mathbf{v}$ for which the decision element will set the TC output to 1
V_i, V_j	Voltages at ports i and j of ESJ model (Fig.3.4)
$V_{Rx_{i(i\pm n)}}$	Voltage in the receiver of track circuit I originating from the transmitter of track circuit (i±n)
$V_{Tx_{(i\pm n)}}$	Voltage of the transmitter of track circuit (i±n)
$\mathbf{v}$	TC response vector
$\mathbf{Y}$	Region of definition of TC output
$\mathbf{y}$	TC output vector

0.2.3 Notation used in Chapter 4

A, B, C, D	Transmission (chain) parameters of a two-port network the particular two-port network being defined with the subscripts as follows: Rx - TC receiver interface network Tx - TC transmitter interface network RT - Rail Track section two port network
C	Rail track capacitance per unit length
$\mathbf{E}$	Electric field vector
$\mathbf{E}_{Eqv.Tx}$	Equivalent voltage source in the equivalent TC transmitter, substituting the TC equipment connected to the rails at the transmitting end (Fig.4-2,b)
$\mathbf{E}_{Tx}$	Equivalent voltage source in TC transmitter Thevenin equivalent circuit (Fig.4-2,a)
G	Rail track conductance per unit length
$\mathbf{H}$	Magnetic field vector
$\mathbf{I}_m^+, \mathbf{I}_m^-$	Magnitudes of the incident and reflected waves of the current in a single phase transmission line (Eqn.4.4.2)
$i(x), \mathbf{I}(x)$	Momentary value and complex phasor of the current in a single phase transmission line at distance x from the beginning of the transmission line (Eqns.4.1.1-4.2.2 and Eqns.4.4.1-4.4.2)
$[\mathbf{I}]$	Column-vector of the phase currents in a multiconductor transmission line
L	Rail track inductance per unit length
M_{12}	Mutual inductance between the two single lines in a two-conductor transmission line
R	Rail track resistance per unit length
$[\mathbf{V}]$	Column vector of the phase voltages in a multiconductor transmission line
$\mathbf{V}_m^+, \mathbf{V}_m^-$	Magnitudes of the incident and reflected waves of the voltage in a single phase transmission line (Eqn.4.4.1)
$v(x), \mathbf{V}(x)$	Momentary value and complex phasor of the voltage between the conductors
x	Distance from the beginning of a transmission line
$\mathbf{Y}$	Rail track shunt admittance per unit length

$[\mathbf{Y}]$	Square matrix of order n describing the shunt admittance per unit length of an n-conductor transmission line
$\mathbf{Y}_{ii}$, $\mathbf{Y}_{ij}$	Elements of matrix $[\mathbf{Y}]$ of an n-conductor transmission line, $\mathbf{Y}_{ii}$ being the self admittance of line i with earth return, and $\mathbf{Y}_{ij}$ being the mutual admittance between lines i and j.
$\mathbf{Y}_m$	Mutual admittance between lines 1 and 2
$\mathbf{Z}$	Rail track series impedance per unit length
$[\mathbf{Z}]$	Square matrix of order n describing the series impedance per unit length of an n-conductor transmission line
$\mathbf{Z}_{ii}$, $\mathbf{Z}_{ij}$	Elements of matrix $[\mathbf{Z}]$ of an n-conductor transmission line, $\mathbf{Z}_{ii}$ being the series self inpedance of line i with earth return, and $\mathbf{Z}_{ij}$ being the mutual impedance between lines i and j.
$\mathbf{Z}_{Eqv.Tx}$, $\mathbf{Z}_{Eqv.Rx}$	Equivalent impedance of TC transmitting/receiving end
$\mathbf{Z}'_{inp.Tx}$, $\mathbf{Z}'_{inp.Rx}$	Equivalent impedance seen looking from the point of connection of TC transmitter/receiver (Fig.4.2)
γ	Propagation constant of a single phase transmission line
$\gamma.l$	TC electrical length
ω	Radian frequency

0.2.4 Notation used in Chapter 5

$\left[\mathbf{A}_{TL}^{(p)}\right],\left[\mathbf{B}_{TL}^{(p)}\right],\left[\mathbf{C}_{TL}^{(p)}\right],\left[\mathbf{D}_{TL}^{(p)}\right]$
$\left[\tilde{\mathbf{A}}_{TL}^{(p)}\right],\left[\tilde{\mathbf{B}}_{TL}^{(p)}\right],\left[\tilde{\mathbf{C}}_{TL}^{(p)}\right],\left[\tilde{\mathbf{D}}_{TL}^{(p)}\right]$

Square (n,n)-order matrices which represent a generalisation of the transmission and the inverse transmission parameters of a two-port network for the case of a section of n-conductor transmission line described in phase quantities.

$\left[\mathcal{A}_{D}^{(p)}\right],\left[\mathcal{B}_{D}^{(p)}\right],\left[\mathcal{C}_{D}^{(p)}\right],\left[\mathcal{D}_{D}^{(p)}\right]$
$\left[\tilde{\mathcal{A}}_{D}^{(p)}\right],\left[\tilde{\mathcal{B}}_{D}^{(p)}\right],\left[\tilde{\mathcal{C}}_{D}^{(p)}\right],\left[\tilde{\mathcal{D}}_{D}^{(p)}\right]$

Square (n,n)-order matrices which represent generalised transmission and the inverse transmission parameters of a (2n+1)-pole lumped parameter network (identified with subscript 'D' or 'D(i)') which represent a discontinuity in a non-homogenous transmission line.

$\left[\mathcal{B}_{D}^{(m)}\right]$, $\left[\mathbf{B}_{TL}^{(m)}\right]$

Square (2n,2n)-order matrix representing a short designation of the generalised inverse transmission parameters matrices of a (2n)-port lumped parameter network (identified with subscript 'D' or 'D(i)) and a section of a n-conductor transmission line described in modal quantities (identified with subscript 'TL').

$\left[\mathcal{B}_{D}^{(p)}\right]$, $\left[\mathbf{B}_{TL}^{(p)}\right]$

Square (2n,2n)-order matrix representing a short designation of the generalised inverse transmission parameters matrices of a (2n+1)-pole lumped parameter network (identified with subscript 'D' or 'D(i)') or a section of n-conductor transmission line described in phase quantities (identified with subscript 'TL').

$\left[\mathbf{B}_{TL_T}^{(m)}\right]$, $\left[\mathbf{B}_{TL_\pi}^{(m)}\right]$
$\left[\mathbf{B}_{TL_T}^{(p)}\right]$, $\left[\mathbf{B}_{TL_\pi}^{(p)}\right]$

Short designation of the generalised inverse transmission parameters of a section of n-conductor transmission line described in modal/phase quantities and represented with an equivalent T or π network.

d, d_i, $i = 1,\ n$

Distance, distance of section 'i'

D, D(i)

Transmission line discontinuity, Discontinuity 'i'

$[D]$, $[D']$, $[D'']$

Diagonal matrix

$\left[\mathbf{E}_{Tx}^{(p)}\right]$

Column (1,n)-order matrix describing the n-phase voltage source in Thevenin equivalent circuit of transmitting end network of a n-conductor transmission line (Fig.5.1)

$\left[\mathbf{G}_{TL}^{(m)}\right],\left[\mathbf{G}_{TL}^{(p)}\right]$

Square (2n,2n)-order matrix representing a short designation of the inverse hybrid parameters matrices of a section of a n-conductor transmission line described in modal/phase quantities.

$\left[\mathbf{H}_{TL}^{(m)}\right],\left[\mathbf{H}_{TL}^{(p)}\right]$

Square (2n,2n)-order matrix representing a short designation of the hybrid parameters matrices of a section

	of a n-conductor transmission line described in modal/phase quantities.
$\left[\mathbf{I}^{(m)}\right]=\left[\mathbf{I}_1^{(m)},\mathbf{I}_2^{(m)},\cdots\mathbf{I}_n^{(m)}\right]$ $\left[\mathbf{I}^{(m)}(x)\right]$ $\left[\mathbf{I}_{(i)}^{(m)}(x)\right]$	Column (1,n)-order matrix of the modal currents of a n-conductor transmission line (in general, and at point 'x' from the beginning of the transmission line). When describing a non-homogenous transmission line (Fig.5.1) a subscript indicates to which section of the transmission line the matrix refers.
$\left[\underline{\mathbf{I}}^{(m)}\right]$	Column (1,n)-order matrix representing the difference between the currents of the incident and the reflected wave of the modal currents (Eqn.5.135.1)
$\left[\bar{\mathbf{I}}^{(m)}\right]$	Column (1,n)-order matrix whose elements represent the complex conjugates of the elements of the matrix of the phase currents $\left[\mathbf{I}^{(m)}\right]$, (Eqn.5.155)
$\left[\mathbf{I}^{(m+)}\right],\left[\mathbf{I}^{(m-)}\right]$	Column (1,n)-order matrices of the amplitudes of the modal currents in the incident (m+) and in the reflected wave (m-).
$\mathbf{I}_c(0)$, $\mathbf{I}_c(x)$	Currents flowing in each conductor of a symmetrical two-conductor transmission line in common mode excitation (at the beginning of the transmission line and at distance x from the beginning)
$\mathbf{I}_c(0)$, $\mathbf{I}_d(x)$	Currents flowing in opposite phases in the conductors of a symmetrical two-conductor transmission line in differential mode excitation (at the beginning of the transmission line and at distance x from the beginning)
$\left[\mathbf{I}_{inc}^{(m)}\right],\left[\mathbf{I}_{refl}^{(m)}\right]$	Column (1,n)-order matrices of the modal currents of the incident and reflected waves (in general, and at point 'x' from the beginning of the transmission line).
$\left[\mathbf{I}_{D(i)}^{I(m)}\right]$, $\left[\mathbf{I}_{D(i)}^{II(m)}\right]$	Column (1,n)-order matrices of the modal currents in the input and output port of an intermediate discontinuity D(i) of a n-conductor transmission line
$\mathbf{I}(0)$, $\mathbf{I}(l)$	General notation for the currents in the transmitting and receiving end of a transmission line described as a two-port network (Fig.5.2, Fig.5.3)
$\mathbf{I}_{ij}^{(p,m)}$	Contribution of the mode j current in the phase i current
$\mathbf{I}_p^I$, $\mathbf{I}_p^{II}$	General notation for the currents in the input and output port of a two-port network (Fig.5.2)

i, j	Indexes. used to identify a particular phase (i.e. phase i), mode (i.e. mode j) or component of a column matrix (i.e. phase current i).
$\left[\mathbf{I}^{(p)}\right]=\left[\mathbf{I}_1^{(p)},\mathbf{I}_2^{(p)},\cdots\mathbf{I}_n^{(p)}\right]$ $\mathbf{I}^{(p)}(x)\right]$ $\mathbf{I}_{()}^{(p)}(x)\right]$	Column (1,n)-order matrix of the phase currents of a n-conductor transmission line (in general, and at point 'x' from the beginning of the transmission line). When describing a non-homogenous transmission line (Fig.5.1) a subscript indicates to which section of the transmission line the matrix refers.
$\mathbf{I}^{p+}\right],\left[\mathbf{I}^{p-}\right]$	Column (1,n)-order matrices of the amplitudes of the phase currents in the incident (p+) and in the reflected wave (p-).
$\mathbf{I}^{(r)}\right]$	Column (1,n)-order matrix representing the difference between the currents of the incident and the reflected wave of the phase currents (Eqn.5.22.1)
$\mathbf{I}^{(r)}\right]$	Column (1,n)-order matrix whose elements represent the complex conjugates of the elements of the matrix of the phase currents $\left[\mathbf{I}^{(p)}\right]$ (Eqn.5.153)
$\left[\mathbf{I}_D^{I^{(r)}}\right],\left[\mathbf{I}_D^{II^{(p)}}\right]$ $\left[\mathbf{I}_{D_i}^{I^{(r)}}\right],\left[\mathbf{I}_{D_i}^{II^{(p)}}\right]$	Column (1,n)-order matrices of the phase currents in the input and output port of intermediate discontinuity D (or D(i)) of a n-conductor transmission line
$\left[\mathbf{I}_{Rx}^{(p)}\right]=\left[\mathbf{I}_{Rx_1}^{(p)},\mathbf{I}_{Rx_2}^{(p)},\cdots\mathbf{I}_{Rx_n}^{(p)}\right]$	Column (1,n)-order matrix of the currents in the terminals of a transmission line receiving end terminating network represented as a (n+1)-pole network
$\left[\mathbf{I}_{Tx}^{(p)}\right]=\left[\mathbf{I}_{Tx_1}^{(p)},\mathbf{I}_{Tx_2}^{(p)},\cdots\mathbf{I}_{Tx_n}^{(p)}\right]$	Column (1,n)-order matrix of the currents in the terminals of a transmission line transmitting end network represented as a (n+1)-pole network
$\left[\mathbf{I}_{inc}^{(p)}\right],\left[\mathbf{I}_{refl}^{(p)}\right],\left[\mathbf{I}_{tr}^{(p)}\right]$ $\left[\mathbf{I}_{inc}^{(p)}(x)\right],\left[\mathbf{I}_{refl}^{(p)}(x)\right],\left[\mathbf{I}_{tr}^{(p)}(x)\right]$ $\left[\mathbf{I}_{inc_{(i)}}^{(p)}(x)\right],\left[\mathbf{I}_{refl_{(i)}}^{(p)}(x)\right],$ $\left[\mathbf{I}_{tr_{(i)}}^{(p)}(x)\right]$	Column (1,n)-order matrices of the phase currents of the incident, reflected and transmitted (refracted) waves (in general, and at point 'x' from the beginning of the transmission line). When describing a non-homogenous transmission line (Fig.5.1) a subscript '(i)' indicates to which section of the transmission line the matrix refer.
$\left[\mathbf{I}_t\right]$	Column (1,n)-order matrix of the terminal currents of a (n+1)-terminal network described in terms of terminal node voltages and terminal currents (Appendix B)
$\mathbf{I}$	General notation for current

$\left[\mathbf{J}_{Tx}^{(m)}\right]$	Column (1,n)-order matrix of the n-phase current source in the Norton equivalent circuit of transmitting end network of a n-conductor transmission line described in modal quantities
$\left[\mathbf{J}_{Tx}^{(p)}\right]$	Column (1,n)-order matrix of the n-phase current source in the Norton equivalent circuit of transmitting end network of a n-conductor transmission line described in phase quantities
$\mathbb{K}$	General notation for reflection operator
$\left[\mathbf{K}_{I}^{(m)}\right], \left[\mathbf{K}_{V}^{(m)}\right]$ $\left[\mathbf{K}_{I_{D(i)}}^{(m)}\right], \left[\mathbf{K}_{V_{D(i)}}^{(m)}\right]$	Square (nun)-order matrices of the current and voltage phase reflection operator in a n-conductor non-homogenous transmission line described in modal quantities. When referred to a particular discontinuity this is indicated by subscript 'D(i)'. When necessary $(\mathbb{Z})$ or $(\mathbb{Y})$ accompany the symbol to indicate whether the reflection operator is expressed in terms of impedances or admittances.
$\left[\mathbf{K}_{I}^{(p)}\right], \left[\mathbf{K}_{V}^{(p)}\right]$ $\left[\mathbf{K}_{I_{D(i)}}^{(p)}\right], \left[\mathbf{K}_{V_{D(i)}}^{(p)}\right]$	Square (n,n)-order matrices of the current and voltage phase reflection operators in a n-conductor non-homogenous transmission line described in phase quantities. When referred to a particular discontinuity this is indicated by subscript 'D(i)'. When necessary $(\mathbb{Z})$ or $(\mathbb{Y})$ accompany the symbol to indicate whether the reflection operator is expressed in terms of impedances or admittances.
$l_1, l_2, \cdots l_n$	Lengths of the sections a non-homogenous transmission line.
$[\mathbf{P}]$	Square (n,n)-order non-diagonal matrix equal to the product of the phase series impedance matrix and the phase shunt admittance matrix of a n-conductor transmission line (Eqn.5.102.1).
$[\tilde{\mathbf{P}}]$	General notation for a (n,n)-order non-diagonal matrix
$[\mathbf{Q}], [\mathbf{Q}']$ $[\mathbf{Q}_{(i)}]$	Square (n,n)-order current transformation matrices of a n-conductor transmission line (Eqns.5.111 and 5.121.2) When necessary a subscript '(i)' identifies to which section of a non-homogenous transmission line the matrix refers.
$\left[\mathbf{R}_{I}^{(p)}\right], \left[\mathbf{R}_{V}^{(p)}\right]$ $\left[\mathbf{R}_{I_{D(i)}}^{(p)}\right], \left[\mathbf{R}_{V_{D(i)}}^{(p)}\right]$	Square (n,n)-order matrices of the current and voltage phase transmission (refraction) operators in a n-conductor non-homogenous transmission line described in phase

quantities.
When referred to a particular discontinuity this is indicated by subscript 'D(i)'.

$[S]$, $[S']$

$[S_{(i)}]$

Square (n,n)-order current transformation matrices of a n-conductor transmission line analytically defined by Eqn.5.111 and Eqn.5.121.2.
When necessary a subscript '(i)' identifies to which section of a non-homogenous transmission line the matrix refers.

$S_C^{(m)}$, $S_V^{(m)}$

Equivalent current and voltage source in the equivalent circuit representation of the receiving end terminating network of a two-conductor transmission line described in modal quantities.

$S_C^{(p)}$, $S_V^{(p)}$

Equivalent current and voltage source in the equivalent circuit representation of the receiving end terminating network of a two-conductor transmission line described in phase quantities.

$\mathbb{S}^{(m)}$, $\mathbb{S}^{(p)}$

Modal and phase complex power of a multiconductor transmission line

$\left[T_D^{(m)}\right]$, $\left[T_{TL}^{(m)}\right]$

Square (2n,2n)-order matrix representing a short designation of the generalised transmission parameters matrices of a (2n)-port lumped parameter network (identified with subscript 'D' or 'D(i)) or a section of a n-conductor transmission line described in modal quantities (identified with subscript 'TL').

$\left[T_D^{(p)}\right]$, $\left[T_{TL}^{(p)}\right]$

Square (2n,2n)-order matrix representing a short designation of the generalised inverse transmission parameters matrices of a (2n+1)-pole lumped parameter network (identified with subscript 'D' or 'D(i)') or a section of n-conductor transmission line described in phase quantities (identified with subscript 'TL').

$\left[T_{TL_T}^{(m)}\right]$, $\left[T_{TL_\pi}^{(m)}\right]$
$\left[T_{TL_T}^{(p)}\right]$, $\left[T_{TL_\pi}^{(p)}\right]$

Short designation of the generalised inverse transmission parameters of a section of n-conductor transmission line described in modal/phase quantities and represented with an equivalent T or π network.

$\left[V^{(m)}\right]=\left[V_1^{(m)}, V_2^{(m)}, \cdots V_n^{(m)}\right]$

$\left[V^{(m)}(x)\right]$
$\left[V_{(i)}^{(m)}(x)\right]$

Column (1,n)-order matrix of the modal voltages of a n-conductor transmission line (in general, and at point 'x' from the beginning of the transmission line).
When describing a non-homogenous transmission line (Fig.5.1) a subscript indicates to which section of the transmission line the matrix refers.

$\left[\underline{V}^{(m)}\right]$

Column (1,n)-order matrix representing the difference between the voltages of the incident and the reflected wave

	of the modal voltages (Eqn.5.135.2)
$\left[\mathbf{V}^{(m+)}\right],\left[\mathbf{V}^{(m-)}\right]$	Column (1,n)-order matrices of the amplitudes of the modal voltages in the incident (m+) and in the reflected wave (m-).
$\left[\mathbf{V}_{inc}^{(m)}\right],\left[\mathbf{V}_{refl}^{(m)}\right]$ $\left[\mathbf{V}_{inc}^{(m)}(x)\right],\left[\mathbf{V}_{refl}^{(m)}(x)\right]$	Column (1,n)-order matrices of the modal voltages of the incident and reflected waves (in general, and at point 'x' from the beginning of the transmission line).
$\left[\mathbf{V}_{D(i)}^{I(m)}\right],\left[\mathbf{V}_{D(i)}^{II(m)}\right]$	Column (1,n)-order matrices of the modal voltages in the input and output port of discontinuity D(i) of a n-conductor transmission line
$\mathbf{V}(0), \mathbf{V}(l)$	General notation for the voltages in the transmitting and receiving end of a transmission line described as a two-port network (Fig.5.2, Fig.5.3)
$\mathbf{V}_{ij}^{(p,m)}$	Contribution of the mode j voltage in the phase i voltage
$\mathbf{V}_p^I,\ \mathbf{V}_p^{II}$	General notation for the voltages in the input and output port of a two-port network (Fig.5.2)
$\left[\mathbf{V}^{(p)}\right]=\left[\mathbf{V}_1^{(p)},\mathbf{V}_2^{(p)},\cdots\mathbf{V}_n^{(p)}\right]$ $\left[\mathbf{V}^{(p)}(x)\right]$ $\left[\mathbf{V}_{(i)}^{(p)}(x)\right]$	Column (1,n)-order matrix of the phase voltages of a n-conductor transmission line (in general, and at point 'x' from the beginning of the transmission line). When describing a non-homogenous transmission line (Fig.5.1) a subscript indicates to which section of the transmission line the matrix refers.
$\left[\mathbf{V}^{p+}\right],\left[\mathbf{V}^{p-}\right]$	Column (1,n)-order matrices of the amplitudes of the phase voltages in the incident (p+) and in the reflected wave (p-).
$\left[\underline{\mathbf{V}}^{(p)}\right]$	Column (1,n)-order matrix representing the difference between the voltages of the incident and the reflected wave of the phase voltages (Eqn.5.22.1)
$\left[\mathbf{V}_D^{I(p)}\right],\left[\mathbf{V}_D^{II(p)}\right]$ $\left[\mathbf{V}_{D_i}^{I(p)}\right],\left[\mathbf{V}_{D_i}^{II(p)}\right]$	Column (1,n)-order matrices of the phase voltages in the input and output port of an intermediate discontinuity D (or D(i)) of a n-conductor transmission line
$\left[\mathbf{V}_{Rx}^{(p)}\right]=\left[\mathbf{V}_{Rx_1}^{(p)},\mathbf{V}_{Rx_2}^{(p)},\cdots\mathbf{V}_{Rx_n}^{(p)}\right]$	Column (1,n)-order matrix of the voltages in the terminals of transmission line receiving end terminating network represented as a (n+1)-pole network
$\left[\mathbf{V}_{Tx}^{(p)}\right]=\left[\mathbf{V}_{Tx_1}^{(p)},\mathbf{V}_{Tx_2}^{(p)},\cdots\mathbf{V}_{Tx_n}^{(p)}\right]$	Column (1,n)-order matrix of the voltages in the terminals of transmission line transmitting end network represented as a (n+1)-pole network

$\left[\mathbf{V}_{inc}^{(p)}\right], \left[\mathbf{V}_{refl}^{(p)}\right], \left[\mathbf{V}_{tr}^{(p)}\right]$ $\left[\mathbf{V}_{inc}^{(p)}(x)\right], \left[\mathbf{V}_{refl}^{(p)}(x)\right],$ $\left[\mathbf{V}_{tr}^{(p)}(x)\right]$ $\left[\mathbf{V}_{inc_{(i)}}^{(p)}(x)\right], \left[\mathbf{V}_{ref_{l(i)l}}^{(p)}(x)\right],$ $\left[\mathbf{V}_{tr_{(i)}}^{(p)}(x)\right]$	Column (1,n)-order matrices of the phase voltages of the incident, reflected and transmitted (refracted) waves (in general, and at point 'x' from the beginning of the transmission line). When describing a non-homogenous transmission line (Fig.5.1) a subscript indicates to which section of the transmission line the matrix refer.
$\mathbb{V}$	General notation for current
$[W]$	A non-singular matrix
$\mathbf{Y}$	Shunt admittance of a single phase transmission line
$\mathbf{Y}_o$	Characteristic admittance of a single phase transmission line
$\left[\mathbf{Y}^{(m)}\right], \left[\mathbf{Y}^{(p)}\right]$	Square (n,n)-order modal and phase shunt admittance matrices of a n-conductor transmission line.
$\left[\mathbf{Y}_{inp}^{(m)}\right], \left[\mathbf{Y}_{inp}^{(m)}(x)\right]$ $\left[\mathbf{Y}_{inp}^{(p)}\right], \left[\mathbf{Y}_{inp}^{(p)}(x)\right]$	Square (n,n)-order matrices of the modal/phase input admittance of a n-conductor transmission (in general, and at point 'x' from the beginning of the transmission line).
$\left[\mathbf{Y}_o^{(m)}\right], \left[\mathbf{Y}_o^{(p)}\right]$	Square (n,n)-order modal and phase characteristic admittance matrices of a n-conductor transmission line.
$\left[\mathbf{Y}_p\right]$	Square (n,n)-order short circuit admittance matrix of an n-port network (Appendix B)
$\left[\mathbf{Y}_\pi^{(m)}\right], \left[\mathbf{Y}_\pi^{(p)}\right]$	Square (2n,2n)-order matrices describing a section of n-conductor transmission line represented by an equivalent lumped parameter π-network in modal and phase quantities
$\left[\mathbf{Y}_{\pi 1}^{(m)}\right], \left[\mathbf{Y}_{\pi 2}^{(m)}\right]$ $\left[\mathbf{Y}_{\pi 1}^{(p)}\right], \left[\mathbf{Y}_{\pi 2}^{(p)}\right]$	Diagonal (n,n)-order matrices whose components represent the components of the lumped parameter equivalent π-network of a section of a n-conductor transmission line described in modal and phase quantities
$\left[\mathbf{Y}_{TL}^{(m)}\right], \left[\mathbf{Y}_{TL}^{(p)}\right]$	Square (2n,2n)-order matrix representing a short designation of the generalised short circuit admittance parameters matrices of a section of a n-conductor transmission line described in modal/phase quantities (identified with subscript 'TL').
$\left[\mathbf{Y}_{TL_T}^{(m)}\right], \left[\mathbf{Y}_{TL_T}^{(p)}\right]$ $\left[\mathbf{Y}_{TL_\pi}^{(m)}\right], \left[\mathbf{Y}_{TL_\pi}^{(p)}\right]$	Short designation of the generalised short circuit admittance parameters of a section of n-conductor transmission line described in modal/phase quantities and represented with an equivalent T or π network.

$\left[\mathbf{Y}^{(m)}_{Tx(Rx)}\right], \left[\mathbf{Y}^{(p)}_{Tx(Rx)}\right]$	Square (n,n)-order matrix of the modal/phase input admittance of the transmitting (or receiving) end terminating network of a n-conductor transmission line
$\mathbf{Y}^{\Delta}_{\star_1}, \mathbf{Y}^{\Delta}_{\star_{12}}, \mathbf{Y}^{\Delta}_{\star_2}$ $\mathbf{Y}^{X}_{\star_1}, \mathbf{Y}^{X}_{\star_{12}}, \mathbf{Y}^{X}_{\star_2}$	Lumped parameter admittances in the equivalent delta/star circuit representation of the definite terminal admittance matrix of a n-conductor transmission line terminating network
$\mathbb{Y}$	General notation for admittance
$\mathbb{Y}_{Tx\,(Rx)}, \mathbb{Z}_{Tx\,(Rx)}$	General notation for the admittance and the impedance of the transmitting/receiving end terminating network of a n-conductor transmission line
$\left[\mathbb{Y}^{(m)}\right], \left[\mathbb{Y}^{(p)}\right]$	General notation for modal/phase admittance matrices
$\mathbf{Z}$	Series impedance of a single phase transmission line
$\mathbf{Z}_o$	Characteristic impedance of a single phase transmission line
$\mathbf{Z}^{(p,m)}_{ij}$	Surge impedance in phase I due to mode j.
$\left[\mathbf{Z}^{(m)}\right], \left[\mathbf{Z}^{(p)}\right]$	Square (n,n)-order modal and phase series impedance matrices of a n-conductor transmission line.
$\left[\mathbf{Z}^{(m)}_{inp}\right], \left[\mathbf{Z}^{(m)}_{inp}(x)\right]$ $\left[\mathbf{Z}^{(p)}_{inp}\right], \left[\mathbf{Z}^{(p)}_{inp}(x)\right]$ $\left[\mathbf{Z}^{(p)}_{inp_{D(i)}}\right]$	Square (n,n)-order matrices of the modal/phase input impedance of a n-conductor transmission (in general, and at point 'x' from the beginning of the transmission line). When necessary a subscript 'D(i)' indicates to which section of a non-homogenous transmission line the matrix refers.
$\left[\mathbf{Z}^{I(p)}_{inp_{D(i)}}\right], \left[\mathbf{Z}^{II(p)}_{inp_{D(i)}}\right]$	Phase input impedance seen looking into the transmission line beyond discontinuity D(i)
$\left[\mathbf{Z}^{(m)}_{o}\right], \left[\mathbf{Z}^{(p)}_{o}\right]$ $\left[\mathbf{Z}^{(m)}_{o_{(i)}}\right], \left[\mathbf{Z}^{(p)}_{o_{(i)}}\right]$	Square (n,n)-order modal and phase characteristic impedance matrices of a n-conductor transmission line. When necessary a subscript '(i)' indicates to which section of a non-homogenous transmission line the matrix refers.
$\left[\mathbf{Z}_t\right]$	Square (n,n)-order definite admittance matrix of a (n+1)-terminal network (Appendix B)
$\left[\mathbf{Z}^{(m)}_{T}\right], \left[\mathbf{Z}^{(p)}_{T}\right]$	Square (2n,2n)-order matrices describing a section of n-conductor transmission line represented by an equivalent lumped parameter T-network in modal and phase quantities
$\left[\mathbf{Z}^{(m)}_{T1}\right], \left[\mathbf{Z}^{(m)}_{T2}\right]$	Diagonal (n,n)-order matrices whose components represent

$\left[\mathbf{Z}_{T1}^{(p)}\right], \left[\mathbf{Z}_{T2}^{(p)}\right]$	the components of the lumped parameter equivalent T-network of a section of a n-conductor transmission line described in modal and phase quantities
$\left[\mathbf{Z}_{TL}^{(m)}\right], \left[\mathbf{Z}_{TL}^{(p)}\right]$	Square (2n,2n)-order matrix representing a short designation of the generalised open circuit impedance parameters matrices of a section of a n-conductor transmission line described in modal/phase quantities (identified with subscript 'TL').
$\left[\mathbf{Z}_{TL_{I,I}}^{(p)}\right], \left[\mathbf{Z}_{TL_{I,II}}^{(p)}\right], \left[\mathbf{Z}_{TL_{II,I}}^{(p)}\right], \left[\mathbf{Z}_{TL_{II,II}}^{(p)}\right]$	Square (n,n)-order matrices which represent components of matrix $\left[\mathbf{Z}_{TL}^{(p)}\right]$
$\left[\mathbf{Z}_{TL_T}^{(m)}\right], \left[\mathbf{Z}_{TL_T}^{(p)}\right]$ $\left[\mathbf{Z}_{TL_\pi}^{(m)}\right], \left[\mathbf{Z}_{TL_\pi}^{(p)}\right]$	Short designation of the generalised open circuit impedance parameters of a section of n-conductor transmission line described in modal/phase quantities and represented with an equivalent T or π network.
$\left[\mathbf{Z}_{transf}^{(m)}\right], \left[\mathbf{Z}_{transf}^{(p)}\right]$	Square (n,n)-order matrix of the modal/phase transfer impedance of a n-conductor transmission line
$\left[\mathbf{Z}_{Tx(Rx)}^{(m)}\right], \left[\mathbf{Z}_{Tx(Rx)}^{(p)}\right]$	Square (n,n)-order matrix of the modal/phase input impedance of the transmitting (or receiving) end terminating network of a n-conductor transmission line
$\left[\mathbf{Z}_{Rx_{(i)}}^{(p)}\right]$	Equivalent phase input impedance of the receiving end of section 'I' of a non-homogenous n-conductor transmission line
$\mathbf{Z}_{*_1}^{\Delta}, \mathbf{Z}_{*_{12}}^{\Delta}, \mathbf{Z}_{*_2}^{\Delta}$ $\mathbf{Z}_{*_1}^{X}, \mathbf{Z}_{*_{12}}^{X}, \mathbf{Z}_{*_2}^{X}$	Lumped parameter impedances in the equivalent delta/star circuit representation of the definite terminal impedance matrix of a n-conductor transmission line terminating network. (Subscript '*' substitutes 'Tx' or 'Rx'.)
$\mathbb{Z}$	General notation for admittance
$\mathbb{Y}_{Tx\,(Rx)}$, $\mathbb{Z}_{Tx\,(Rx)}$	General notation for the admittance and the impedance of the transmitting/receiving end terminating network of a n-conductor transmission line
$\left[\mathbb{Z}^{(m)}\right], \left[\mathbb{Z}^{(p)}\right]$	General notation for modal/phase admittance matrices
$\left[\mathbb{Z}_{inp}\right]$	General notation for input impedance
$\left[\mathbb{Z}_{transf}\right]$	General notation for transfer impedance
α,	Attenuation coefficient of a transmission line
α_i	Attenuation coefficient of mode i of a n-conductor

	transmission line
$\chi_V^{(p)}$, $\chi_I^{(p)}$	See Eqns.5.64 and 5.73
$[\gamma]$	Diagonal (n,n)-order matrix of the modal propagation constants of a n-conductor transmission line
η_1, η_2	Coefficients
$[\Lambda]$	Diagonal (n,n)-order matrix whose elements represent the eigenvalues of matrix $[\mathbf{P}]$
$[\nu_E^{(p)}]$, $[\nu_J^{(p)}]$	See Eqns.5.93.2 and 5.94.2
$[\Psi_I]$	Square (n,n)-order voltage phase propagation matrix of a n-conductor transmission line
$[\Psi_V]$	Square (n,n)-order current phase propagation matrix of a n-conductor transmission line

0.2.5 Notation used in Appendix A

$\mathbf{B}$, B_o	Vector of magnetic flux density and its magnitude
C_d	Capacitance of the double layer at electrode-electrolyte interface (Fig.A.5)
C_p	Polarisation capacitance (Fig.A.4)
C_r	Rail-to-rail capacitance (Fig.A.4)
D	Diameter of conductor (Eqns.(A.19) and (A.20))
D_e	Equivalent depth of earth return conductor
D_{ij}	Distance between conductors i and j (Figs.A.3 and A.4)
D'_{ij}	Distance between conductor i and the mirror image of conductor j (Figs.A.3 and A.4)
d_1, d_2	Horizontal separation of rails 1 and 2 from the origin (Eqn.(A.18.2))
d_{ij}	Distance between the projections of conductors i and j (Figs.A.2 and A.3)
E_g	Electromotive force of galvanic element due to the potential difference between the rails as electrodes (Fig.A.4)
f	Frequency
G_{12}	Rail-to-rail conductance (Fig.A.5-b)
G_1, G_2	Rail-to-earth conductance (Fig.A.6)
$\mathbf{H}$, H_o	Vector of magnetic field strength and its magnitude
H_i, H_j	Heights of conductors i and j above earth plane (Figs.A.2 and A.3)
i, j	Conductors i and j (Figs.A.2 and A.3)
i′, j′	Mirror images of conductors i and j, (Figs.A.2 and A.3)
I_o, I_1	Modified Bessel functions of the first kind
k_o, k_1, k_2	Coefficients (Tab.A.2)
K_1	Modified Bessel function of the second kind
k_s	Correction coefficient characterising rail shape effect on rail

	internal impedance (Eqn.(A.12))
p	Complex penetration depth (Fig.A.3)
R_e	Electrolyte resistance (Fig.A.5)
R_i	Resistance accounting for energy loss due to ionic reactions at electrode-electrolyte interfaces (Fig.A.5)
R_p	Polarisation resistance (Fig.A.5)
R_{r-m}	Rail-fastening interface resistance (Fig.A.5)
r_r	Radius of a circular conductor equivalent to the rail (Eqns.(A.16.1) and (A.16.2))
r_i, r_j	Radiuses of conductors i and j (Figs.A.2 and A.3)
S	Distance between the centres of conductors (Eqns.A.19 and A.20)
u	Perimeter of rail cross section
X	Reactance
$\mathbf{Z}_e$	Conductor (earth) component rail - ground loop self impedance
$[\mathbf{Z}]$	Series impedance matrix of rail track regarded as a two conductor transmission line over lossy ground.
$\mathbf{Z}_{ii}$, $i = 1, 2$	Diagonal elements of matrix $[\mathbf{Z}]$ each representing the self impedance of a rail-ground loop regarded as a single phase transmission line
$\mathbf{Z}_{ij}$, $i = 1, 2$; $j = 1, 2$	Off-diagonal elements of matrix $[\mathbf{Z}]$ each representing the mutual impedance between the two rail-ground loops regarded as single phase transmission lines
$\mathbf{Z}_{ii_{ext}}$	External component of the series self impedance of rail track regarded as a two conductor transmission line over lossy ground.
$[\mathbf{Z}_{int}]$	Diagonal matrix the elements of which represent the internal components of rail-ground loops' self impedances.
$\mathbf{Z}'_{int_r}$, $\mathbf{Z}'_{int_c}$	Internal impedances of a hollow rail conductor and a hollow equivalent circular conductor
$\mathbf{Z}'_{ii_{ext}}$	Modified external impedance, accounting for the effect of the earth return path (Eqn.A.4)

$\mathbf{Z}'_{ij_{ext}}$	Modified rail-to-rail mutual impedance accounting for the effect of the earth return path
$\left[\mathbf{Z}'_{ext}\right]$	Square matrix in which the diagonal elements equal zero and the off-diagonal elements represent the modifies external impedance components of rail-ground loops
$\mathbf{Z}_r$	Conductor (rail) component rail - ground loop self impedance
$\mathbf{Z}_{r-e}$	Mutual inductive impedance between the rail and earth
$\mathbf{Z}_{r_{ext}}$	External component of rail-ground loop self inductance
$\mathbf{Z}_{r_{int}}$	Internal component of rail-ground loop self inductance
$[\mathbf{Y}]$	Shunt admittance matrix of rail track regarded as a two conductor transmission line over lossy ground.
$\mathbf{Y}_{ii}$, i = 1, 2	Diagonal elements of matrix $[\mathbf{Y}]$ each representing the self admittance of a rail-ground loop regarded as a single phase transmission line.
$\mathbf{Y}_{ij}$, i = 1, 2; i ≠ j	Off-diagonal elements of matrix $[\mathbf{Y}]$ each representing the mutual admittance between the two rail-ground loops regarded as a single phase transmission lines.
δ	Defined in Tab.A.2
γ_o	Propagation constant in free space
γ	Propagation constant in the earth medium
ε_r	Relative permittivity
ε_o	Permittivity of free space
μ	Magnetic permeability
$\hat{\mu}$	Complex magnetic permeability
μ_o, μ_r	Magnetic permeability of free space and relative permeability
σ	Conductivity
θ	Hysteresis angle
ω	Radian velocity
φ	Hysteresis angle

0.2.6 Notation used in Appendix B

$[\mathcal{A}_{2t}], [\mathcal{B}_{2t}], [C_{2t}], [\mathcal{D}_{2t}]$ Components of matrix $[\mathbf{T}_{2t}]$

$[\tilde{\mathcal{A}}_{2t}], [\tilde{\mathcal{B}}_{2t}], [\tilde{C}_{2t}], [\tilde{\mathcal{D}}_{2t}]$ Components of matrix $[\mathbf{B}_{2t}]$

$[\mathbf{B}_{2t}]$ Square (2n,2n)-order matrix of the inverse transmission parameters of a (2n+1)-pole network (Fig.B.5-b, Table B.1)

$\mathbf{C}$ 2m-pole current source network (Fig.B.3)

$[\mathbf{E}_p]$ Column (1,n)-order matrix describing the 2n-port voltage source in the Thevenin equivalent diagram of an active n-port network (Fig.B.7-b, Eqn.B.32)

$[\mathbf{E}_t]$ Column (1,n)-order matrix describing the 2n-pole voltage source in the Thevenin equivalent diagram of an active (n+1)-terminal network (Fig.B.4, Eqn.B.21)

$[\mathbf{G}_{2t}]$ Square (2n,2n)-order matrix of the hybrid parameters of a (2n+1)-pole network (Fig.B.5-b, Table B.1)

$[\mathbf{H}_{2t}]$ Square (2n,2n)-order matrix of the inverse hybrid parameters of a (2n+1)-pole network (Fig.B.5-b, Table B.1)

$[\mathbf{I}_p]$ Column (1,n)-order matrix of the port currents of a n-port network (Fig.B.6)

$[\tilde{\mathbf{I}}_p]$ Column (1,n)-order matrix of constants characterising the internal energy sources of an active n-port network. The components of $[\tilde{\mathbf{I}}_p]$ are equal to the currents flowing in the ports when all ports are short circuited.

$[\mathbf{I}_t]$ Column (1,n)-order matrix of the terminal currents of a (n+1)-terminal network described in terms of terminal node voltages and currents and definite admittance matrix (Fig.B.1, Eqns.B.B15.1 and B.15.2)

$[\tilde{\mathbf{I}}_t]$ Column (1,n)-order matrix of constants characterising an active (n+1)-terminal network described in terms of terminal node voltages and currents. The components of $[\tilde{\mathbf{I}}_t]$ are equal to the currents flowing in the terminals as response of the internal energy sources when all terminals of the network are grounded.

$[I_t]$ Column (1,n)-order matrix of the loop currents of a (n+1)-terminal network described in terms terminal-to-terminal voltages and loop currents and definite impedance matrix

(Fig.B.2, Eqns.B.16.1 and B.16.2)

$[\mathbf{I}_{2t}^{I}], [\mathbf{I}_{2t}^{II}]$ Column (1,n)-order matrices of the terminal currents of the input and output port terminals of a (2n+1)-terminal network (Fig.B.5-b)

$[\mathbf{I}_{2t}^{I}], [\mathbf{I}_{2t}^{II}]$ Column (1,n)-order matrices of the port currents of the input and output ports of a 2n-port network (Fig.B.5-b)

$[\mathbf{J}_{p}]$ Column (1,n)-order matrix describing the 2n-port current source in Norton's equivalent diagram of an active n-port network (Fig.B.7-a, Eqn.B.30).

$[\mathbf{J}_{t}]$ Column (1,m)-order matrix describing the 2m-pole current source in Norton's equivalent diagram of an active (m+1)-terminal network (Fig.B.3, Eqn.B.18)

M Active multipole (multiterminal) network

P Passive multipole (multiterminal) network

$[\mathbf{T}_{2p}]$ Square (2n,2n)-order matrix of the transmission parameters of a 2n-port network (Fig.B.8)

$[\mathbf{T}_{2t}]$ Square (2n,2n)-order matrix of the transmission parameters of a (2n+1)-pole network (Fig.B.5-b, Table B.1)

V 2n-pole voltage source

$[\mathbf{V}_{p}]$ Column (1,n)-order matrix of the port voltages of a n-port network (Fig.B.6)

$[\mathbf{V}_{t}]$ Column (1,n)-order matrix of the terminal node voltages of a (n+1)-terminal network described in terms of terminal node voltages and currents and definite admittance matrix (Fig.B.1)

$[\mathbf{V}_{2t}^{I}], [\mathbf{V}_{2t}^{II}]$ Column (1,n)-order matrices of the terminal voltages of the input and output port terminals of a (2n+1)-terminal network (Fig.B.5-b)

$[\mathbf{V}_{2p}^{I}], [\mathbf{V}_{2p}^{II}]$ Column (1,n)-order matrices of the port voltages of the input and output ports of a 2n-port network (Fig.B.8)

$[\mathcal{V}_{t}]$ Column (1,n)-order matrix of the terminal-to-terminal voltages of a (n+1)-terminal network described in terms terminal-to-terminal voltages and loop currents and definite impedance matrix (Fig.B.2)

$[\mathbf{V}_{t}^{-}]$ Column (1,n)-order matrix of constants characterising an active (n+1)-terminal network described in terms terminal-to-terminal

	voltages and loop currents (Fig.B.2) the elements of which are equal to the terminal-to-terminal voltages when all terminals are open circuit.
$[\mathbf{Y}_p]$	Short-circuit admittance matrix of order (n,n) of a n-port network (Fig.B.6)
$[\mathbf{Y}_t']$, $[\mathbf{Y}_t]$	Indefinite (n+1, n+1)-order and definite (n,n)-order terminal admittance matrix of a (n+1)-terminal network described in terms of terminal node voltages and currents (Fig.B.1)
$[\mathbf{Y}_{2t}]$	Square (2n,2n)-order matrix of the short circuit admittance parameters of a (2n+1)-pole network (Fig.B.5-b, Table B.1)
$[\mathbf{Z}_p]$	Open-circuit impedance matrix of order (n,n) of a n-port network (Fig.B.6)
$[\mathbf{Z}_{2p}]$	Square (n,n)-order matrix of the open circuit impedance parameters of a 2n-port network (Fig.B.8, Eqn.B.34)
$[\mathcal{Z}_t']$, $[\mathcal{Z}_t]$	Indefinite (n+1, n+1)-order and definite (n,n)-order terminal admittance matrix of a (n+1)-terminal network described in terms of terminal-to-terminal voltages and loop currents (Fig.B.1)
$[\mathbf{Z}_{2t}]$	Square (2n,2n)-order matrix of the transmission parameters of a (2n+1)-pole network (Fig.B.5-b, Table B.1)
δ	Arbitrary constant

Chapter 1

INTRODUCTION

The ever increasing demands for higher speeds and greater traffic capacities in railways together with the availability of modern microelectronics and microcomputer technology have stimulated a revolution in the field of railway signalling and control. The last fifteen - twenty years have seen the development of sophisticated and highly automated signalling and control systems providing effective, stable and safe performance of the railway transportation process.

The most fundamental element of all signalling and train control systems is the train detection system. Despite the advances in the development of modern, transmission-based methods for train detection, track circuits are and are likely to remain the principal and most widespread train detection system for urban and high-speed railways for a considerable time.

Track circuits have evolved from a simple DC circuit, using the rails as the transmission path between a battery and a DC relay, to sophisticated devices employing digital techniques. The latest achievements in track circuit design are the audio-frequency jointless track circuits which are the subject of this thesis. Their development has been brought about and stimulated by two main factors: the possibility of eliminating the insulating block joints, which are the most unreliable track circuit component and the necessity to increase substantially the capacity of track-to-train data transmission, calling for a shift of track circuit operating signals towards the audio-frequency range.

1.1 THE PROBLEM OF TRACK CIRCUIT DESIGN AND OPTIMISATION. THE NEED FOR SOFTWARE TOOLS FOR TRACK CIRCUIT SIMULATION AND DESIGN

To meet the stringent requirements for safe and highly reliable operation in an increasingly hostile environment of interferences from modern traction control and other systems track circuits are undergoing continuous improvement and development to optimise their performance. This involves solving problems such as:

- Checking the correct performance of a track circuit after modifications and improvements
- Setting up tables for adjustment of track circuit parameters according to different environmental conditions after modifications to the design

- Investigation of track circuit behaviour for a particular set of operating and environmental conditions following reports of faulty operation
- Investigation of the effect of a particular type of interference on track circuit operation
- Optimisation of track circuit design to achieve better performance.

The above tasks are not trivial, especially when modern audio-frequency jointless track circuits are concerned. Significant difficulties are related to the following specific features of track circuits:

- Track circuits do not have a fixed operating point but must maintain fail-safe operation over a wide range of dynamically varying operating conditions
- Track circuit performance depends on a number of design parameters which may be mutually related
- Track circuit performance cannot be characterised with a single operating criterion but rather with a set of criteria for various operating conditions. Some track circuit design parameters may need to be optimised with respect to various performance criteria
- Track circuits are open systems and their performance is susceptible to changing external environmental factors.

In formal terms, track circuit design and optimisation require a specifically controlled directed search through a multidimensional space, defined by constraints on design parameters, for a set of parameters which will guarantee the specified track circuit performance. Thus, the investigation and the design and optimisation of track circuits require versatile tools which allow the following to performed:

- Evaluation of track circuit performance for specific values of design parameters, operating conditions and environmental factors
- Repeated simulations to evaluate track circuit performance

In addition, when the design or optimisation problem is concerned:

- A way of assessing track circuit performance and defining the best or optimum performance.

1.2 AIM AND SCOPE OF THE RESEARCH WORK

The aim of the present research work is to develop a computer program for track circuit analysis and design (TCADP), which will enable the solution of the above formulated problems. TCADP shall be applicable to all types of track circuits, but will be particularly suited for the investigation of the audio-frequency jointless track circuits.

Contrary to track circuit simulation tools using professional software for electric and electronic circuit simulation, TCADP shall be purpose built so that it implements the track circuit specific requirements in the most efficient way. It shall operate on the basis of a track circuit model which shall be developed with reference to a specific application but shall incorporate provisions to enable its universal application for various track circuit designs and configurations.

The work shall include as well validation of the implemented track circuit model and verification of the viability of TCADP through its application for the modelling and investigation of an established track circuit design.

The development of the computer track circuit simulation tool requires the setting up of a realistic and versatile track circuit model, such that:

- It represents a precise and realistic description of the physical processes occurring in track circuits, with an optimum balance between detail and approximation to achieve the necessary modelling accuracy without undue increase in complexity.
- It allows simulation of the track circuit operation under the full range of design parameter variations and environmental conditions, and accounts for both 'static' and dynamically changing conditions.

1.3 METHODOLOGY OF THE RESEARCH WORK. ORGANISATION OF THE THESIS

The methodology and the stages of TCADP development and validation process are illustrated in Fig.1.1. This figure gives as well indication of the organisation of the thesis and where the different stages of the research work are presented.

Fig.1.1 represents the modelling process as an iterative, feedback/feedthrough process carried out with continuous reference to the modelling specification. The requirements which the model should meet follow from the purpose of the simulation tool and the problems which are to be solved. They are initially formulated in this chapter and further developed and specified in detail in parallel to the model building process.

The model building process is performed in two parts:

- Analysis of real track circuits as modelling object to determine and describe in an appropriate way the set of their fundamental properties, characteristics, functional behaviour, etc. which basically define track circuits as such and which would have to be implemented in the track circuit model, and
- Synthesis of a track circuit model consisting in building up an abstract structure with the required set of properties, characteristics, etc.

The analysis starts by a review of the principle types of audio-frequency (AF) jointless track circuits (JTCs) which have been well established in main line and rapid transit railway systems. This review provides a systematic knowledge of the functions performed by AF JTCs and their performance characteristics, correlated with the particular technical solutions and indicates the required ways of track circuit design optimisation.

Based on the background provided by the review of AF JTCs, the analysis continues further in two parallel streams - functional and physical modelling.

On one side, in Chapter 3, track circuits are analysed from the point of view of the particular functions which they perform and their functional algorithm is defined in a formal way. This formulation is enough general to embrace all types of track circuits. At the same time, recognising that each track circuit design and application are particular, the functional analysis indicates the way of applying the general functional model to a particular case. Chapter 3 introduces as well the concept of track circuit performance criteria as a 'measure' of track circuit performance.

On the other hand, Chapter 4 aims to identify the track circuit as a physical system in the form of an electric network. Based on the electric network theory suitable physical models for the various track circuit components are chosen and justified. This is done with view to a 'maximum' model which is able to incorporate the most complex configurations of track circuits in electrified railway areas as well as interfering external networks. The formulation of the physical model calls for some more specialised knowledge which is reviewed and included for reference. This includes experimental and theoretical methods for determination of rail track parameters, summarised in Appendix A and methods for description and solution of multiterminal and multiport networks, reviewed in Appendix B.

The implementation of the physical model requires formulation of the conceptual physical models in a suitable analytical form as well as devising convenient and powerful solution procedure. To this end Chapter 5 provides a presentation of the mathematical apparatus for describing multiconductor transmission lines with reference to its application to track circuit modelling. It introduces the set of physical variables necessary for the description and solution of multiconductor transmission lines (MTLs) both in the phase and in the modal domain and defines a universal solution procedure for a MTL with discontinuities.

The ultimate aim is to integrate the functional and physical track circuit models. This is achieved in an analytical form by relating the physical variables introduced to describe track circuit functional algorithm to those describing track circuit design parameters, operating and environmental conditions. This is implemented in the track circuit computer model described in Chapter 6. By implementing and solving the analytical relationships on computer the need for an explicit solution is obviated.

The solution of the TC model for a particular set of design parameters and operating conditions constitutes the kernel of the TCADP. To enable the use of the TC model for performing simulations and solving various track circuit analysis and optimisation problems a special control logic is implemented in the computer program. The structure, operation and use of the simulation tool are explained in details in Chapter 6.

Fig.1.1 shows that in parallel to the modelling process a continuous validation analysis is being carried out. The results of this analysis are summarised at the end of Chapter 6. The validation process culminates in a 'overall system' validation of the model by application of the TCADP for the investigation of a real track circuit design and comparison of the results obtained by simulation with the preliminary known track circuit characteristics. The results of the simulations of the established track circuit FS 2000 (Westinghouse Signals Limited) are analysed and presented in Chapter 7 together with a final conclusion on the validity of the track circuit model.

Finally, Chapter 8 summarises the results of the research work presented in this thesis and outlines the directions for further work for the development of the simulation tool towards a universal, user friendly software tool and its application for investigation and optimisation of track circuits.

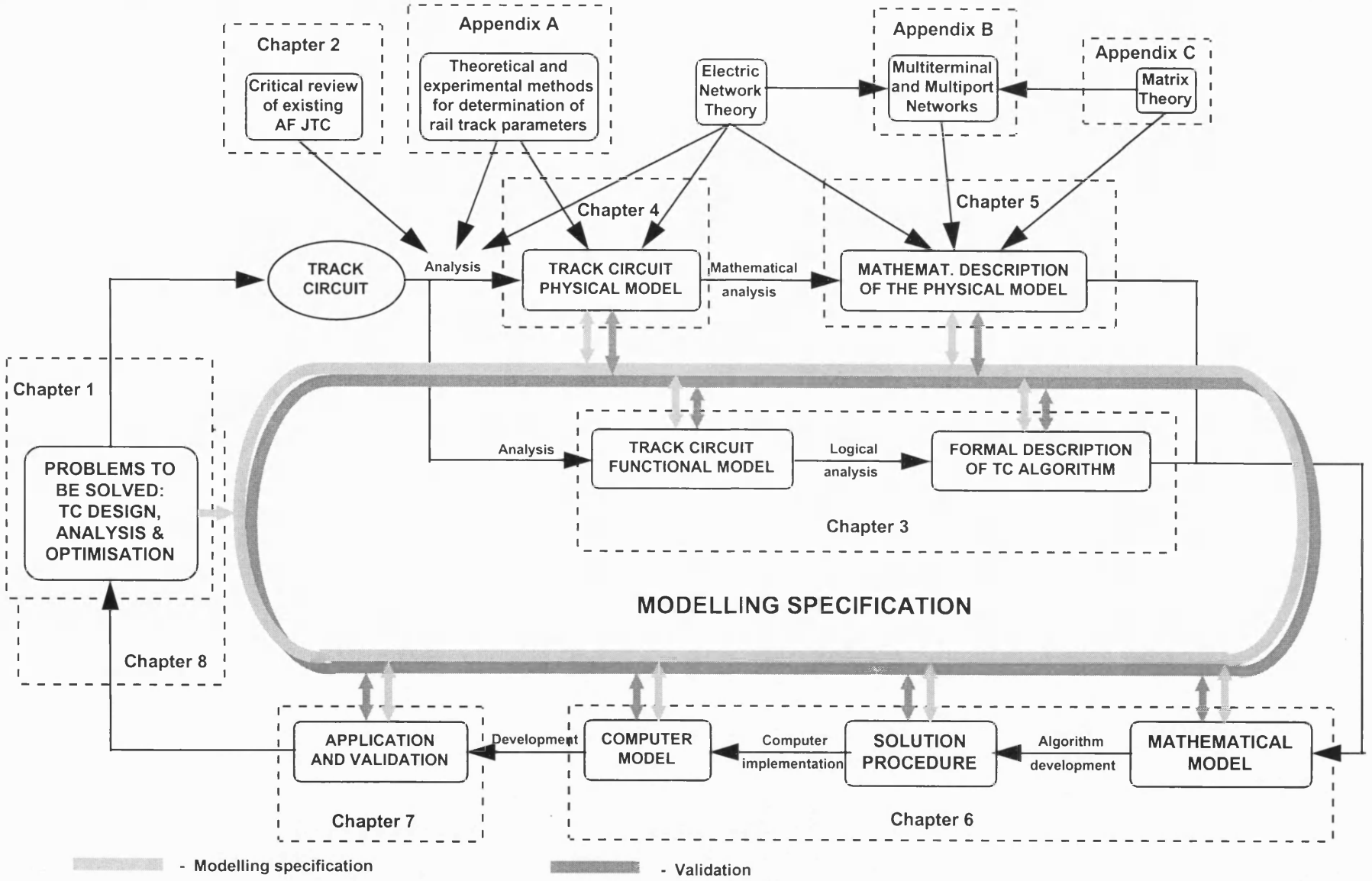

FIG.1.1 Process of development and validation of track circuit model. Structure of the thesis.

Chapter 2

AUDIO-FREQUENCY TRACK CIRCUITS

Audio frequency (AF) track circuits have been used as overlay track circuits for level crossing control since the mid 1950s [2-6]. However, it is only during the last two decades that their advantages for main lines, and especially for urban and suburban railways, have been fully recognised. The major suppliers of signalling equipment have all proposed different versions of AF track circuits. Table 2.1 summarises the characteristics and performance of each and illustrates the variety of design concepts available ([2-1]-[2-57]).

AF track circuit operation is based on the same principle as other types incorporating insulating joints. However, the operating frequency is in the range 0.3 - 20 kHz. Examination of the various features of AF track circuit operation reveals the main design problems which have resulted in shorter detection lengths, elimination of insulating joints and the implementation of digital and microprocessor techniques (Fig. 2.1).

2.1 TRACK CIRCUIT TERMINATIONS

The design of AF track circuit terminating areas must consider the problems of coupling the transceiver equipment to the track, and separation of adjacent track circuits.

2.1.1 Coupling of transmitter and receiver to rail track

As for conventional track circuits, the receiver equipment can be connected to the track by voltage or current coupling. The method of coupling determines the principle of operation of the track circuit receiver and also affects the general design of the AF track circuit. The main classification criterion for AF track circuits is whether they are voltage or current operated.

Unlike conventional track circuits which exclusively use voltage coupling of the transmitter, both voltage and current coupling can be utilised in AF track circuits. Thus four combinations 'voltage/current transmitter - voltage/current receiver' are possible. According to [2-48], the preferred combination is a 'voltage transmitter with a current receiver', giving a reduced dynamic range. Table 2.2 gives a summary of the various types of voltage and current transceivers available for AF track circuits.

2.1.2 Track circuit separation

The complete separation of adjacent track circuits is a necessary condition for precise train position detection. The normal way to achieve this is to use distinct frequencies for

adjacent track circuits. This can take the form of different carrier and/or modulation frequencies depending on the type of TC. From the view points of receiver design and power dissipation, it is, however, desirable to limit the presence of the operating signals to within the track circuit physical boundaries.

There are two aspects that must be considered for track circuit separation. These are the concept of non-separation (i.e. boundless track circuits) and the concept of electrical separating joints. In either case both voltage and current coupling methods for the transceivers can be used.

In boundless track circuits, no specific means for track circuit demarcation are provided. The extent of the detection length relies only on the TC signal attenuation. Voltage operated boundless TCs (e.g. AF 1000 W, Table 2.1-g) have an extended shunt area (Fig.2.2-a) the length of which is strongly dependent on the ballast resistance. Current operated boundless TCs (e.g. TI 21, Table 2.1-c), however, may give rise to dangerous situations because of proximity effects (Fig.2.2-b). The first problem can be solved with careful design including system performance assessment [G-9], but the second is more intransigent. Much effort has been put into solving the problems, however, since boundless track circuits have the undeniable advantage of simplicity.

The function of electrical separating joints differs for voltage and current operated AF track circuits. Electrical separation of track circuits using voltage-sensitive receivers is achieved by short-circuiting the rails together at the track circuit extremities. As Table 2.3 shows, the short circuit may be performed either by a low impedance rail-rail bond or by a series resonant circuit. To limit the power consumption, however, it is desirable to have a high terminating impedance. A suitable compromise is the use of a parallel resonance circuit, tuned at the track circuit operating frequency, combined with a series resonant circuit defining the actual track circuit boundary (e.g. TI 21, UM 71, in Table 2.1-e and c). Other types of termination which reduce the transmitter output impedance are transformer coupling (e.g. AF 1000, Wee-Zee, in Table 2.1-g and h) and inductive loop coupling (e.g. WELCO track circuit in Table 2.1-i). These also provide galvanic isolation.

It is usually not possible to ensure exact delineation of adjacent AF TCs. The 'dead zone,' arising from shunting problems near the short circuit termination, may be eliminated in favour of overlap zone using specially shaped bonds (e.g. 'D', 'Z', 'S' or '8' in Table 2.3), or by staggering the transmitter and receiver connections at the boundary between adjacent track circuits.

Current-sensitive receivers using inductive coils or loops within the track give a very precise definition of the track circuit extremities. To further improve their performance, however, short circuiting bonds or series resonant circuits are also used (e.g. FME L 20/80, CVCM-75 in Table 2.1-d and j). The use of short circuiting connections, however

should be carefully considered for any particular application as they can have important safety implications [2-1]. To achieve optimum performance, particularly to increase the shunting sensitivity, some designers have used combined voltage/current sensitive receivers (e.g. Reed track circuits in Table 2.1-k).

2.2 TRACK CIRCUIT MODULATION AND CODING. TRAIN DETECTION AND TRACK-TO-TRAIN TRANSMISSION. INTERFERENCE TOLERANT DESIGN.

The choice of operating frequency is the central problem in AF track circuit design. The exact frequency represents a trade-off between several factors: ease of establishing tuned TC separation areas, maximisation of track circuit detection length, reduction of transmitter power, protection against feed-through and crosstalk from adjacent TCs, and avoidance of interference from traction and propulsion systems. The last problem is particularly significant and one solution is a twin channel design based on a carefully chosen relationship between the two channel frequencies (e.g. TI-21 in Table 2.1-c).

The track circuit energisation can propagate along the rails as a continuous wave or a modulated carrier signal. Continuous wave track circuits are normally used in non-electrified areas (e.g. Aster, Aster-U in Table 2.1-e). On electrified lines, however, such track circuits are very vulnerable to malfunction from traction or power supply interference. Thus other protective measures are employed. The CVCM 75 track circuit, for instance, operates with a continuous signal with stringent frequency, level and phase checking to eliminate interference signals.

A basic principle to provide immunity against EMI is to ensure that the track circuit operating signal is dissimilar from any spurious signals which are likely to occur. Thus a high signal-to-noise ratio at the operating frequency is necessary. The most common modulation techniques used to achieve this requirement are amplitude and frequency shift keying (ASK and FSK). Analysis performed in [2-5] on the workability of ASK and FSK for track circuit applications concludes the suitability of FSK. ASK is considered to be unsuitable without the use of sophisticated detection techniques. This is illustrated by reported instances of faulty operation of GRS and US&S ASK-modulated AF track circuits on several systems after chopper-controlled trains were introduced into service. The problem is that during the OFF-period in ASK modulation, the receiver is highly susceptible to noise. To solve the interference problem, GRS developed a true frequency-division multiplexed signal with a fixed 1 Hz code rate track signal for train detection, and a variable code rate train signal for cab signalling with increased receiver selectivity [2-46]. US&S, however, developed a new coherent code-selective track circuit in which

the code rate recovered at the receiving end is compared with a reference code rate from the transmitter.

FSK modulation has advantages both in operation and in implementation [2-5]. The most widely used implementation involves a different carrier frequency and/or modulation rate for adjacent track circuits. A completely interference tolerant design may be achieved with FSK by incorporating in the AF track circuit receiver stringent checks of the operating signal parameters, such as frequency, voltage level, timing relationships and modulation rate with an additional operating time delay to eliminate transient effects. At the time of writing, the most sophisticated examples of such an AF track circuits are the track circuits FTG S 917 and FS 2500 (Table 2.1-a and b), incorporating a microprocessor based receiver. In FS 2500 track circuit, the received signal is analysed using digital signal processing techniques to verify its frequency spectrum. The use of microprocessors, however, in safety systems has involved a new problem of software validation.

In most track circuits with FSK, different modulation rates are provided for information transmission from track to train. The information capacity, however, is relatively low: there are only 6 possible information bits in the TI-21, 18 in the UM-21, and 14 in the FS 2000 track circuit. An alternative method of transmitting information to the train is by digital coding, such as in the BART AF TC ([2-50] to [2-52]) where there is capacity for 8 different messages with a 6-bit comma free code. In the Siemens FTG S 917 track circuit ([2-7] to [2-13]), however, message telegrams are provided with a length of 60 bits, transmitted at 200 bauds. The digital coding provides an increased signal-to-noise ratio, and each track section is assigned a particular code which is then checked in the receiver. No practical examples of track circuits using other types of modulation have been reported. However, phase shift keying may be a suitable technique for achieving enhanced data transmission rates in the presence of electromagnetic noise.

A problem in the use of AF track circuits for cab signalling is the correct transmission and reception of the signal in the train receiver. The presence of overlap at the ESJs could cause mixed reception of signals from adjacent track circuits.

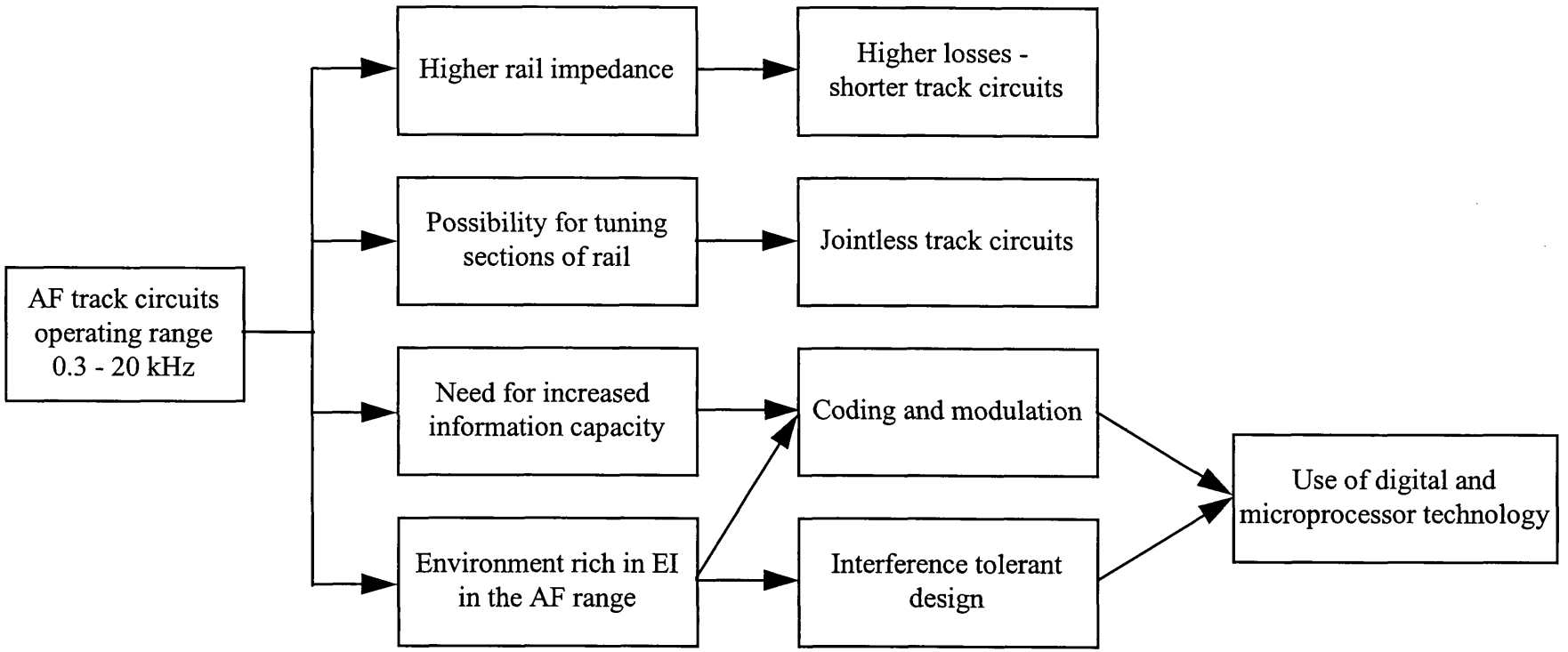

Fig.2.1 Problems and features of AF track circuits design

TABLE 2.1-a

Manufacturer	**SIEMENS**	TC type	**FTG S**	**1**

APPLICATION
Main line Rapid transit Overlay track circuit
Non-electrified lines DC electrified lines AC electrified lines
Standard layout Points & crossings layout Centre-fed layout
Continuous welded rail Non-sleepered permanent way

TRACK CIRCUIT TERMINATION

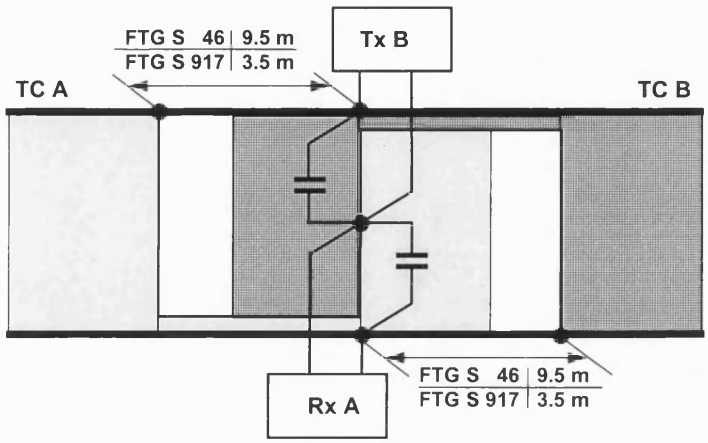

FUNCTIONS
Train detection
Broken rail detection
Overlay track circuit
Transmission of information for signalling without lineside cables
Transmission of information for cab signalling, ATP or ATO system
Equalisation of traction return current

OPERATIONAL CHARACTERISTICS	
Nominal TC length (standard layout)	
FTG S 46	600-750 m
FTG S 917	300-400 m
Maximum train shunt resistance	0.5-1.0 Ω
Specific ballast resistance	
Min	1.5 Ω.km
Max	2.5 Ω.km
Max distance of TC equipment from track	
FTG S 46	6500 m
FTG S 917	4500 m
Definition of TC boundaries	Overlap
MTBF per TC per year	0.2 faults

TRACK CIRCUIT OPERATING SIGNAL	
TC operating frequencies FTG S 46 FTG S 917	Six fequencies spaced at 1 kHz in the band 4.75, 5.25, 5.75, 6.25 kHz 9.5, 10.5 11.5, 12.5, 13.5, 14.5, 15.5, 16.5 kHz Adjacent TC frequencies should differ by at least 2 kHz.
Modulation and coding	FSK modulation with modulation rate 100 Hz and deviation frequency ±75 Hz is used for digital coding of the operating signal. Each track circuit is allocated one of 15 code pattern for unique TC identification. FTG S is also available without modulation.
Information capacity	When a TC is occupied telegrams can be transmitted to the train at a rate of 200 bauds using a 32 bit CRC protection code and optimisation of telegram length.

TABLE 2.1-a

Manufacturer	**SIEMENS**	TC type	**FTG S**	**2**

ELECTRICAL SEPARATING JOINT	
ESJ design	S-shaped bond forming together with short sections of rails two inductive loops. Each loop is tuned with a capacitor in parallel resonance at the frequency of its own TC but represents a low impedance at the frequency of the adjecent TC. With coupling factor between loop and rail equal 1 (practically 0.85) a pronounced directional effect is produced in the direction of the circuit towards which the conductor loop is open.
Tx coupling Centre-fed TC Single TC	 Direct connection to the rails Voltage coupling to the Tx S half loop with parallel resonance tunir
Rx coupling	Voltage coupling to the Rx S half loop with parallel resonance tunir
Train shunt detection	A train axle entering the ESJ progressively reduces the inductance of the loop formed by rail and bond thus disturbing the parallel resonance tuning and decreasing the voltage across the Tx / Rx. An axle within the S-bond occupies two TC resulting in overlapping of train detection sections thus providing uninterrupted monitoring of all axles within the entire ESJ area.

SAFETY AND RELIABILITY	
Safety design	Two-channel design of the receiving equipment Same switching state of both track relays, fault detection through different switching state of the two track relays.
Immunisation against EM Interferences	The modulation renders the TC signal distiguishable from any harmonic products of the electric traction supply. Immunisation against: • chopper thyristor propulsion equipment interfernce • disturbance of traction current when metallic structures are earthed to the rail
Availability	In-doors installation of equipment except the maintenance free tuning units Extensive diagnostic indications Simple maintenance

TABLE 2.1-b

Manufr . **WESTINGHOUSE**	TC type **FS2500**	**1**

APPLICATION
Main line Metro
Non-electrified lines DC electrified lines AC electrified lines Lines used by chopper controlled trains
Standard layout Points & crossings layout Centre-fed layout Continuous welded rail
Remote feeding

TRACK CIRCUIT TERMINATION
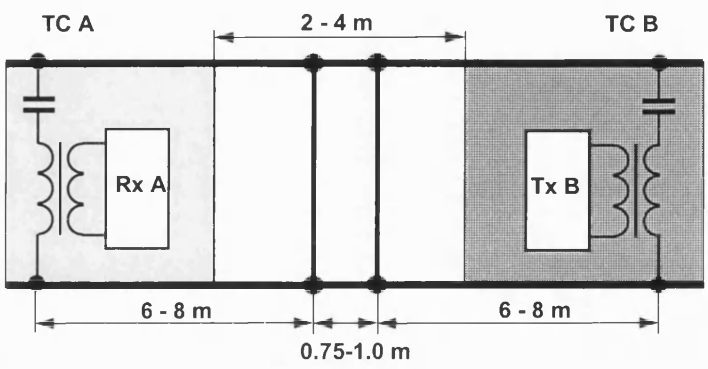

FUNCTIONS
Train detection
Broken rail detection (in most instances)
Transmission of up to 14 speed information to the train
Equalisation of traction return current
Cut section track circuits to obtain longer track circuits

OPERATIONAL CHARACTERISTICS	
Main line version	
Min /max TC length main line (end fed)	50/600 m
Min/max TC length main.l. (centre fed)	1.0/1.8 km
Max axle resistance	0.3 Ω
Metro version	
Max TC length Short type	40-100 m
Max TC length Long type	100-400 m
Max axle resistance (outside/inside ESJ)	0.5/0.15 Ω
Specific ballast resistance min/max	2/1000Ω.km
Remote feed-in/feed-out	max 2000 m
Definition of TC boundaries	'Dead' zone

TRACK CIRCUIT OPERATING SIGNAL	
TC operating frequencies Main line version Metro version	4 carrier frequencies in the range 1700 - 2600 Hz Track I - 4080 (V), 4560 (W), 5280 (M) Hz Track II - 4320 (K), 5040 (X), 5520 (Y) Hz Spare - 4800 (L), 6000 (Z) Hz
Modulation	FSK by ±40 Hz from the nominal frequency is used. On the standard version (no ATP) a single modulation frequency is used for all track circuits. In the ATP metro version one of 14 modulation frequencies is selected. These frequencies are from the range 28 to 80 Hz spaced by 4 Hz. The main line version uses 4 modulation frequencies
Information capacity	14 different speed codes can be transmitted to the train

TABLE 2.1-b

Manufr . **WESTINGHOUSE**	TC type **FS2500**	**2**

ELECTRICAL SEPARATING JOINT	
ESJ design	Track circuit is terminated at either end by two shorting bonds, 6-8 m apart from the points of connection of the Tx/Rx. To reduce the high power losses to an acceptable level, each end is resonated by circuits tuned to parallel resonance for the respective track circuit frequency. Two bonds are used to eliminate the longitudinal leakage due to mutual coupling between track circuits of the same frequency.
Tx coupling	Voltage coupling with series resonance tuning.
Rx coupling	Voltage coupling with series resonance tuning.
Train shunt detection	A train axle moving past the termination bonds and into the track circuit progressively reduces the inductance of the loop formed by rails and TBs thus reducing the Q of the parallel tuned circuit. At some point the tuning collapses causing reduction of the current through the tuning unit and de-energisation of the track relay. As the train axle moves into the TCT of the Tx end the series tuned circuit condition is nullified and a reduction of voltage occurs on the Tx TU. The current output to the rails is decreased and the TC relay is maintained de-energised. As the train axle moves away from the Tx TU the conditions change until at some point the receiver no longer detects the TC occupancy.

SAFETY AND RELIABILITY	
Safety design	The system uses digital signal processing techniques to provide a very high level of safety. The transmitter is so designed as to ensure that no failure can lead to an incorrect carrier frequency been produced. It delivers a constant output power, regardless of variations in supply voltage and load characteristics. In the receiver the safety is achieved by using conventional fail-safe techniques (fail-safe passive filters, threshold level detectors, etc.) as well as validated safe software and various safety checks.
Immunisation against EM Interferences	The FS 2500 track circuit is highly immune to interferences of various sources. This is achieved by the use of an 'intelligent' microprocessor based receiver which performs stringent checks of the incoming signal, namely: • it has the correct complex waveform • it is above a pre-defined threshold level and • no failures, noise or interferences can cause the track circuit to show 'unoccupied'.

TABLE 2.1-c

Manufacturer	**ADtranz**	TC type	**TI21**	**1**

APPLICATION
Main line Rapid transit
Non-electrified lines DC electrified lines AC electrified lines Areas with high levels of interference signals
Plain line layout
End/Centre fed layout
Continuous welded rail
Remote feeding

TRACK CIRCUIT TERMINATION

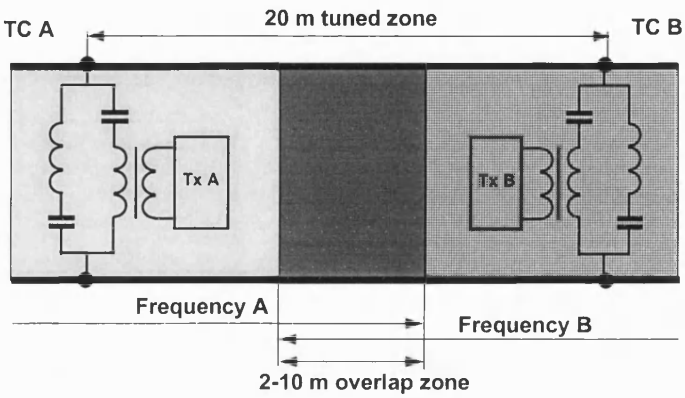

FUNCTIONS
Train detection
Broken rail detection (in most instances)
Equalisation of traction return current
Normal/low power mode

OPERATIONAL CHARACTERISTICS	
Min/max track circuit length	
Low power	50-250 m
Normal power end fed	200-1100 m
Normal power centre fed (each half)	300-1000 m
Min/max length (main line)	200-2400 m
Min specific ballast resistance	2 Ω.km
Max axle resistance (outside/inside ESJ)	0.5/0.15 Ω
Definition of TC boundaries (around the centre of the tuned zone)	
Main line	max ±5 m
Rapid transit	max ±1.5 m

TRACK CIRCUIT OPERATING SIGNAL	
TC operating frequencies	
Main line	4 carrier frequencies: Track I - 1699 Hz, 2296 Hz Track II - 1996 Hz, 2593 Hz
Rapid transit	Frequencies up to 10 kHz are employed depending upon application.
Modulation	FSK technique is used where the carrier frequency is shifted by 34 Hz at a low modulation rate and with mark/space ratio of 1. A single modulation rate of 4.8 Hz is used in all track circuits.

TABLE 2.1-c

Manufacturer	**ADtranz**	TC type	**TI21**	**2**

ELECTRICAL SEPARATING JOINT	
ESJ design	Electrical separation between adjacent track circuits is achieved by tuning a short length of track using two tuning units the tuned length varying with the application. Each tuned circuit presents a low impedance to one of the frequencies present in the ESJ so that transmission does not occur beyond this point. A relatively high impedance is present to the other frequency so that transmission of this signal occurs in the required direction. For a particular frequency , there is a ratio of approximately 15:1 between the voltage across the tuning unit of that frequency and the voltage across the other tuning unit. The low impedance circuits in the tuning units also serve the very important function of shorting the rail to rail traction harmonic voltages at the track frequencies thus keeping their level at the input of the receiver low.
Tx coupling	Voltage coupling with resonance tuning
Rx coupling	Voltage coupling with resonance tuning.
Train shunt detection	On entering the tuned area the train axles cause disturbance of the resonance tuning and hence, reduction of the level of the incoming signal causing the track circuit relay to drop. In the middle part of the tuned zone trains are detected by both track circuits (overlap zone). The exact length of the overlap shunting zone is between 2 and 10 m and depends upon the ballast conditions and train axle resistance.

SAFETY AND RELIABILITY	
Safety design	The track circuit receiver performs a number of checks to ensure very high security against false operation, such as • both audio frequency signals are checked independently by narrow bandwidth filters • The amplitude of each frequency • the mark/space ratio of frequency shift should be 1 • the correct sequence of both frequencies • the correct modulation rate.
Immunisation against EM Interferences	The TI21 track circuit can operate reliably in areas where high values of interference may be present, both in AC and DC electrification areas. It is considered to be an universal type of track circuit.

TABLE 2.1-d

Manufacturer	**SEL**	TC type **FME L20/80**	**1**

APPLICATION
High density railroads Rapid tramsit
Railway lines with traction return current via both rails
Standard layout Points & crossings areas Short track circuits
Continuous welded rail
Areas with high level of EM Interferences

TRACK CIRCUIT TERMINATION

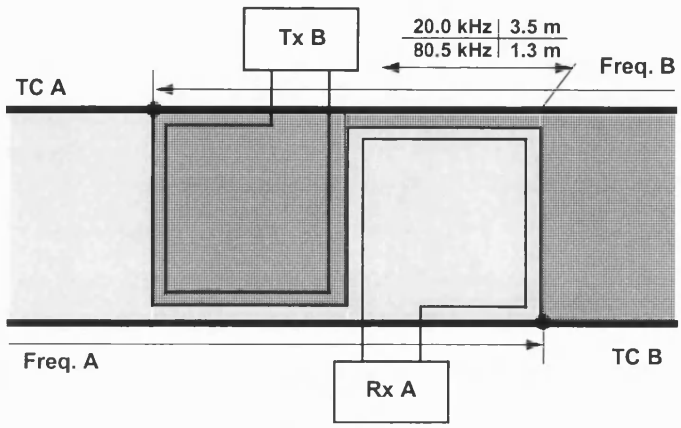

FUNCTIONS
Train detection
Broken rail detection (in most instances)
Overlapping track vacancy detection
Cab signalling
Joint fault detection
Equalisation of traction return current
Remote feeding
High reliability

OPERATIONAL CHARACTERISTICS	
Max TC length (standard layout) single end fed centre fed	 300 m 750 m
Maximum train shunt resistance	0.5 Ω
Min specific ballast resistance	2.5 Ω.km
Max distance of TC equipment from track	1.0 km
Definition of TC boundaries	Overlap
Response time	300 ms

TRACK CIRCUIT OPERATING SIGNAL	
TC operating frequencies Up to 750 m Up to 100 m For point track circuits	 Six frequencies in the band 20 to 25 kHz with spacing of 1 kHz Six frequencies in the band 80.5 to 85.5 kHz with spacing of kHz Adjacent TC frequencies should differ by 2 kHz. Frequencies from the range of 80 kHz.
Modulation and coding	Track circuit carrier signal is binary coded using FSK modulation. Each track circuit is allocated an individual 8 bit comma free code combimation. the code provides 30 different self-synchronising codes.

TABLE 2.1-d

Manufacturer	**SEL**	TC type	**FMEL20/80**	**2**

ELECTRICAL SEPARATING JOINT	
ESJ design	The ESJ is formed by a copper cable in a 'S'-shaped configuration fixed to each of the running rails and two inductive loops for coupling the transmitter and the receiver. The Tx loop is mounted adjacent to one half of the 'S'bond, the Rx loop is mounted to the other half. Both loops are coupled to the half on the outer side of the track circuit boundary. The bonding cable can also perform the function of balancing traction power return current through the rails.
Tx coupling Centre/fed TC Single TC	 Direct voltage connection to the rails Inductive coupling via the Tx inductive loop
Rx coupling	Inductive coupling via the Rx inductive loop
Train shunt detection	The train shunt detection in the ESJ area is characterised by the presence of an overlap area where both track circuits are detected. Its length depends on the application and equals approximately the 'S'-bond's lendth. A track circuit will only be released after the last train axles has vacated the S-bond and the adjacent track circuit has indicated 'occupied'.

SAFETY AND RELIABILITY	
Safety design	High selective receiver with phase sensitive rectifier referenced to the transmitter fequency.
Immunisation against EM Interferences	Highly immune

TABLE 2.1-e

Manufacturer	**CSEE**	TC type	**UM71**	**1**

APPLICATION
Main line
Non-electrified lines DC electrified lines AC electrified lines
Compatible with locomotives with thyristor and chopper control
Plain line layout
End/Centre fed layout
Continuous welded rail
Remote feeding

TRACK CIRCUIT TERMINATION

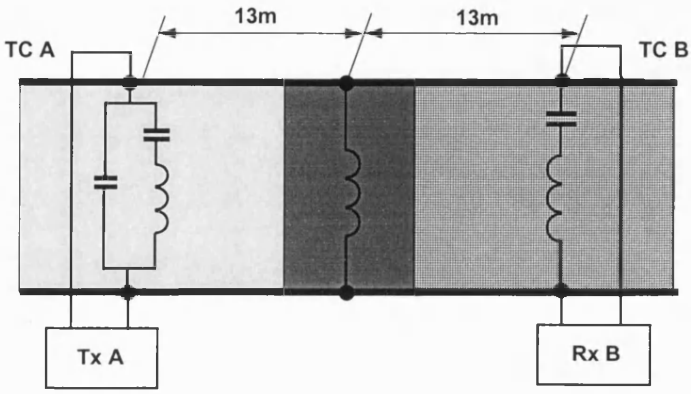

FUNCTIONS
Train detection
Broken rail detection (in most instances)
Cab signalling
End-to-end transmission
Equalisation of traction return current
Reversible mode
Capacitive compensation

OPERATIONAL CHARACTERISTICS	
Min track circuit length (end/centre fed)	50/100 m
Max track circuit length	
Simplified/normal joint	500/750 m
Normal joint, centre fed	1500 m
With capacitive compensation	5-10 km
Max length of ASTER-U (centre fed)	1.0-2.0 km
Min specific ballast resistance	2 Ω.km
Max axle resistance (outside/inside ESJ)	0.25 Ω
Definition of TC boundaries	Overlap 1m

TRACK CIRCUIT OPERATING SIGNAL	
TC operating frequencies	Track I - 1700 Hz, 2300 Hz Track II - 1900 Hz, 2500 Hz
Modulation	The carrier signal is either continuous wave (in the earlier track circuit version ASTER U) or modulated by frequency shift keying by ±10 Hz at a low frequency rate. In track circuits without cab signalling each carrier frequency is assigned a fixed modulation rate: 13.3, 18.0, 15.6 and 20.3 Hz For cab signalling the same carrier frequency as for train detection are used but the modulation rate varies and carries specific speed information.
Information capacity	18 modulation frequencies from the interval 10.3 to 29 Hz with a step of 1.1 Hz are available for transmission of speed information.

TABLE 2.1-e

Manufacturer	**CSEE**	TC type	**UM71**	**2**

ELECTRICAL SEPARATING JOINT	
ESJ design	The ESJ comprises inductances, capacitors and short sections of rails which are specially tuned as to provide directional effect and best conditions for coupling of track circuit transmitter and receiver. At the frequency of the track circuit the tuning circuits present a high impedance while at the frequency of the adjacent track circuit they act as a series resonance. Two types of ESJ are available: normal, incorporating an impedance bond for equalisation of traction return currents and simplified - without impedance bond.
Tx coupling	Voltage coupling with resonance tuning
Rx coupling	Voltage coupling with resonance tuning.
Train shunt detection	The presence of train axles in the ESJ area disturb the resonance tuning and decrease the signal in the track circuit receiver giving indication 'occupied'.

SAFETY AND RELIABILITY	
Safety design	The modulation makes the track circuit signal distinguishable from any harmonic products of the electric traction supply.
Immunisation against EM Interferences	The design of UM71 track circuit ensures immunisation against: • chopper thyristor propulsion equipment interference • disturbance of traction current when metallic structures are earthed to the rail.

TABLE 2.1-f

Manufacturer	**ASTER**	TC type	**ASTER**

APPLICATION
ASTER- 1W Non-electrified lines DC electrified lines
ASTER - 16 W DC electrified lines AC electrified lines
Plain line layout
End fed layout
Continuous welded rail

TRACK CIRCUIT TERMINATION

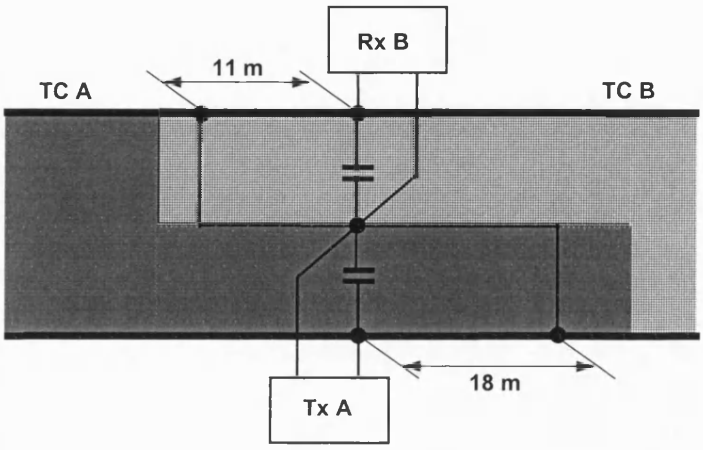

FUNCTIONS
Train detection
Broken rail detection
Equalisation of traction return current

OPERATIONAL CHARACTERISTICS	
Max track circuit length	880 m
Min specific ballast resistance	2 Ω.km
Max axle resistance	Ω
Definition of TC boundaries	Overlap 29 m

TRACK CIRCUIT OPERATING SIGNAL		
TC operating frequencies	ASTER 1W	ASTER 16W
Track I	1620 Hz, 2100, 2580 Hz	1700, 2100, 2500 Hz
Track II	1860 Hz, 2340, 2820 Hz	1900, 2300, 2700 Hz
	Continuous wave	

ELECTRICAL SEPARATING JOINT	
ESJ design	The ESJ represents a 'Z'-shaped bond which together with short sections of rails forms two inductive loops. Being inductive, each loop is tuned by a capacitor to resonate at the frequency of the adjacent track circuit.
Tx/Rx coupling	Voltage coupling across the capacitors on which significant impedance is developed
Train detection	Overlap of adjacent track circuits of about 30 m.

SAFETY AND IMMUNISATION	
Safety and immunisation	ASTER 1W - Susceptible to wrong-side failures because of the odd harmonics of 50 Hz produced by traction drives. ASTER 16W - TC frequencies chosen to be equal to even harmonics of 50 Hz. Receiver susceptibility reduced to 25%.

TABLE 2.1-g

Manufacturer	**ANSALDO**	TC type	**AF 1000 W**

APPLICATION
Rapid Mass Transit Systems
Non-electrified lines DC electrified lines AC electrified lines
Plain line layout Point & crossings areas
End/centre fed
Continuous welded rail

TRACK CIRCUIT TERMINATION

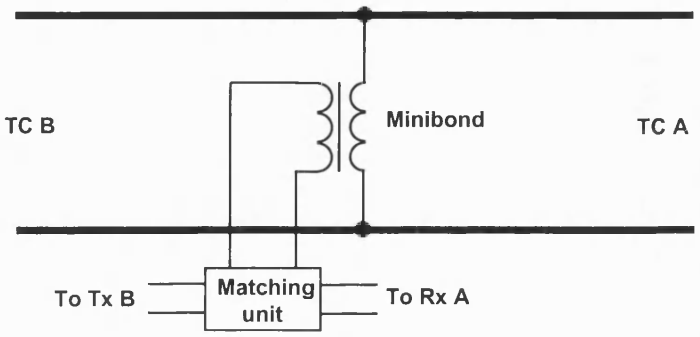

FUNCTIONS
Train detection
Broken rail detection
A single pair of conductors used for connection of a Tx and a Rx.

OPERATIONAL CHARACTERISTICS	
Max track circuit length	1400 m
Min specific ballast resistance	2 - 20 Ω.km
Max axle resistance	0.25 Ω

TRACK CIRCUIT OPERATING SIGNAL	
TC operating frequencies Modulation	Four carrier frequencies (2375, 2925, 3525 and 4175Hz) amplitude modulated by ON/OFF modulation with side band suppression by six frequency codes (2,3,4.5, 6.8, 10.1 and 15.3Hz). A carrier frequency and its associated code of each track circuit are selected such as to be as far as possible from those of the adjacent track circuits.

ELECTRICAL SEPARATING JOINT	
ESJ design	No mechanical insulating joints are required, except at points. The ESJ comprises a Tx transformer, a Rx transformer and an impedance bond (Minibond) for traction current return. Due to their low impedance, the track transformers act as an electrical barrier delimiting one track circuit from another with a good degree of precision.
Tx/Rx coupling	Inductive coupling via track transformers

SAFETY AND IMMUNISATION	
Safety and immunisation	The system operates with two tones. Track circuit clear indication is given only when both tones are present and there is a particular phase relationship between the signal applied to the track and the signal received.

TABLE 2.1 -h

Manufacturer	**GRS**	TC type	**Wee-Zee**	**1**

APPLICATION
Rapid transit WMATA MARTA

TRACK CIRCUIT TERMINATION

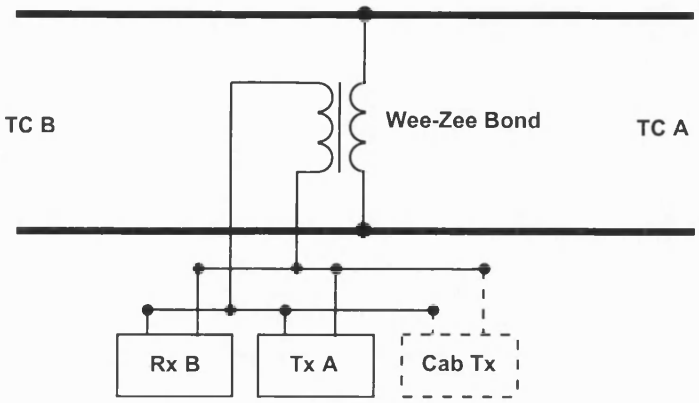

FUNCTIONS
Train detection
Broken rail detection (in most instances)
Cab signalling
Equalisation of traction return current

OPERATIONAL CHARACTERISTICS	
Max length of ASTER-U (centre fed)	m
Min specific ballast resistance	Ω.km
Max axle resistance	Ω
Definition of TC boundaries	Dead zone

TRACK CIRCUIT OPERATING SIGNAL		
TC operating frequencies	MARTA	WMATA
Track I	2970,3510,3870,4410 Hz	2100,2320,2580,2820 Hz
Track II	3330,3690,4230,4950 Hz	3100,3370,3660,3900 Hz
Cab signal frequencies	2340 Hz in all TCs	4550, 5225 Hz
Modulation freq's.	2, 3, 4,5, 6.83, 10.1, 15,3, 21.5 Hz	
Modulation	Train detection carrier frequencies are ON-OFF modulated with a fixed code rate of 2 Hz when unoccupied and with a special code rate for cab signalling transmission when a train enters the track circuit. the mark/space ratio is equal to 1. Cab signalling carrier frequency is transmitted during the OFF periods of train detection carrier frequency. The modulation frequency is chosen according to the speed code.	
Information capacity	8 modulation frequencies are available for transmission of speed information.	

TABLE 2.1 -h

Manufacturer	**GRS**	TC type	**Wee-Zee**	**2**

ELECTRICAL SEPARATING JOINT	
ESJ design	Track circuit boundaries are defined by impedance bonds being the common primary winding of three step-up transformers, the secondary windings being tuned in parallel resonance correspondingly to the Tx, Rx and Cab signalling Tx frequencies. The impedance bond known as Wee-Zee bond is of special design. It consists of a two-turn winding made of heavy copper conductor threaded through three or four toroidal iron core reactors.
Tx/Rx coupling	Transformer coupling with parallel resonance tuning
Train shunt detection	This ESJ relies upon the rail impedance to define the ends of the track circuit. They are used where some imprecision of the definition of the track circuit boundaries can be tolerated.

SAFETY AND RELIABILITY	
Safety design and immuni-sation against EMI	A steady receiver output is interpreted as circuit failure and causes the TC to show 'occupied'. For improved selectivity against EMI a separately coded signal and a highly selective receiver are used for train detection as opposed to the conventional 'all rate' receiver and signals with a common code rate for both train commands and track occupancy detection. The new GRS TC design employed at MARTA utilises frequency division multiplexed signal consisting of a fixed code rate (1 Hz) track signal and a variable code rate train signal.

TABLE 2.1-i

Manufacturer	**WELCO**	TC type	**WELCO**	**1**

APPLICATION
Rapid tramsit BART Sao Paulo Metro
DC electrification

TRACK CIRCUIT TERMINATION

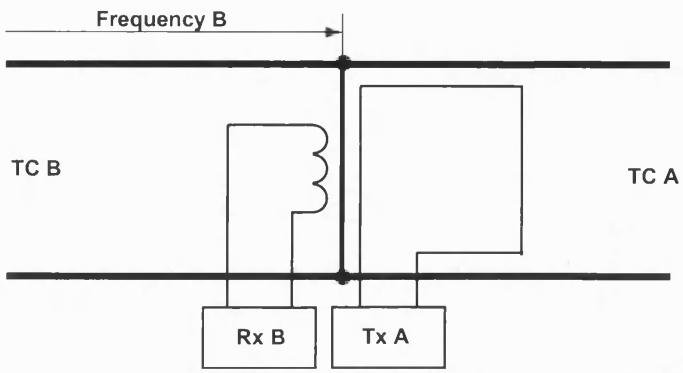

FUNCTIONS
Train detection
Broken rail detection (in most instances)
Cab signalling
Equalisation of traction return current

OPERATIONAL CHARACTERISTICS	
Max TC length	330 m
Maximum train shunt resistance	0.06 Ω
Min specific ballast resistance	2.5 km
Definition of TC boundaries	

TRACK CIRCUIT OPERATING SIGNAL	
TC operating frequencies	Each track circuit is assigned a pair of carrier frequencies used for train detection and speed code transmission. Four sets of frequency pairs (A,B,C and F) are used in order for consecutive track circuits to operate at diffrent frequencies: A (5783, 7775 Hz), B (5841, 8762 Hz), C (6623, 9935 Hz), F (5599, 8399 Hz)
Modulation and coding	Speed information is transmitted by binary coding achieved by switching between the two frequencies assigned to the track circuit (instead of turning on and off a fixed frequency). Adjacent track circuits use different frequency pair and a different code phase to avoid interference. The binary coding is at 18 bits per second. A 6 comma free code is used to transmit a maximum of 8 speed codes.

TABLE 2.1-i

Manufacturer	**WELCO**	TC type	**WELCO**	**2**

ELECTRICAL SEPARATING JOINT	
ESJ design	Track circuit extremities are defined by a substantial short - circuiting bond connected from rail-to-rail.
Tx coupling	Inductive coupling via a multiturn inductive loop.
Rx coupling	Inductive coupling via current sensors attached to the track sh bond.
Train shunt detection	The shunting sensityvity in the vicinity of the short-circuiting bond is low.

SAFETY AND RELIABILITY	
Safety design and immunisa-tion against EM interferences	To ensure high immunity against interferences in the occupancy detection circuitry speed code data sent out to each individual transmitter are compared with the data returning from those of the associated reciever. If the code sent out is identical to the code returned, the detector produces an 'unoccupied' indication.

TABLE 2.1-j

Manufacturer **ALSTHOM**	TC type **CVCM 75**	**1**

APPLICATION
Mass transit railways
Railways with chopper controlled propulsion systems and regenerative braking
Standard layout Points & crossings areas
Continuous welded rail

TRACK CIRCUIT TERMINATION

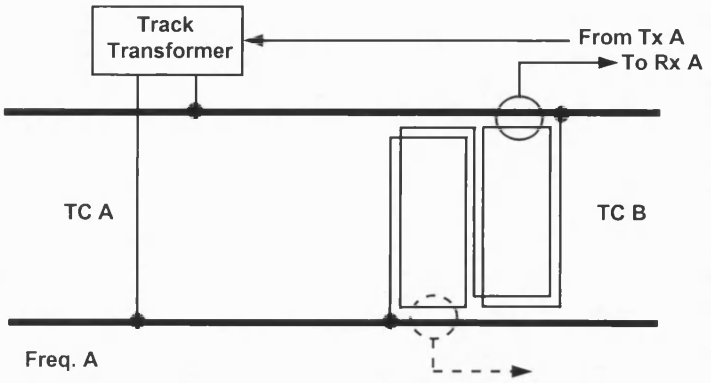

FUNCTIONS
Train detection
Broken rail detection (at any point of the TC)
Precise definition of TC boundaries
Detection of axles with higher resistance
Equalisation of traction return current
Local/central location of equipment

OPERATIONAL CHARACTERISTICS	
Min/max track circuit length	20 m
Max TC length (cascade operation)	600 m
Min specific ballast resistance	0.25 Ω
Max distance of remote feeding	2 km
Definition of TC boundaries	±0.25 m
Maximum train shunt resistance	0.5 Ω/km

TRACK CIRCUIT OPERATING SIGNAL	
TC operating frequencies	
Track I	8.2, 9.2, 10.6 kHz
Track II	8.6, 10, 11 kHz
For TCs at crossings	12.3 kHz
Modulation and coding	None

TABLE 2.1-j

Manufacturer	**ALSTHOM**	TC type	**CVCM 75**	**2**

ELECTRICAL SEPARATING JOINT	
ESJ design	Track circuit extremities are very strictly defined by LC series tuned circuit or '8'-shaped multiturn inductive loop fixed between the rails. The signal currents flowing in the loop add their effect to those present in the rail above the antenna resulting in a better coupling when the track circuit is not occupied. Compared to the LC circuit the inductive loop has the following advantages: • the drop shunt of the track circuit is significantly higher • the loop provides an equipotential connection for traction return currents in the two rails and can also be used for track-to-track connections.
Tx coupling	Direct voltage coupling in the centre of the track circuit.
Rx coupling	Inductive coupling with antenna fixed under the flange of the rail

SAFETY AND RELIABILITY	
Safety design Immunisation against EM Interferences	The CVCM 75 track circuit is highly immune to EM interferences. This is achieved by special design of the receiver where several checks of the in-coming signals are performed: • the correct operating frequency • the correct level • the correct phase relation between the signals picked up from the two-half sections of the track circuit.

TABLE 2.1-k

Manufacturer	**GEC**	TC type	**REED AF TC**

APPLICATION
Main line Suburban railways
Non-electrified lines AC electrified lines DC electrified lines
Overlay track circuits
Continuous welded rail
Areas with high level of EM Interferences

TRACK CIRCUIT TERMINATION

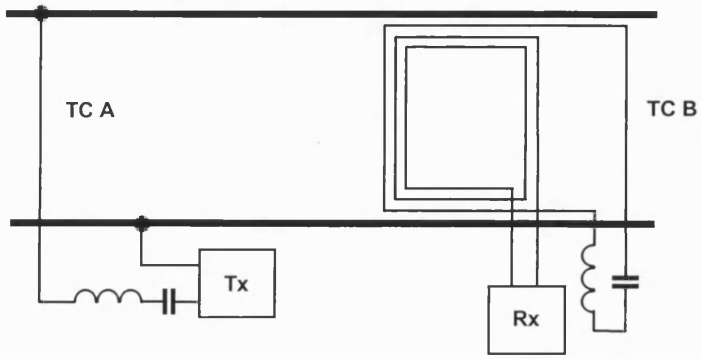

FUNCTIONS
Train detection
Overlapping track vacancy detection

OPERATIONAL CHARACTERISTICS	
Max TC length	3000 m
Maximum train shunt resistance	0.5 Ω
Specific ballast resistance	1.6-70 Ω.km
Definition of TC boundaries	5m overlap

TRACK CIRCUIT OPERATING SIGNAL	
TC operating frequencies	The track circuit operates with eight carrier frequencies in the band between the 7th and the 8th harmonic spaced at as little as 3 Hz. This is achieved by the use of special fail-safe reed filters.
Track I	363, 369, 375, 381 Hz
Track II	366, 372, 378, 384 Hz

ELECTRICAL SEPARATING JOINT	
ESJ design	The relay ends of reed track circuits are defined by a 5 m long pick-up multiturn cable loop laid in the track. For optimum performance the receiver end incorporates a series tuned circuit connected across the rails which provides additional component of voltage in the receiver sensing loop.
Tx coupling	Direct coupling via a series tuned circuit . Centre fed.
Rx coupling	Current coupling with inductive component.
Train shunt detection	The ends of the adjacent track circuits are overlapped so that both track circuits are detected as occupied as the train passes over the common section.
Safety design	The reed filter rejects spurious signals and ensures that the relay responds only to signals of the correct frequency.

Table 2.2 VOLTAGE AND CURRENT COUPLING OF TRANSMITTER AND RECEIVER EQUIPEMENT IN AF TRACK CIRCUIT

VOLTAGE COUPLING		CURRENT COUPLING		CURRENT & VOLTAGE COUPLING
TRANSMITTER	RECEIVER	TRANSMITTER	RECEIVER	RECEIVER
a. DIRECT 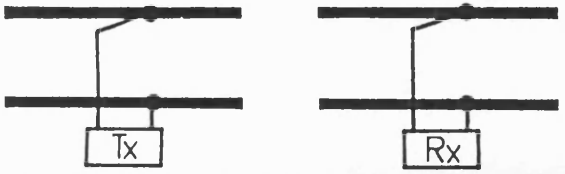		**e.** INDUCTIVE LOOP BIDIRECTIONAL TRANSMISSION 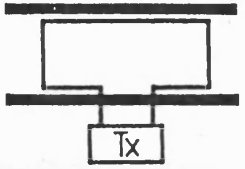	**h.** INDUCTIVE LOOP BOUNDLESS TRACK CIRCUIT **i.** INDUCTIVE COIL(S) 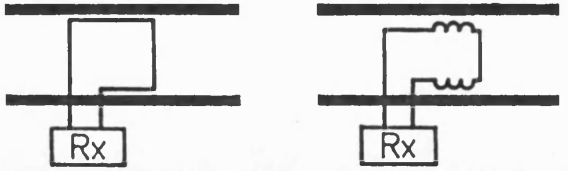	**p.** INDUCTIVE LOOP 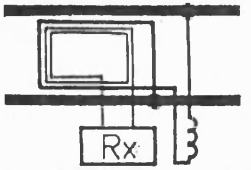
b. TRANSFORMER 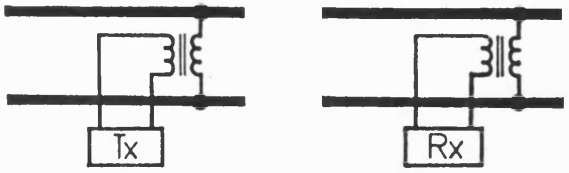		**f.** ONE DIRECTION TRANSMISSION 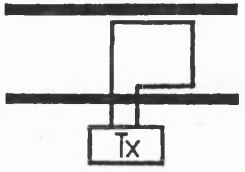	**j.** SHUNT BOND TERMINATION **k.** 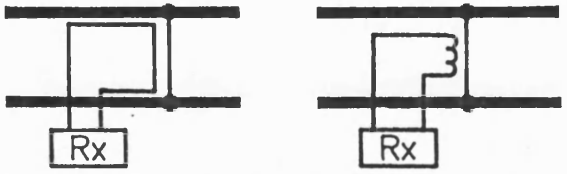	**q.** 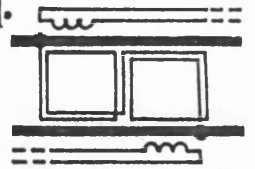
c. PARALLEL RESONANT * 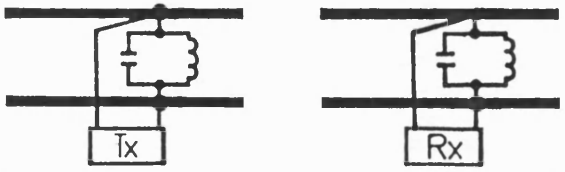		**g.** S-BOND 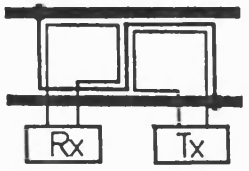	**l.** RESONANT CIRCUIT TERMINATION **m.** 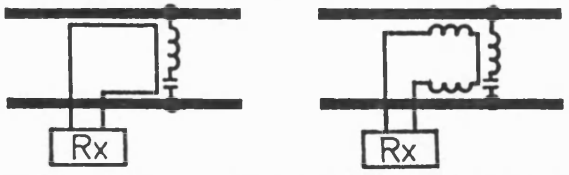	
d. SERIES RESONANT 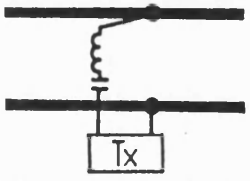			**n.** S-BOND **o.** Z-SHAPED 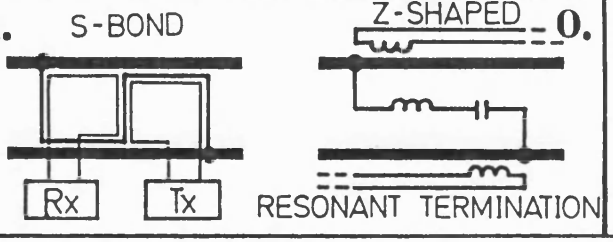	

* This is a symbolic representation of the track circuit terminations shown in Table 2.3 a-f

Table 2.3 TRACK CIRCUIT TERMINATIONS

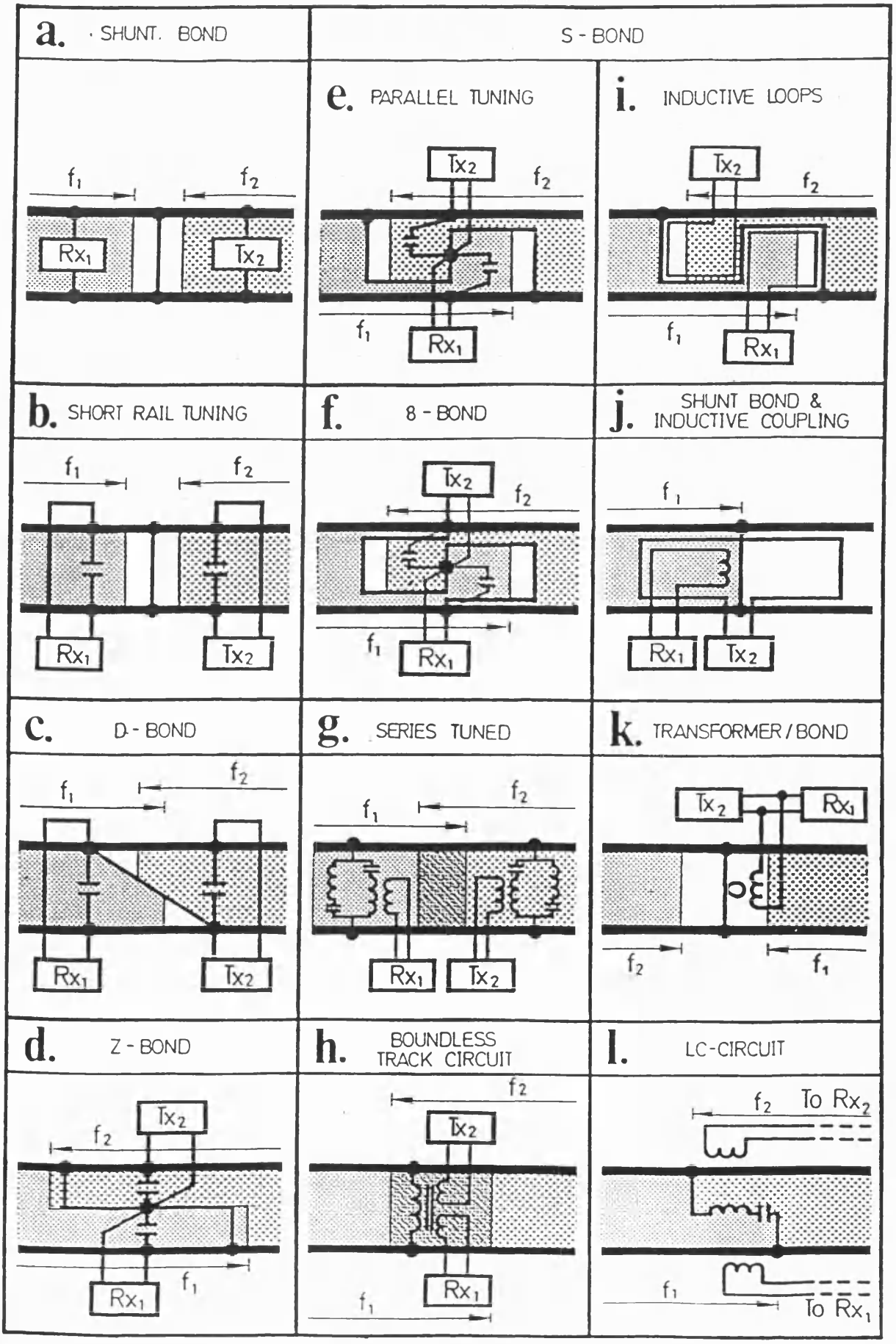

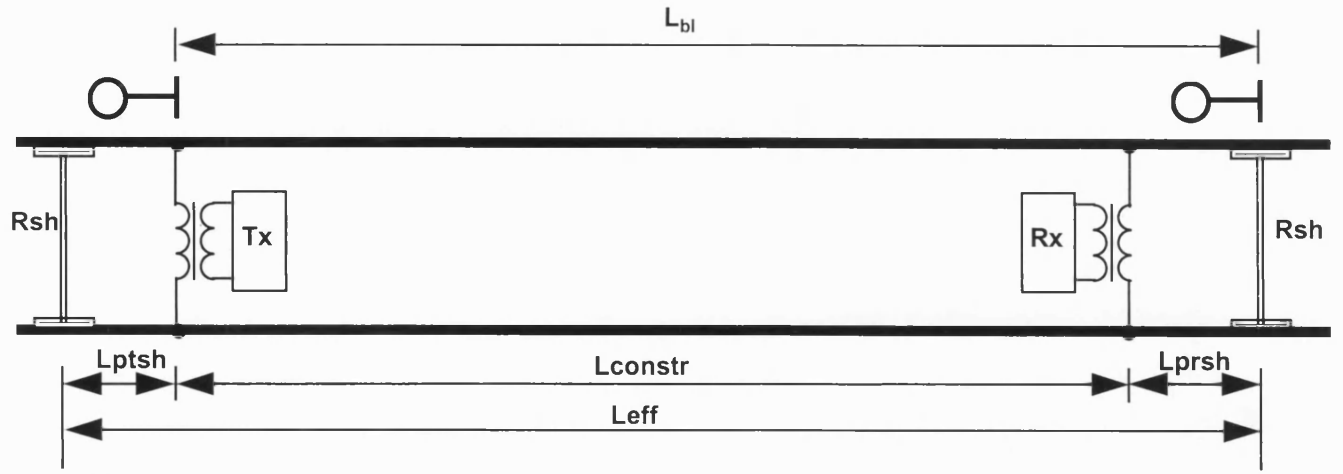

(a) Extended shunt area in voltage operated track circuits

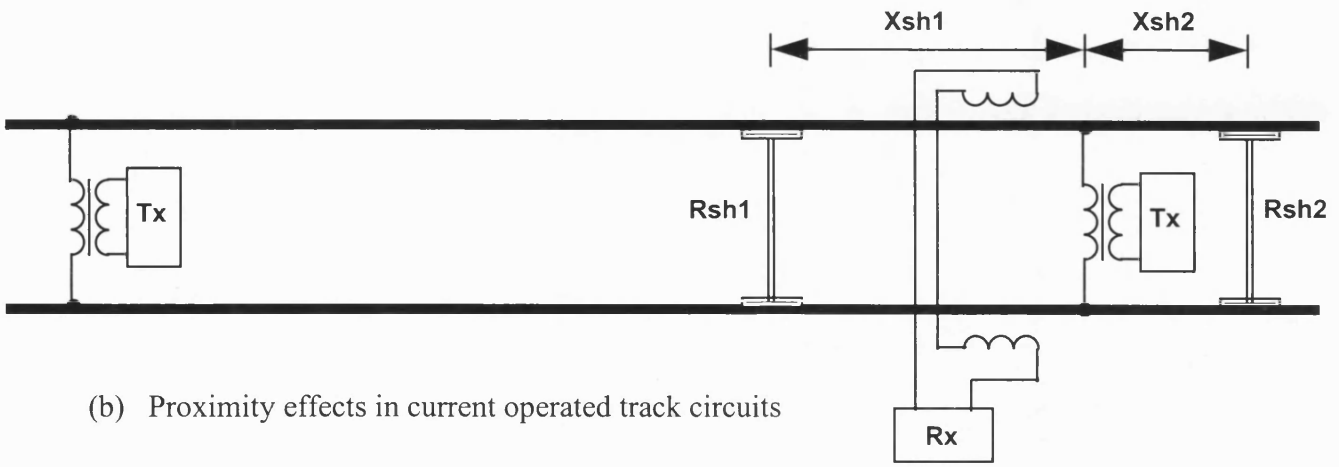

(b) Proximity effects in current operated track circuits

Lprsh - pre-shunting area length, **Lptsh** - postshunting area length, **Lbl** - block section length,
Lconstr - construction length, **Leff** - effective track circuit length

Fig.2.2 Boundless track circuits

Chapter 3

TRACK CIRCUIT FUNCTIONAL MODEL

The objective of this chapter is to analyse track circuits from the point of view of the particular functions which they perform and to derive a suitable track circuit functional model. The track circuit functional model is first defined non-mathematically, and then given a formal mathematical description. A method of analysis based on decomposition of a functional algorithm into several modes of operation is introduced. This is applied first to the relatively simple case of conventional bounded track circuits (with insulated block joints), and then in a revised and extended form to the case of track circuits without physical insulating joints.

3.1 GENERAL TRACK CIRCUIT FUNCTIONAL MODEL

3.1.1 Track circuit purpose and application

The track circuit is an essential component of many signalling, interlocking and level-crossing protection systems. It is an electrical and/or electronic fail-safe system associated with a particular section of rail track, performing either or both the functions of train detection and track-to-train communication link. Although performed on the same physical circuit, these two functions are very different in nature. Hence, when setting up a track circuit functional model it is convenient to examine these functions separately. The following model is concerned only with the track circuit primary function of train detection.

The primary purpose of a track circuit is to continuously monitor the state of occupancy of a track section by a vehicle and generate, within the complete range of track circuit operating conditions, vital 'Clear' indication if, and only if, the track section is free of vehicles and the track circuit equipment is in good working order. Otherwise, non-vital 'Occupied' information is generated. The 'Occupied' and 'Clear' indications are strictly and unambiguously related to a pre-defined section of rail track.

The above definition implies that a track circuit is designed on the principle of fail-safe operation which requires that no component failure may cause an occupied track circuit to give 'Clear' indication. This requirement equally applies to the running rails. They form the transmission path for the track circuit operating signal and as such represent a particular type of track circuit component. Hence, the requirement that a track circuit should be able to detect rail breaks (provided it is accompanied by a significant reduction in the rail electrical continuity) can be regarded as a direct consequence of the requirement for fail-safe operation. Railway engineers and track circuit manufacturers

have adopted various positions with regard to the significance of the broken rail detection function of track circuits. The author has the opinion that since the rail break detection capability exists, it must whenever possible be implemented for safety reasons. Hence, in the following sections, it will be considered that the purpose of track circuits is to detect the presence of vehicles as well as broken rails.

In some cases cab track circuits operate in conjunction with an on-board receiver (cab signalling). For such applications the same functional algorithm applies as for the track circuits with track receiver.

3.1.2 Functional structure and principle of operation

The track circuit algorithm of operation described above is performed by the electrical circuit shown in block diagram form in Fig.3.1. This figure shows a simple functional structure including a transmitter and a receiver connected to both ends of a section of running rails. The transmitter provides a standard operating signal. The receiver is where the output information is formed and stored. The section of running rails forms the transmission path between transmitter and receiver, at the same time, being the object monitored by the track circuit system.

The principle of operation is based on the fact that the application of a train shunt across the running rails or a broken rail affects the transmission characteristics of the rails, causing discrete changes of the operating signal in the receiver. These changes are then assessed and the appropriate output indication is given.

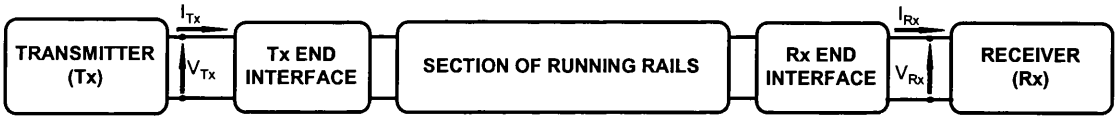

Fig.3.1 Track circuit block diagram

It is essential to note that the running rails are sensitive not only to the two monitored effects - the presence of a rail vehicle and a broken rail. A number of other factors such as geological conditions, humidity, temperature etc., may as well influence their transmission characteristics and affect track circuit operation. In addition, electric signals from other track circuits or other electric networks may as well penetrate the track circuit and add to the standard operating signal at any time and in any combination, thus changing the expected operating signal in a random way. This makes the interpretation of the signal in the receiver more difficult and requires the use of more sophisticated techniques.

3.1.3 Formal track circuit system model

A suitable track circuit model, which provides a high degree of generality, is conveniently based on the system approach. The definition of such a model (Fig.3.2) requires specification of the TC input, output and the TC function which is the relationship between input and output.

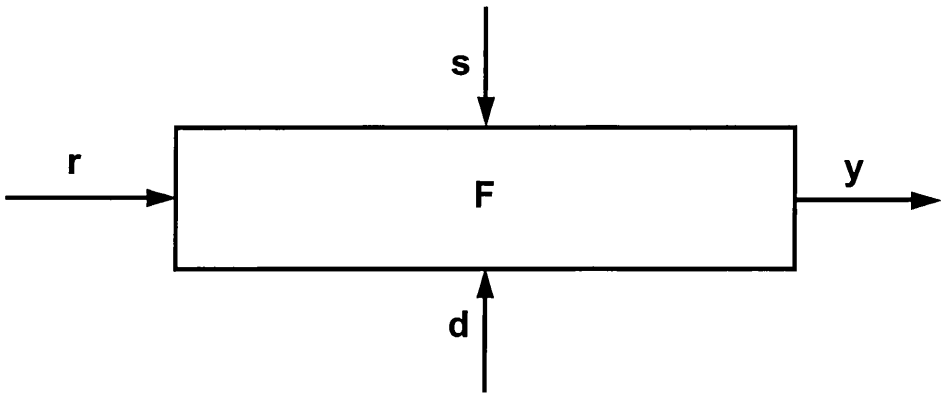

Fig. 3.2 General track circuit system model

The TC input can be described by a set of three vectors:

- Vector of TC input operating effects

$$\mathbf{r} = (r_1, r_2, \cdots r_j \cdots r_m) \tag{3.1}$$

describes the actual track circuit operating state i.e. 'unoccupied', 'occupied', train shunt position, broken rail position, position of second train shunt on an adjacent track circuit, train shunt resistance, etc. These input effects are well defined. For each set of these input effects the track circuit functional algorithm strictly defines what the track circuit output (indication) should be.

- Vector of TC environmental effects

$$\mathbf{s} = (s_1, s_2, \cdots s_k \cdots s_n) \tag{3.2}$$

takes into account such factors as the instability of rail track parameters with geological and weather conditions, rail track asymmetry, crosstalk or feedthrough interference from other track circuits on the same or on a parallel track, electro-magnetic interferences originating from the traction system, thyristor controlled locomotives, etc. All these can be qualified as spurious input effects and may result in both continuous and discrete changes of the track circuit operating signal. They are not defined in the functional algorithm but have to be accounted for, so that they do not lead to wrong output.

- Vector of TC design parameters

$$\mathbf{d} = (d_1, d_2, \cdots d_i \cdots d_l) \tag{3.3}$$

defines track circuit operating parameters such as track circuit length, operating frequency, electrical separating joint parameters, track circuit layout, remote feeding, etc. as well as the electrical parameters of track circuit equipment itself. These parameters are considered as a particular type of input effect in order to include them in the frame of the track circuit functional model. This is necessary because choosing, maintaining and monitoring the correct values of track circuit design parameters is essential for achieving the required fail-safe functional algorithm.

On the basis of the above definitions the track circuit input can be described by a vector of track circuit (input) status

$$\mathbf{x} = (\mathbf{d},\mathbf{r},\mathbf{s}) = (x_1, x_2, \cdots x_j \cdots x_{l+m+n}) \tag{3.4}$$

where each of the vectors **d**, **x**, **s** and **r** represents an ordered finite set of real or complex numbers. The number of components in each of the vectors and their physical meaning depends on the particular problem being solved and the required level of accuracy and design detail. Each vector component may assume values from an associated definition interval. The set of definition intervals imposed on all vector elements define the boundaries of a domain in a multidimensional space. This domain represents the region of definition of the corresponding vector. The specification of TC input and output includes definition of the following regions of definition:

- Region of definition of TC design parameters $\mathbf{D_D}$
- Region of existence of a track circuit **D**
- Region of definition of the specified design parameters $\mathbf{D_o}$
- Region of definition of TC input operating effects **R**
- Region of safety critical input operating effects $\mathbf{R_o}$
- Region of definition of the TC environmental conditions **S**
- Region of definition of TC status **X**
- Region of definition of TC safety critical status $\mathbf{X_o}$
- Region of definition of TC output **Y**.

The region of definition of TC design parameters $\mathbf{D_D}$ is defined by the general constraints on the track circuit design parameters. Some of these constraints may be expressed explicitly (e.g. the track circuit length has a real positive value greater than the minimum track circuit length defined from operational requirements); others can be expressed implicitly by specifying a restriction on some design or performance characteristic which is itself a function of the TC design parameters (e.g. the maximum length of the 'dead' zone at the boundary of two jointless track circuits).

The region of existence of a track circuit **D** is defined as a subset of $\mathbf{D_D}$ within which the track circuit will perform its specified function (i.e. the operation of the track circuit according to the functional requirements is guaranteed).

The region of the specified design parameters $\mathbf{D_o}$ is a subset of $\mathbf{D}$ and is defined as:

$$\mathbf{D_o} = \left\{ d_{o_i} : d_{o_i} \in \bar{d}_{o_i} + \Delta d_{o_i},\ i = 1 \ldots l \right\} \tag{3.5}$$

where vectors $\bar{\mathbf{d}}_\mathbf{o}$ and $\Delta\bar{\mathbf{d}}_\mathbf{o}$ are correspondingly the vector of the specified design parameters and the vector of the specified design tolerances as defined as result of track circuit design and set in the specification. These values are defined on the basis of some optimisation criteria and have to be maintained during the whole lifecycle to ensure a proper and optimum track circuit performance. The design tolerances provide the necessary margins for operation and adjustment as well as margins for safety.

The region of definition of TC input operating conditions $\mathbf{R}$ is defined by the set of constraints on the components of the vector $\mathbf{r}$, i.e.

$$\mathbf{R} = \left\{ r_j :\ r_j \in \Delta r_j,\ j = 1 \cdots m \right\} \tag{3.6}$$

The boundaries of $\mathbf{R}$ are defined by good engineering judgement in the context of the requirements for the overall signalling or control system in which the track circuits are used. Physically, the region covers the complete set of possible operating conditions.

The region of safety critical input operating effects $\mathbf{R_o}$ is defined as a subset of $\mathbf{R}$ including the safe, non-occupied track circuit operating conditions.

The region of definition of the TC environmental conditions $\mathbf{S}$ is defined by the set of constraints on the components of the vector $\mathbf{s}$, i.e.

$$\mathbf{S} = \left\{ s_k :\ s_k \in \Delta s_k,\ k = 1 \cdots n \right\} \tag{3.7}$$

The definition intervals Δs_k are defined for each particular problem on the basis of reasonable assumptions and statistical data. This definition region specifies the boundaries of the environmental conditions within which correct track circuit operation is provided.

The region of definition of TC status $\mathbf{X}$ is defined as a combination of the $\mathbf{D}$, $\mathbf{R}$ and $\mathbf{S}$ definition regions. The $\mathbf{X}$ region is bounded and contains the infinite set of vectors $\mathbf{x}$ which the track circuit may assume.

The region of the TC safety critical status $\mathbf{X_o}$ is defined as

$$\mathbf{X_o} = \{ \mathbf{x_o} : (\mathbf{d} \in \mathbf{D_o}) \cap (\mathbf{r} \in \mathbf{R_o}) \cap (\mathbf{s} \in \mathbf{S}) \} \tag{3.8}$$

The TC output can be described by the track circuit output $\mathbf{y}$ with its definition area $\mathbf{Y}$. The definition area is a set of two elements, one corresponding to the TC safety critical output, and the other corresponding to the TC non-safety critical output. These elements are usually denoted by 1 and 0 respectively.

3.1.4 Track circuit function

The track circuit algorithm defined in Section 3.1.1 can be formally expressed by the following system of equations:

$$\begin{aligned} \mathbf{F}(\mathbf{x} \in \mathbf{X}_0) &= 1 \\ \mathbf{F}(\mathbf{x} \notin \mathbf{X}_0) &= 0 \end{aligned} \tag{3.9}$$

The TC function **F** defines a relation of surjection which maps each element of **U** into one of the two elements of **Y** i.e. $\mathbf{F}: \mathbf{X} \rightarrow \mathbf{Y}$. For the purposes of TC analysis, design and optimisation, it is necessary to translate the above relations into a lower level of formalisation, based on TC physical principles of operation.

Physically, the TC function **F** is performed by transformation of the characteristic(s) of track circuit operating signal which is/are chosen to be sensitive to the track circuit input effects. The function **F** is performed in two stages as shown in Fig.3-3.

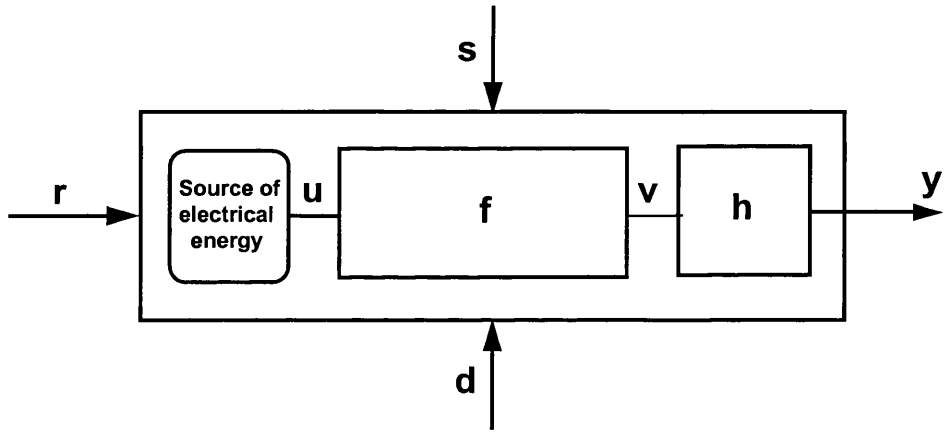

Fig.3-3 Two stage performance of TC function

On the first stage, the input operating signal described with the input vector **u** is transformed according to the TC status to the TC output operating signal, or TC response, described with vector **v**.

$$\mathbf{v} = \mathbf{f}(\mathbf{u}) \tag{3.10}$$

The vectors **u** and **v** are defined with the set of physical parameters, i.e. amplitudes, phases, carrier and modulation frequencies, phase relationships, etc., describing track circuit electric operating signal (or signals) in TC transmitter and at the input of TC receiver. Their definition areas are correspondingly **U** and **V**. The function of track circuit response **f** is defined in a complex way by track circuit input status **x**.

At the second stage the TC response is assessed by an output decision element which is, in general, designed as a voltage or current driven amplitude selector, and an output is given according to the following algorithm:

$$\mathbf{y} = \mathbf{h}(\mathbf{v} \in \mathbf{V}_o) = 1 \tag{3.11.1}$$

$$\mathbf{y} = \mathbf{h}(\mathbf{v} \notin \mathbf{V}_o) = 0 \tag{3.11.2}$$

where

$\mathbf{h}$ is the function of the decision element and

$\mathbf{V}_o$ is a subset of $\mathbf{V}$ including those values of $\mathbf{v}$ for which the decision element will set the TC output to 1.

Track circuit design must ensure that the function of the track circuit response $\mathbf{f}$ and the function of the decision element $\mathbf{h}$ are strictly co-ordinated. More specifically, the following two conditions must be met:

$$\mathbf{v} \in \mathbf{V}_o \quad \text{for} \quad \forall \quad \mathbf{x} \in \mathbf{X}_o \tag{3.12.1}$$

$$\mathbf{v} \notin \mathbf{V}_o \quad \text{for} \quad \forall \quad \mathbf{x} \notin \mathbf{X}_o \tag{3.12.2}$$

Relations (3.12.1) and (3.12.2) in conjunction with relations (3.11.1) and (3.11.2) represent a formal expression of track circuit algorithm of operation. Furthermore, relations (3.12.2) and (3.11.2) state the condition for a track circuit to operate in a fail-safe manner, while (3.12.1) in conjunction with (3.11.1) expresses the condition for a track circuit to operate reliably. The non-fulfilment of (3.12.2) and (3.11.2) constitutes a wrong side failure. If either of (3.12.1) or (3.11.1) is not met there is a right side failure.

3.1.5 'Worst case' TC status

It is of particular interest that relation (3.12.1) should be achieved for every value of $\mathbf{x}$ belonging to region $\mathbf{X}_o$, and correspondingly, relation (3.12.2) should be met for every value of $\mathbf{x}$ belonging to region $\mathbf{X} \setminus \mathbf{X}_o$. This is important in order to estimate how (and whether) the set of vectors $\mathbf{v}$ corresponding to all possible values of $\mathbf{x} \in \mathbf{X}_o$ map into region $\mathbf{V}_o$ and even more importantly, how (and whether) the set of vectors $\mathbf{v}$ corresponding to all possible values of $\mathbf{x} \notin \mathbf{X}_o$ fall outside region $\mathbf{V}_o$. From point of view of providing reliable and stable track circuit operation it is desirable that in neither case do the actual vectors $\mathbf{v}$ come closer to the boundaries of $\mathbf{V}_o$ (on the relevant side) than a pre-defined safety margin. For track circuit design it is essential to identify that track circuit status (vector $\mathbf{x}$) the corresponding vector $\mathbf{v}$ of which falls the closest to the boundary of $\mathbf{V}_o$. It is appropriate to identify this vector as 'worst case' TC status vector ($\mathbf{x}_w$). Using this definition track circuit function can be re-written as follows:

$$\left(\mathbf{f}(\mathbf{x}_w \in \mathbf{X}_o)\right) \in \mathbf{V}_o \tag{3.13.1}$$

$$\left(\mathbf{f}(\mathbf{x}_w \notin \mathbf{X}_o)\right) \notin \mathbf{V}_o \tag{3.13.2}$$

Naturally, $\mathbf{x}_w \in \mathbf{X}_o$ would be different from $\mathbf{x}_w \notin \mathbf{X}_o$. Furthermore, considering that $\mathbf{x} = (\mathbf{d},\mathbf{r},\mathbf{s})$ it is clear that in general $\mathbf{x}_w$ is a set of 'worst case' vectors **d**, **r** and **s**.

The practical application of the above described functional model for track circuit design, analysis or optimisation requires this model to be analytically expressed at a lower level of formalisation. This can only be done in the context of a particular problem where all vector quantities and their regions of definition have to be identified in detail in physical terms. Analysis of the design and the particular track circuit application will enable the decomposition of the general functional algorithm into a set of operating conditions and deduce a set of analytical expressions, written in terms of physical variables which implement relations (3.11.1), (3.11.2), (3.12.1) and (3.12.2). The number of operating conditions (operating modes) which in conjunction describe fully TC algorithm depends on the complexity of TC design and layout as well as on the number of parameters determining TC operating signal. An example of an analytical definition of the functional model of a simple track circuit is presented in the following section.

3.1.6 Track circuit modes of operation and performance criteria

For the simplest case of a DC track circuit with insulated block joints and an electromechanical relay for receiver, the functional algorithm defined with relations (3.11.1), (3.11.2), (3.12.1) and (3.12.2) can be expressed with a system of three inequalities. These inequalities are written in terms of one single physical variable describing track circuit operating signal - in this case the amplitude of the current in TC relay.

- TC operating mode (1) - TC unoccupied, no broken rail or equipment failure

$$I_{Rx}^{w} = \underline{I_{Rx}} + \sum_i (-\Delta I_{Rx})_{max_i} \geq \underline{I^{\uparrow}} + \Delta I^{\uparrow} = I^{\uparrow} \qquad (3.14.1)$$

- TC operating mode (2) -TC occupied

$$I_{Rx}^{sh.w} = \underline{I_{Rx}^{sh.w}} + \sum_i (+\Delta I_{Rx})_{max_i} \leq \underline{I_{\downarrow}} - \Delta I_{\downarrow} = I_{\downarrow} \qquad (3.14.2)$$

- TC operating mode (3)- broken rail or equipment failure

$$I_{Rx}^{br.w} = \underline{I_{Rx}^{br.w}} + \sum_i (+\Delta I_{Rx})_{max_i} \leq \underline{I_{\downarrow}} - \Delta I_{\downarrow} = I_{\downarrow} \qquad (3.14.3)$$

In Eqns.(3.14.1) to (3.14.3)

I_{Rx} is the current in TC receiver (relay) and is specifically defined with the associated symbols as follows:

No first superscript refers to TC operating mode (1),

First superscript 'sh' (train shunt) refers to TC operating mode (2),

First superscript 'br' (broken rail) refers to TC operating mode (3),

Second superscript 'w' refers to worst conditions,

ΔI_{Rx} is the summary destabilising effect (+or -) of all input effects

$I^{\uparrow}$ and $I_{\downarrow}$ denote the levels of energisation and de-energisation of TC relay

$+\Delta I^{\uparrow}$ and $-\Delta I_{\downarrow}$ define the safety margins necessary to account for the instability of TC receiver levels of energisation and de-energisation.

Underscored symbols refer to actual values, and non-underscored symbols refer to values specified in the design.

In this simple example the functional algorithm has been decomposed into three operating modes which are the main operating modes of every track circuit. Taking into account that the actual value of TC operating parameter (I_{Rx} in this case) is a function of TC design parameters it is clear that the system of inequalities (3.14.1) - (3.14.3) defines in a concise and symbolic form the particular relations between track circuit design parameters which ensure that the TC operates according to the specified algorithm. The exact relationships can be exposed by substituting the TC output response symbolic notations ($I_{Rx}, I_{Rx}^{sh.w}, I_{Rx}^{br.w}$) with their exact expressions as functions of the specific TC input effects. A detailed analytical formulation of the functional algorithm can be used both for TC analysis and for synthesis.

TABLE 3.1 Criteria of track circuit performance

Oper. mode	State value method	State change method	Absolute value method
(1)	Coefficient of energisation $K = \frac{I_{Rx}^{w}}{I^{\uparrow}} \geq 1$		
(2)	Train shunt sensitivity $K_{sh} = \frac{I_{\downarrow}}{\underline{I_{Rx}^{sh.w}}} \geq 1$	Reaction to train shunt $F_{sh}(R_{sh}, x_{sh}) = \frac{I_{Rx}^{b}}{\underline{I_{Rx}^{sh.w}}}$	Absolute shunt $R_{sh} \geq \underline{R_{sh.min}}$
(3)	Broken rail sensitivity $K_{br} = \frac{I_{\downarrow}}{\underline{I_{Rx}^{br.w}}} \geq 1$	Reaction to broken rail $F_{br}(x_{br}) = \frac{I_{Rx}^{b}}{\underline{I_{Rx}^{br.w}}}$	

Note: The notation used in the table is explained with reference to Eqns.(14.1)-(14.3). In addition second superscript 'b' stands for 'best case conditions'.

The above example is useful to illustrate the idea of performance criteria. Since the functional algorithm has been decomposed into a system of operating modes it is sensible

to describe TC performance with a system of performance criteria, each relating to a particular operating mode. The performance criteria give a quantitative indication of 'how well' a particular operating mode is performed, or, in other words, what is the safety margin of performance for a given set of operational and environmental input effects. They may be used for an alternative analytical formulation of track circuit algorithm and form the basis of track circuit optimisation when different operating modes impose contradictory requirements on some design parameters.

3.2 FUNCTIONAL MODEL OF JOINTLESS AF TRACK CIRCUITS

When considering the functional model of jointless track circuits (JTC) with electrical separating joints, it is essential to examine how the lack of perfect insulation between adjacent track circuits affects their operation. An immediate observation is that JTCs cannot, unlike bounded TCs, be regarded as independent circuits as they are galvanically and functionally interconnected through the electrical separating joints. Therefore, it is more appropriate to consider the functional model of a system of JTCs, rather than that of a single JTC. Without loss of generality the simplest system of two adjacent jointless track circuits is sufficient to derive the typical characteristics of the model.

The functional model of a system of two adjacent JTCs can be thought of as incorporating the functional algorithms of each of the two TCs (as described earlier) and, in addition, some other functions which can be called 'functions of separation'. These functions provide that the functional algorithms of the two adjacent track circuits are independent, or, in other words, the operational state or the change of operational state of one, cannot in any way affect the operational state of the other. In the case of bounded track circuits these functions are provided by the insulated block joints (IBJs). This observation suggests the following procedure of defining the additional functionality of a system of two adjacent JTCs which specifically refers to their interface area:

- Determination of the functions of IBJs in bounded track circuits
- Analysis of IBJ's functions to establish:

(a) Which IBJ functions are absolutely essential for correct track circuit operation and, therefore, should be performed in JTCs in alternative ways, but with the same level of performance as provided by IBJs, and

(b) Which IBJ functions are essential, but can be performed with some tolerance; how the magnitude of the tolerance affects the track circuit operation, and what is the maximum tolerance for any particular function.

- Determination of any 'new' functions which do not have an IBJs' equivalent but are required to ensure a complete functional algorithm of the system of two JTCs.

3.2.1 Function of the physical insulating joints

IBJs provide perfect galvanic insulation between adjacent track circuits. More specifically, the effect of this insulation consists in the following:

- The track circuit operating signal of each track circuit is strictly confined within the boundaries of its own track circuit
- Any changes in the topology or parameters of a track circuit electric network occurring as result of different operating or environmental conditions do not have any effect on the electric network of the adjacent TC.

Formally, IBJ function can be defined as 'inhibiting the set of logical transitions given in Table 3.2'.

Table 3.2 Definition of IBJ's 'functions

Operational state of TC1	Effect of TC1 on TC2	Operational state of TC2		Safety aspect	Ref.
		Initial	Resultant		
1	→1	1	1	Not important	
1	→0	1	0	Right side failure	(a)
1	→1	0	1	Wrong side failure	(b)
1	→0	0	0	Not important	
0	→1	1	1	Not important	
0	→0	1	0	Right side failure	(c)
0	→1	0	1	Wrong side failure	(d)
0	→0	0	0	Not important	

Note: The symbols → 1 and → 0 denote transition into the indicated operational state.

Inspection of Table 3.2 shows that the IBJ function consists in preventing the four transitions which cause a change in the operational state of TC2 and represent either right or wrong side failures (the highlighted transitions).

The next step is to consider each of the transitions (a) to (d) with respect to a system of adjoining JTCs and decide on whether they can be performed adequately by ESJs or alternative solutions should be applied.

3.2.2 Separation of jointless track circuits

Transitions (a) and (b) in Table 3.2 consist essentially in de-energising and energising the receiver of track circuit TC_1 by the operating signal of the adjacent track circuit TC_2. Such a connection between the transmitter of one track circuit and the receiver of another one is not permitted. Hence, both logical transitions should be excluded without any

degree of tolerance. This is particularly true of the second transition which results in a wrong side failure. Since absolute prevention of these two transitions cannot be guaranteed by an ESJ the solution of the problem lies in using alternative methods. Despite the variety of practical applications they all use essentially the same method. It consists in assigning to each track circuit operating signal some specific, individual features and making the corresponding track circuit receiver responsive only to those particular characteristics. These features can be carrier or modulation frequency, code pattern or specific timing relationship. These special features can be made unique for every track circuit, but in practice a limited number of them is used, being assigned in a particular order to the successive track circuits.

Transitions (a) and (b) can, in principle, occur between track circuits which are not immediately adjacent e.g. between two successive track circuits on the same track which have identical operating features. To prevent such transitions the TCs with identical specific characteristics should be sufficiently spaced to ensure that the signal from one TC practically does not reach the receiver of the other. This is mainly achieved by the attenuation provided by the rail sections of the intermediate track circuits but sometimes, the attenuation is implemented by the ESJs. This helps as well to prevent dissipation of energy in the unwanted direction and create a more economic design.

Analytically, the longitudinal leakage (feedthrough) can be generally characterised as

$$K_{ft} = \frac{\left|\mathbf{V}_{Rx_{i(i\pm n)}}\right|}{\left|\mathbf{V}_{Tx_{(i\pm n)}}\right|} \tag{3.15}$$

where

n is the number of TC distinctive operating characteristics (i.e. frequencies) used in the same rail track,

$\mathbf{V}_{Tx_{(i\pm n)}}$ is the voltage of the transmitter of track circuit (i±n), and

$\mathbf{V}_{Rx_{i(i\pm n)}}$ is the voltage in the receiver of track circuit i originating from the transmitter of track circuit (i±n).

Transitions (c) and (d) in Table 3.2 consist in one track circuit reacting to a train shunt on the adjacent track circuit. Strictly speaking, transition (c) leads to a right side failure. However, because it only occurs when the train shunt is just outside the track circuit, it can be regarded as an imperfection of TC shunt sensitivity rather than a failure. The extended zones of train detection of the two adjacent track circuits overlap, yielding a zone of ambiguity, where a train is detected by both track circuits. Such zones are acceptable but their length should be minimised so that they do not affect the headway between trains.

Transition (d) constitutes a wrong side failure and should be excluded without any tolerance. In track circuits with ESJs this is achievable by appropriate design of TC terminations. Such transition could only occur in unbounded track circuits (without any form of separation between the adjacent track circuits), in rare operational situations. In such cases the dangerous situation has to be prevented by alternative measures on a system level. The requirements as to whether and how strictly should transition (d) be prevented should be established in the context of the particular track circuit application with reference to the overall signalling system design.

3.2.3 Additional functions

An important difference between an IBJ and an ESJ is their longitudinal dimension. Unlike IBJs which practically have no physical length, ESJs could extend up to a considerable length (e.g. 30m). ESJ design should therefore be responsible for ensuring adequate train shunt sensitivity within the section of track occupied by its physical length. Absolute train detection in any point of ESJ's length is not always achievable. Depending on the design there could be a smaller or larger zone where a vehicle remains undetected. Such discontinuities are in principle acceptable, as long as it is ensured that the shortest vehicle operating on the line is not lost while passing over a 'dead' zone.

Another 'new' function of the ESJ, which has no equivalent with regard to an IBJ is the function of coupling the TC transmitter and receiver equipment to the rail track. This function is incorporated in the ESJ design itself in such a way as to ensure adequate performance of its vital functions, but is subject to optimisation within the restrictions imposed by ESJ design. The aim of the optimisation is to minimise the power consumed by the track circuit.

3.2.4 ESJ model and track circuit separation criterion

An ESJ can be conveniently represented as a four-port network (Fig.3.4). For some types of ESJ, some of the ports may coincide. The model can be defined by the open-circuit impedance matrix or short-circuit admittance matrix given in Appendix B. Alternatively, the four-port network may be described by a set of port-to-port transfer functions:

$$K_{ij} = \frac{|\mathbf{V}_j|}{|\mathbf{V}_i|}; \qquad \text{for i, j = 1, 2, 3, 4} \tag{3.16}$$

where

K_{ij} is the transfer function from port i to port j and

$\mathbf{V}_i$, and $\mathbf{V}_j$ are the voltages at ports i and j respectively.

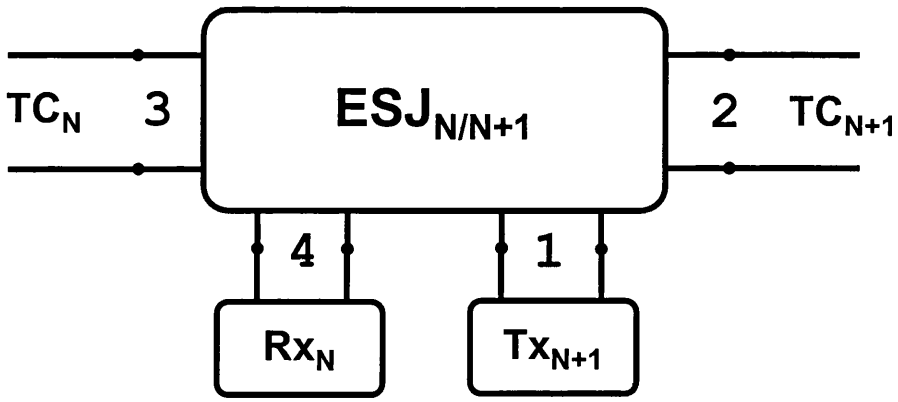

Fig. 3.4 ESJ transfer functions

With reference to this model, to achieve the functional requirements stated in the previous sections transfer coefficients K_{13}, K_{14} and K_{32} should be minimised and transfer coefficient K_{12} should be maximised. It is a matter of the detailed application specific design to define to what extent these requirements are vital for the proper track circuit performance and to what extent they are optimisation requirements.

To summarise the considerations regarding the functional model of JTCs the following conclusions can be made:

- Jointless track circuits should be modelled as a system of several successive track circuits, rather than in isolation. This system may include as many track circuits as necessary to analyse and achieve the required space separation between track circuits with identical operating parameters.
- The functional algorithm of a system of JTCs incorporates the functional algorithms of each individual track circuit as well as the functions of the ESJs.
- The performance criteria of each ESJ function depends strictly on the particular application and is decided with reference to the design of the overall signalling system.

Chapter 4

PHYSICAL MODEL OF TRACK CIRCUITS

The objective of this chapter is to describe the track circuit as a physical system in the form of an electric network. This involves choosing circuit models for the various components which accurately describe the physical phenomena occuring during track circuit operation. The criteria for choice of model are applicability, conveniance of use and acceptable approximations.

4.1 TRACK CIRCUIT PHYSICAL STRUCTURE

From the point of view of electric network theory, track circuits can be treated as an electrical network built of both distributed and lumped parameters components (Fig.4.1). The components with distributed parameters are in the form of a transmission line representing the rail track. The lumped parameters components represent the equipment of track circuit terminations. In some applications, an additional distributed parameter network must be considered in the form of a cable transmission line connecting the centrally located track circuit equipment to the rail track.

In most track circuits the track circuit transmitter is connected to the rail track by a potential (galvanic) connection, although a few types of track circuit do use inductive coupling. The track circuit receiving equipment can also be connected to the rail track either potentially or inductively.

4.2 LUMPED PARAMETER NETWORK MODELLING

Modelling the lumped parameter networks (transmitter, receiver, interface networks, such as impedance bonds, track capacitors and transformers, ESJ, etc.) on the basis of component-by-component substitution with appropriate electric circuit analogs may not always result in an efficient model. To create a concise and convenient track circuit model, it is desirable to abandon features of the network internal structure which are not directly relevant to the tasks of track circuit analysis and synthesis. On the other hand, it is necessary to retain access to parameters which do have a direct impact on track circuit performance. The above requirements can be achieved by using equivalent circuits for the lumped parameter networks, selected on the basis of either:

- Identical input-output transfer functions (e.g. track), or
- Functional equivalence (e.g. receiver)

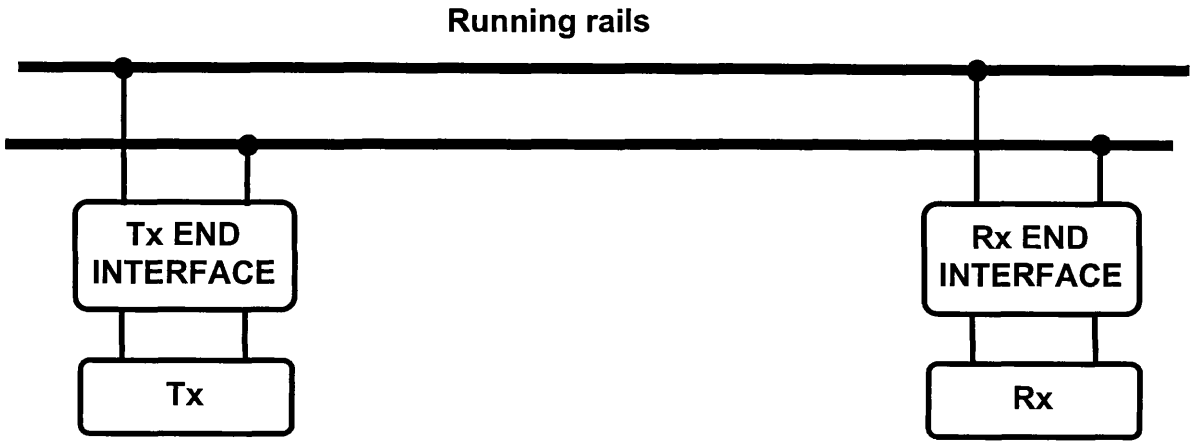

(a) Track circuit with insulated block joints

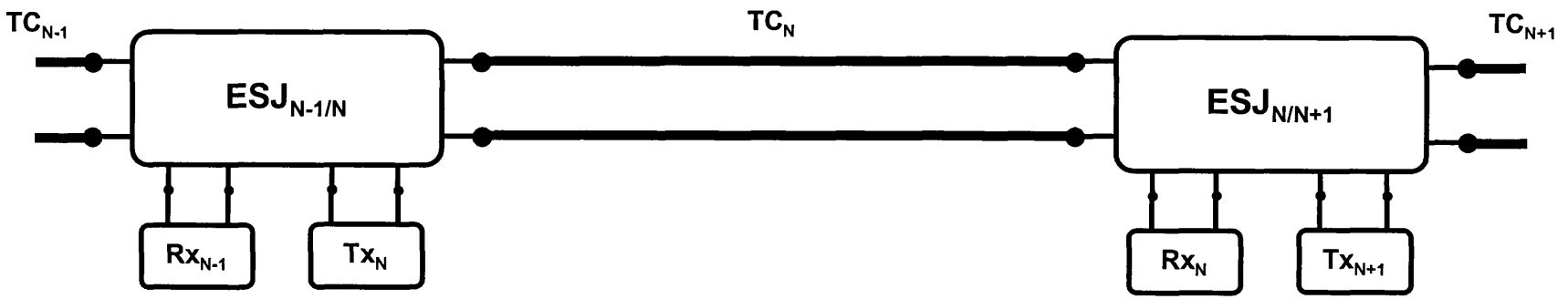

(b) Track circuit with electrical separating joints (ESJ)

Fig. 4.1 Track circuit block diagram

The latter implies not only equivalent electric circuit representation but as well specification of appropriate parameters to account for receiver energisation and de-energisation.

Such an approach has been applied in [G-8] for the modelling of bounded DC and power frequency AC track circuits. In these types of track circuits, the effect of the interface networks on the track circuit operating signal is amplitude and phase change. These networks can be modelled by linear electric networks. Furthermore, as they are independent of the exact track circuit mode of operation, the internal structure of the interface networks is not important in the track circuit analysis. They may then be described with equivalent passive linear two-port networks, as shown in Fig.4.2-a. Their transfer coefficients, calculated by the conventional methods of electric circuit theory should be identical to those of the actual equipment.

The transmitter and receiver can be represented as equivalent two-pole Thevenin or Norton networks. A further simplification, resulting in a more concise equivalent circuit, may be made by applying Thevenin's theorem looking from the rail track section into the track circuit equipment (Fig.4.2-b). The benefit of this model is that after substitution of the rail track section by an equivalent two-port representation, it will be straightforward to define an overall track circuit transfer function.

The above considerations have been applied to the modelling of jointed track circuits [G-8] but in principle, with appropriate adjustments this method is applicable to jointless track circuits as well. Due to the variety of JTCs available, setting up the equivalent circuits for the termination areas requires an individual approach for each case. However, some general points apply.

4.2.1 Electrical Separating Joint Modelling

In general, ESJs have a mixed structure in that they comprise lumped parameter components with sections of cables and rail track. However, it is usually appropriate to model ESJs as lumped component networks because:

- The cable and rail track sections are too short with respect to the transmission wavelength, to show significant transmission line effects, and
- When simulating a train shunt moving along the ESJ area, the cable and rail track sections must be divided into very short sections to provide for the insertion of the train shunt model in the equivalent circuit.

ESJs can be represented as equivalent four-port networks described with a set of transfer coefficients between any pair of poles (Section 3.2.4). Different sets of transfer

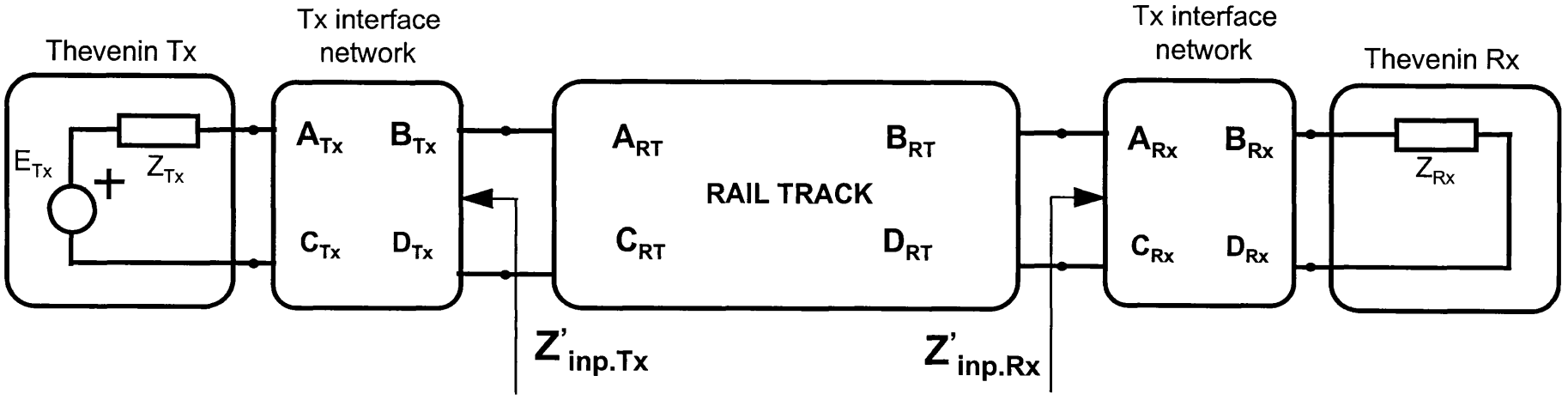

(a) Track circuit equivalent network

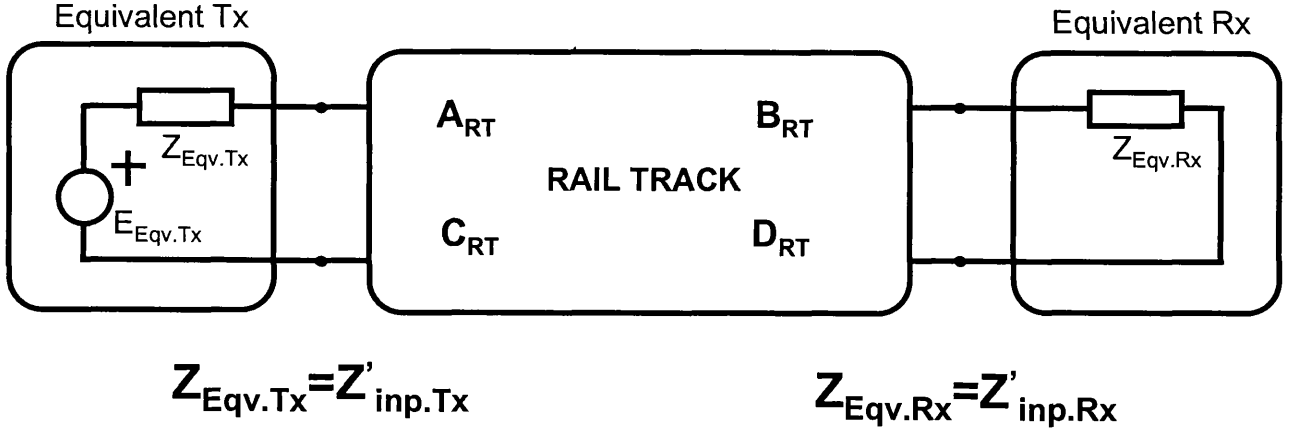

(b) Concise track circuit equivalent network

Fig.4.2 Track circuit equivalent networks

coefficients will apply for the different ESJ operating modes - unoccupied, occupied, etc.

4.2.2 Modelling AF JTC receiver

In audio-frequency track circuits, the receiver is a multistage electronic circuit, often incorporating microcomputer control. The main function of the receiver is to assess the signal incoming from the rails and make a decision about the condition of the track circuit. An additional requirement is to protect the system from malfunctions due to electrical interference. As far as a particular group of problems are concerned not all stages of signal transformation (filtering, demodulation, decoding, etc.) are of interest and need to be included in the model. The aim is to keep the model simple but still incorporating all important features. This can be achieved by using the concept of an equivalent receiver, the equivalence being based on the parameters used in the decision making stage.

An illustration of the above technique of equivalent circuit modelling is given in Chapter 6 using as an example the FS 2000 audio frequency jointless track circuit.

4.3 DISTRIBUTED PARAMETER NETWORK MODELLING

4.3.1 Rail track as a transmission line

A single rail track with no electrification or parallel cables of other systems may be regarded as a two-conductor transmission line presenting a number of particular properties. The conductors are made of ferromagnetic material and their cross section has a very irregular shape. They are laid at the interface of two half-space regions, the upper (air) being a perfect homogeneous dielectric, and the lower (ground), being a complex, non-homogeneous medium with poor conductance but having good electrical contact with the conductors (Fig.4.3).

The properties of a transmission line are characterized by its primary and secondary parameters. Fig.4.4,a-d gives typical rail track primary parameter data compiled from various sources. The values quoted correspond to differential mode (rail to rail) excitation, i.e. they are the loop parameters of the line. This is the normal case for track circuit applications. The spread in values on the graphs is due to the wide variety of rail types in use worldwide, the environmental conditions in which the data were measured, and local track substructure conditions. Nevertheless, the curves do show the expected trend with frequency. The graphs in Fig.4.5,a-d represent rail track secondary parameters, including the wavelength and phase velocity as function of frequency.

The graphs of Figs.4.4 and 4.5 show that:

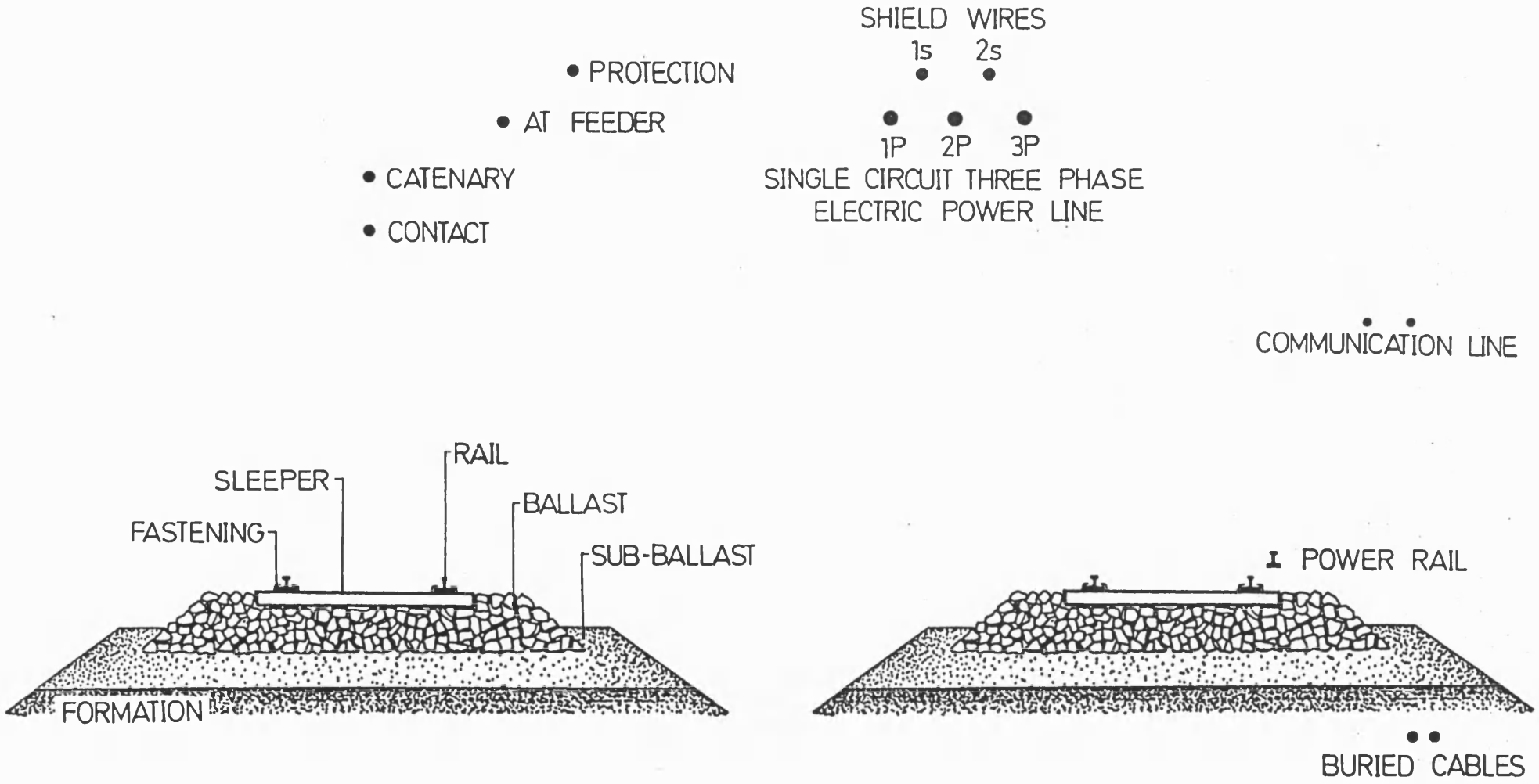

a. AC TRACTION POWER SUPPLY

b. DC TRACTION POWER SUPPLY WITH THIRD RAIL CONFIGURATION

Fig.4.3 RAIL TRACK STRUCTURES & TYPICAL CONFIGURATIONS OF TRANSMISSION LINES

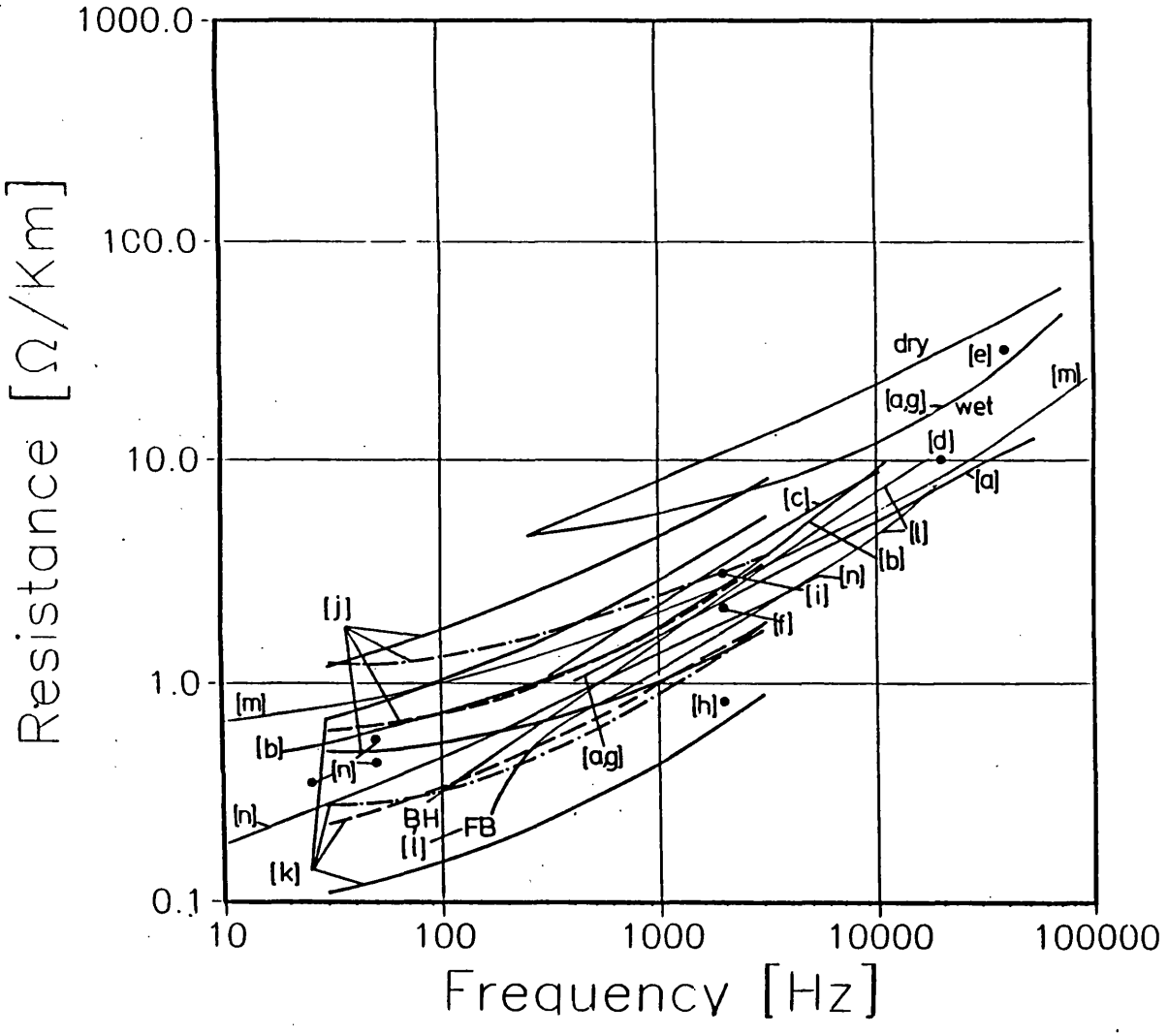

[a]	Experimental curves for dry and wet conditions and theoretical curve for the resistance	[4-1]
[b]	Experimental curves for dry weather but ground dump	[4-2]
[c]	Experimental curves for 90 lb/yard rail	[2-4]
[d]	Measured values	[4-3]
[e]	Measured values	[4-4]
[f]	Experimental curves for dry and wet conditions	[4-5]
[g]	Measured values for BH rail on wooden sleepers	[4-6]
[h]	Measured values for rails S-49	[G-12]
[i]	Measured values for rails S-49	[G-13]
[j] [k]	Theoretical high and low limiting curves (————) Corrected theoretical curves (— — —) Experimental curves (- · - · - ·) for rail types 40 [j] and 60 [k]	[4-7]
[l]	Experimental curves for BH and FB rails for wet and dry weather conditions	[2-5]
[m]	Experimental curves	[4-8]
[n]	Experimental curves for rail types R43 and R65	[G-9]
[o]	Measured values	[2-30]
FB	Flat bottom rail	
BH	Bull head rail	

FIG.4.4 Rail track primary parameters: (a) Rail track resistance as function of frequency

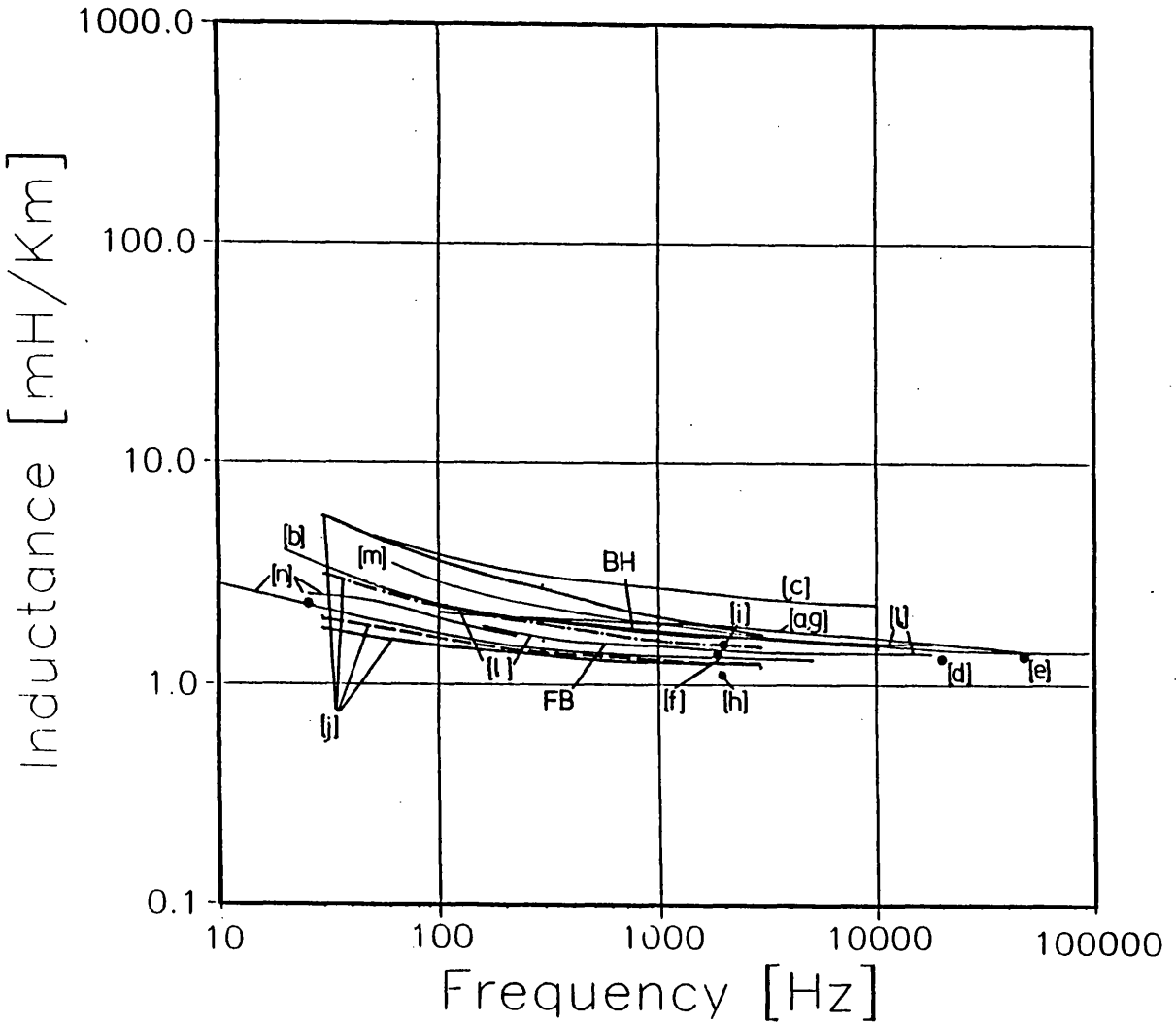

[a]	Experimental curves for dry and wet conditions and theoretical curve for the resistance	[4-1]
[b]	Experimental curves for dry weather but ground dump	[4-2]
[c]	Experimental curves for 90 lb/yard rail	[2-4]
[d]	Measured values	[4-3]
[e]	Measured values	[4-4]
[f]	Experimental curves for dry and wet conditions	[4-5]
[g]	Measured values for BH rail on wooden sleepers	[4-6]
[h]	Measured values for rails S-49	[G-12]
[i]	Measured values for rails S-49	[G-13]
[j] [k]	Theoretical high and low limiting curves (————) Corrected theoretical curves (— — —) Experimental curves (- - - - -) for rail types 40 [j] and 60 [k]	[4-7]
[l]	Experimental curves for BH and FB rails for wet and dry weather conditions	[2-5]
[m]	Experimental curves	[4-8]
[n]	Experimental curves for rail types R43 and R65	[G-9]
[o]	Measured values	[2-30]
FB	Flat bottom rail	
BH	Bull head rail	

FIG.4.4 Rail track primary parameters: (b) Rail track inductance as function of frequency

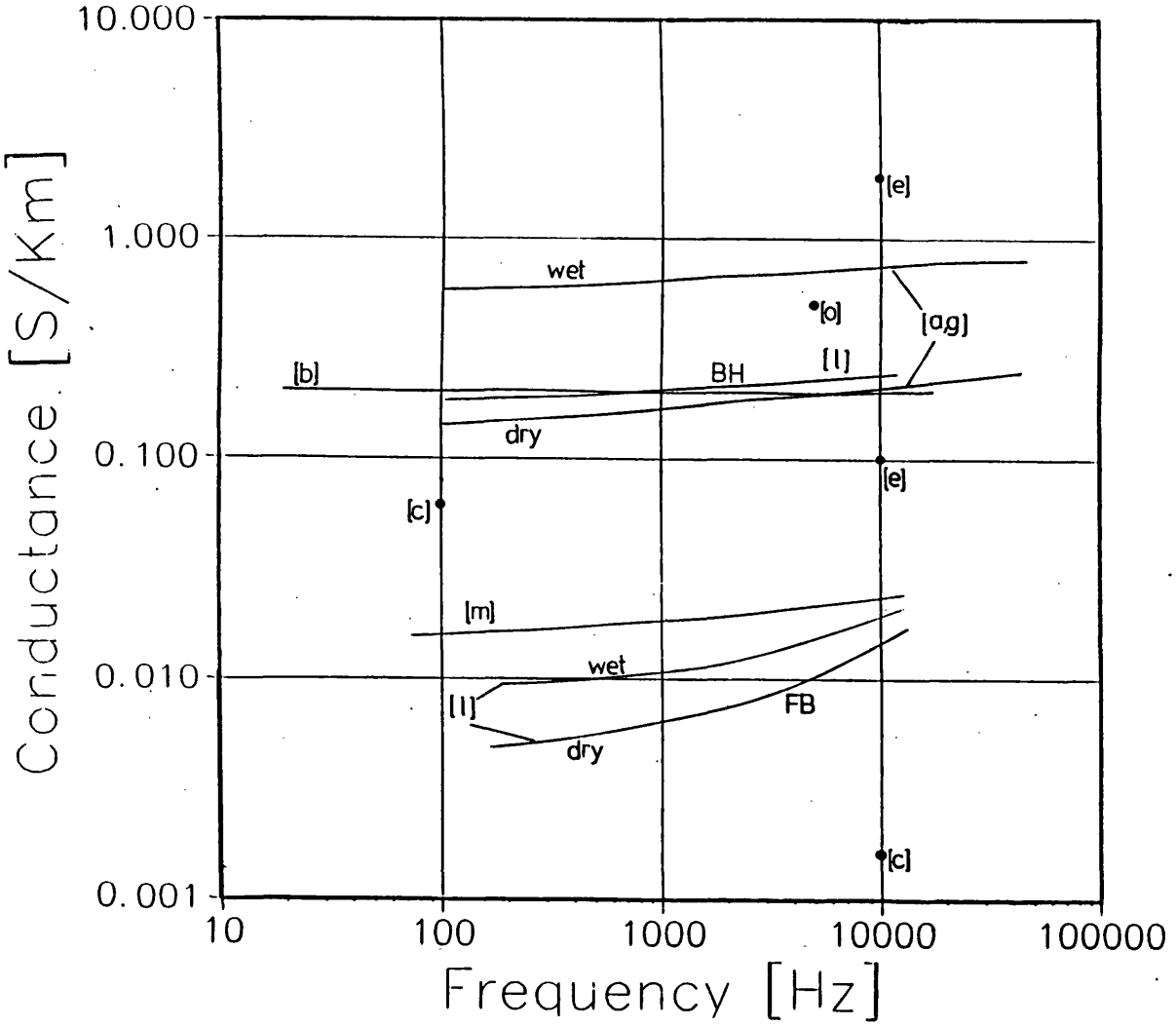

[a]	Experimental curves for dry and wet conditions and theoretical curve for the resistance	[14]
[b]	Experimental curves for dry weather but ground dump	[13]
[c]	Experimental curves for 90 lb/yard rail	[27]
[d]	Measured values	[16]
[e]	Measured values	[17]
[f]	Experimental curves for dry and wet conditions	[18]
[g]	Measured values for BH rail on wooden sleepers	[23]
[h]	Measured values for rails S-49	[24]
[i]	Measured values for rails S-49	[25]
[j] [k]	Theoretical high and low limiting curves (————) Corrected theoretical curves (– – –) Experimental curves (– · – · –) for rail types 40 [j] and 60 [k]	[64]
[l]	Experimental curves for BH and FB rails for wet and dry weather conditions	[33]
[m]	Experimental curves	[75]
[n]	Experimental curves for rail types R43 and R65	[8]
[o]	Measured values	[21]
FB	Flat bottom rail	
BH	Bull head rail	

FIG.4.4 Rail track primary parameters: (c) Rail track conductance as function of frequency

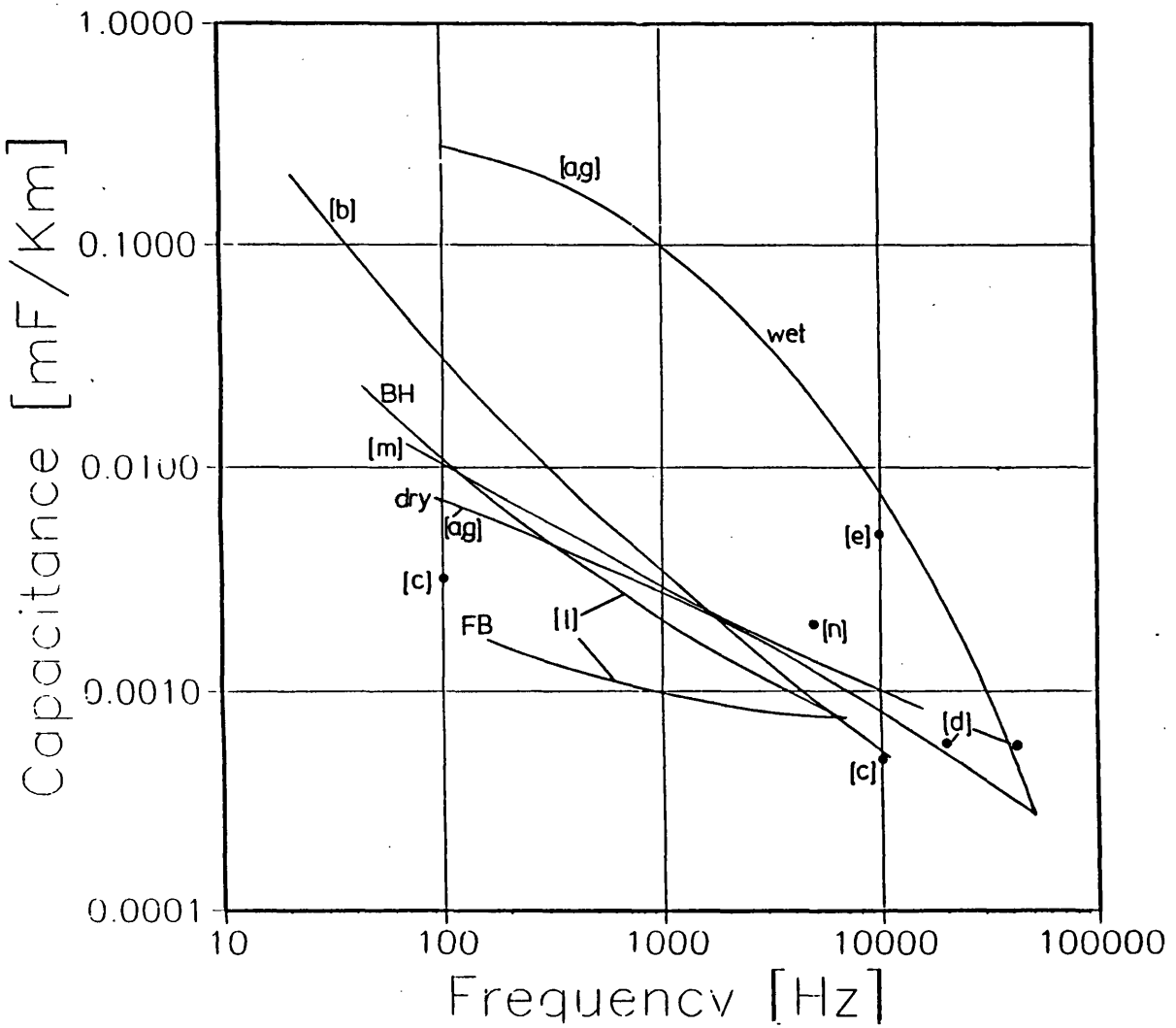

[a]	Experimental curves for dry and wet conditions and theoretical curve for the resistance	[14]
[b]	Experimental curves for dry weather but ground dump	[13]
[c]	Experimental curves for 90 lb/yard rail	[27]
[d]	Measured values	[16]
[e]	Measured values	[17]
[f]	Experimental curves for dry and wet conditions	[18]
[g]	Measured values for BH rail on wooden sleepers	[23]
[h]	Measured values for rails S-49	[24]
[i]	Measured values for rails S-49	[25]
[j] [k]	Theoretical high and low limiting curves (————) Corrected theoretical curves (— — —) Experimental curves (- · - · - · -) for rail types 40 [j] and 60 [k]	[64]
[l]	Experimental curves for BH and FB rails for wet and dry weather conditions	[33]
[m]	Experimental curves	[75]
[n]	Experimental curves for rail types R43 and R65	[8]
[o]	Measured values	[21]
FB	Flat bottom rail	
BH	Bull head rail	

FIG.4.4 Rail track primary parameters: (d) Rail track capacitance as function of frequency

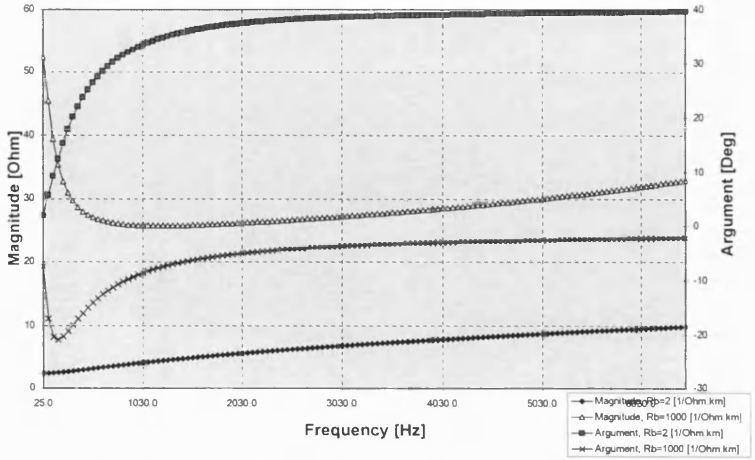

(a) Characteristic impedance $\mathbf{Z}_o$ as function of frequency

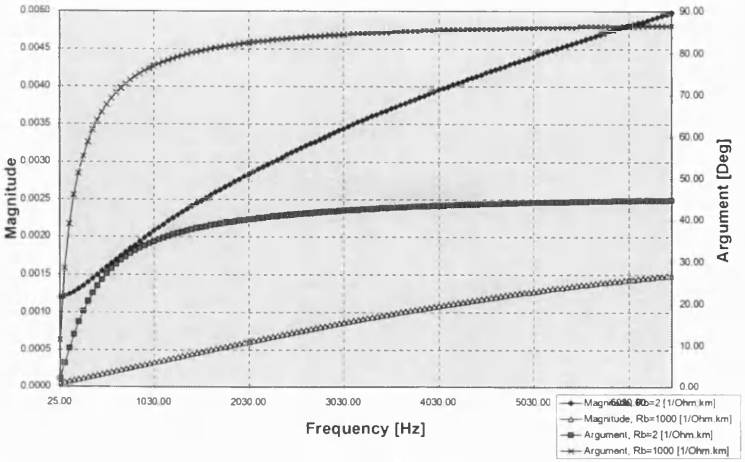

(b) Propagation constant γ as function of frequency

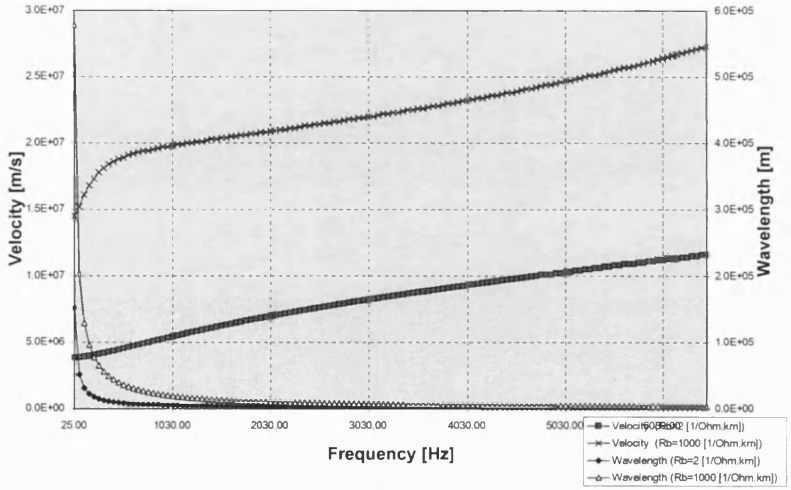

(c) Phase velocity v and wavelength λ as function of frequency

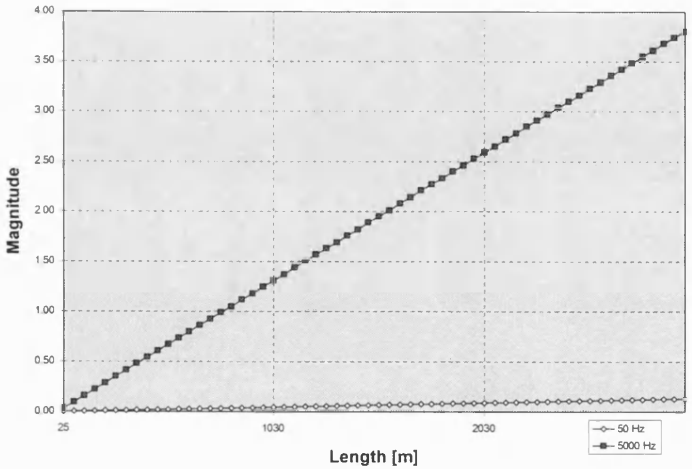

(d) Electric length ($|\gamma l|$) as function of length

FIG. 4.5 Secondary parameters of rail track transmission line

- Rail track is inefficient both for power transmission, because of the large losses, and as a communication line, because the distortionless criterion is not satisfied ($R/L << G/C$).

- The phase electromagnetic wave propagation velocity along the rail track is much smaller than the phase velocity in empty space, and a factor of 10 to 100 times smaller than the phase velocity along cables and overhead transmission lines.

- The phase propagation velocity decreases rapidly with increase of track conductance.

- At power frequencies, the wavelength is several times greater than the maximum track circuit length of about 2.5 km, while at audio frequencies the wavelength approaches the track circuit length. This observation confirms that the rail track must be considered as a distributed parameter network.

- At audio frequencies, the track circuit electrical length $|\gamma l|$ increases. When $|\gamma l| > 2.3$, the amplitude of the reflected voltage wave at the beginning of the line will be 100 times smaller than that of the incident wave. The reflected wave can thus be neglected, and the line can be considered electrically long.

- The wavelength is much larger than the geometrical dimensions of the rail track cross-section.

The last observation is important when considering the mode of propagation for electromagnetic waves along the track. The dominant mode on two-conductor lines is the TEM (Transverse-Electromagnetic Waves) mode, where the electric-field vector **E** and the magnetic-field vector **H** both have only components perpendicular to the direction of propagation along the line (the z axis). Theoretically, this mode can exist only in transmission lines with perfect conductors and a homogeneous dielectric. In the presence of a non-homogeneous dielectric and/or conductors with finite conductivity, z-components of the electric-field and magnetic-field vectors will appear, and the waves will propagate with a combination of the TE (Transverse-Electric) and TM (Transverse-Magnetic) modes. However, where the maximum cross-sectional dimensions of the line are much smaller than the wavelength, the longitudinal field components are much smaller than the transverse components. These hybrid waves can thus be approximated by TEM waves, and are called *essentially* TEM waves. Solution of Maxwell's equations for the TEM propagation mode, based on the assumption of quasi-static fields, is then identical with that describing uniform plane waves propagating in a lossy unbounded medium [G-1].

For a transmission line, it is appropriate to solve Maxwell's equations in terms of voltages and currents. For a two-wire line exited by the TEM mode, this is achieved by deriving a pair of coupled differential equations:

$$\frac{dv(x)}{dx} = -\left(R.i + L.\frac{di(x)}{dt}\right) \tag{4.1.1}$$

$$\frac{di(x)}{dx} = -\left(G.v + C.\frac{dv(x)}{dt}\right) \tag{4.1.2}$$

or in complex time-harmonic form at a specific frequency:

$$\frac{d\mathbf{V}(x)}{dx} = -\mathbf{Z}.\mathbf{I}(x) \tag{4.2.1}$$

$$\frac{d\mathbf{I}(x)}{dx} = -\mathbf{Y}.\mathbf{V}(x) \tag{4.2.2}$$

In the above equations,

$v(x)$ and $\mathbf{V}(x)$ are the momentary value and complex phasor of the voltage between the conductors(or conductor and earth), i.e. the conductor (phase) voltage

$i(x)$ and $\mathbf{I}(x)$ are the momentary value and complex phasor of the current in the conductors

R, L, G and C are the primary (distributed) parameters of the transmission line specified per unit length and

$\mathbf{Z}$ and $\mathbf{Y}$ are the series impedance and the shunt admittance per unit length for a specific frequency i.e.

$$\mathbf{Z} = R + j\omega L \tag{4.3.1}$$

$$\mathbf{Y} = G + j\omega C \tag{4.3.2}$$

Eqns.(4.2.1) and (4.2.2) give the following solutions for the voltage and current:

$$\mathbf{V}(x) = \mathbf{V}_m^+.e^{-\gamma x} + \mathbf{V}_m^-.e^{\gamma x} \tag{4.4.1}$$

$$\mathbf{I}(x) = \mathbf{I}_m^+.e^{-\gamma x} + \mathbf{I}_m^-.e^{\gamma x} = \frac{\mathbf{V}_m^+}{\mathbf{Z}_o}.e^{-\gamma x} + \frac{\mathbf{V}_m^-}{\mathbf{Z}_o}.e^{\gamma x} \tag{4.4.2}$$

where

γ is the propagation constant per unit length and

$\mathbf{Z}_o$ is the characteristic impedance (Ω).

4.3.2 Rail track as a two-phase transmission line over a conductive earth plane

All equations in Section 4.3.1 refer to a single-phase, symmetrical, isolated transmission line. The symmetry is for both electrical and magnetic conditions with respect to the axis

of geometrical symmetry. Such lines can be characterized with a single voltage and a single current at any point along the line.

The presence of other conductors and conductive surfaces in close proximity to the transmission line can cause a redistribution of the electromagnetic fields around the line, disturbing the balance between the two conductors. This is the case for rail track, which is laid on a conductive medium (the ground) and has a good electrical contact with it. In such conditions, any electrical asymmetry between the rails gives rise to longitudinal earth-return currents, even in the absence of any rails-to-ground excitation. To account for the effect of the conductive earth plane on wave propagation, the earth can be included within the transmission line model as a special reference conductor. The assumption that the earth is a perfect conductor simplifies the mathematical formulation of the transmission line model. However, such an assumption is usually unrealistic as the lossy ground is likely to affect the overall transmission line parameters. The effect of a weakly conducting earth is hence taken into account when determining the equivalent parameters of the conductors.

Special techniques are available for the calculation of the rail conductor parameters, accounting for the effect of the lossy ground. These are considered in detail in Appendix A.

4.3.3 Mathematical model of two-conductor transmission line above conductive earth plane

The mathematical formulation of the model of a two-conductor transmission line above a conductive surface can be derived on the basis of the mathematical description of a two-conductor line given in Eqns.4.1.1 to 4.4.2 The total series impedance and shunt admittance of the transmission line per unit length is ascribed to one of the conductors, with the other regarded as a perfect, voltage reference conductor. The equations describe a single-phase line with earth return, where R, L, G and C are the self parameters per unit length. Such a line is illustrated in Fig.4.6.

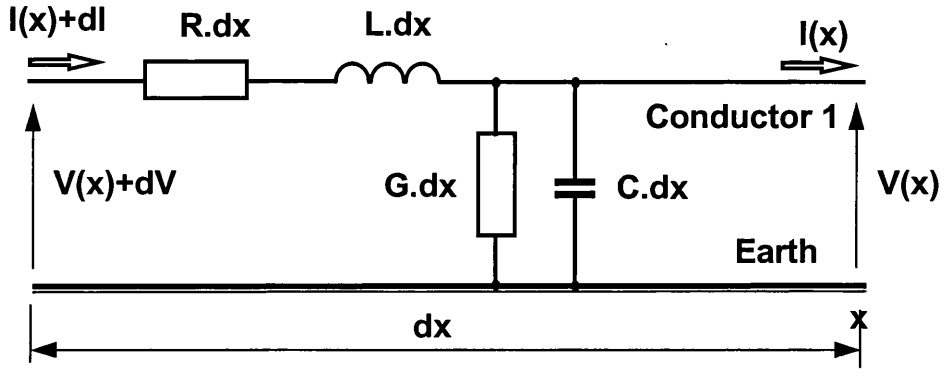

FIG.4.6 Equivalent diagram of an incremental length of a single phase transmission line

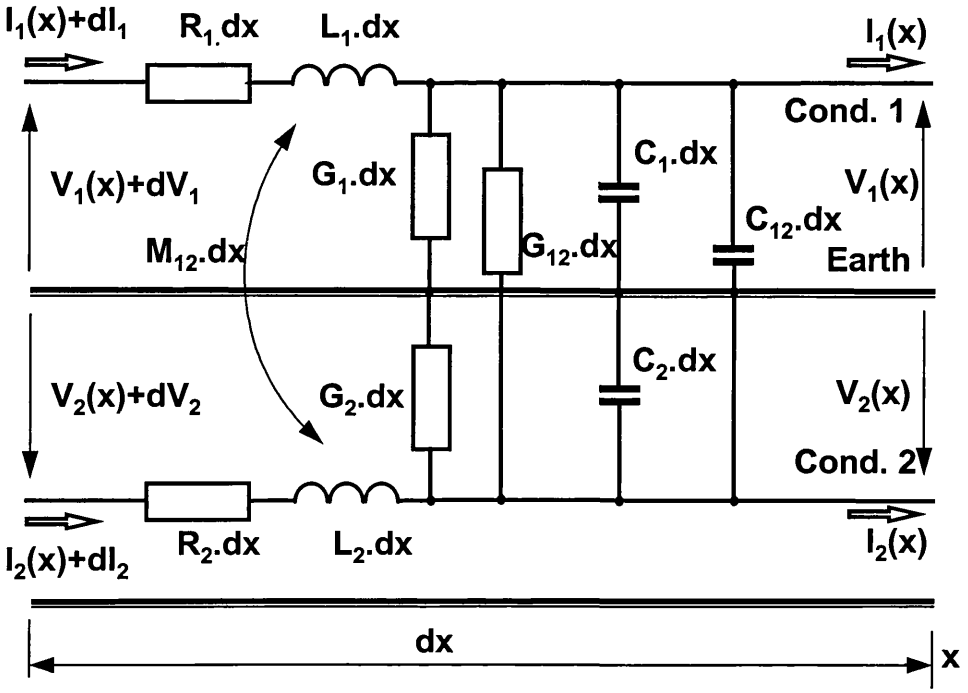

FIG.4.7 Equivalent diagram of an incremental length of a two phase transmission line

A transmission line consisting of two conductors in close proximity to a conductive ground can be regarded as a system of two single-phase transmission lines with a common earth-return (Fig.4.7). These single-phase lines are mutually coupled through inductive and conductive effects which are accounted for in Fig.4.7 by the mutual parameters M , G and C per unit length. These parameters are the mutual parameters between the two single-phase lines, rather than between the two conductors. They are therefore calculated with consideration of the effect of the lossy ground. The self parameters of the equivalent earth conductor and the mutual conductor-earth parameters are also 'hidden' within the self-parameters of the single-phase lines. By applying Kirchoff's laws for the two circuit loops shown in Fig.4.7 and Ohm's law for nodes 1 and 2, the following matrix equations describing the two-conductor transmission line above a conductive earth can be derived:

$$\frac{d[\mathbf{V}]}{dx} = -[\mathbf{Z}].[\mathbf{I}] \tag{4.5.1}$$

$$\frac{d[\mathbf{I}]}{dx} = -[\mathbf{Y}].[\mathbf{V}] \tag{4.5.2}$$

In the above equations, $[\mathbf{V}]$ and $[\mathbf{I}]$ are the column vectors of the phase (conductor-to-ground) voltages and the phase (conductor) currents. $[\mathbf{Z}]$ and $[\mathbf{Y}]$ are the series impedance and the shunt admittance matrices which can be expressed by the matrices of the primary line parameters as:

$$[\mathbf{Z}] = [\mathrm{R}] + j\omega[\mathrm{L}] \tag{4.6.1}$$

$$[\mathbf{Y}] = [\mathrm{R}] + j\omega[\mathrm{L}] \tag{4.6.2}$$

The $[\mathbf{Z}]$ and $[\mathbf{Y}]$ matrices are second-order, square, complex and symmetric. Their elements can be defined as follows:

The diagonal element $\mathbf{Z}_{ii}$ (i=1,2) represents the series self impedance of the line i with earth return, while the off-diagonal element $\mathbf{Z}_{ij}$ (i=1,2; j=1,2) is the series mutual impedance between lines i and j.

The $[\mathbf{Y}]$ matrix is in nodal form. The diagonal element $\mathbf{Y}_{ii}$ (i=1,2) constitutes the nodal admittances of conductor i and is given as the sum of the self and mutual shunt admittances of line i. The off-diagonal element $\mathbf{Y}_{ij}$ (i=1,2, j=1,2) is the negative of the mutual admittance between lines i and j. Hence

$$\mathbf{Y} = \begin{bmatrix} \mathbf{Y}_{11} & \mathbf{Y}_{12} \\ \mathbf{Y}_{21} & \mathbf{Y}_{22} \end{bmatrix} = \begin{bmatrix} \mathbf{Y}_1 + \mathbf{Y}_m & -\mathbf{Y}_m \\ -\mathbf{Y}_m & \mathbf{Y}_2 + \mathbf{Y}_m \end{bmatrix} \tag{4.7}$$

where

$\mathbf{Y}_i$ (i= 1,2) is the the self-admittance of line i with earth return and

$\mathbf{Y}_m$ is the mutual admittance between lines 1 and 2.

To complete the model of rail track as a two-conductor transmission line above a conductive earth plane, it is necessary to determine the components of the $[\mathbf{Z}]$ and $[\mathbf{Y}]$ matrices. This is not straightforward, given that the rail track is a particular type of transmission line. Particular difficulties arise from rails being ferrous conductors with irregular shape, the close proximity of the conductive ground, and the good electrical contact between the conductors and ground.

Generally, there is no rigorous theoretical solution for the series impedance and shunt admittance, which can account for all rail track peculiarities. The most convenient representation relies on the adoption of simplified models. The determination of effective values for the geometrical, electrical and magnetic parameters of the system then allows the simplified model to approach the real system by using a combination of numerical methods and experimental measurements. A review of some existing methods for determination of the rail track parameters in terms of the $[\mathbf{Z}]$ and $[\mathbf{Y}]$ matrices is given in Appendix A.

4.3.4 Multiconductor transmission line modelling of rail track

Generally, the railroad right-of-way can accommodate various parallel electrical networks, such as track circuits on adjacent tracks, traction power supply cables, signalling cables, telephone and other communication cables, power transmission lines

and pipelines (Fig.4.3). Due to the close physical proximity of these parallel conductors above, on and under the ground surface, the corresponding transmission networks are mutually coupled by inductive and conductive and ground effects. These coupling effects produce interfering signals which can penetrate the track circuit and disturb its operation. Hence in track circuit modelling, provision should be made to model the interference effects. A suitable technique to achieve this is to combine the potential interference networks with the rail track as a multiconductor system.

The concept of a multiconductor transmission line above a conductive earth is readily derived from the model of the two-conductor line. An n-conductor transmission line is described by the same matrix equations as the two-conductor line, except that the order of the column matrices $[\mathbf{V}]$ and $[\mathbf{I}]$ will be (n by 1) and the $[\mathbf{Z}]$ and $[\mathbf{Y}]$ matrices will be square (n by n).

In the determination of the $[\mathbf{Z}]$ and $[\mathbf{Y}]$ matrix elements, well established methods used for power systems modelling can be applied [G-15]. A particular case which presents significant difficulties is that of three and four rail configurations, commonly used for urban metro DC electrification. An investigation of the parameters of a typical three rail configuration is given in [A-36, A-37].

Chapter 5

MULTICONDUCTOR TRANSMISSION LINE ANALYSIS WITH SPECIAL REFERENCE TO TRACK CIRCUIT ANALYSIS

The objective of this chapter is to develop the necessary mathematical techniques for the analysis of multiconductor transmission lines (MTL). The rationale is to provide a mathematical solution for the model described in the previous chapter. Starting with single-phase transmission line theory, both phase and modal variables are considered for the description and analysis of a MTL with discontinuities. The applicability and efficiency of phase and modal analyses for this application is considered in detail, and a step-by-step solution procedure developed. Finally, the results obtained are applied to the detailed analysis of a two-conductor transmission line. This provides the appropriate mathematical background for the later modelling and analysis of track circuits along a single non-electrified rail line.

5.1 ANALYSIS OF MULTICONDUCTOR TRANSMISSION LINE IN PHASE QUANTITIES

5.1.1 Solution of the wave equations for a multiconductor transmission line. Phase characteristic impedance matrix and phase propagation matrix

The propagation of electromagnetic waves arising from harmonic excitation of a multiconductor line above a conductive earth plane is described with a pair of differential equations (Eqns.4.5) as follows

$$\frac{d\left[\mathbf{V}^{(p)}(x)\right]}{dx} = -\left[\mathbf{Z}^{(p)}\right].\left[\mathbf{I}^{(p)}(x)\right] \tag{5.1.1}$$

$$\frac{d\left[\mathbf{I}^{(p)}(x)\right]}{dx} = -\left[\mathbf{Y}^{(p)}\right].\left[\mathbf{V}^{(p)}(x)\right] \tag{5.1.2}$$

This system of matrix differential equations can be solved by separating the variables to yield

$$\frac{d^2\left[\mathbf{V}^{(p)}(x)\right]}{dx^2} = \left[\mathbf{Z}^{(p)}\right].\left[\mathbf{Y}^{(p)}\right].\left[\mathbf{V}^{(p)}(x)\right] \tag{5.2.1}$$

$$\frac{d^2\left[\mathbf{I}^{(p)}(x)\right]}{dx^2} = \left[\mathbf{Y}^{(p)}\right].\left[\mathbf{Z}^{(p)}\right].\left[\mathbf{I}^{(p)}(x)\right] \tag{5.2.1}$$

and then applying the method of variation of parameters. The technique involves finding the general form of a particular solution by a trial-and-error technique, and then determining the unknown coefficients and functions by back substitution of the solutions into the equations. It can be easily verified that the solutions for the phase voltages and currents are of the same form as those for a single phase transmission line given by Eqns.(4.4.1) and (4.4.2), namely:

$$\left[\mathbf{V}^{(p)}(x)\right] = e^{-[\Psi_v]x}.\left[\mathbf{V}^{p+}\right] + e^{[\Psi_v]x}.\left[\mathbf{V}^{p-}\right] \tag{5.3.1}$$

$$\left[\mathbf{I}^{(p)}(x)\right] = e^{-[\Psi_I]x}.\left[\mathbf{I}^{p+}\right] + e^{[\Psi_I]x}.\left[\mathbf{I}^{p-}\right] \tag{5.3.2}$$

In the above equations, $\left[\mathbf{V}^{p+}\right]$, $\left[\mathbf{V}^{p-}\right]$, $\left[\mathbf{I}^{p+}\right]$ and $\left[\mathbf{I}^{p-}\right]$ are column matrices of the coefficients of integration, which are determined from the terminal conditions.

$\left[\Psi_v\right]$ and $\left[\Psi_I\right]$ are square matrices which will be referred to as voltage and current phase propagation matrices. Contrary to the single phase lines, in which the voltage and current waves have the same propagation constant γ, here different propagation matrices have been assumed for the voltage and the current waves in MTL. This is a reasonable assumption since Eqns. (5.1) and (5.2), from which the voltage and current propagation matrices are defined, are written in terms of matrices which in general do not inhibit the property of commutivity.

Differentiating twice Eqns. (5.3) yields:

$$\frac{d^2\left[\mathbf{V}^{(p)}(x)\right]}{dx^2} = \left[\Psi_v\right]^2.\left[\mathbf{V}^{(p)}(x)\right] \tag{5.4.1}$$

$$\frac{d^2\left[\mathbf{I}^{(p)}(x)\right]}{dx^2} = \left[\Psi_I\right]^2.\left[\mathbf{I}^{(p)}(x)\right] \tag{5.4.2}$$

Comparing Eqns.(5.2) and (5.4), the phase propagation matrices can be expressed through the transmission line parameters as follows:

$$\left[\Psi_v\right] = \left(\left[\mathbf{Z}^{(p)}\right].\left[\mathbf{Y}^{(p)}\right] \right)^{\frac{1}{2}} \tag{5.5.1}$$

$$\left[\Psi_I\right] = \left(\left[\mathbf{Y}^{(p)}\right].\left[\mathbf{Z}^{(p)}\right] \right)^{\frac{1}{2}} \tag{5.5.2}$$

and since $\left[\mathbf{Z}^{(p)}\right]$ and $\left[\mathbf{Y}^{(p)}\right]$ are symmetric matrices it can be shown that the relationship between the phase propagation matrices for the voltage and current waves is:

$$\left[\Psi_v\right] = \left[\Psi_I\right]^T \tag{5.6}$$

Alternative expressions for the phase voltages and currents may be obtained by differentiating Eqns.(5.3.1) and (5.3.2), substituting into Eqns.(5.1.2) and (5.1.1) respectively and solving for $\left[\mathbf{V}^{(p)}\right]$ and $\left[\mathbf{I}^{(p)}\right]$:

$$\left[\mathbf{V}^{(p)}(x)\right]=\left[\mathbf{Y}^{(p)}\right]^{-1}.\left[\Psi_I\right].\left(e^{-[\Psi_I]x}.\left[\mathbf{I}^{p+}\right]-e^{-[\Psi_I]x}.\left[\mathbf{I}^{p-}\right] \right) \tag{5.7.1}$$

$$\left[\mathbf{I}^{(p)}(x)\right]=\left[\mathbf{Z}^{(p)}\right]^{-1}.\left[\Psi_V\right].\left(e^{-[\Psi_V]x}.\left[\mathbf{V}^{p+}\right]-e^{-[\Psi_V]x}.\left[\mathbf{V}^{p-}\right] \right) \tag{5.7.2}$$

As for the single phase transmission lines, the solutions for the phase voltages and currents imply the existence of incident and reflected waves. From Eqns.(5.3.1) and (5.7.2) the incident waves of the phase voltages and currents can be written as:

$$\left[\mathbf{V}_{inc}^{(p)}(x)\right]=e^{-[\Psi_V]x}.\left[\mathbf{V}^{p+}\right] \tag{5.8}$$

$$\left[\mathbf{I}_{inc}^{(p)}(x)\right]=\left[\mathbf{Z}^{(p)}\right]^{-1}.\left[\Psi_V\right].e^{-[\Psi_V]x}.\left[\mathbf{V}^{p+}\right] \tag{5.9}$$

On comparing the last two equations the following relation follows:

$$\left[\mathbf{I}_{inc}^{(p)}(x)\right]=\left[\mathbf{Z}^{(p)}\right]^{-1}.\left[\Psi_V\right].\left[\mathbf{V}_{inc}^{(p)}(x)\right] \tag{5.10}$$

In the above equation, the term $\left[\mathbf{Z}^{(p)}\right]^{-1}.\left[\Psi_V\right]$ has the dimensions of admittance and will be further designated by the symbol $\left[\mathbf{Y}_o^{(p)}\right]$.

$$\left[\mathbf{I}_{inc}^{(p)}(x)\right]=\left[\mathbf{Y}_o^{(p)}\right].\left[\mathbf{V}_{inc}^{(p)}(x)\right] \tag{5.11}$$

The same procedure applied to the reflected wave components of the phase voltages and currents, yields:

$$\left[\mathbf{I}_{refl}^{(p)}(x)\right]=-\left[\mathbf{Y}_o^{(p)}\right].\left[\mathbf{V}_{refl}^{(p)}(x)\right] \tag{5.12}$$

From of Eqns.(5.11) and (5.12), $\left[\mathbf{Y}_o^{(p)}\right]$ can be defined as the admittance seen by the incident or reflected travelling waves in a MTL. Since it depends only on the transmission line parameters and frequency, it is named the phase characteristic admittance matrix of the MTL:

$$\left[\mathbf{Y}_o^{(p)}\right]=\left[\mathbf{Z}^{(p)}\right]^{-1}.\left[\Psi_V\right] \tag{5.13}$$

In many instances it might be more convenient to use the reciprocal quantity, the phase characteristic impedance matrix, defined as the inverse of the phase characteristic admittance:

$$\left[\mathbf{Z}_o^{(p)}\right]=\left[\mathbf{Y}_o^{(p)}\right]^{-1}=\left[\Psi_V\right]^{-1}.\left[\mathbf{Z}^{(p)}\right] \tag{5.14}$$

Comparing the components of the incident (or reflected) waves of the phase voltages and currents in Eqns.(5.3.2) and (5.7.1) yields the following alternative formulae for the phase characteristic impedance and admittance:

$$\left[\mathbf{Z}_o^{(p)}\right] = \left[\mathbf{Y}_o^{(p)}\right]^{-1} . \left[\Psi_I\right] \tag{5.15}$$

$$\left[\mathbf{Y}_o^{(p)}\right] = \left[\Psi_I\right]^{-1} . \left[\mathbf{Y}^{(p)}\right] \tag{5.16}$$

By expressing $\left[\mathbf{Y}^{(p)}\right]$ from Eqn.(5.5.2) and substituting into Eqn.(5.16), another alternative formula of $\left[\mathbf{Z}_o^{(p)}\right]$ is obtained:

$$\left[\mathbf{Z}_o^{(p)}\right] = \left[\mathbf{Z}^{(p)}\right] . \left[\Psi_I\right]^{-1} \tag{5.17}$$

Using Eqn.(5.6) and taking into account that the $\left[\mathbf{Z}^{(p)}\right]$ matrix is symmetric, Eqn.(5.14) can be rewritten as follows:

$$\left[\mathbf{Z}_o^{(p)}\right] = \left[\Psi_V\right]^{-1} . \left[\mathbf{Z}^{(p)}\right] = \left(\left[\Psi_I\right]^T \right)^{-1} . \left[\mathbf{Z}^{(p)}\right]^T = \left(\left[\mathbf{Z}^{(p)}\right] . \left[\Psi_I\right]^{-1} \right)^T \tag{5.18}$$

Then noting Eqn.(5.17) it follows that

$$\left[\mathbf{Z}_o^{(p)}\right] = \left[\mathbf{Z}_o^{(p)}\right]^T \tag{5.19}$$

Thus the phase characteristic impedance matrix, and correspondingly also the phase characteristic admittance matrix, are both symmetric matrices.

The expressions of $\left[\mathbf{Y}_o^{(p)}\right]$ and $\left[\mathbf{Z}_o^{(p)}\right]$ given by Eqns.(5.13) to (5.17) all have the same form as the corresponding expressions of characteristic impedance and admittance of a single phase line. The data of Table 5.1. explores fully this analogy. A list of all possible expressions of $\mathbf{Z}_o$, $\mathbf{Y}_o$ and γ is given for a single phase line written in terms of the scalar quantities, with the corresponding expressions for a MTL written in terms of matrix quantities. To complete the analogy between the secondary parameters of a single phase line and a MTL it can be noted that the relationship

$$\mathbf{Z}_o^2 = \frac{\mathbf{Z}}{\mathbf{Y}} \tag{5.20}$$

for a single phase line corresponds to the matrix equation

$$\left[\mathbf{Z}_o^{(p)}\right] . \left[\mathbf{Y}^{(p)}\right] . \left[\mathbf{Z}_o^{(p)}\right] = \left[\mathbf{Z}^{(p)}\right] \tag{5.21}$$

for a MTL.

With the knowledge of the phase characteristic impedance and admittance matrices, Eqns. (5.7) may be rewritten in the form:

$$\left[\mathbf{V}^{(p)}(x)\right] = \left[\mathbf{Y}_o^{(p)}\right]^{-1} . \left(e^{-[\Psi_I]x} . \left[\mathbf{I}^{p+}\right] - e^{[\Psi_I]x} . \left[\mathbf{I}^{p-}\right] \right) = \left[\mathbf{Z}_o^{(p)}\right] . \left[\underline{\mathbf{I}}^{(p)}\right] \tag{5.22.1}$$

$$\left[\mathbf{I}^{(p)}(x)\right] = \left[\mathbf{Z}_o^{(p)}\right]^{-1} . \left(e^{-[\Psi_V]x} . \left[\mathbf{V}^{p+}\right] - e^{[\Psi_V]x} . \left[\mathbf{V}^{p-}\right] \right) = \left[\mathbf{Y}_o^{(p)}\right] . \left[\underline{\mathbf{V}}^{(p)}\right] \tag{5.22.2}$$

which will be useful in the analysis to follow.

Table 5.1 Analogy between the mathematical description of single phase and multiconductor transmission lines on phase and modal quantities

Quantity	Single phase line	Multiconductor (n+1)-phase transmission line	
		Phase quantities	Modal quantities
$\mathbf{Z}_o$	$\mathbf{Z}.\gamma^{-1}$	$[\mathbf{Z}^{(p)}].[\Psi_I]^{-1}$	$[\mathbf{Z}^{(m)}].[\gamma]^{-1}$
	$\gamma^{-1}.\mathbf{Z}$	$[\Psi_V]^{-1}.[\mathbf{Z}^{(p)}]$	$[\gamma]^{-1}.[\mathbf{Z}^{(m)}]$
	$\gamma.\mathbf{Y}^{-1}$	$[\Psi_V].[\mathbf{Y}^{(p)}]^{-1}$	$[\gamma].[\mathbf{Y}^{(m)}]^{-1}$
	$\mathbf{Y}^{-1}.\gamma$	$[\mathbf{Y}^{(p)}]^{-1}.[\Psi_I]$	$[\mathbf{Y}^{(m)}]^{-1}.[\gamma]$
$\mathbf{Y}_o$	$\mathbf{Z}^{-1}.\gamma$	$[\mathbf{Z}^{(p)}]^{-1}.[\Psi_I]$	$[\mathbf{Z}^{(m)}]^{-1}.[\gamma]$
	$\gamma.\mathbf{Z}^{-1}$	$[\Psi_I].[\mathbf{Z}^{(p)}]^{-1}$	$[\gamma].[\mathbf{Z}^{(m)}]^{-1}$
	$\mathbf{Y}.\gamma^{-1}$	$[\mathbf{Y}^{(p)}].[\Psi_V]^{-1}$	$[\mathbf{Y}^{(m)}].[\gamma]^{-1}$
	$\gamma^{-1}.\mathbf{Y}$	$[\Psi_I]^{-1}.[\mathbf{Y}^{(p)}]$	$[\gamma]^{-1}.[\mathbf{Y}^{(m)}]$
γ	$(\mathbf{Z}.\mathbf{Y})^{1/2}$	$([\mathbf{Z}^{(p)}].[\mathbf{Y}^{(p)}])^{1/2}=[\Psi_V]$	$([\mathbf{Z}^{(m)}].[\mathbf{Y}^{(m)}])^{1/2}=[\gamma]$
	$(\mathbf{Y}.\mathbf{Z})^{1/2}$	$([\mathbf{Y}^{(p)}].[\mathbf{Z}^{(p)}])^{1/2}=[\Psi_I]$	$([\mathbf{Y}^{(m)}].[\mathbf{Z}^{(m)}])^{1/2}=[\gamma']=[\gamma]$
	$\mathbf{Z}_o.\mathbf{Y}$	$[\mathbf{Z}_o^{(p)}].[\mathbf{Y}^{(p)}]=[\Psi_V]$	$[\mathbf{Z}_o^{(m)}].[\mathbf{Y}^{(m)}]=[\gamma]$
	$\mathbf{Y}.\mathbf{Z}_o$	$[\mathbf{Y}^{(p)}].[\mathbf{Z}_o^{(p)}]=[\Psi_I]$	$[\mathbf{Y}^{(m)}].[\mathbf{Z}_o^{(m)}]=[\gamma]$
	$\mathbf{Z}.\mathbf{Z}_o^{-1}$	$[\mathbf{Z}^{(p)}].[\mathbf{Z}_o^{(p)}]^{-1}=[\Psi_I]$	$[\mathbf{Z}^{(m)}].[\mathbf{Z}_o^{(m)}]^{-1}=[\gamma]$
	$\mathbf{Z}_o^{-1}.\mathbf{Z}$	$[\mathbf{Z}_o^{(p)}]^{-1}.[\mathbf{Z}^{(p)}]=[\Psi_V]$	$[\mathbf{Z}_o^{(m)}]^{-1}.[\mathbf{Z}^{(m)}]=[\gamma]$
	$\mathbf{Y}.\mathbf{Y}_o^{-1}$	$[\mathbf{Y}^{(p)}].[\mathbf{Y}_o^{(p)}]^{-1}=[\Psi_I]$	$[\mathbf{Y}^{(m)}].[\mathbf{Y}_o^{(m)}]^{-1}=[\gamma]$
	$\mathbf{Y}_o^{-1}.\mathbf{Y}$	$[\mathbf{Y}_o^{(p)}]^{-1}.[\mathbf{Y}^{(p)}]=[\Psi_V]$	$[\mathbf{Y}_o^{(m)}]^{-1}.[\mathbf{Y}^{(m)}]=[\gamma]$
	$\mathbf{Z}.\mathbf{Y}_o$	$[\mathbf{Z}^{(p)}].[\mathbf{Y}_o^{(p)}]=[\Psi_V]$	$[\mathbf{Z}^{(m)}].[\mathbf{Y}_o^{(m)}]=[\gamma]$
	$\mathbf{Y}_o.\mathbf{Z}$	$[\mathbf{Y}_o^{(p)}].[\mathbf{Z}^{(p)}]=[\Psi_I]$	$[\mathbf{Y}_o^{(m)}].[\mathbf{Z}^{(m)}]=[\gamma]$

The complete solution for the phase voltages and currents given by Eqns.(5.3) and (5.7) requires determination of the column matrices of the coefficients of integration $[\mathbf{V}^{p+}]$, $[\mathbf{V}^{p-}]$, $[\mathbf{I}^{p+}]$ and $[\mathbf{I}^{p-}]$. These are determined from boundary conditions which impose an additional relationship between the phase voltages and currents at the terminations of each homogeneous distributed parameter section. The application of the boundary conditions for the MTL is trivial. However, the termination networks, or in more general terms the boundary lumped parameter networks, in the MTL are more complicated and require some preliminary consideration which is given in the next section.

5.1.2 Discontinuities in a multiconductor transmission line and their mathematical formulation

In general, transmission lines may consist of a number of homogeneous sections with distributed parameters and a number of lumped parameter networks connected at the source and load ends of the transmission line, and between the homogeneous distributed parameter sections. All these lumped parameter networks are termed discontinuities, referring to their effect on electromagnetic wave propagation. Phase transpositions and direct junctions between line sections with different primary and secondary parameters also represent particular types of discontinuities. In order to incorporate discontinuities into the general transmission line description, it is necessary to introduce an equivalent, consistent, mathematical description of the discontinuities. This implies that at interface points, the discontinuities must be described in terms of the same quantities as those introduced for the transmission line, i.e. phase currents and voltages measured with respect to earth. Furthermore, to ensure compatibility at the interface, the equivalent diagram of the discontinuity network must have the same number of terminals as the number of conductors of the adjacent transmission line section. The above considerations imply that a general discontinuity in a (n+1) conductor transmission line must be represented with an equivalent multipole (multiterminal) network (Fig.5.1). In particular, the terminal discontinuities represent (n+1) pole active or passive networks, while the intermediate discontinuities are [2 x (n+1)]-pole networks. Here, 2 is the number of ports (or groups of poles) and (n+1) is the number of poles (terminals) in each port. This equivalent diagram is fully consistent with the description of the transmission line sections which themselves can be represented as [2 x (n+1)]-pole networks.

With reference to Appendix B which contains a brief outline of relevant multipole network theory, the following observations about the most appropriate methods for the analytical description of MTL discontinuities can be made:

(1) Multipole networks of transmission line discontinuities should be described with their definite admittance matrix formulation because the nodal voltages

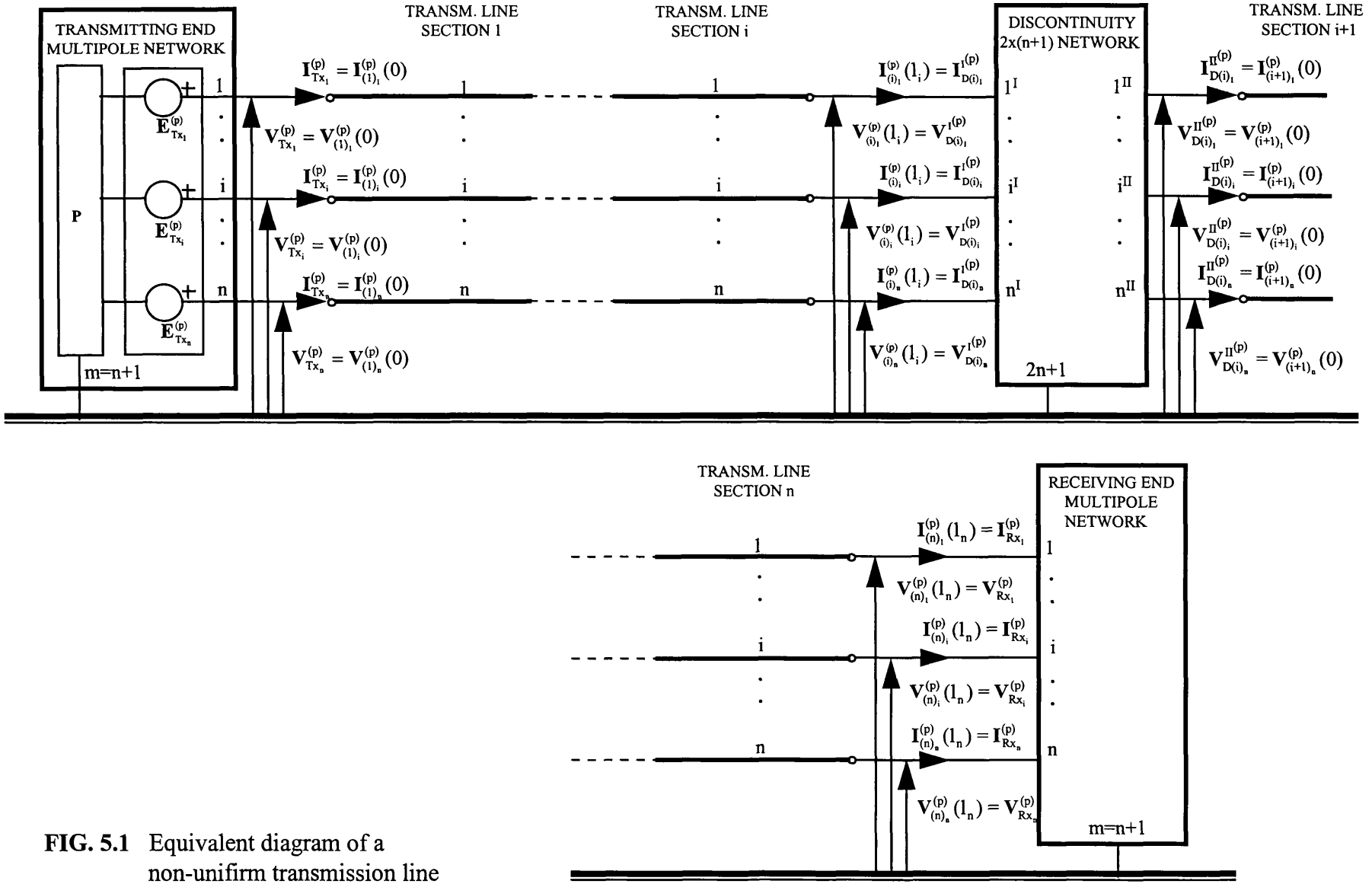

FIG. 5.1 Equivalent diagram of a non-unifirm transmission line

and currents associated with multipole terminals are then equivalent to phase voltages and currents at the MTL terminals.

- The transmitting end termination network is represented by its equivalent Norton or Thevenin multipole diagram according to Eqns.(B.18) and (B.21) and Figs.B.3 and B.4. These equations are rewritten below for convenience, but in a modified form according to a different convention for the positive directions of the currents (as shown in Fig.5.1), which is more appropriate for the transmitting end termination network:

$$\left[\mathbf{I}_{\mathrm{Tx}}^{(p)}\right] = -\left[\mathbf{Y}_{\mathrm{Tx}}^{(p)}\right].\left[\mathbf{V}_{\mathrm{Tx}}^{(p)}\right] + \left[\mathbf{J}_{\mathrm{Tx}}^{(p)}\right] \tag{5.23}$$

$$\left[\mathbf{I}_{\mathrm{Tx}}^{(p)}\right] = -\left[\mathbf{Y}_{\mathrm{Tx}}^{(p)}\right]^{-1}.\left(\left[\mathbf{V}_{\mathrm{Tx}}^{(p)}\right] - \left[\mathbf{E}_{\mathrm{Tx}}^{(p)}\right]\right) \tag{5.24}$$

- The receiving end termination network is represented as an equivalent passive m-pole network described with its terminal admittance matrix formulation as follows:

$$\left[\mathbf{I}_{\mathrm{Rx}}^{(p)}\right] = \left[\mathbf{Y}_{\mathrm{Rx}}^{(p)}\right].\left[\mathbf{V}_{\mathrm{Rx}}^{(p)}\right] \tag{5.25}$$

- The intermediate discontinuities are described by the transmission parameter form (Table B.1)

$$\left[\begin{bmatrix}\mathbf{V}_{\mathrm{D}}^{\mathrm{I}(p)}\\ \mathbf{I}_{\mathrm{D}}^{\mathrm{I}(p)}\end{bmatrix}\right] = \left[\begin{bmatrix}\mathcal{A}_{\mathrm{D}}^{(p)}\end{bmatrix} \begin{bmatrix}\mathcal{B}_{\mathrm{D}}^{(p)}\end{bmatrix}\right] \cdot \left[\begin{bmatrix}\mathbf{V}_{\mathrm{D}}^{\mathrm{II}(p)}\\ \mathbf{I}_{\mathrm{D}}^{\mathrm{II}(p)}\end{bmatrix}\right] = \left[\mathrm{T}_{\mathrm{D}}^{(p)}\right] \cdot \left[\begin{bmatrix}\mathbf{V}_{\mathrm{D}}^{\mathrm{II}(p)}\\ \mathbf{I}_{\mathrm{D}}^{\mathrm{II}(p)}\end{bmatrix}\right] \tag{5.26}$$

In Eqns.(5.23)-(5.26) the general subscript 't' standing for 'terminal' in Appendix B has been replaced with subscripts corresponding to the particular discontinuity i.e. 'Tx' for transmitting end network, 'Rx' for receiving end network and 'D' for an intermediate discontinuity in general or D(i) for the intermediate discontinuity.

The superscript '(p)' is added for consistency with the phase domain analysis of the multiconductor transmission line.

5.1.3 Effect of transmission line discontinuities on wave propagation. Phase reflection and refraction operators.

In the general case, both terminal and intermediate discontinuities disturb the propagation of the phase voltage and current incident waves $\left[\mathbf{V}_{\mathrm{inc}}^{(p)}\right]$ and $\left[\mathbf{I}_{\mathrm{inc}}^{(p)}\right]$ by giving rise to reflected waves $\left[\mathbf{V}_{\mathrm{refl}}^{(p)}\right]$ and $\left[\mathbf{I}_{\mathrm{refl}}^{(p)}\right]$ and transmitted or refracted waves $\left[\mathbf{V}_{\mathrm{tr}}^{(p)}\right]$ and $\left[\mathbf{I}_{\mathrm{tr}}^{(p)}\right]$. The incident, reflected and transmitted (or refracted) wave components at a general discontinuity D(i) (Fig.5.1) are related by the following node matrix equations:

- At the input (port I) of the discontinuity network:

$$\left[\mathbf{V}_{(\mathrm{i})}^{(p)}(l_i)\right] = \left[\mathbf{V}_{\mathrm{inc}_{(\mathrm{i})}}^{(p)}(l_i)\right] + \left[\mathbf{V}_{\mathrm{refl}_{(\mathrm{i})}}^{(p)}(l_i)\right] = \left[\mathbf{V}_{\mathrm{D(i)}}^{\mathrm{I}(p)}\right] \tag{5.27}$$

$$\left[\mathbf{I}_{(i)}^{(p)}(l_i)\right]=\left[\mathbf{I}_{inc_{(i)}}^{(p)}(l_i)\right]+\left[\mathbf{I}_{refl_{(i)}}^{(p)}(l_i)\right]=\left[\mathbf{I}_{D(i)}^{I^{(p)}}\right] \tag{5.28}$$

$$\left[\mathbf{V}_{inc_{(i)}}^{(p)}(l_i)\right]=\left[\mathbf{Z}_{o_{(i)}}^{(p)}\right].\left[\mathbf{I}_{inc_{(i)}}^{(p)}(l_i)\right] \tag{5.29}$$

$$\left[\mathbf{V}_{refl_{(i)}}^{(p)}(l_i)\right]=-\left[\mathbf{Z}_{o_{(i)}}^{(p)}\right].\left[\mathbf{I}_{refl_{(i)}}^{(p)}(l_i)\right] \tag{5.30}$$

$$\left[\mathbf{V}_{D(i)}^{I^{(p)}}\right]=\left[\mathbf{Z}_{inp_{D(i)}}^{I^{(p)}}\right].\left[\mathbf{I}_{D(i)}^{I^{(p)}}\right] \tag{5.31}$$

where $\left[\mathbf{Z}_{inp_{D(i)}}^{I^{(p)}}\right]$ is the matrix of the input impedance looking into the discontinuity.

- At the discontinuity network:

$$\left[\begin{bmatrix}\mathbf{V}_{D(i)}^{I^{(p)}}\\ \mathbf{I}_{D(i)}^{I^{(p)}}\end{bmatrix}\right]=\left[\begin{bmatrix}\mathcal{A}_{D(i)}^{(p)} & \mathcal{B}_{D(i)}^{(p)}\\ C_{D(i)}^{(p)} & \mathcal{D}_{D(i)}^{(p)}\end{bmatrix}\right].\left[\begin{bmatrix}\mathbf{V}_{D(i)}^{II^{(p)}}\\ \mathbf{I}_{D(i)}^{II^{(p)}}\end{bmatrix}\right]=\left[\mathbf{T}_{D(i)}^{(p)}\right].\left[\begin{bmatrix}\mathbf{V}_{D(i)}^{II^{(p)}}\\ \mathbf{I}_{D(i)}^{II^{(p)}}\end{bmatrix}\right] \tag{5.32}$$

- At the output (port II) of the discontinuity network:

Assumming for simplicity that in the transmission line section 'i+1', there are no reflected waves

$$\left[\mathbf{V}_{tr_{(i+1)}}^{(p)}(0)\right]=\left[\mathbf{V}_{inc_{(i+1)}}^{(p)}(0)\right]=\left[\mathbf{V}_{D_{(i)}}^{II^{(p)}}\right] \tag{5.33}$$

$$\left[\mathbf{I}_{tr_{(i+1)}}^{(p)}(0)\right]=\left[\mathbf{I}_{inc_{(i+1)}}^{(p)}(0)\right]=\left[\mathbf{I}_{D_{(i)}}^{II^{(p)}}\right] \tag{5.34}$$

$$\left[\mathbf{V}_{inc_{(i+1)}}^{(p)}(0)\right]=\left[\mathbf{Z}_{o_{(i+1)}}^{(p)}\right].\left[\mathbf{I}_{inc_{(i+1)}}^{I^{(p)}}(0)\right] \tag{5.35}$$

$$\left[\mathbf{V}_{D(i)}^{II^{(p)}}\right]=\left[\mathbf{Z}_{inp_{D(i)}}^{II^{(p)}}\right].\left[\mathbf{I}_{D(i)}^{I^{(p)}}\right] \tag{5.36}$$

where $\left[\mathbf{Z}_{inp_{D(i)}}^{II^{(p)}}\right]$ is the matrix of the phase input impedance seen looking into the transmission line beyond the discontinuity network

By analogy with single phase transmission line theory, the effect of a discontinuity in a MTL can be expressed in terms of matrix phase reflection and phase refraction operators defined by the equations:

$$\left[\mathbf{V}_{refl}^{(p)}\right]=\left[\mathbf{K}_{V}^{(p)}\right].\left[\mathbf{V}_{inc}^{(p)}\right] \tag{5.37}$$

$$\left[\mathbf{I}_{refl}^{(p)}\right]=-\left[\mathbf{K}_{I}^{(p)}\right].\left[\mathbf{I}_{inc}^{(p)}\right] \tag{5.38}$$

$$\left[\mathbf{V}_{tr}^{(p)}\right]=\left[\mathbf{R}_{V}^{(p)}\right].\left[\mathbf{V}_{inc}^{(p)}\right] \tag{5.39}$$

$$\left[\mathbf{I}_{tr}^{(p)}\right]=\left[\mathbf{R}_{I}^{(p)}\right].\left[\mathbf{I}_{inc}^{(p)}\right] \tag{5.40}$$

where:

$\left[\mathbf{K}_V^{(p)}\right]$ and $\left[\mathbf{K}_I^{(p)}\right]$ are (n,n)-order matrices representing the voltage and current phase reflection operators and

$\left[\mathbf{R}_V^{(p)}\right]$ and $\left[\mathbf{R}_I^{(p)}\right]$ are (n,n)-order matrices representing the voltage and current phase refraction (or transmission) operators.

At this point, the following observations can be made:

- While in single phase transmission lines, the reflection/refraction of the voltage and current waves is described in terms of the same reflection/refraction scalar coefficients, in a MTL described in terms of matrices, it is necessary to assume the existence of different reflection/refraction operators for the phase voltages and currents. This assumption, verified later, is suggested by the existence of different matrix phase propagation constants $\left[\Psi_V\right]$ and $\left[\Psi_I\right]$.

- The physical interpretation of the matrix formulation of the reflection and refraction operators is that the different MTL phases are mutually dependent, both in the distributed and in the lumped parameter sections. This means that the i-th phase of the reflected/refracted wave, will also include components which are due to the reflection/refraction of all the other phases of the incident wave.

In the analysis of multiconductor transmission lines, it is useful to derive expressions for the phase reflection and refraction operators in terms of the transmission line and discontinuity parameters. To obtain expressions of the voltage and current phase reflection operator, the receiving end of a homogeneous multiconductor transmission line of length l will be considered.

The receiving end network is described by Eqn.(5.25). Taking into consideration the equivalence between the quantities specifying the transmission line receiving end terminals and the terminals of the receiving end network i.e.

$$\left[\mathbf{V}_t\right]=\left[\mathbf{V}_{Rx}^{(p)}\right]=\left[\mathbf{V}^{(p)}(l)\right] \tag{5.41.1}$$

$$\left[\mathbf{I}_t\right]=\left[\mathbf{I}_{Rx}^{(p)}\right]=\left[\mathbf{I}^{(p)}(l)\right] \tag{5.41.2}$$

and i

$$\left[\mathbf{V}_t\right]=\left[\mathbf{V}_{Rx}^{(p)}\right]=\left[\mathbf{V}^{(p)}(l)\right] \tag{5.41.1}$$

$$\left[\mathbf{I}_t\right]=\left[\mathbf{I}_{Rx}^{(p)}\right]=\left[\mathbf{I}^{(p)}(l)\right] \tag{5.41.2}$$

and introducing the notation $\left[\mathbf{Z}_{Rx}^{(p)}\right]$ for the inverse of the definite admittance matrix $\left[\mathbf{Z}_t\right]$. the following equation is obtained:

$$\left[\mathbf{V}^{(p)}(l)\right]=\left[\mathbf{Z}_{Rx}^{(p)}\right].\left[\mathbf{I}^{(p)}(l)\right] \tag{5.42}$$

5.1.3.1 Voltage phase reflection operator

Substituting $\left[\mathbf{V}^{(p)}(l)\right]$ from Eqn.(5.3.1) and $\left[\mathbf{I}^{(p)}(l)\right]$ from Eqn.(5.22.2) into Eqn.(5.42) and rearranging gives:

$$\left(\left[\mathbf{Z}_{Rx}^{(p)}\right].\left[\mathbf{Y}_{o}^{(p)}\right]+[1]\right).\left[\mathbf{V}_{refl}^{(p)}\right]=\left(\left[\mathbf{Z}_{Rx}^{(p)}\right].\left[\mathbf{Y}_{o}^{(p)}\right]-[1]\right).\left[\mathbf{V}_{inc}^{(p)}\right] \tag{5.43}$$

or alternatively:

$$\left[\mathbf{V}_{refl}^{(p)}(l)\right]=\left(\left[\mathbf{Z}_{Rx}^{(p)}\right].\left[\mathbf{Y}_{o}^{(p)}\right]+[1]\right)^{-1}.\left(\left[\mathbf{Z}_{Rx}^{(p)}\right].\left[\mathbf{Y}_{o}^{(p)}\right]-[1]\right).\left[\mathbf{V}_{inc}^{(p)}(l)\right] \tag{5.44}$$

Comparing the above equation with Eqn.(5.37), it follows that

$$\left[\mathbf{K}_{V}^{(p)}\right]=\left(\left[\mathbf{Z}_{Rx}^{(p)}\right].\left[\mathbf{Y}_{o}^{(p)}\right]+[1]\right)^{-1}.\left(\left[\mathbf{Z}_{Rx}^{(p)}\right].\left[\mathbf{Y}_{o}^{(p)}\right]-[1]\right) \tag{5.45}$$

Premultiplying Eqn.(5.43) with $\left[\mathbf{Z}_{Rx}^{(p)}\right]^{-1}$ and solving for $\left[\mathbf{K}_{V}^{(p)}\right]$ gives an alternative expression:

$$\left[\mathbf{K}_{V}^{(p)}\right]=\left(\left[\mathbf{Y}_{o}^{(p)}\right]+\left[\mathbf{Y}_{Rx}^{(p)}\right]\right)^{-1}.\left(\left[\mathbf{Y}_{o}^{(p)}\right]-\left[\mathbf{Y}_{Rx}^{(p)}\right]\right) \tag{5.46}$$

In some applications it might be more convenient to use a formula for $\left[\mathbf{K}_{V}^{(p)}\right]$ expressed through the impedances. Expressing the admittance matrices by the inverse of the impedance matrices and manipulating yields the formula:

$$\left[\mathbf{K}_{V}^{(p)}\right]=\left(\left[\mathbf{Z}_{Rx}^{(p)}\right]-\left[\mathbf{Z}_{o}^{(p)}\right]\right).\left(\left[\mathbf{Z}_{Rx}^{(p)}\right]+\left[\mathbf{Z}_{o}^{(p)}\right]\right)^{-1} \tag{5.47}$$

5.1.3.2 Current phase reflection operator

Starting again with Eqn.(5.42) and following a similar procedure leads to the following equation:

$$\left[\mathbf{I}_{refl}^{(p)}(l)\right]=-\left(\left[\mathbf{Y}_{o}^{(p)}\right].\left[\mathbf{Z}_{Rx}^{(p)}\right]+[1]\right)^{-1}.\left(\left[\mathbf{Y}_{o}^{(p)}\right].\left[\mathbf{Z}_{Rx}^{(p)}\right]-[1]\right).\left[\mathbf{I}_{inc}^{(p)}(l)\right] \tag{5.48}$$

Comparing Eqn.(5.48) with Eqn.(5.38) yields:

$$\left[\mathbf{K}_{I}^{(p)}\right]=\left(\left[\mathbf{Y}_{o}^{(p)}\right].\left[\mathbf{Z}_{Rx}^{(p)}\right]+[1]\right)^{-1}.\left(\left[\mathbf{Y}_{o}^{(p)}\right].\left[\mathbf{Z}_{Rx}^{(p)}\right]-[1]\right) \tag{5.49}$$

Manipulation of Eqn.(5.49) leads to the following two expressions for the current phase reflection coefficient:

$$\left[\mathbf{K}_{I}^{(p)}\right]=\left(\left[\mathbf{Z}_{Rx}^{(p)}\right]+\left[\mathbf{Z}_{o}^{(p)}\right]\right)^{-1}.\left(\left[\mathbf{Z}_{Rx}^{(p)}\right]-\left[\mathbf{Z}_{o}^{(p)}\right]\right) \tag{5.50}$$

$$\left[\mathbf{K}_{I}^{(p)}\right]=\left(\left[\mathbf{Y}_{o}^{(p)}\right]-\left[\mathbf{Y}_{Rx}^{(p)}\right]\right).\left(\left[\mathbf{Y}_{o}^{(p)}\right]+\left[\mathbf{Y}_{Rx}^{(p)}\right]\right)^{-1} \tag{5.51}$$

5.1.3.3 Relationship between voltage and current phase reflection operators

Manipulating the expression of $\left[\mathbf{K}_{V}^{(p)}\right]$ from Eqn.(5.47) yields the following relationships between the voltage and current reflection operators:

$$\left[\mathbf{K}_{V}^{(p)}\right]=\left[\mathbf{Z}_{Rx}^{(p)}\right].\left[\mathbf{K}_{I}^{(p)}\right].\left[\mathbf{Z}_{Rx}^{(p)}\right]^{-1} \tag{5.52}$$

$$\left[\mathbf{K}_{V}^{(p)}\right]=\left[\mathbf{Y}_{Rx}^{(p)}\right]^{-1}.\left[\mathbf{K}_{I}^{(p)}\right].\left[\mathbf{Y}_{Rx}^{(p)}\right] \tag{5.53}$$

Similarly, manipulating Eqn.(5.46) gives another two forms for the same relationship but expressed through the characteristic impedance/admittance:

$$\left[\mathbf{K}_{V}^{(p)}\right]=\left[\mathbf{Z}_{o}^{(p)}\right].\left[\mathbf{K}_{I}^{(p)}\right].\left[\mathbf{Z}_{o}^{(p)}\right]^{-1} \tag{5.54}$$

$$\left[\mathbf{K}_{V}^{(p)}\right]=\left[\mathbf{Y}_{o}^{(p)}\right]^{-1}.\left[\mathbf{K}_{I}^{(p)}\right].\left[\mathbf{Y}_{o}^{(p)}\right] \tag{5.55}$$

Equations (5.52) to (5.55) show that $\left[\mathbf{K}_{V}^{(p)}\right]$ and $\left[\mathbf{K}_{I}^{(p)}\right]$ are similar matrices.

5.1.3.4 Reflection operators at an intermediate discontinuity

The voltage and current phase reflection operators at an intermediate discontinuity can be derived from Eqn.(5.31). Substituting Eqns.(5.27) and (5.28) into Eqn.(5.31) yields:

$$\left[\mathbf{V}_{(i)}^{(p)}(l_i)\right]=\left[\mathbf{Z}_{inp_{D(i)}}^{I^{(p)}}\right].\left[\mathbf{I}_{(i)}^{(p)}(l_i)\right] \tag{5.56}$$

which is identical in form to Eqn.(5.42). The difference is that instead of the phase load impedance matrix $\left[\mathbf{Z}_{Rx}^{(p)}\right]$, Eqn. (5.56) contains the matrix of the phase input impedance looking into the discontinuity. Considering this matrix as an equivalent load matrix for the section of the transmission line to the left of the discontinuity (Fig.5.1), the case of an intermediate discontinuity can be reduced to that of a terminal discontinuity. Hence the reflection operators of an intermediate discontinuity can be calculated using Eqns. (5.45) to (5.47) and (5.49) to (5.51) provided that the phase input impedance matrix $\left[\mathbf{Z}_{inp_{D(i)}}^{I^{(p)}}\right]$ is known. It can be calculated from Eqn.(5.32) as

$$\left[\mathbf{Z}_{inp_{D(i)}}^{I^{(p)}}\right]=\left(\left[\mathcal{A}_{D(i)}^{(p)}\right].\left[\mathbf{Z}_{inp_{D(i)}}^{II^{(p)}}\right]+\left[\mathcal{B}_{D(i)}^{(p)}\right]\right).\left(\left[C_{D(i)}^{(p)}\right].\left[\mathbf{Z}_{inp_{D(i)}}^{II^{(p)}}\right]+\left[\mathcal{D}_{D(i)}^{(p)}\right]\right)^{-1} \tag{5.57}$$

5.1.3.5 Refraction operators

Refraction operators are associated only with intermediate discontinuities. Expressions for the refraction operators can be derived from Eqn.(5.32) which describes the intermediate discontinuity network.

Using Eqns.(5.27), (5.28), (5.37) and (5.38), the matrix of the input port voltages and currents can be expressed as follows:

$$\begin{bmatrix}\begin{bmatrix}\mathbf{V}^{I^{(p)}}_{D(i)}\\ \mathbf{I}^{I^{(p)}}_{D(i)}\end{bmatrix}\end{bmatrix}=\begin{bmatrix}[1]+\left[\mathbf{K}^{(p)}_{V_{D(i)}}\right] & \\ & [1]-\left[\mathbf{K}^{(p)}_{I_{D(i)}}\right]\end{bmatrix}\cdot\begin{bmatrix}\begin{bmatrix}\mathbf{V}^{(p)}_{inc_{(i)}}(1_i)\end{bmatrix}\\ \begin{bmatrix}\mathbf{I}^{(p)}_{inc_{(i)}}(1_i)\end{bmatrix}\end{bmatrix}=$$

$$=\begin{bmatrix}[1]+\left[\mathbf{K}^{(p)}_{V_{D(i)}}\right] & \\ & [1]-\left[\mathbf{K}^{(p)}_{I_{D(i)}}\right]\end{bmatrix}\cdot\begin{bmatrix}[1]\\ \left[\mathbf{Z}^{(p)}_{o_{(i)}}\right]^{-1}\end{bmatrix}\cdot\left[\mathbf{V}^{(p)}_{inc_{(i)}}(1_i)\right]=$$

$$=\begin{bmatrix}[1]+\left[\mathbf{K}^{(p)}_{V_{D(i)}}\right] & \\ & [1]-\left[\mathbf{K}^{(p)}_{I_{D(i)}}\right]\end{bmatrix}\cdot\begin{bmatrix}\left[\mathbf{Z}^{(p)}_{o_{(i)}}\right]\\ [1]\end{bmatrix}\cdot\left[\mathbf{I}^{(p)}_{inc(i)}(1_i)\right] \qquad (5.58)$$

Using Eqns.(5.33) and (5.34), the matrix of the output port voltages and currents can be expressed as:

$$\begin{bmatrix}\begin{bmatrix}\mathbf{V}^{II^{(p)}}_{D(i)}\\ \mathbf{I}^{II^{(p)}}_{D(i)}\end{bmatrix}\end{bmatrix}=\begin{bmatrix}\begin{bmatrix}\mathbf{V}^{(p)}_{inc_{(i+1)}}(0)\end{bmatrix}\\ \begin{bmatrix}\mathbf{I}^{(p)}_{inc_{(i+1)}}(0)\end{bmatrix}\end{bmatrix}=\begin{bmatrix}\mathbf{V}^{(p)}_{tr_{(i+1)}}(1_i)\\ \mathbf{I}^{(p)}_{tr_{(i+1)}}(1_i)\end{bmatrix}=$$

$$=\begin{bmatrix}[1]\\ \left[\mathbf{Z}^{II^{(p)}}_{inp_{D(i)}}\right]^{-1}\end{bmatrix}\cdot\left[\mathbf{V}^{(p)}_{tr_{(i+1)}}(0)\right]=\begin{bmatrix}\left[\mathbf{Z}^{II^{(p)}}_{inp_{D(i)}}\right]\\ [1]\end{bmatrix}\cdot\left[\mathbf{I}^{(p)}_{tr_{(i+1)}}(0)\right] \qquad (5.59)$$

Substituting Eqns.(5.58) and (5.59) into (5.31) and manipulating gives:

$$\begin{bmatrix}[1]+\left[\mathbf{K}^{(p)}_{V_{D(i)}}\right]\\ \left([1]-\left[\mathbf{K}^{(p)}_{I_{D(i)}}\right]\right)\cdot\left[\mathbf{Z}^{(p)}_{o_i}\right]^{-1}\end{bmatrix}\cdot\left[\mathbf{V}^{(p)}_{inc_{(i)}}(1_i)\right]=\begin{bmatrix}\left[\mathcal{A}^{(p)}_{D(i)}\right]+\left[\mathcal{B}^{(p)}_{D(i)}\right]\cdot\left[\mathbf{Z}^{II^{(p)}}_{inp_{D(i)}}\right]^{-1}\\ \left[C^{(p)}_{D(i)}\right]+\left[\mathcal{D}^{(p)}_{D(i)}\right]\cdot\left[\mathbf{Z}^{II^{(p)}}_{inp_{D(i)}}\right]^{-1}\end{bmatrix}\cdot\left[\mathbf{V}^{(p)}_{tr_{(i+1)}}(0)\right] \qquad (5.60)$$

from which the voltage phase refraction coefficient can be expressed in two ways:

$$\left[\mathbf{R}^{(p)}_{V_{D(i)}}\right]=\left(\left[\mathcal{A}^{(p)}_{D(i)}\right]+\left[\mathcal{B}^{(p)}_{D(i)}\right]\cdot\left[\mathbf{Z}^{II^{(p)}}_{inp_{D(i)}}\right]^{-1}\right)^{-1}\cdot\left([1]+\left[\mathbf{K}^{(p)}_{V_{D(i)}}\right]\right)=$$

$$=\left(\left[C^{(p)}_{D(i)}\right]+\left[\mathcal{D}^{(p)}_{D(i)}\right]\cdot\left[\mathbf{Z}^{II^{(p)}}_{inp_{D(i)}}\right]^{-1}\right)^{-1}\cdot\left([1]-\left[\mathbf{K}^{(p)}_{I_{D(i)}}\right]\right)\cdot\left[\mathbf{Z}^{(p)}_{o_{(i)}}\right]^{-1} \qquad (5.61)$$

In a similar manner, the current phase refraction coefficients can be obtained as:

$$\left[\mathbf{R}^{(p)}_{I_{D(i)}}\right]=\left(\left[\mathcal{A}^{(p)}_{D(i)}\right]\cdot\left[\mathbf{Z}^{II^{(p)}}_{inp_{D(i)}}\right]+\left[\mathcal{B}^{(p)}_{D(i)}\right]\right)^{-1}\cdot\left([1]+\left[\mathbf{K}^{(p)}_{V_{D(i)}}\right]\right)\cdot\left[\mathbf{Z}^{(p)}_{o_{(i)}}\right]=$$

$$=\left(\left[C^{(p)}_{D(i)}\right]\cdot\left[\mathbf{Z}^{II^{(p)}}_{inp_{D(i)}}\right]+\left[\mathcal{D}^{(p)}_{D(i)}\right]\right)^{-1}\cdot\left([1]-\left[\mathbf{K}^{(p)}_{I_{D(i)}}\right]\right) \qquad (5.62)$$

Eqns.(5.61) and (5.62) give expressions for the phase refraction operators for the most general case of discontinuity, which is when it represents a 2(n+1)-pole network. In practice, a discontinuity may have a much simpler structure such as that of a series impedance or shunt admittance matrix or a direct junction between two transmission line

sections with different parameters. Ref.[5-1] contains a full set of reflection and refraction operator formulae for various types of discontinuity networks.

Calculation of the reflection and refraction operators associated with an intermediate discontinuity requires preliminary knowledge of the matrix $\left[\mathbf{Z}^{II^{(p)}}_{inp_{D(i)}}\right]$ The determination of this matrix is treated in the next section.

5.1.4 Transmission line solution including boundary conditions

The aim of this subsection is to derive the exact solution for the voltages and currents at any point along the transmission line taking into account the boundary conditions. This can be done by using the reflection coefficient.

5.1.4.1 Transmitting end conditions

At the point x = 0, the phase voltages are

$$\left[\mathbf{V}^{(p)}(0)\right]=\left[\mathbf{V}^{(p)}_{inc}(0)\right]+\left[\mathbf{V}^{(p)}_{refl}(0)\right]=\left[\mathbf{V}^{(p)}_{inc}(0)\right]+e^{-[\Psi_v]l}.\left[\mathbf{V}^{p}_{refl}(l)\right]=$$

$$=\left[\mathbf{V}^{(p)}_{inc}(0)\right]+e^{-[\Psi_v]l}.\left[\mathbf{K}^{(p)}_{V}\right].\left[\mathbf{V}^{(p)}_{inc}(l)\right]=\left[\mathbf{V}^{(p)}_{inc}(0)\right]+e^{-[\Psi_v]l}.\left[\mathbf{K}^{(p)}_{V}\right].e^{-[\Psi_v]l}.\left[\mathbf{V}^{(p)}_{inc}(0)\right]=$$

$$=\left(\left[1\right]+e^{-[\Psi_v]l}.\left[\mathbf{K}^{(p)}_{V}\right].e^{-[\Psi_v]l}\right).\left[\mathbf{V}^{(p)}_{inc}(0)\right]=\left(\left[1\right]+\left[\chi^{(p)}_{V}\right]\right).\left[\mathbf{V}^{(p)}_{inc}(0)\right] \quad (5.63)$$

where
$$\left[\chi^{(p)}_{V}\right]=e^{-[\Psi_v]l}.\left[\mathbf{K}^{(p)}_{V}\right].e^{-[\Psi_v]l} \quad (5.64)$$

From Eqn.(5.22.2) the current can be found as:

$$\left[\mathbf{I}^{(p)}(0)\right]=\left[\mathbf{Y}^{(p)}_{o}\right].\left[\underline{\mathbf{V}}^{(p)}(0)\right]=\left[\mathbf{Y}^{(p)}_{o}\right].\left(\left[1\right]-\left[\chi^{(p)}_{V}\right]\right).\left[\mathbf{V}^{(p)}_{inc}(0)\right] \quad (5.65)$$

5.1.4.2 General conditions at any point along the transmission line

At any point x along the transmission line, the phase voltages are:

$$\left[\mathbf{V}^{(p)}(x)\right]=\left[\mathbf{V}^{(p)}_{inc}(x)\right]+\left[\mathbf{V}^{(p)}_{refl}(x)\right] \quad (5.66)$$

The incident and reflected waves of the voltage can be expressed as follows:

$$\left[\mathbf{V}^{(p)}_{inc}(x)\right]=e^{-[\Psi_v]x}.\left[\mathbf{V}^{(p)}_{inc}(0)\right] \quad (5.67)$$

$$\left[\mathbf{V}^{(p)}_{refl}(x)\right]=e^{-[\Psi_v](l-x)}.\left[\mathbf{V}^{(p)}_{refl}(l)\right]=$$

$$=e^{-[\Psi_v](l-x)}.\left[\mathbf{K}^{(p)}_{V}\right].\left[\mathbf{V}^{(p)}_{inc}(l)\right]=e^{-[\Psi_v](l-x)}.\left[\mathbf{K}^{(p)}_{V}\right].e^{-[\Psi_v]l}.\left[\mathbf{V}^{(p)}_{inc}(0)\right] \quad (5.68)$$

Substituting Eqns.(5.67) and (5.68) into Eqn.(5.66) gives:

$$\left[\mathbf{V}^{(p)}(x)\right]=\left(e^{-[\Psi_v]x}+e^{-[\Psi_v](l-x)}.\left[\mathbf{K}^{(p)}_{V}\right].e^{-[\Psi_v]l}\right).\left[\mathbf{V}^{(p)}_{inc}(0)\right] \quad (5.69)$$

Similarly, using Eqn.(5.22.2) the following expression can be obtained for the current:

$$\left[\mathbf{I}^{(p)}(x)\right]=\left[\mathbf{Y}_0^{(p)}\right].\left(e^{-[\Psi_v]x}-e^{-[\Psi_v](l-x)}.\left[\mathbf{K}_V^{(p)}\right].e^{-[\Psi_v]l}\right).\left[\mathbf{V}_{inc}^{(p)}(0)\right] \tag{5.70}$$

Substituting $\left[\mathbf{V}_{inc}^{(p)}(0)\right]$ from Eqn.(5.63) into Eqns.(5.69) and (5.70) yields:

$$\left[\mathbf{V}^{(p)}(x)\right]=\left(e^{-[\Psi_v]x}+e^{-[\Psi_v](l-x)}.\left[\mathbf{K}_V^{(p)}\right].e^{-[\Psi_v]l}\right).\left([1]+\left[\chi_V^{(p)}\right]\right)^{-1}.\left[\mathbf{V}^{(p)}(0)\right] \tag{5.71}$$

$$\left[\mathbf{I}^{(p)}(x)\right]=\left[\mathbf{Y}_0^{(p)}\right].\left(e^{-[\Psi_v]x}-e^{-[\Psi_v](l-x)}.\left[\mathbf{K}_V^{(p)}\right].e^{-[\Psi_v]l}\right).\left([1]+\left[\chi_V^{(p)}\right]\right)^{-1}.\left[\mathbf{V}^{(p)}(0)\right] \tag{5.72}$$

The above two equations give the voltages and currents at any point along the transmission line expressed through the voltage phase reflection operator $\left[\mathbf{K}_V^{(p)}\right]$, the voltage phase propagation matrix $\left[\Psi_V\right]$ and the voltages at the transmitting end. Alternative expressions using the current phase reflection operator $\left[\mathbf{K}_I^{(p)}\right]$, the current phase propagation matrix $\left[\Psi_I\right]$ and the voltages and currents at the transmitting or at the receiving end may also be derived through:

$$\left[\chi_I^{(p)}\right]=e^{-[\Psi_I]l}.\left[\mathbf{K}_I^{(p)}\right].e^{-[\Psi_I]l} \tag{5.73}$$

For particular applications the phase voltages and currents at any point along the transmission line may be expressed through the voltages or currents at the receiving end.

In the next section, two additional forms are derived which are particularly useful for several applications.

5.1.4.3 Input and transfer phase impedances/admittances

Solving Eqn.(5.72) for $\left[\mathbf{V}^{(p)}(0)\right]$ and substituting into Eqn.(5.71) yields:

$$\left[\mathbf{V}^{(p)}(x)\right]=\left(e^{-[\Psi_v]x}+e^{-[\Psi_v](l-x)}.\left[\mathbf{K}_V^{(p)}\right].e^{-[\Psi_v]l}\right).\left(e^{-[\Psi_v]x}-e^{-[\Psi_v](l-x)}.\left[\mathbf{K}_V^{(p)}\right].e^{-[\Psi_v]l}\right)^{-1}.\left[\mathbf{Z}_o^{(p)}\right].\left[\mathbf{I}^{(p)}(x)\right] \tag{5.74}$$

from where it follows that the MTL phase input impedance looking into the transmission line at point x towards the receiving end may be defined as:

$$\left[\mathbf{Z}_{inp}^{(p)}(x)\right]=\left(e^{-[\Psi_v]x}+e^{-[\Psi_v](l-x)}.\left[\mathbf{K}_V^{(p)}\right].e^{-[\Psi_v]l}\right).\left(e^{-[\Psi_v]x}-e^{-[\Psi_v](l-x)}.\left[\mathbf{K}_V^{(p)}\right].e^{-[\Psi_v]l}\right)^{-1}.\left[\mathbf{Z}_o^{(p)}\right] \tag{5.75}$$

Alternatively, the phase input impedance can be expressed through the current phase reflection operator as:

$$\left[\mathbf{Z}_{inp}^{(p)}(x)\right]=\left[\mathbf{Z}_0^{(p)}\right].\left(e^{-[\Psi_I]x}+e^{-[\Psi_I](l-x)}.\left[\mathbf{K}_I^{(p)}\right].e^{-[\Psi_I]l}\right).\left(e^{-[\Psi_I]x}-e^{-[\Psi_I](l-x)}.\left[\mathbf{K}_I^{(p)}\right].e^{-[\Psi_I]l}\right)^{-1} \tag{5.76}$$

At x = 0, Eqns. (5.75) and (5.76) yield

$$\left[\mathbf{Z}_{inp}^{(p)}(0)\right]=\left(\left[1\right]+\left[\chi_V^{(p)}\right]\right).\left(\left[1\right]-\left[\chi_V^{(p)}\right]\right)^{-1}.\left[\mathbf{Z}_0^{(p)}\right] \tag{5.77}$$

$$\left[\mathbf{Z}_{inp}^{(p)}(0)\right]=\left[\mathbf{Z}_o^{(p)}\right].\left(\left[1\right]+\left[\chi_I^{(p)}\right]\right).\left(\left[1\right]-\left[\chi_I^{(p)}\right]\right)^{-1} \tag{5.78}$$

The above two formulae can be applied for the calculation of the matrix $\left[\mathbf{Z}_{inp_{D(i)}}^{II^{(p)}}\right]$ which is necessary for the calculation of the phase reflection and refraction operators.

Additional expressions may be obtained for the input admittance as follows:

$$\left[\mathbf{Y}_{inp}^{(p)}(x)\right]=\left[\mathbf{Y}_0^{(p)}\right].\left(e^{-[\Psi_v]x}-e^{-[\Psi_v](l-x)}.\left[\mathbf{K}_V^{(p)}\right].e^{-[\Psi_v]l}\right).\left(e^{-[\Psi_v]x}-e^{-[\Psi_v](l-x)}.\left[\mathbf{K}_V^{(p)}\right].e^{-[\Psi_v]l}\right)^{-1} \tag{5.79}$$

$$\left[\mathbf{Y}_{inp}^{(p)}(0)\right]=\left[\mathbf{Y}_0^{(p)}\right].\left(\left[1\right]-\left[\chi_V^{(p)}\right]\right).\left(\left[1\right]+\left[\chi_V^{(p)}\right]\right)^{-1} \tag{5.80}$$

Using the phase reflection operator, the relationship between the transmitting end voltage and the receiving end current becomes

$$\left[\mathbf{V}^{(p)}(0)\right]=\left[\mathbf{V}_{inc}^{(p)}(0)\right]+\left[\mathbf{V}_{refl}^{(p)}(0)\right]=e^{[\Psi_v]l}.\left[\mathbf{V}_{inc}^{(p)}(1)\right]+e^{-[\Psi_v]l}.\left[\mathbf{K}_V^{(p)}\right].\left[\mathbf{V}_{inc}^{(p)}(1)\right]=$$

$$\left(e^{[\Psi_v]l}+e^{-[\Psi_v]l}.\left[\mathbf{K}_V^{(p)}\right]\right).\left[\mathbf{Z}_o^{(p)}\right].\left[\mathbf{I}_{inc}^{(p)}(1)\right]=\left(e^{[\Psi_v]l}+e^{-[\Psi_v]l}.\left[\mathbf{K}_V^{(p)}\right]\right).\left[\mathbf{Z}_o^{(p)}\right]\left(\left[1\right]-\left[\mathbf{K}_I^{(p)}\right]\right)^{-1}.\left[\mathbf{I}^{(p)}(1)\right] \tag{5.81}$$

By comparison of Eqn.(5.81) with the equation

$$\left[\mathbf{V}^{(p)}(0)\right]=\left[\mathbf{Z}_{transf}^{(p)}\right].\left[\mathbf{I}^{(p)}(1)\right] \tag{5.83}$$

the MTL phase transfer impedance may be defined as:

$$\left[\mathbf{Z}_{transf}^{(p)}\right]=\left(e^{[\Psi_v]l}+e^{-[\Psi_v]l}.\left[\mathbf{K}_V^{(p)}\right]\right).\left[\mathbf{Z}_o^{(p)}\right].\left(\left[1\right]-\left[\mathbf{K}_I^{(p)}\right]\right)^{-1} \tag{5.84}$$

$\left[\mathbf{Z}_{transf}^{(p)}\right]$ represents an equivalent impedance which can substitute for the transmission line between the transmitting and receiving ends. At alternative expression for the phase transfer impedance can be obtained using the phase load impedance matrix $\left[\mathbf{Z}_{Rx}^{(p)}\right]$:

$$\left[\mathbf{Z}_{transf}^{(p)}\right]=\left(e^{[\Psi_v]l}+e^{-[\Psi_v]l}.\left[\mathbf{K}_V^{(p)}\right]\right).\left(\left[1\right]-\left[\mathbf{K}_V^{(p)}\right]\right)^{-1}.\left[\mathbf{Z}_{Rx}^{(p)}\right] \tag{5.85}$$

5.1.4.4 Two-port formulation of the transmission line solution

The two-port representation of a transmission line (Fig.5.2) gives a convenient model for problems concerned with the input-output transfer function of the transmission line.

One method of deriving the two-port formulation is to apply the boundary conditions to Eqns.(5.3.1) and (5.22.2) to determine the column matrices of the coefficients of integration.

$$\left[\mathbf{I}^{(p)}(0)\right] = \left[\mathbf{Y}_o^{(p)}\right].\left(\left[\mathbf{V}^{p+}\right] - \left[\mathbf{V}^{p-}\right]\right) \tag{5.87}$$

- At x = l, Eqns.(5.3.1) and (5.22.2) give

$$\left[\mathbf{V}^{(p)}(l)\right] = e^{-[\Psi_v]l}.\left[\mathbf{V}^{p+}\right] + e^{[\Psi_v]l}.\left[\mathbf{V}^{p-}\right] \tag{5.88}$$

$$\left[\mathbf{I}^{(p)}(l)\right] = \left[\mathbf{Y}_o^{(p)}\right]\left(e^{-[\Psi_v]l}.\left[\mathbf{V}^{p+}\right] - e^{[\Psi_v]l}.\left[\mathbf{V}^{p-}\right]\right) \tag{5.89}$$

Solving Eqns.(5.86) and (5.87) for $\mathbf{V}^{p+}$ and $\mathbf{V}^{p-}$ and substituting into Eqns.(5.88) and (5.89) gives, after manipulation, the following matrix equation:

$$\begin{bmatrix}\left[\mathbf{V}^{(p)}(l)\right] \\ \left[\mathbf{I}^{(p)}(l)\right]\end{bmatrix} = \begin{bmatrix}\left[\tilde{\mathbf{A}}_{TL}^{(p)}\right] & \left[\tilde{\mathbf{B}}_{TL}^{(p)}\right] \\ \left[\tilde{\mathbf{C}}_{TL}^{(p)}\right] & \left[\tilde{\mathbf{D}}_{TL}^{(p)}\right]\end{bmatrix}.\begin{bmatrix}\left[\mathbf{V}^{(p)}(0)\right] \\ \left[\mathbf{I}^{(p)}(0)\right]\end{bmatrix} =$$

$$= \begin{bmatrix} \cosh\left(\left[\Psi_v\right]l\right) & -\sinh\left(\left[\Psi_v\right]l\right).\left[\mathbf{Z}_o^{(p)}\right] \\ -\left[\mathbf{Z}_o^{(p)}\right]^{-1}.\sinh\left(\left[\Psi_v\right]l\right). & \left[\mathbf{Z}_o^{(p)}\right]^{-1}.\sinh\left(\left[\Psi_v\right]l\right).\left[\mathbf{Z}_o^{(p)}\right] \end{bmatrix}.\begin{bmatrix}\left[\mathbf{V}^{(p)}(0)\right] \\ \left[\mathbf{I}^{(p)}(0)\right]\end{bmatrix} \tag{5.90}$$

The above equation represents the inverse transmission parameter formulation of the two-port equations. All six two-port formulations of a MTL can be derived by noting that the matrix hyperbolic functions and their inverses & squares are commutative .The resulting parameter set is given in Table 5.2-a. The full forms of the two-port equations are identical with those of a two-port multipole network (Table B.1 in Appendix B), using the notation for the transmission line voltages and currents shown in Fig.5.2.

(a) Two-port network notation

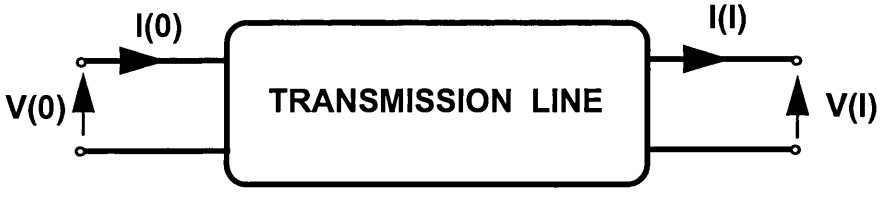

(b) Transmission line notation

FIG.5.2 Convention for two-port network formulation of a transmission line

TABLE 5.2-a: Multiconductor transmission line two-port equations in phase quantities

Open circuit impedance parameters
$\left[\mathbf{Z}_{TL}^{(p)}\right] = \begin{bmatrix} \coth\left(\left[\Psi_v\right]l\right).\left[\mathbf{Z}_o^{(p)}\right] & \left(\sinh\left(\left[\Psi_v\right]l\right)\right)^{-1}.\left[\mathbf{Z}_o^{(p)}\right] \\ \left(\sinh\left(\left[\Psi_v\right]l\right)\right)^{-1}.\left[\mathbf{Z}_o^{(p)}\right] & \coth\left(\left[\Psi_v\right]l\right).\left[\mathbf{Z}_o^{(p)}\right] \end{bmatrix}$
Short circuit admittance parameters
$\left[\mathbf{Y}_{TL}^{(p)}\right] = \begin{bmatrix} \left[\mathbf{Z}_o^{(p)}\right]^{-1}.\coth\left(\left[\Psi_v\right]l\right) & -\left[\mathbf{Z}_o^{(p)}\right]^{-1}.\left(\sinh\left(\left[\Psi_v\right]l\right)\right)^{-1} \\ -\left[\mathbf{Z}_o^{(p)}\right]^{-1}.\left(\sinh\left(\left[\Psi_v\right]l\right)\right)^{-1} & \left[\mathbf{Z}_o^{(p)}\right]^{-1}.\coth\left(\left[\Psi_v\right]l\right) \end{bmatrix}$
Transmission (chain or ABCD) parameters
$\left[\mathbf{T}_{TL}^{(p)}\right] = \begin{bmatrix} \cosh\left(\left[\Psi_v\right]l\right) & \sinh\left(\left[\Psi_v\right]l\right).\left[\mathbf{Z}_o^{(p)}\right] \\ \left[\mathbf{Z}_o^{(p)}\right]^{-1}.\sinh\left(\left[\Psi_v\right]l\right) & \left[\mathbf{Z}_o^{(p)}\right]^{-1}.\cosh\left(\left[\Psi_v\right]l\right).\left[\mathbf{Z}_o^{(p)}\right] \end{bmatrix}$
Inverse transmission parameters
$\left[\mathbf{B}\right]_{TL}^{(p)} = \begin{bmatrix} \cosh\left(\left[\Psi_v\right]l\right) & \sinh\left(\left[\Psi_v\right]l\right).\left[\mathbf{Z}_o^{(p)}\right] \\ \left[\mathbf{Z}_o^{(p)}\right]^{-1}.\sinh\left(\left[\Psi_v\right]l\right) & \left[\mathbf{Z}_o^{(p)}\right]^{-1}.\cosh\left(\left[\Psi_v\right]l\right).\left[\mathbf{Z}_o^{(p)}\right] \end{bmatrix}$
Hybrid parameters
$\left[\mathbf{H}_{TL}^{(p)}\right] = \begin{bmatrix} \tanh\left(\left[\Psi_v\right]l\right).\left[\mathbf{Z}_o^{(p)}\right] & \left(\cosh\left(\left[\Psi_v\right]l\right)\right)^{-1} \\ -\left[\mathbf{Z}_o^{(p)}\right]^{-1}.\left(\cosh\left(\left[\Psi_v\right]l\right)\right)^{-1}.\left[\mathbf{Z}_o^{(p)}\right] & \left[\mathbf{Z}_o^{(p)}\right]^{-1}.\tanh\left(\left[\Psi_v\right]l\right) \end{bmatrix}$
Inverse hybrid parameters
$\left[\mathbf{G}_{TL}^{(p)}\right] = \begin{bmatrix} \left[\mathbf{Z}_o^{(p)}\right].\tanh\left(\left[\Psi_v\right]l\right) & -\left[\mathbf{Z}_o^{(p)}\right]^{-1}.\left(\cosh\left(\left[\Psi_v\right]l\right)\right)^{-1}.\left[\mathbf{Z}_o^{(p)}\right] \\ \left(\cosh\left(\left[\Psi_v\right]l\right)\right)^{-1} & \tanh\left(\left[\Psi_v\right]l\right).\left[\mathbf{Z}_o^{(p)}\right] \end{bmatrix}$

TABLE 5.2-b: Two-port equations parameters of a MTL equivalent multphase/multimode T- and p- lumped parameter networks

Multiphase/multimode T sections

Open circuit impedance parameters
$\left[\mathbf{Z}^{*}_{\mathrm{TL_T}}\right]=\begin{bmatrix}\left[\mathbf{Z}^{*}_{\mathrm{T1}}\right]+\left[\mathbf{Z}^{*}_{\mathrm{T2}}\right] & -\left[\mathbf{Z}^{*}_{\mathrm{T2}}\right]\\ \left[\mathbf{Z}^{*}_{\mathrm{T2}}\right] & -\left(\left[\mathbf{Z}^{*}_{\mathrm{T1}}\right]+\left[\mathbf{Z}^{*}_{\mathrm{T2}}\right]\right)\end{bmatrix}$
Transmission (ABCD) parameters
$\left[\mathbf{T}^{*}_{\mathrm{TL_T}}\right]=\begin{bmatrix}\left[\mathbf{Z}^{*}_{\mathrm{T1}}\right].\left[\mathbf{Z}^{*}_{\mathrm{T2}}\right]^{-1}+[1] & \left[\mathbf{Z}^{*}_{\mathrm{T1}}\right].\left(\left[\mathbf{Z}^{*}_{\mathrm{T2}}\right]^{-1}.\left[\mathbf{Z}^{*}_{\mathrm{T1}}\right]+2[1]\right)\\ \left[\mathbf{Z}^{*}_{\mathrm{T2}}\right]^{-1} & \left[\mathbf{Z}^{*}_{\mathrm{T2}}\right]^{-1}.\left[\mathbf{Z}^{*}_{\mathrm{T1}}\right]+[1]\end{bmatrix}$
Inverse transmission parameters
$\left[\mathbf{B}^{*}_{\mathrm{TL_T}}\right]=\begin{bmatrix}\left[\mathbf{Z}^{*}_{\mathrm{T1}}\right].\left[\mathbf{Z}^{*}_{\mathrm{T2}}\right]^{-1}+[1] & -\left[\mathbf{Z}^{*}_{\mathrm{T1}}\right].\left(\left[\mathbf{Z}^{*}_{\mathrm{T2}}\right]^{-1}.\left[\mathbf{Z}^{*}_{\mathrm{T1}}\right]+2[1]\right)\\ -\left[\mathbf{Z}^{*}_{\mathrm{T2}}\right]^{-1} & \left[\mathbf{Z}^{*}_{\mathrm{T2}}\right]^{-1}.\left[\mathbf{Z}^{*}_{\mathrm{T1}}\right]+[1]\end{bmatrix}$
$\left[\mathbf{Z}^{*}_{\mathrm{T1}}\right]=\tanh\left(0.5\left[\Psi_{\mathrm{v}}\right]l\right).\left[\mathbf{Z}^{*}_{\mathrm{o}}\right]$ $\qquad$ $\left[\mathbf{Z}^{*}_{\mathrm{T2}}\right]=\sinh\left(\left[\Psi_{\mathrm{v}}\right]l\right).\left[\mathbf{Z}^{*}_{\mathrm{o}}\right]$

Multiphase/multimode π-sections

Short circuit admittance parameters
$\left[\mathbf{Y}^{*}_{\mathrm{TL}_\pi}\right]=\begin{bmatrix}\left[\mathbf{Y}^{*}_{\pi1}\right]+\left[\mathbf{Y}^{*}_{\pi2}\right] & -\left[\mathbf{Y}^{*}_{\pi2}\right]\\ \left[\mathbf{Y}^{*}_{\pi2}\right] & -\left(\left[\mathbf{Y}^{*}_{\pi1}\right]+\left[\mathbf{Y}^{*}_{\pi2}\right]\right)\end{bmatrix}$
Transmission (ABCD) parameters
$\left[\mathbf{T}^{*}_{\mathrm{TL}_\pi}\right]=\begin{bmatrix}\left[\mathbf{Y}^{*}_{\pi2}\right]^{-1}.\left[\mathbf{Y}^{*}_{\pi1}\right]+[1] & \left[\mathbf{Y}^{*}_{\pi2}\right]^{-1}\\ \left[\mathbf{Y}^{*}_{\pi1}\right].\left(\left[\mathbf{Y}^{*}_{\pi2}\right]^{-1}.\left[\mathbf{Y}^{*}_{\pi1}\right]+2.[1]\right) & \left[\mathbf{Y}^{*}_{\pi1}\right].\left[\mathbf{Y}^{*}_{\pi2}\right]^{-1}+[1]\end{bmatrix}$
Inverse transmission parameters
$\left[\mathbf{B}^{*}_{\mathrm{TL}_\pi}\right]=\begin{bmatrix}\left[\mathbf{Y}^{*}_{\pi2}\right]^{-1}.\left[\mathbf{Y}^{*}_{\pi1}\right]^{-1}+[1] & -\left[\mathbf{Y}^{*}_{\pi2}\right]^{-1}.\\ -\left[\mathbf{Y}^{*}_{\pi1}\right].\left(\left[\mathbf{Y}^{*}_{\pi2}\right]^{-1}.\left[\mathbf{Y}^{*}_{\pi1}\right]+2.[1]\right) & \left[\mathbf{Y}^{*}_{\pi1}\right].\left[\mathbf{Y}^{*}_{\pi2}\right]^{-1}+[1]\end{bmatrix}$
$\left[\mathbf{Y}^{*}_{\pi1}\right]=\left[\mathbf{Z}^{*}_{\mathrm{o}}\right]^{-1}.\tanh\left(0.5\left[\Psi_{\mathrm{v}}\right]l\right)$ $\qquad$ $\left[\mathbf{Y}^{*}_{\pi2}\right]=\left[\mathbf{Z}^{*}_{\mathrm{o}}\right]^{-1}.\sinh\left(\left[\Psi_{\mathrm{v}}\right]l\right)^{-1}$

Note: The superscript (*) stands for (p) or (m)

FIG.5.3 Equivalent lumped parameter networks of a section of transmission line in the phase domain

	Equivalent lumped parameter networks of a transmission line section	
	SymmetricT-network	Symmetric π-network
Single phase transm. line	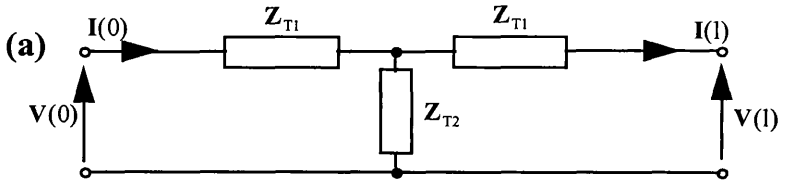	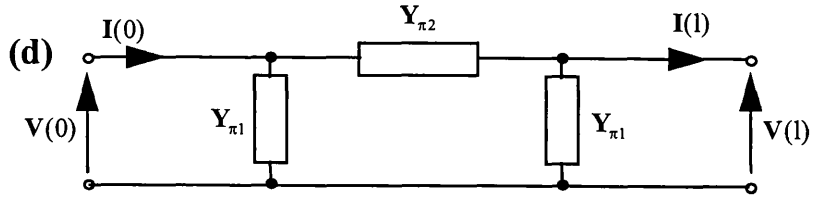
MTL desribed in phase quantities	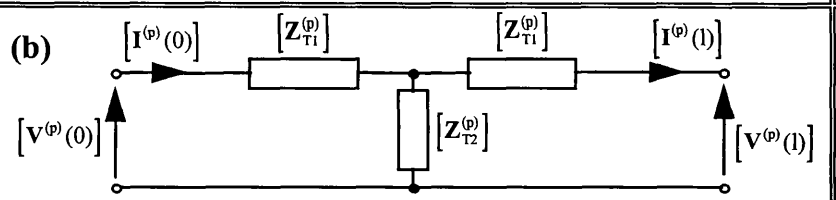 $[Z^{(p)}_{T1}] = \tanh(0.5[\Psi_V]l).[Z^{(p)}_o]$ $[Z^{(p)}_{T2}] = (\sinh(0.5[\Psi_V]l))^{-1}.[Z^{(p)}_o]$	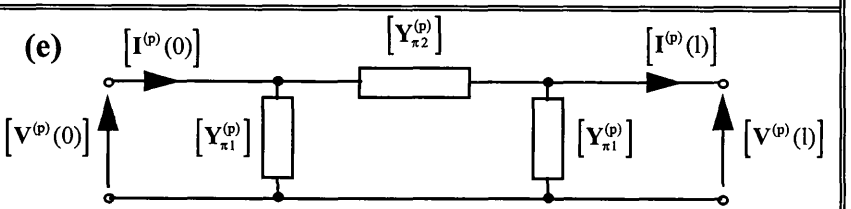 $[Y^{(p)}_{\pi 1}] = [Z^{(p)}_o]^{-1}.\tanh(0.5[\Psi_V]l)$ $[Y^{(p)}_{\pi 2}] = [Z^{(p)}_o].(\sinh(0.5[\Psi_V]l))^{-1}$
MTL desribed in modal quantities	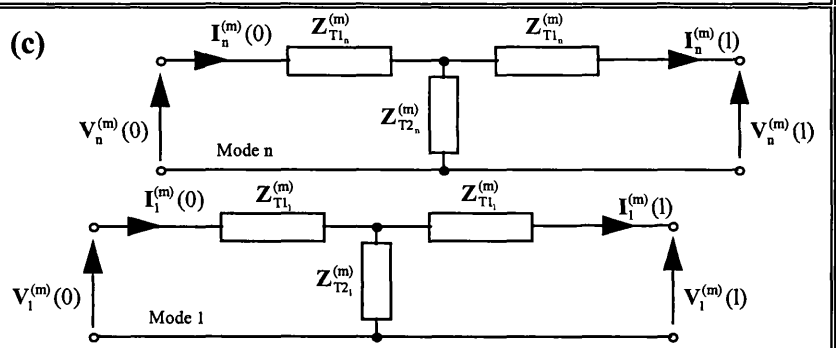 $Z^{(m)}_{Tl_i} = \tanh(0.5\gamma_i l).Z^{(m)}_{o_i}$ $Z^{(m)}_{T2_i} = (\sinh(0.5\gamma_i l))^{-1}.Z^{(m)}_o$	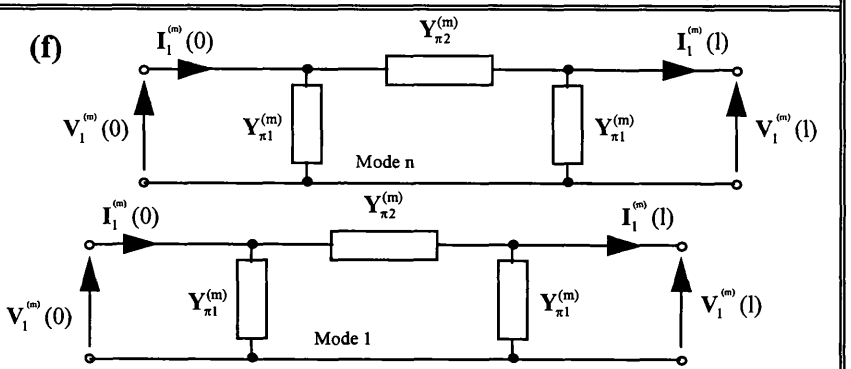 $Y^{(m)}_{\pi l_i} = Z^{(m)^{-1}}_o.\tanh(0.5\gamma_i l)$ $Y^{(m)}_{\pi 2_i} = Z^{(m)}_o.(\sinh(0.5\gamma_i l))^{-1}$

Consider the Z-form of two port equations:

$$\left[\mathbf{V}^{(p)}(0)\right]=\left[\mathbf{Z}^{(p)}_{TL_{I,I}}\right].\left[\mathbf{I}^{(p)}(0)\right]+\left[\mathbf{Z}^{(p)}_{TL_{I,II}}\right].\left[\mathbf{I}^{(p)}(l)\right] \tag{5.91.1}$$

$$\left[\mathbf{V}^{(p)}(l)\right]=\left[\mathbf{Z}^{(p)}_{TL_{II,I}}\right].\left[\mathbf{I}^{(p)}(0)\right]+\left[\mathbf{Z}^{(p)}_{TL_{II,II}}\right].\left[\mathbf{I}^{(p)}(l)\right] \tag{5.91.2}$$

Substituting $\left[\mathbf{V}^{(p)}(l)\right]$ by $\left[\mathbf{Z}^{(p)}_{Rx}\right].\left[\mathbf{I}^{(p)}(l)\right]$ yields two equations with three unknowns. Eliminating $\left[\mathbf{I}^{(p)}(l)\right]$ gives:

$$\left[\mathbf{V}^{(p)}(0)\right]=\left[\left[\mathbf{Z}^{(p)}_{TL_{I,I}}\right]+\left[\mathbf{Z}^{(p)}_{TL_{II,I}}\right].\left(\left[\mathbf{Z}^{(p)}_{Rx}\right]+\left[\mathbf{Z}^{(p)}_{TL_{II,II}}\right]\right)^{-1}.\left[\mathbf{Z}^{(p)}_{TL_{II,I}}\right]\right].\left[\mathbf{I}^{(p)}(l)\right] \tag{5.92.1}$$

and eliminating $\left[\mathbf{I}^{(p)}(0)\right]$ gives:

$$\left[\mathbf{V}^{(p)}(0)\right]=\left[\left[\mathbf{Z}^{(p)}_{TL_{I,I}}\right].\left[\mathbf{Z}^{(p)}_{TL_{II,I}}\right]^{-1}.\left(\left[\mathbf{Z}^{(p)}_{Rx}\right]+\left[\mathbf{Z}^{(p)}_{TL_{II,II}}\right]\right)-\left[\mathbf{Z}^{(p)}_{TL_{I,II}}\right]\right].\left[\mathbf{I}^{(p)}(l)\right] \tag{5.92.2}$$

From Eqns.(5.92.1) and (5.92.2), alternative expressions for the input and transfer impedance, not involving the reflection operators, can be derived.

The derivation method for the transfer characteristics between the MTL transmitting and receiving end terminals derived above can be extended to include the transfer characteristics from the MTL source to the receiver.

Noting that

$$\left[\mathbf{V}^{(p)}(0)\right]=\left[\mathbf{Z}^{(p)}_{inp}(0)\right].\left[\mathbf{I}^{(p)}(0)\right] \tag{5.93}$$

Eqns. (5.23) and (5.24) can be rearranged to yield the following expressions:

$$\begin{bmatrix}\left[\mathbf{V}^{(p)}(0)\right]\\ \left[\mathbf{I}^{(p)}(0)\right]\end{bmatrix}=\begin{bmatrix}\left[\mathbf{Z}^{(p)}_{inp}(0)\right]\\ [1]\end{bmatrix}.\left[\nu^{(p)}_{E}\right].\left[\mathbf{E}^{(p)}_{Tx}\right] \tag{5.93.1}$$

where

$$\left[\nu^{(p)}_{E}\right]=\left(\left[\mathbf{Z}^{(p)}_{Tx}\right]+\left[\mathbf{Z}^{(p)}_{inp}(0)\right]\right)^{-1} \tag{5.93.2}$$

and

$$\begin{bmatrix}\left[\mathbf{V}^{(p)}(0)\right]\\ \left[\mathbf{I}^{(p)}(0)\right]\end{bmatrix}=\begin{bmatrix}\left[\mathbf{Z}^{(p)}_{inp}(0)\right]\\ [1]\end{bmatrix}.\left[\nu^{(p)}_{J}\right].\left[\mathbf{J}^{(p)}_{Tx}\right] \tag{5.94.1}$$

where

$$\left[\nu^{(p)}_{J}\right]=\left(\left[1\right]+\left[\mathbf{Z}^{(p)}_{Tx}\right]^{-1}.\left[\mathbf{Z}^{(p)}_{inp}(0)\right]\right)^{-1} \tag{5.94.2}$$

Substituting Eqn.(5.93.1) or (5.94.1) into the MTL two-port matrix equations (5.90) gives the desired two-port transfer equations between the MTL voltage or current source and the MTL receiver:

$$\begin{bmatrix}\left[\mathbf{V}^{(p)}(l)\right]\\ \left[\mathbf{I}^{(p)}(l)\right]\end{bmatrix}=\left[\mathbf{B}^{(p)}_{TL}\right].\begin{bmatrix}\left[\mathbf{Z}^{(p)}_{inp}(0)\right]\\ -[1]\end{bmatrix}.\left[\nu^{(p)}_{E}\right].\left[\mathbf{E}^{(p)}_{Tx}\right] \tag{5.95}$$

$$\begin{bmatrix}[\mathbf{V}^{(p)}(l)]\\ [\mathbf{I}^{(p)}(l)]\end{bmatrix}=[\mathbf{B}_{TL}^{(p)}].\begin{bmatrix}[\mathbf{Z}_{inp}^{(p)}(0)]\\ -[1]\end{bmatrix}.[\nu_J^{(p)}].[\mathbf{J}_{Tx}^{(p)}] \tag{5.96}$$

The phase source/receiver transfer impedance/admittance can be derived from Eqns.(5.95) and (5.96).

5.1.4.5 Equivalent lumped networks of multiconductor transmission lines

The open circuit impedance formulation of the two-port MTL equations (Table B.1 and Table 5.2) can be represented in the form:

$$\begin{bmatrix}[\mathbf{V}^{(p)}(0)]\\ [\mathbf{I}^{(p)}(0)]\end{bmatrix}=\begin{bmatrix}[\mathbf{Z}_{T1}^{(p)}]+[\mathbf{Z}_{T2}^{(p)}] & -[\mathbf{Z}_{T2}^{(p)}]\\ [\mathbf{Z}_{T2}^{(p)}] & -([\mathbf{Z}_{T1}^{(p)}]+[\mathbf{Z}_{T2}^{(p)}])\end{bmatrix}.\begin{bmatrix}[\mathbf{I}^{(p)}(0)]\\ [\mathbf{I}^{(p)}(l)]\end{bmatrix} \tag{5.97.1}$$

where

$$[\mathbf{Z}_{T1}^{(p)}]=\tanh(0.5[\Psi_v]l).[\mathbf{Z}_o^{(p)}] \tag{5.97.2}$$

and

$$[\mathbf{Z}_{T2}^{(p)}]=\sinh([\Psi_v]l).[\mathbf{Z}_o^{(p)}] \tag{5.97.3}$$

The above matrix equation is identical in form with the system of two scalar mesh equations describing a symmetrical T-network with reference voltages and currents as shown in Fig.5.3-a. On the basis of this identity a section of MTL can be represented with the multiphase T-network shown in generalised form in Fig.5.3-b.

Similarly, a section of MTL can be represented with an equivalent multiphase lumped parameter π-network. It can be derived on the basis of the short circuit admittance form of the MTL two-port equations rearranged in the form:

$$\begin{bmatrix}[\mathbf{I}^{(p)}(0)]\\ [\mathbf{I}^{(p)}(l)]\end{bmatrix}=\begin{bmatrix}[\mathbf{Y}_{\pi1}^{(p)}]+[\mathbf{Y}_{\pi2}^{(p)}] & -[\mathbf{Y}_{\pi2}^{(p)}]\\ [\mathbf{Y}_{\pi2}^{(p)}] & -([\mathbf{Y}_{\pi1}^{(p)}]+[\mathbf{Y}_{\pi2}^{(p)}])\end{bmatrix}.\begin{bmatrix}[\mathbf{V}^{(p)}(0)]\\ [\mathbf{V}^{(p)}(l)]\end{bmatrix} \tag{5.98.1}$$

where

$$[\mathbf{Y}_{\pi1}^{(p)}]=[\mathbf{Z}_o^{(p)}]^{-1}.\tanh(0.5[\Psi_v]l) \tag{5.98.2}$$

and

$$[\mathbf{Y}_{\pi2}^{(p)}]=[\mathbf{Z}_o^{(p)}]^{-1}.\sinh([\Psi_v]l) \tag{5.98.3}$$

The above system of equations is identical in form with the system of two scalar node equations describing the symmetrical π-network shown in Fig.5.3-d. Hence, Eqns.5.98 describe mathematically a multiphase lumped parameter π-network represented in generalised form in Fig.5.3-e.

It should be noted that the equivalent T- and π– multiphase lumped parameter networks of a section of n conductor transmission line above conductive earth plane represent [2 x (n+1)]-pole networks and their representation on Fig.5.3-b and d is only generalised. An exact network representation of these T- and π– multiphase networks in which the

network components are expressed through the elements of the $\left[\mathbf{Z}_{T1}^{(p)}\right]$ and $\left[\mathbf{Z}_{T2}^{(p)}\right]$ or $\left[\mathbf{Y}_{\pi 1}^{(p)}\right]$ and $\left[\mathbf{Y}_{\pi 2}^{(p)}\right]$ correspondingly is in principle possible but being very complicated is not convenient for practical application. The equivalent T- and π– multiphase networks are more often used with their mathematical description and more particularly in the form of the transmission or inverse transmission two-port equations. The $\left[\mathbf{T}_{TL}^{(p)}\right]$ and $\left[\mathbf{B}_{TL}^{(p)}\right]$ parameters of the T- and π– multiphase networks can be derived from Eqns.(5.97) and (5.98) and are given in Table 5.2-b for reference.

5.1.5 Numerical computation

The numerical computation of the different matrix quantities describing multiconductor transmission lines involves calculation of an exponential function with a matrix argument in addition to functions using such matrix exponents hyperbolic trigonometric functions.

The matrix exponential function of [A] is defined by the following power series:

$$e^{[A]} = [1] + \frac{[A]}{1!} + \frac{[A]^2}{2!} + \frac{[A]^3}{3!} + \ldots = \sum_{k=0}^{k=\infty} \frac{[A]^k}{k!} \tag{5.99}$$

To avoid overflow, the matrix functions are usually expressed in terms of negative exponents, or $e^{-[A]}$.

An alternative method for the calculation of $e^{[A]}$, and of the matrix functions, is to apply Sylvester's theorem [5-2]. According to this theorem, if F([A]) is a function with a matrix argument, and the matrix has distinct eigenvalues, then

$$F([M]) = \sum \frac{F(\mu_k)}{p'(\mu_k)} . [A(\mu_k)] \tag{5.100}$$

where:

[M] is a square matrix of order (n,n)

μ_k, k = 1,2..n are the eigenvalues of the matrix [M]

$A(\mu_k)$ is the eigenvector corresponding to the eigenvalue μ_k

$p'(\mu) = \frac{dp}{d\mu} . \mu$, evaluated at $\mu = \mu_k$

$p(\mu)$ is the characteristic polynomial.

The above technique requires determination of the eigenvalues and the eigenvectors of the matrix comprising the argument of the matrix function. Solution of the wave differential equations by determining the eigenvalues of the phase propagation matrix leads to the concept of natural modes. This procedure provides an insight into the process of wave propagation along multiconductor transmission lines, and will be considered in detail in the next section.

5.2 APPLICATION OF THE THEORY OF NATURAL MODES FOR THE ANALYSIS OF MULTICONDUCTOR TRANSMISSION LINES

5.2.1 Solution of the wave equations by diagonalisation

The MTL wave equations given in Eqns.(5.2) may be expressed in the form

$$\frac{\left[d^2\left[\mathbf{V}^{(p)}(x)\right]\right]}{dx^2} = [\mathbf{P}].\left[\mathbf{V}^{(p)}(x)\right] \tag{5.101.1}$$

$$\frac{\left[d^2\left[\mathbf{I}^{(p)}(x)\right]\right]}{dx^2} = [\mathbf{P}]^T.\left[\mathbf{I}^{(p)}(x)\right] \tag{5.101.2}$$

where

$$[\mathbf{P}] = \left[\mathbf{Z}^{(p)}\right].\left[\mathbf{Y}^{(p)}\right] = [\Psi_V]^2 \tag{5.102.1}$$

$$[\mathbf{P}]^T = \left[\mathbf{Y}^{(p)}\right].\left[\mathbf{Z}^{(p)}\right] = [\Psi_I]^2 \tag{5.102.1}$$

Matrices $[\mathbf{P}]$ and $[\mathbf{P}]^T$ are (n,n)-order non-diagonal matrices. Hence the phase voltages and currents are mutually coupled, i.e. the derivative of any phase voltage or current depends on all the other phase voltages or currents. One way of solving the system of equations (5.98) is to change the variables $\left[\mathbf{V}^{(p)}\right]$ and $\left[\mathbf{I}^{(p)}\right]$ such that the phase equations become decoupled. This implies that the variables and their derivatives should be related by a diagonal matrix. A matrix $[\mathbf{P}]$ can be converted to an alternative form (say $[\tilde{\mathbf{P}}]$) by applying a similarity transformation given by the equation

$$[\tilde{\mathbf{P}}] = [\mathbf{W}]^{-1}.[\mathbf{P}].[\mathbf{W}] \tag{5.103}$$

where $[\mathbf{W}]$ is a non-singular matrix.

In this particular case, the similar, or transformed, matrix should be diagonal, i.e.

$$[\tilde{\mathbf{P}}] = [\Lambda] \tag{5.104}$$

where $[\Lambda]$is a diagonal matrix. Suppose the matrix linking $[\mathbf{P}]$ and its similar diagonal matrix $[\Lambda]$ is some matrix $[\mathbf{S}]$ i.e.

$$[\Lambda] = [\mathbf{S}]^{-1}.[\mathbf{P}].[\mathbf{S}] \tag{5.105.1}$$

then

$$[\mathbf{P}].[\mathbf{S}] = [\mathbf{S}].[\Lambda] \tag{5.105.2}$$

Eqn.(5.105.2) coincides with the form of the equation defining the characteristic vectors and characteristic values of a matrix. It therefore follows that the elements of the diagonal matrix $[\Lambda]$ are the eigenvalues of the matrix $[\mathbf{P}]$ and the columns of matrix $[\mathbf{S}]$

are the right eigenvectors of $[\mathbf{P}]$ calculated for the corresponding eigenvalues. The n eigenvalues can be found by solving the equation

$$\det([\mathbf{P}]-\lambda[1])=1 \tag{5.106}$$

The n corresponding eigenvectors can be obtained from

$$\left[\quad \mathbf{P} \quad\right].\left[\mathbf{S}_i\right]=\lambda_i\left[\mathbf{S}_i\right], \qquad i=1,2\ldots n \tag{5.107.1}$$

or

$$\left[[\mathbf{P}]-\lambda_i[1]\right].\left[\mathbf{S}_i\right]=\left[0\right] \qquad i=1,2\ldots n \tag{5.107.2}$$

which represents a system of n linear homogeneous equations. As the determinant of the square matrix $\left[[\mathbf{P}]-\lambda_i[1]\right]$ vanishes for λ_i, i = 1, 2....n (this follows from the definition of the eigenvalues), the rank of this system of equations is less than the number of unknowns and one of the equations is linear combination of the others. This means that the above system of equations has a non-trivial solution (i.e. different from $[\mathbf{S}_i]=[0]$), which is unique to within a multiplicative constant. In other words any (n-1) elements of an eigen-vector can be expressed in a unique way through the remaining n-th element.

Using a similar procedure, a matrix [**Q**] can be found that transforms the matrix $[\mathbf{P}]^T$ from Eqn.(5.98.2) into a similar diagonal matrix $[\Lambda']$ i.e.

$$[\Lambda']=[\mathbf{Q}]^{-1}.[\mathbf{P}]^T.[\mathbf{Q}] \tag{5.108}$$

The matrices [**P**] and its transpose $[\mathbf{P}]^T$ have equal determinants and hence the same eigenvalues i.e

$$[\Lambda]=[\Lambda'] \tag{5.109}$$

Consequently

$$[\mathbf{P}]^T.[\mathbf{Q}]=[\mathbf{Q}].[\Lambda] \tag{5.110}$$

Transposing the above equation gives

$$[\mathbf{Q}]^T.[\mathbf{P}]=[\Lambda].[\mathbf{Q}]^T \tag{5.111}$$

from which the [**Q**] matrix can be identified as the matrix of the left eigenvalues of matrix [**P**].

Substituting [**P**] from Eqn.(5.105.1) into Eqn.(5.101.1) and $[\mathbf{P}]^T$ from Eqn.(5.108) into Eqn.(5.101.2) yields

$$\frac{d^2\left[\mathbf{V}^{(p)}(x)\right]}{dx^2} = [\mathbf{S}].[\Lambda].[\mathbf{S}]^{-1}.\left[\mathbf{V}^{(p)}(x)\right] \tag{5.112.1}$$

$$\frac{d^2\left[\mathbf{I}^{(p)}(x)\right]}{dx^2} = [\mathbf{Q}].[\Lambda].[\mathbf{Q}]^{-1}.\left[\mathbf{I}^{(p)}(x)\right] \tag{5.112.2}$$

The above equations can be rewritten in the form

$$\frac{d^2\left([\mathbf{S}]^{-1}.\left[\mathbf{V}^{(p)}(x)\right]\right)}{dx^2} = [\Lambda].\left([\mathbf{S}]^{-1}.\left[\mathbf{V}^{(p)}(x)\right]\right) \tag{5.113.1}$$

$$\frac{d^2\left([\mathbf{Q}]^{-1}.\left[\mathbf{I}^{(p)}(x)\right]\right)}{dx^2} = [\Lambda].\left([\mathbf{Q}]^{-1}.\left[\mathbf{I}^{(p)}(x)\right]\right) \tag{5.113.2}$$

which is the required transformed diagonalized formulation of Eqns.(5.98). Introducing the new variables $\left[\mathbf{V}^{(m)}\right]$ and $\left[\mathbf{I}^{(m)}\right]$ defined by

$$\left[\mathbf{V}^{(m)}(x) = [\mathbf{S}]^{-1}.\left[\mathbf{V}^{(p)}(x)\right]\right] \tag{5.114.1}$$

$$\left[\mathbf{I}^{(m)}(x) = [\mathbf{Q}]^{-1}.\left[\mathbf{I}^{(p)}(x)\right]\right] \tag{5.114.2}$$

and defining a matrix $[\gamma]$ such that

$$[\gamma] = \left([\Lambda]\right)^{1/2} \tag{5.115}$$

the MTL wave equations can be written in terms of the transformed variables as follows:

$$\frac{d^2\left[\mathbf{V}^{(m)}(x)\right]}{dx^2} = [\gamma]^2.\left[\mathbf{V}^{(m)}(x)\right] \tag{5.116.1}$$

$$\frac{d^2\left[\mathbf{I}^{(m)}(x)\right]}{dx^2} = [\gamma]^2.\left[\mathbf{I}^{(m)}(x)\right] \tag{5.116.2}$$

It is apparent that the transformed equations are themselves wave equations, but in diagonal or decoupled form. Each represents a system of n independent scalar equations of the form:

$$\frac{d^2\mathbf{V}_i^{(m)}(x)}{dx^2} = \gamma_i^2.\mathbf{V}_i^{(m)}(x), \qquad i = 1, 2....n \tag{5.117.1}$$

$$\frac{d^2\mathbf{I}_i^{(m)}(x)}{dx^2} = \gamma_i^2.\mathbf{I}_i^{(m)}(x), \qquad i = 1, 2....n \tag{5.117.2}$$

Eqns.(5.117.1) and (5.117.2) can be regarded as a set of n pairs of differential equations, each describing a different single phase transmission line. The solutions for the voltage and the current waves along each line are given by the usual expressions:

$$\mathbf{V}_i^{(m)}(x) = e^{(-\gamma_i.x)}.\mathbf{V}_i^{(m+)} + e^{(\gamma_i.x)}.\mathbf{V}_i^{(m-)}, \qquad i = 1, 2....n \tag{5.118.1}$$

$$\mathbf{I}_i^{(m)}(x) = e^{(-\gamma_i.x)}.\mathbf{I}_i^{(m+)} + e^{(\gamma_i.x)}.\mathbf{I}_i^{(m-)}, \qquad i = 1, 2....n \tag{5.118.2}$$

or in matrix form

$$\left[\mathbf{V}^{(m)}(x)\right] = e^{-[\gamma]x}.\left[\mathbf{V}^{m+}\right] + e^{[\gamma]x}.\left[\mathbf{V}^{m-}\right] \tag{5.119.1}$$

$$\left[\mathbf{I}^{(m)}(x)\right] = e^{-[\gamma]x}.\left[\mathbf{I}^{m+}\right] + e^{[\gamma]x}.\left[\mathbf{I}^{m-}\right] \tag{5.119.2}$$

The original variables can be found using the back transformation equations:

$$\left[\mathbf{V}^{(p)}(x) = [\mathbf{S}].\left[\mathbf{V}^{(m)}(x)\right]\right] \tag{5.120.1}$$

$$\left[\mathbf{I}^{(p)}(x) = [\mathbf{Q}].\left[\mathbf{I}^{(m)}(x)\right]\right] \tag{5.120.2}$$

By inspection of Eqns.(5.117 - 5.118), the propagation of electromagnetic waves along a MTL may be regarded as taking place along a number of a single phase lines, called modes of propagation, there being the same number of modes as the number of distinct eigenvalues of [**P**]. Each propagation mode is uniquely defined by its modal propagation constant γ_i , which is a function of the transmission line parameters only(Eqns.(5.105.1) and (5.115)). The modes are thus known as natural modes. Consequently, the transformed variables are called modal voltages $\left[\mathbf{V}^{(m)}(x)\right]$ and modal currents $\left[\mathbf{I}^{(m)}(x)\right]$, and the transformation matrices [**S**] and [**Q**] are called the voltage and current transformation matrices respectively.

The concept of natural modes of propagation in a MTL is illustrated graphically by Fig.5.4.

To complete the mathematical representation, it is necessary to state certain properties of the transformation matrices. Proof of these properties follows from matrix algebra and can be found in Ref.[G-14].

(1) The [**S**] and [**Q**] matrices are not unique. This follows from the fact that the right, as well as the left eigenvectors can be determined only to within a multiplicative constant. In matrix terms this means that postmultiplying matrices [**S**] and [**Q**] by any diagonal matrix yields other matrices [**S**] and [**Q**] which would also diagonalize matrix [**P**] and its transpose:

$$[\mathbf{S}] = [\mathbf{S}].[\mathbf{D}'] \tag{5.121.1}$$

$$[\mathbf{Q}'] = [\mathbf{Q}].[\mathbf{D}''] \tag{5.121.2}$$

where $[\mathbf{D}']$ and $[\mathbf{D}'']$ are diagonal matrices.

The choice of voltage and current transformation matrices does not affect the MTL mathematical solution, since with the back mode-to-phase transformations their effect is cancelled. However, from the computational point of view, careful choice of the transformation matrices can be advantageous. The process of scaling the matrices by postmultiplying them with a properly chosen diagonal matrix is called normalization.

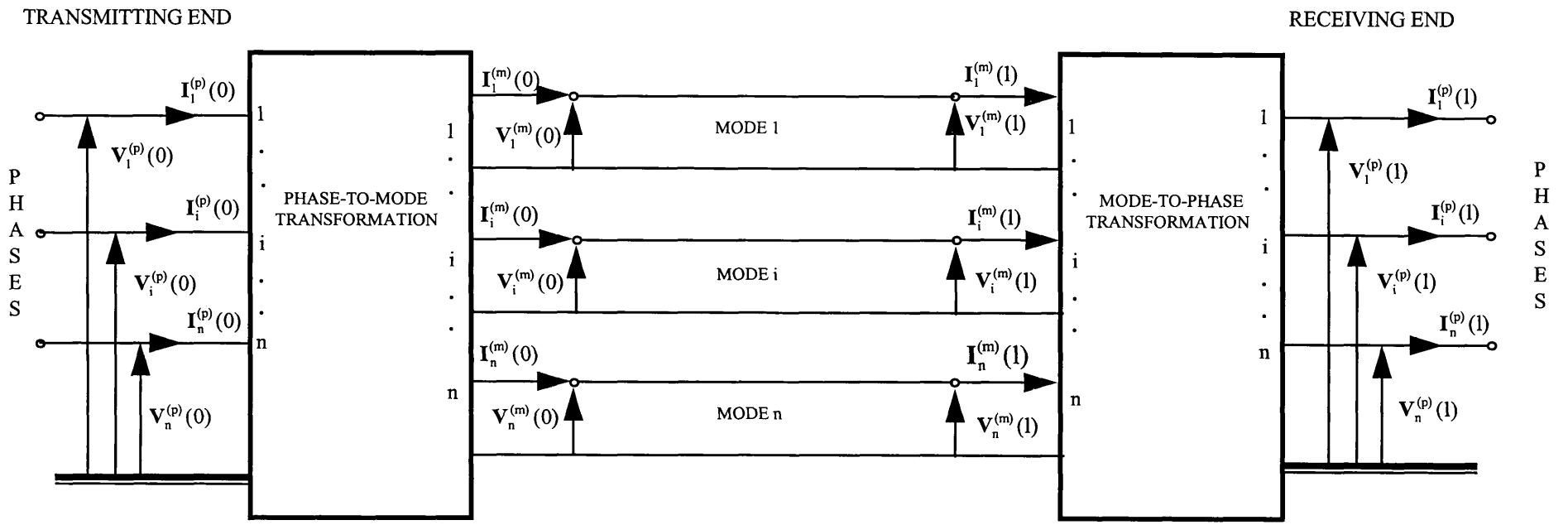

FIG. 5.4 Equivalent diagram of a multiconductor transmission line in the modal domain

(2) If the matrix [**P**] is symmetric, the [**S**] and [**Q**] matrices are related by the equation

$$[\mathbf{S}]=[\mathbf{Q}].[\mathbf{D}] \tag{5.122}$$

(3) The [**S**] and [**Q**] matrices are not orthogonal:

$$[\mathbf{S}].[\mathbf{S}]^{T} \neq [\mathbf{D}] \tag{5.123.1}$$

$$[\mathbf{Q}].[\mathbf{Q}]^{T} \neq [\mathbf{D}] \tag{5.123.2}$$

where [**D**] is a diagonal matrix.

(4) The [**S**] and [**Q**] matrices are not unitary:

$$[\mathbf{S}].[\mathbf{S}]^{*} \neq [\mathbf{D}] \tag{5.124.1}$$

$$[\mathbf{Q}].[\mathbf{Q}]^{*} \neq [\mathbf{D}] \tag{5.124.2}$$

where $[\mathbf{S}]^{*}=\left[\overline{\mathbf{S}}\right]^{T}$ denotes the transpose of the complex conjugate of the matrix [**S**] (similar considerations apply to matrix [**Q**]).

(5) The [**S**] and [**Q**] matrices are mutually orthogonal:

$$[\mathbf{S}]^{T}.[\mathbf{Q}]=[\mathbf{Q}]^{T}.[\mathbf{S}]=[\mathbf{D}] \tag{5.125.1}$$

or, with proper normalization,

$$[\mathbf{S}]^{T}=[\mathbf{Q}]^{-1} \tag{5.125.2.1}$$

$$[\mathbf{Q}]^{T}=[\mathbf{S}]^{-1} \tag{5.125.2.2}$$

(6) The [**S**] and [**Q**] matrices are not mutually unitary:

$$[\mathbf{S}]^{*}.[\mathbf{Q}]=[\mathbf{Q}]^{*}.[\mathbf{S}]\neq[\mathbf{D}] \tag{5.126}$$

5.2.2 Physical interpretation of the natural modes and their properties

The concept of natural modes of propagation in multiconductor transmission lines can have specific physical significance in certain circumstances.

It has been shown in the previous section that at any point of a MTL, the phase voltages and currents can be transformed into natural modes (Eqns.(5.114)), and inversely at any point, the modal voltages and currents can be summed to yield the phase voltages and currents (Eqns.(5.120)). Hence a transmission line consisting of n conductors above a conductive plane can be regarded as having n parallel channels (or modes) for the propagation of electromagnetic waves. These channels are uniquely defined with their own attenuation constants and velocities of propagation, and are specific for a particular MTL. Under these conditions, the phase voltages and currents appearing at the input of the line are first distributed between the channels, then transmitted to the receiving end

where they are again redistributed into the separate phases and supplied to the receiver terminals.

Analysis of the modes of propagation gives an insight into multiphase wave propagation and enables direct practical conclusions to be made. However, as the [**S**] and [**Q**] transformation matrices are defined both in a unique and in a non-unique way, it is necessary to establish some physically measurable quantities which uniquely characterise the modes. It is also of interest to establish what is the physical meaning of the uniqueness/non-uniqueness properties of the process of resolution of phases into modes.

According to Eqns.(5.120), each phase voltage/current can be represented as a linear combination of the modal voltages/currents:

$$\mathbf{V}_i^{(p)} = \sum \mathbf{S}_{ij} . \mathbf{V}_j^{(m)} = \sum_{j=1}^{j=n} \mathbf{V}_{ij}^{(p,m)} \tag{5.127.1}$$

$$\mathbf{I}_i^{(p)} = \sum \mathbf{Q}_{ij} . \mathbf{I}_j^{(m)} = \sum_{j=1}^{j=n} \mathbf{I}_{ij}^{(p,m)} \tag{5.127.2}$$

From the above equations, the elements of the transformation matrices can be given the following definitions:

$\mathbf{S}_{ij}$ defines the portion of the mode j voltage contributing to the phase i voltage

$\mathbf{Q}_{ij}$ defines the portion of the mode j current contributing to the phase i current

$\mathbf{V}_{i,j}^{(p,m)} = \mathbf{S}_{ij} . \mathbf{V}_j^{(m)}$ is the contribution of the mode j voltage in the phase i voltage

$\mathbf{I}_{i,j}^{(p,m)} = \mathbf{Q}_{ij} . \mathbf{I}_j^{(m)}$ is the contribution of the mode j current in the phase i current

Using these definitions and the properties of the [**S**] and [**Q**] matrices, the uniqueness of the modal decomposition process implies a specific relationship between the contributions of each mode (voltage or current) to the different phases (voltages or currents). The non-uniqueness means that each phase (voltage or current) can be regarded as the sum of arbitrary contributions from all modes (voltages or currents).

Furthermore, the ratio of $\mathbf{V}_{ij}^{(p,m)}$ to $\mathbf{I}_{ij}^{(p,m)}$ represents the impedance which phase i presents to mode j. It is:

$$\mathbf{Z}_{ij}^{(p,m)} = \frac{\mathbf{S}_{ij} . \mathbf{V}_j^{(m)}}{\mathbf{Q}_{ij} . \mathbf{I}_j^{(m)}} \tag{5.128}$$

and is known as the surge impedance in phase i due to mode j. It can be expressed as follows (Ref.[G-14]):

$$\mathbf{Z}_{ij}^{(p,m)} = \frac{\sum_{m=1}^{m=n} \mathbf{Z}_{im}^{(p)} \cdot \frac{\mathbf{Q}_{mj}}{\mathbf{Q}_{ij}}}{\sum_{m=1}^{m=n} \mathbf{Y}_{im}^{(p)} \cdot \frac{\mathbf{S}_{mj}}{\mathbf{S}_{ij}}} \qquad (5.129)$$

From Eqn.(5.129) and recalling that the eigenvalues of a matrix are unique, it follows that the modes of propagation existing in a multiconductor transmission line are uniquely defined by their propagation constants γ_i (i = 1, 2 ... n) and a set of n^2 scalar surge impedances $\mathbf{Z}_{ij}^{(p,m)}$ (i = 1, 2 ... n, j = 1, 2 ... n) which depend only on the transmission line parameters.

5.2.3 Modal characteristics. Phase-to-modal and modal-to-phase

The abstract mathematical solution can be developed further by stating the requirements for equivalence of a multiconductor line to a system of single phase transmission lines. The conditions are first, that the same propagation characteristics ensue and second, that there is no mutual coupling with the terminating networks of the single phase lines. The terminating networks have the function of distributing the phases into modes at the sending end, and redistributing the modes into phases at the receiving end. This procedure is illustrated later with a two-conductor transmission line.

A consequence of the above argument is that a single phase transmission line can be regarded as a linear combination of a set of actual transmission line conductors. Thus a system of n wires above a conducting earth is equivalent to n single phase isolated transmission lines which reuse the physical conductors in different configurations. From a modelling viewpoint, the possibility of reducing a multiconductor line to a system of isolated single phase lines is beneficial. The approach requires a full set of quantities characterising the transmission line to be defined for each. The modal propagation constant matrix [γ] has been defined by Eqns.(5.105.1), (5.108), (5.109) and (5.115). Considering Eqns.(5.102) and extracting the square root yields the following two equations relating the phase voltage and current propagation constant matrices with the modal propagation constant matrix:

$$[\gamma] = [\mathbf{S}]^{-1} \cdot [\Psi_V] \cdot [\mathbf{S}] \qquad (5.130.1)$$

$$[\gamma'] = [\gamma] = [\mathbf{Q}]^{-1} \cdot [\Psi_I] \cdot [\mathbf{Q}] \qquad (5.130.2$$

Applying the phase-to-modal transformation (Eqns.5.120) to Eqns.(5.1) gives:

$$[\mathbf{S}] \cdot \frac{d[\mathbf{V}^{(m)}(x)]}{dx} = -[\mathbf{Z}^{(p)}] \cdot [\mathbf{Q}] \cdot [\mathbf{I}^{(m)}(x)] \qquad (5.131.1)$$

$$[\mathbf{Q}] \cdot \frac{d[\mathbf{I}^{(m)}(x)]}{dx} = -[\mathbf{Y}^{(p)}] \cdot [\mathbf{S}] \cdot [\mathbf{V}^{(m)}(x)] \qquad (5.131.2)$$

Manipulating the above equations and introducing the notation

$$[S]^{-1}.[Z^{(p)}].[Q]=[Z^{(m)}] \tag{5.132.1}$$

$$[Q]^{-1}.[Y^{(p)}].[S]=[Y^{(m)}] \tag{5.132.2}$$

yields the pair of MTL first order differential equations in terms of their modal quantities:

$$\frac{d[V^{(m)}(x)]}{dx}=-[Z^{(m)}].[I^{(m)}(x)] \tag{5.133.1}$$

$$\frac{d[I^{(m)}(x)]}{dx}=-[Y^{(m)}].[V^{(m)}(x)] \tag{5.133.2}$$

Expressions (5.132) fit the definition of the modal series impedance matrix and modal shunt admittance matrix if they also satisfy Eqns.(5.117). The condition is equivalent to:

$$[Z^{(m)}].[Y^{(m)}]=[\gamma]^2 \tag{5.134.1}$$

$$[Y^{(m)}].[Z^{(m)}]=[\gamma]^2 \tag{5.134.2}$$

The above equations can be proved correct by substitution using Eqns.(5.102) and (5.130). Hence Eqns. (5.132) define the modal series impedance and modal shunt admittance matrices, and the phase-to-modal & modal-to-phase transformations of the series impedance and shunt admittance matrices.

As the matrix $[\gamma]$ is diagonal, it follows from Eqns.(5.134) that the $[Z^{(m)}]$ and $[Y^{(m)}]$ matrices are also diagonal. Hence the $[\gamma]$, $[Z^{(m)}]$ and $[Y^{(m)}]$ matrices are commutative. This enables definition of the modal characteristic impedance $[Z_o^{(m)}]$ and modal characteristic admittance $[Y_o^{(m)}]$ matrices directly from the scalar formulae of Z_o and Y_o for a single phase transmission line (Table 5.1) by substituting the scalar quantities with their corresponding modal quantities. The formulae obtained are given in column 4 of Table 5.1 and can be checked for consistency with the phase-to-modal transformations by applying the transformations to the formulae of the phase modal characteristic impedance/admittance matrices (column 3 of Table 5.1). The procedure yields in addition the equations relating the phase and modal characteristic impedance/admittance matrices. $[Z_o^{(m)}]$ and $[Y_o^{(m)}]$ are also diagonal since they are the products of two diagonal matrices. Using the definitions of $[Z_o^{(m)}]$ and $[Y_o^{(m)}]$ Eqns.(5.119) can be manipulated as

$$[V^{(m)}]=[Z_o^{(m)}].[\underline{I}^{(m)}] \tag{5.135.1}$$

$$[I^{(m)}]=[Y_o^{(m)}].[\underline{V}^{(m)}] \tag{5.135.2}$$

The primary and secondary parameters of a multiconductor line are defined in the modal domain, so it is straightforward to derive all the other quantities describing the line, such as the reflection and refraction coefficients, input impedance/admittance and transfer impedance. The procedures for their derivation are analogous to those used in Section 5.1 for the description of the multiconductor transmission line in the phase domain. The expressions obtained are also identical in form to those obtained in Section 5.1, and can be directly deduced by substituting the superscript '(p)' by '(m)' and the quantity Ψ_v (Ψ_I) with γ .

In general, it can be shown that any phase quantity with dimensions of impedance, say $\left[\mathbf{Z}^{(p)}\right]$ can be transformed to a corresponding modal quantity, $\left[\mathbf{Z}^{(m)}\right]$, by the equation

$$\left[\mathbf{Z}^{(m)}\right] = [\mathbf{S}]^{-1}.\left[\mathbf{Z}^{(p)}\right].[\mathbf{Q}] \tag{5.136.1}$$

while the inverse transformation is given by the equation

$$\left[\mathbf{Z}^{(p)}\right] = [\mathbf{S}].\left[\mathbf{Z}^{(m)}\right].[\mathbf{Q}]^{-1} \tag{5.136.2}$$

Similarly, the transformation equations for quantities having the dimensions of admittance are as follows:

$$\left[\mathbf{Y}^{(m)}\right] = [\mathbf{Q}]^{-1}.\left[\mathbf{Y}^{(p)}\right].[\mathbf{S}] \tag{5.137.1}$$

$$\left[\mathbf{Y}^{(p)}\right] = [\mathbf{Q}].\left[\mathbf{Z}^{(m)}\right].[\mathbf{S}]^{-1} \tag{5.137.2}$$

The same formulae can also be used to obtain the phase-to-modal and modal-to-phase transformations of all other quantities describing the transmission line since those quantities can always be expressed as functions of voltages, currents and impedances/admittances. Formulae compiled in this way are summarized in Tables 5.3 and 5.4 for reference. Equivalent lumped parameter T- and π -networks in the modal domain can also be derived by applying the phase-to-modal transformation formulae to Eqns.(5.97) and (5.98). This yields for the T- equivalent section

$$\begin{bmatrix}\mathbf{V}^{(m)}(0)\\ \mathbf{V}^{(m)}(1)\end{bmatrix} = \begin{bmatrix}\left[\mathbf{Z}_{T1}^{(m)}\right]+\left[\mathbf{Z}_{T2}^{(m)}\right] & -\left[\mathbf{Z}_{T2}^{(m)}\right]\\ \left[\mathbf{Z}_{T2}^{(m)}\right] & -\left(\left[\mathbf{Z}_{T1}^{(m)}\right]+\left[\mathbf{Z}_{T2}^{(m)}\right]\right)\end{bmatrix}.\begin{bmatrix}\mathbf{I}^{(m)}(0)\\ \mathbf{I}^{(m)}(1)\end{bmatrix} \tag{5.138}$$

where $\left[\mathbf{Z}_{T1}^{(m)}\right] = \tanh\left(0.5.[\gamma]l\right).\left[\mathbf{Z}_o^{(m)}\right]$ and $\left[\mathbf{Z}_{T2}^{(m)}\right] = \left(\sinh\left([\gamma]l\right)\right).\left[\mathbf{Z}_o^{(m)}\right]$,

$$\begin{bmatrix}\mathbf{I}^{(m)}(0)\\ \mathbf{I}^{(m)}(1)\end{bmatrix} = \begin{bmatrix}\left[\mathbf{Y}_{\pi1}^{(m)}\right]+\left[\mathbf{Y}_{\pi2}^{(m)}\right] & -\left[\mathbf{Y}_{\pi2}^{(m)}\right]\\ \left[\mathbf{Y}_{\pi2}^{(m)}\right] & -\left(\left[\mathbf{Y}_{\pi1}^{(m)}\right]+\left[\mathbf{Y}_{\pi2}^{(m)}\right]\right)\end{bmatrix}.\begin{bmatrix}\mathbf{V}^{(m)}(0)\\ \mathbf{V}^{(m)}(1)\end{bmatrix} \tag{5.139}$$

where $\left[\mathbf{Y}_{\pi1}^{(m)}\right] = \left[\mathbf{Z}_o^{(m)}\right]^{-1}.\left(\tanh\left(.[\gamma]l\right)\right)^{-1}$ and $\left[\mathbf{Y}_{\pi2}^{(m)}\right] = \left[\mathbf{Z}_o^{(m)}\right]^{-1}.\left(\sinh\left(.[\gamma]l\right)\right)^{-1}$

TABLE 5.3: Phase -to-modal and mopdal-to-phase tramnsformations of the quantities describing multiconductor transmission lines

Quan-tity	MODAL-TO-PHASE TRANSFORMATIONS	PHASE_TO_MODAL TRANSFORMATIONSS
$\mathbb{V}$	$\left[\mathbf{V}^{(m)}\right]=[\mathbf{S}]^{-1}.\left[\mathbf{V}^{(p)}\right]$	$\left[\mathbf{V}^{(p)}\right]=[\mathbf{S}].\left[\mathbf{V}^{(m)}\right]$
$\mathbb{I}$	$\left[\mathbf{I}^{(m)}\right]=[\mathbf{Q}]^{-1}.\left[\mathbf{I}^{(p)}\right]$	$\left[\mathbf{I}^{(p)}\right]=[\mathbf{Q}].\left[\mathbf{I}^{(m)}\right]$
γ	$[\gamma]=[\mathbf{S}]^{-1}.[\Psi_V].[\mathbf{S}]$ $[\gamma']=[\gamma]=[\mathbf{Q}]^{-1}.[\Psi_I].[\mathbf{Q}]$	$[\Psi_V]=[\mathbf{S}].[\gamma].[\mathbf{S}]^{-1}$ $[\Psi_I]=[\mathbf{Q}].[\gamma].[\mathbf{Q}]^{-1}$
$\mathbb{Z}$ $\mathbb{Y}$	$\left[\mathbf{Z}^{(m)}\right]=[\mathbf{S}]^{-1}.\left[\mathbf{Z}^{(p)}\right].[\mathbf{Q}]$ $\left[\mathbf{Y}^{(m)}\right]=[\mathbf{Q}]^{-1}.\left[\mathbf{Y}^{(p)}\right].[\mathbf{S}]$	$\left[\mathbf{Z}^{(p)}\right]=[\mathbf{S}].\left[\mathbf{Z}^{(m)}\right].[\mathbf{Q}]^{-1}$ $\left[\mathbf{Y}^{(p)}\right]=[\mathbf{Q}].\left[\mathbf{Y}^{(m)}\right].[\mathbf{S}]^{-1}$
$\mathbb{Z}_o$ $\mathbb{Y}_o$	$\left[\mathbf{Z}_o^{(m)}\right]=[\mathbf{S}]^{-1}.\left[\mathbf{Z}_o^{(p)}\right].[\mathbf{Q}]$ $\left[\mathbf{Y}_o^{(m)}\right]=[\mathbf{Q}]^{-1}.\left[\mathbf{Y}_o^{(p)}\right].[\mathbf{S}]$	$\left[\mathbf{Z}_o^{(p)}\right]=[\mathbf{S}].\left[\mathbf{Z}_o^{(m)}\right].[\mathbf{Q}]^{-1}$ $\left[\mathbf{Y}_o^{(p)}\right]=[\mathbf{Q}].\left[\mathbf{Y}_o^{(m)}\right].[\mathbf{S}]^{-1}$
$\mathbb{Z}_{Tx(Rx)}$ $\mathbb{Y}_{Tx(Rx)}$	$\left[\mathbf{Z}_{Tx(Rx)}^{(m)}\right]=[\mathbf{S}]^{-1}.\left[\mathbf{Z}_{Tx(Rx)}^{(p)}\right].[\mathbf{Q}]$ $\left[\mathbf{Y}_{Tx(Rx)}^{(m)}\right]=[\mathbf{Q}]^{-1}.\left[\mathbf{Y}_{Tx(Rx)}^{(p)}\right].[\mathbf{S}]$	$\left[\mathbf{Z}_{Tx(Rx)}^{(p)}\right]=[\mathbf{S}].\left[\mathbf{Z}_{Tx(Rx)}^{(m)}\right].[\mathbf{Q}]^{-1}$ $\left[\mathbf{Y}_{Tx(Rx)}^{(p)}\right]=[\mathbf{Q}].\left[\mathbf{Y}_{Tx(Rx)}^{(m)}\right].[\mathbf{S}]^{-1}$
$\mathbb{K}$	$\left[\mathbf{K}_V^{(m)}(\mathbb{Y})\right]=[\mathbf{S}]^{-1}.\left[\mathbf{K}_V^{(p)}(\mathbb{Y})\right].[\mathbf{S}]$ $\left[\mathbf{K}_V^{(m)}(\mathbb{Z})\right]=[\mathbf{Q}]^{-1}.\left[\mathbf{K}_V^{(p)}(\mathbb{Z})\right].[\mathbf{Q}]$ $\left[\mathbf{K}_I^{(m)}(\mathbb{Y})\right]=[\mathbf{S}]^{-1}.\left[\mathbf{K}_I^{(p)}(\mathbb{Y})\right].[\mathbf{S}]$ $\left[\mathbf{K}_I^{(m)}(\mathbb{Z})\right]=[\mathbf{Q}]^{-1}.\left[\mathbf{K}_I^{(p)}(\mathbb{Z})\right].[\mathbf{Q}]$	$\left[\mathbf{K}_V^{(p)}(\mathbb{Y})\right]=[\mathbf{S}].\left[\mathbf{K}_V^{(m)}(\mathbb{Y})\right].[\mathbf{S}]^{-1}$ $\left[\mathbf{K}_V^{(p)}(\mathbb{Z})\right]=[\mathbf{Q}].\left[\mathbf{K}_V^{(m)}(\mathbb{Z})\right].[\mathbf{Q}]^{-1}$ $\left[\mathbf{K}_I^{(p)}(\mathbb{Y})\right]=[\mathbf{S}].\left[\mathbf{K}_I^{(m)}(\mathbb{Y})\right].[\mathbf{S}]^{-1}$ $\left[\mathbf{K}_I^{(p)}(\mathbb{Z})\right]=[\mathbf{Q}].\left[\mathbf{K}_I^{(m)}(\mathbb{Z})\right].[\mathbf{Q}]^{-1}$
$\mathbb{Z}_{inp}$	$\left[Z_{inp}^{(m)}\right]=[\mathbf{S}]^{-1}.\left[\mathbf{Z}_{inp}^{(p)}\right].[\mathbf{Q}]$	$\left[\mathbf{Z}_{inp}^{(p)}\right]=[\mathbf{S}].\left[\mathbf{Z}_{inp}^{(m)}\right].[\mathbf{Q}]^{-1}$
$\mathbb{Z}_{transf}$	$\left[\mathbf{Z}_{transf}^{(m)}\right]=[\mathbf{S}]^{-1}.\left[\mathbf{Z}_{transf}^{(p)}\right].[\mathbf{Q}]$	$\left[\mathbf{Z}_{transf}^{(p)}\right]=[\mathbf{S}].\left[\mathbf{Z}_{transf}^{(m)}\right].[\mathbf{Q}]^{-1}$

TABLE 5.3 (continuation): Phase-to-modal transformations of a multiconductor transmission line two-port equations

Open circuit impedance parameters
$\left[\mathbf{Z}_{TL}^{(p)}\right] = \begin{bmatrix} [S] & \\ & [S] \end{bmatrix} \cdot \left[\mathbf{Z}_{TL}^{(m)}\right] \cdot \begin{bmatrix} [Q]^{-1} & \\ & [Q]^{-1} \end{bmatrix}$
Short circuit admittance parameters
$\left[\mathbf{Y}_{TL}^{(p)}\right] = \begin{bmatrix} [Q] & \\ & [Q] \end{bmatrix} \cdot \left[\mathbf{Y}_{TL}^{(M)}\right] \cdot \begin{bmatrix} [S]^{-1} & \\ & [S]^{-1} \end{bmatrix}$
Transmission (chain or ABCD) parameters
$\left[\mathbf{T}_{TL}^{(p)}\right] = \begin{bmatrix} [S] & \\ & [Q] \end{bmatrix} \cdot \left[\mathbf{T}_{TL}^{(m)}\right] \cdot \begin{bmatrix} [S]^{-1} & \\ & [Q]^{-1} \end{bmatrix}$
Inverse transmission parameters
$\left[\mathbf{B}_{TL}^{(p)}\right] = \begin{bmatrix} [S] & \\ & [Q] \end{bmatrix} \cdot \left[\mathbf{B}_{TL}^{(m)}\right] \cdot \begin{bmatrix} [S]^{-1} & \\ & [Q]^{-1} \end{bmatrix}$
Hybrid parameters
$\left[\mathbf{H}_{TL}^{(p)}\right] = \begin{bmatrix} [S] & \\ & [Q] \end{bmatrix} \cdot \left[\mathbf{H}_{TL}^{(m)}\right] \cdot \begin{bmatrix} [Q]^{-1} & \\ & [S]^{-1} \end{bmatrix}$
Inverse hybrid parameters
$\left[\mathbf{G}_{TL}^{(p)}\right] = \begin{bmatrix} [Q] & \\ & [S] \end{bmatrix} \cdot \left[\mathbf{G}_{TL}^{(m)}\right] \cdot \begin{bmatrix} [S]^{-1} & \\ & [Q]^{-1} \end{bmatrix}$

TABLE 5.4: Multiconductor transmission line two-port equations in modal quantities

Open circuit impedance parameters
$\mathbf{Z}_{TL}^{(m)} = \begin{bmatrix} \coth([\gamma]l).[\mathbf{Z}_o^{(m)}] & (\sinh([\gamma]l))^{-1}.[\mathbf{Z}_o^{(m)}] \\ (\sinh([\gamma]l))^{-1}.[\mathbf{Z}_o^{(m)}] & \coth([\gamma]l).[\mathbf{Z}_o^{(m)}] \end{bmatrix}$
Short circuit admittance parameters
$\mathbf{Y}_{TL}^{(m)} = \begin{bmatrix} [\mathbf{Z}_o^{(m)}]^{-1}.\coth([\gamma]l) & -[\mathbf{Z}_o^{(m)}]^{-1}.(\sinh([\gamma]l))^{-1} \\ -[\mathbf{Z}_o^{(m)}]^{-1}.(\sinh([\gamma]l))^{-1} & [\mathbf{Z}_o^{(m)}]^{-1}.\coth([\gamma]l) \end{bmatrix}$
Transmission (chain or ABCD) parameters
$\mathbf{T}_{TL}^{(m)} = \begin{bmatrix} \cosh([\gamma]l) & \sinh([\gamma]l).[\mathbf{Z}_o^{(m)}] \\ [\mathbf{Z}_o^{(m)}]^{-1}.\sinh([\gamma]l) & .\cosh([\gamma]l). \end{bmatrix}$
Inverse transmission parameters
$\mathbf{B}_{TL}^{(m)} = \begin{bmatrix} \cosh([\gamma]l) & \sinh([\gamma]l).[\mathbf{Z}_o^{(m)}] \\ [\mathbf{Z}_o^{(m)}]^{-1}.\sinh([\gamma]l) & \cosh([\gamma]l) \end{bmatrix}$
Hybrid parameters
$\mathbf{H}_{TL}^{(m)} = \begin{bmatrix} \tanh([\gamma]l).[\mathbf{Z}_o^{(m)}] & (\cosh([\gamma]l))^{-1} \\ -.(\cosh([\gamma]l))^{-1}. & [\mathbf{Z}_o^{(m)}]^{-1}.\tanh([\gamma]l) \end{bmatrix}$
Inverse hybrid parameters
$\mathbf{G}_{TL}^{(m)} = \begin{bmatrix} [\mathbf{Z}_o^{(m)}]^{-1}.\tanh([\gamma]l) & -(\cosh([\gamma]l))^{-1}. \\ (\cosh([\gamma]l))^{-1} & \tanh([\gamma]l).[\mathbf{Z}_o^{(m)}] \end{bmatrix}$

Equations (5.138) and (5.139) describe the equivalent T- and π -networks of a section of MTL in the modal domain. It can be observed that the matrix components of the $\left[\mathbf{Z}_{T}^{(m)}\right]$ and $\left[\mathbf{Y}_{\pi}^{(m)}\right]$ matrices are diagonal matrices. Hence, each of the above systems of matrix equations can be regarded as a set of n uncoupled pairs of scalar equations each corresponding to a particular mode and describing an independent T- or π - symmetrical network. The sets of all n independent T- or π - networks constitute 2n port networks as those shown in Fig.5.3,c and f. As these figures show the equivalent modal T- and π - networks of a section of MTL have straightforward network representation which can be conveniently used while working in the modal domain. The corresponding modal transmission and inverse transmission parameters may also be derived by phase-to-modal transformation of the formulae given in Table 5.2-b.

5.2.4 Electrically long (infinite) and electrically short MTL

Similarly to the single phase lines in MTL analysis it could prove useful to introduce approximations for electrically long and electrically short lines. For single phase lines the criteria for such approximations are usually expressed through the value of γl (αl) i.e.

$$|\alpha l| \geq 2.3 \tag{5.140}$$

for electrically long or infinite lines and

$$|\gamma l| << 1 \tag{5.141}$$

for electrically short lines. When considering MTL, corresponding criteria can only be introduced in the modal domain of analysis for the following reasons:

- In the phase domain MTL are described in terms of non-diagonal matrices including the voltage and current phase propagation matrices $\left[\Psi_{V}\right]$ and $\left[\Psi_{I}\right]$. In such terms the criteria given with Eqns.(5.140) and (5.141) are meaningless.

- As already stated the propagation of the electromagnetic waves along MTL is effected through several modes uniquely characterised with their modal propagation constants. In the general case the values of these constants may vary in large range and all modes may not satisfy the above criteria simultaneously. This means that strictly speaking the approximations for electrically long or short MTLs have to be understood and applied with respect to every individual mode. Then the following criteria may be introduced:

For electrically long MTLs

$$|\alpha_{i} l| \geq 2.3, \qquad i=1,2....n \tag{5.142}$$

and for electrically short MTLs

$$|\gamma_{i} l| << 1 \qquad i=1,2....n \tag{5.143}$$

The non-fulfilment of one or more of the above conditions may lead to errors. When all modes satisfy the criteria for electrically long or short lines the approximations may be generalised in terms of matrix modal quantities.

If the criteria given with Eqns.(5.142) are satisfied the term $e^{-[\gamma]l}$ can be neglected with respect to the term $e^{[\gamma]l}$ which means that the reflected waves of the modes at the transmitting end of the MTL are negligible. The following approximations apply:

$$\sinh([\gamma]l) = \cosh([\gamma]l) \cong 0.5.e^{[\gamma]l} \tag{5.144}$$

and the transmission two port equations of a MTL reduce to

$$\begin{bmatrix} \mathbf{V}^{(m)}(0) \\ \mathbf{I}^{(m)}(0) \end{bmatrix} = 0.5.e^{[\gamma]l}.\begin{bmatrix} 1 & [\mathbf{Z}^{(m)}] \\ [\mathbf{Z}_o^{(m)}]^{-1} & 1 \end{bmatrix}.\begin{bmatrix} \mathbf{V}^{(m)}(l) \\ \mathbf{I}^{(m)}(l) \end{bmatrix} \tag{5.145}$$

The input impedance of electrically long lines is almost constant and equals the characteristic impedance. It does not depend on the terminating impedance.

$$[\mathbf{Z}_{inp}^{(m)}(0)] \cong [\mathbf{Z}_o^{(m)}] \tag{5.146}$$

By applying the phase-to-modal transformations it can be shown that the relations given with Eqns.(5.143) and (5.144) as well as any other relations which can be derived for electrically long lines are equally valid in the phase domain.

When according to the criteria given with Eqns.(5.141) the modal propagation constants have very small values $(|\gamma_i l| < 0.2)$ the attenuation and phase shift in each mode along the MTL are negligible. The wave propagation processes in such MTL are not well apparent. Instead, such MTL approach lumped parameter circuits and the relations between voltages and currents can be described in terms of the primary parameters. Indeed, for small values of $|\gamma l|$ | the following approximations hold

$$\sinh(\gamma l) \cong (\gamma l) \tag{5.147.1}$$

$$\cosh(\gamma l) \cong 1 \tag{5.147.2}$$

$$\tanh(\gamma l) \cong (\gamma l) \tag{5.147.3}$$

and the expressions for the components of the equivalent T- and π- sections become correspondingly:

$$[\mathbf{Z}_{T1}^{(m)}] = 0.5.[\mathbf{Z}^{(m)}].1 \qquad [\mathbf{Z}_{T2}^{(m)}] = ([\mathbf{Y}^{(m)}].1)^{-1} \tag{5.148.1}$$

$$[\mathbf{Y}_{\pi 1}^{(m)}] = 0.5.[\mathbf{Y}^{(m)}].1 \qquad [\mathbf{Y}_{\pi 2}^{(m)}] = ([\mathbf{Z}^{(m)}].1)^{-1} \tag{5.148.2}$$

The same formulae can be obtained for the corresponding phase quantities. Taking into account Eqns.(5.146) and Table 5.2-b the two-port equations parameters of an electrically short MTL can be derived. The most commonly used formulations of electrically short

MTLs are given in Table 5.5. The open circuit impedance and the short circuit admittance parameters correspond to the T-and π - lumped parameter 2n port networks shown in Fig.5.5.

For the approximations given with Eqns.(5.147.1) and (5.147.2) the modal input impedance looking from the transmitting end into the MTL is determined mainly by the modal terminating impedance and does not depend on the characteristic impedance.

$$\left[\mathbf{Z}_{\text{inp}}^{(m)}(0)\right] \cong \left[\mathbf{Z}_{\text{Rx}}^{(m)}\right] \tag{5.149}$$

5.2.5 Analysis of multiconductor transmission lines using modal quantities

It has been shown in the previous section that the derivation of a full set of quantities describing a non-uniform MTL in the modal domain is mathematically straightforward. The applicability of the formulae to MTL modal analysis however, requires careful consideration of the implication regarding terminating networks & discontinuities, and uniqueness.

5.2.5.1 Modal transformation of MTL terminating networks and discontinuities

The modal transformations for MTL terminating networks are given by the formulae of Table 5.3. From the electrical circuit viewpoint, the transformations relate active or passive multipole networks into active or passive multiport networks. The modal admittance matrices of the terminating networks $\left[\mathbf{Y}_{\text{Tx}}^{(m)}\right]$ and $\left[\mathbf{Y}_{\text{Rx}}^{(m)}\right]$ are thus defined by the equations

$$\left[\mathbf{I}^{(m)}(0)\right] = \left[\mathbf{Y}_{\text{Tx}}^{(m)}\right].\left[\mathbf{V}^{(m)}(0)\right] - \left[\tilde{\mathbf{J}}_{\text{Tx}}^{(m)}\right] \tag{5.150.1}$$

$$\left[\mathbf{I}^{(m)}(0)\right] = \left[\mathbf{Y}_{\text{Rx}}^{(m)}\right].\left[\mathbf{V}^{(m)}(1)\right] \tag{5.150.2}$$

and are short-circuit admittance matrices $\left[\mathbf{Y}_{\text{p}}\right]$ of active and passive multiport networks, defined in Section B.3 of Appendix B.

With reference to the modal transformation formulae in Table 5.3, it may be shown that since the phase admittance matrix of the transmitter is symmetric, the modal transmitter/receiver admittance matrix is also symmetric. However generally this matrix is not diagonal, so the modal voltages and currents at the MTL termination are coupled. As shown later, the modal termination matrix is diagonal only in special cases, for which full decoupling of the modes, including the transmitter and receiver end networks, is possible.

The modal reflection operators are not in general diagonal matrices since they are functions of the terminating network modal admittance matrix. This is illustrated by their expressions which are identical with Eqns.(5.46), (5.47), (5.50) and (5.51) with subscript

TABLE 5.5: Two-port equations parameters of electrically shorty MTL equivalent networks in modal quantities

Open circuit impedance parameters for equivalent T section

$$\left[\mathbf{Z}_{TL_T}^{(m)\prime}\right]=\begin{bmatrix}\frac{\left[\mathbf{Z}^{(m)}\right]1}{2}+\left(\left[\mathbf{Y}^{(m)}\right]1\right)^{-1} & -\frac{\left[\mathbf{Z}^{(m)}\right]1}{2}\\ \frac{\left[\mathbf{Z}^{(m)}\right]1}{2} & -\left(\frac{\left[\mathbf{Z}^{(m)}\right]1}{2}+\left(\left[\mathbf{Y}^{(m)}\right]1\right)^{-1}\right)\end{bmatrix}$$

Transmission (ABCD) parameters for equivalent T section

$$\left[\mathbf{T}_{TL_T}^{(m)\prime}\right]=\begin{bmatrix}\frac{\left[\mathbf{Z}^{(m)}\right]1.\left[\mathbf{Y}^{(m)}\right]1}{2}+[1] & \left[\mathbf{Z}^{(m)}\right]1.\left(\frac{\left[\mathbf{Y}^{(m)}\right]1.\left[\mathbf{Z}^{(m)}\right]1}{4}+[1]\right)\\ \left[\mathbf{Y}^{(m)}\right]1 & \frac{\left[\mathbf{Y}^{(m)}\right]1.\left[\mathbf{Z}^{(m)}\right]1}{2}+[1]\end{bmatrix}$$

Inverse transmission parameters for equivalent T section

$$\left[\mathbf{B}_{TL_T}^{(m)\prime}\right]=\begin{bmatrix}\frac{\left[\mathbf{Z}^{(m)}\right]1.\left[\mathbf{Y}^{(m)}\right]1}{2}+[1] & -\left[\mathbf{Z}^{(m)}\right]1.\left(\frac{\left[\mathbf{Y}^{(m)}\right]1.\left[\mathbf{Z}^{(m)}\right]1}{4}+[1]\right)\\ -\left[\mathbf{Y}^{(m)}\right]1 & \frac{\left[\mathbf{Y}^{(m)}\right]1.\left[\mathbf{Z}^{(m)}\right]1}{2}+[1]\end{bmatrix}$$

Short circuit admittance parameters for equivalent π section

$$\left[\mathbf{Y}_{TL_\pi}^{(m)\prime}\right]=\begin{bmatrix}\frac{\left[\mathbf{Y}^{(m)}\right]1}{2}+\left(\left[\mathbf{Z}^{(m)}\right]1\right)^{-1} & -\left(\left[\mathbf{Z}^{(m)}\right]1\right)^{-1}\\ \left(\left[\mathbf{Z}^{(m)}\right]1\right)^{-1} & -\left(\frac{\left[\mathbf{Y}^{(m)}\right]1}{2}+\left(\left[\mathbf{Z}^{(m)}\right]1\right)^{-1}\right)\end{bmatrix}$$

Transmission (ABCD) parameters for equivalent π section

$$\left[\mathbf{T}_{TL_\pi}^{(m)\prime}\right]=\begin{bmatrix}\frac{\left[\mathbf{Z}^{(m)}\right]1.\left[\mathbf{Y}^{(m)}\right]1}{2}+[1] & \left[\mathbf{Z}^{(m)}\right]1\\ \left[\mathbf{Y}^{(m)}\right]1.\left(\frac{\left[\mathbf{Z}^{(m)}\right]1.\left[\mathbf{Y}^{(m)}\right]1}{4}+[1]\right) & \frac{\left[\mathbf{Z}^{(m)}\right]1.\left[\mathbf{Y}^{(m)}\right]1}{2}+[1]\end{bmatrix}$$

Inverse transmission parameters for equivalent π section

$$\left[\mathbf{G}_{TL_\pi}^{(m)\prime}\right]=\begin{bmatrix}\frac{\left[\mathbf{Z}^{(m)}\right]1.\left[\mathbf{Y}^{(m)}\right]1}{2}+[1] & -\left[\mathbf{Z}^{(m)}\right]1\\ -\left[\mathbf{Y}^{(m)}\right]1.\left(\frac{\left[\mathbf{Z}^{(m)}\right]1.\left[\mathbf{Y}^{(m)}\right]1}{4}+[1]\right) & \frac{\left[\mathbf{Y}^{(m)}\right]1.\left[\mathbf{Z}^{(m)}\right]1}{2}+[1]\end{bmatrix}$$

FIG.5.5 Equivalent lumped parameter networks of a section of transmission line in the phase domain

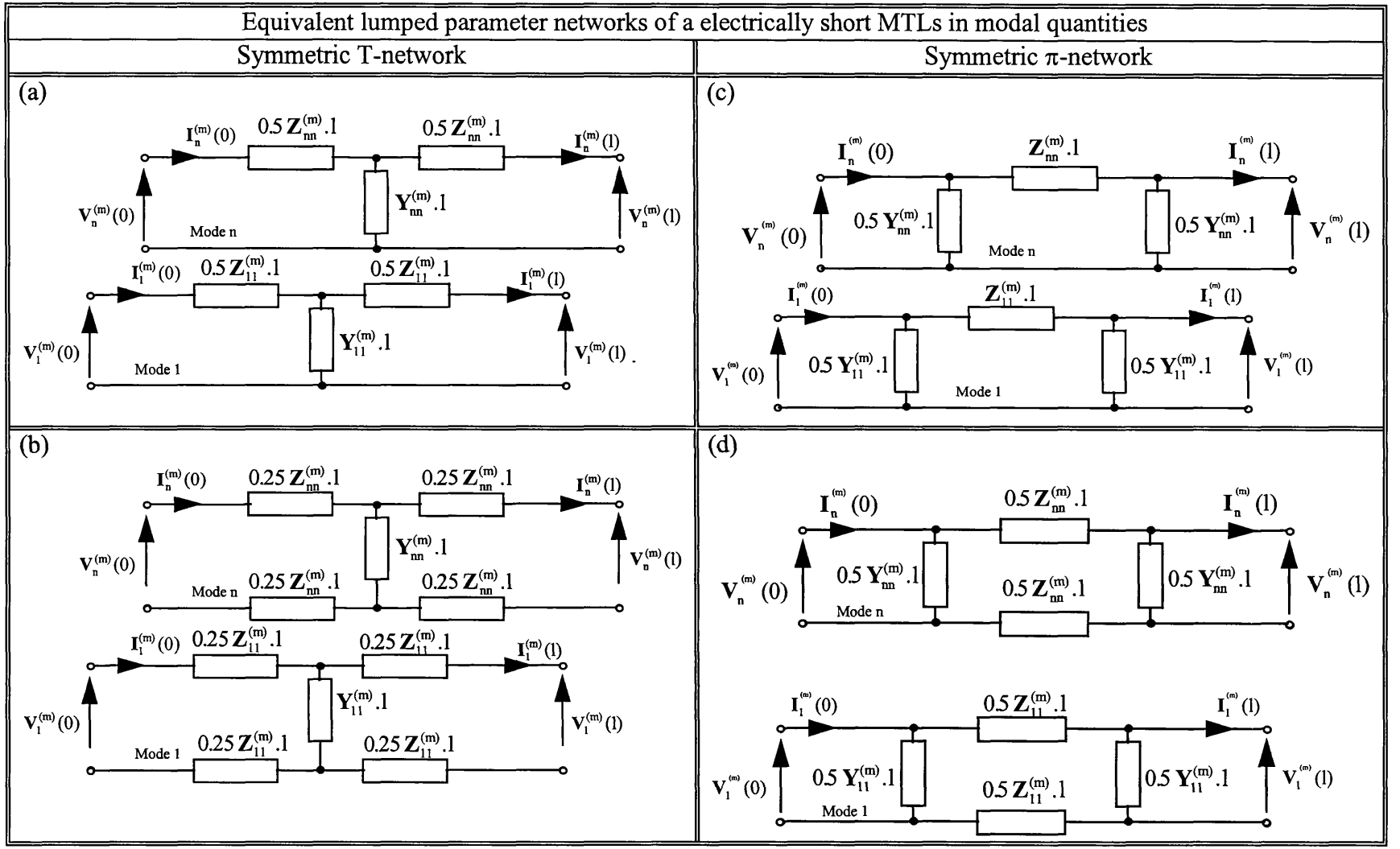

'(p)' instead of '(m)'. These expressions also show that, as for the phase reflection operators, the reflection of the modal voltages and currents is governed by different operators. From the equations

$$\left[\mathbf{V}_{\text{refl}}^{(m)}\right]=\left[\mathbf{K}_{\text{V}}^{(m)}\right].\left[\mathbf{V}_{\text{inc}}^{(m)}\right] \tag{5.151.1}$$

$$\left[\mathbf{I}_{\text{refl}}^{(m)}\right]=\left[\mathbf{K}_{\text{V}}^{(m)}\right].\left[\mathbf{I}_{\text{inc}}^{(m)}\right] \tag{5.151.2}$$

it can be seen that the reflection operators are rectangular matrices. The incident wave of each modal voltage/current component reflects into each other modal voltage/current component, and the element $\mathbf{K}_{\text{V}_{ij}}^{(m)}$ defines the portion of the incident wave of mode j which has reflected into mode i.

Hence the terminations and intermediate discontinuities of a MTL act as mode-coupling networks, as can be seen from the modal transform of the two-port formulation equations (i.e. the transmission parameters formulation)

$$\begin{bmatrix}\mathbf{V}_{\text{D(i)}}^{\text{II}^{(m)}}\\ \mathbf{I}_{\text{D(i)}}^{\text{II}^{(m)}}\end{bmatrix}=\begin{bmatrix}[\mathbf{S}_{(i)}] & \\ & [\mathbf{Q}_{(i)}]\end{bmatrix}^{-1}.\begin{bmatrix}[\mathcal{A}_{\text{D(i)}}^{(p)}] & [\mathcal{B}_{\text{D(i)}}^{(p)}]\\ [C_{\text{D(i)}}^{(p)}] & [\mathcal{D}_{\text{D(i)}}^{(p)}]\end{bmatrix}.\begin{bmatrix}[\mathbf{S}_{(i)}] & \\ & [\mathbf{Q}_{(i)}]\end{bmatrix}.\begin{bmatrix}\mathbf{V}_{\text{D(i)}}^{\text{I}^{(m)}}\\ \mathbf{I}_{\text{D(i)}}^{\text{I}^{(m)}}\end{bmatrix} \tag{5.152}$$

In conclusion, it is noted that the natural modes in a MTL are independent provided the boundary conditions are not applied. The attempt to incorporate transmission line terminations and discontinuities into a modal analysis produces coupling in the modes, and loss of simplicity in the solution by diagonalisation.

Another disadvantage of the full modal description of a non-uniform MTL is that by applying phase-to-modal transforms to the terminating and discontinuity networks, equivalent transformed networks are obtained which are described mathematically rather than physically. A back modal-to-phase transformation must then be applied in order to retrieve the physical meaning.

5.2.5.2 Uniqueness of MTL modal analysis

It has been shown that the quantities describing a MTL in the modal domain, except the propagation constants and the surge impedances in phase i due to mode j, are not unique. Hence the modal analysis is also not unique, so the question arises about the exact conditions of the equivalence of MTL analysis in the modal and phase domains. A necessary condition for this equivalence is the power invariance of the phase-to-modal transformations which is considered below. The complex power of an MTL described in phase quantities is

$$\mathbf{S}^{(p)}=\left[\bar{\mathbf{I}}^{(p)}\right]^{T}.\left[\mathbf{V}^{(p)}\right] \tag{5.153}$$

and in the modal domain is

$$\mathbf{S}^{(m)} = \left[\bar{\mathbf{I}}^{(m)}\right]^{T}.\left[\mathbf{V}^{(m)}\right] \tag{5.154}$$

Applying the phase-to-modal transforms to the first equation gives:

$$\mathbf{S}^{(p)} = \left(\overline{[\mathbf{Q}].\left[\mathbf{I}^{(m)}\right]}\right)^{T}.\left([\mathbf{S}].\left[\mathbf{V}^{(m)}\right]\right) = \left[\bar{\mathbf{I}}^{(m)}\right]^{T}.\left[\overline{\mathbf{Q}}\right]^{T}.[\mathbf{S}].\left[\mathbf{V}^{(m)}\right] \tag{5.155}$$

Comparing with the expression for the modal complex power, it follows that the modal transformations defined by the [**S**] and [**Q**] matrices are power invariant if

$$\left[\overline{\mathbf{Q}}\right]^{T}.[\mathbf{S}] = [\mathbf{Q}]^{*}.[\mathbf{S}] = [1] \tag{5.156}$$

which is the condition for the matrices [**S**] and [**Q**] to be mutually unitary. According to property (6) in Section 5.2, this condition is not satisfied, so the modal transformations are not power invariant. Eqn.(5.144) can also be expressed as:

$$\left[\overline{\mathbf{Q}}\right] = [\mathbf{Q}] \qquad \text{or} \qquad \left[\overline{\mathbf{S}}\right] = [\mathbf{S}] \tag{5.157}$$

which is satisfied if the matrices [**S**] and [**Q**] are real. The transformation matrices are real only for a lossless and perfectly transposed line, in which case the [**P**] matrix is also real and has real eigenvalues.

To conclude, in the general case, the phase-to-modal transformations are not power invariant and the modal analysis of a MTL is not equivalent to the analysis in phase quantities.

5.3. PROCEDURE FOR MTL ANALYSIS

Considering the advantages and disadvantages of the phase and modal description of MTLs, an analysis procedure is suggested based on the combination of the two methods as follows:

- The transmission line sections are described in modal quantities exploiting the simplified solution of the uncoupled modes;
- The lumped parameter networks at the line terminations and intermediate discontinuities are described in terms of the real physical quantities. This enables access to the voltages and currents of interest and enables them to be monitored.
- Phase-to-modal and modal-to-phase transformations are made at every transmission line section termination to provide a compatible interface.

The procedure is essentially a phase domain analysis making use of the solution by diagonalisation to simplify the numerical procedures.

5.4. ANALYSIS OF TWO-CONDUCTOR TRANSMISSION LINE ABOVE EARTH PLANE

The procedure for MTL modal analysis presented in the previous section is applied on a two-conductor transmission line. The results obtained form the immediate background for detailed track circuit analysis. For convenience, the results are presented in several tables (Tables 5.6 to 5.10) which will be used further as reference. Here, simplified formulae derived for two-conductor symmetrical and asymmetrical transmission lines, are used to give a comprehensive physical interpretation of the concept of natural modes.

5.4.1 Modes in a two-conductor transmission line

In two-conductor transmission lines there are two natural modes of propagation. In the particular case of symmetrical two-conductor transmission lines, these modes are known as common or earth mode (mode 1) and differential mode (mode 2). In this simple case, the physical manifestation of the natural modes is apparent. To illustrate this, consider a symmetrical two-conductor transmission line with symmetrical lumped parameter transmitting and receiving end networks. Assume that the voltage and current transformation matrices are

$$[\mathbf{S}]=\begin{bmatrix}1 & 0.5\\ 1 & 0.5\end{bmatrix}; \qquad [\mathbf{Q}]=\begin{bmatrix}0.5 & 1\\ -0.5 & 1\end{bmatrix} \tag{5.158}$$

It is shown later that a symmetrical transmission line with symmetrical terminating networks can be fully decoupled in the modal domain. Hence the presence of a particular mode depends only on the manner of line excitation, i.e. whether the corresponding modal source voltage is zero or non-zero.

Consider the transmission line for the following two cases:

(1) Excitation for common mode only (Fig.5.6-a)

The two-conductor transmission line is excited such that

$$\mathbf{V}_1^{(p)}(0)=\mathbf{V}_2^{(p)}(0)=\mathbf{V}_c(0) \tag{5.159}$$

From the assumptions made earlier, it follows that the phase voltages and currents are equal and in phase at any point along the line:

$$\mathbf{V}_1^{(p)}(x)=\mathbf{V}_2^{(p)}(x)=\mathbf{V}_c(x) \tag{5.160.1}$$

$$\mathbf{I}_1^{(p)}(x)=\mathbf{I}_2^{(p)}(x)=\mathbf{I}_c(x) \tag{5.160.2}$$

Using the modal transformation matrices given by Eqns.(5.145), the modal voltages and currents are:

$$\mathbf{V}_1^{(m)}(x) = \mathbf{V}_c(x); \qquad \mathbf{V}_2^{(m)}(0) = 0 \tag{5.161.1}$$

$$\mathbf{I}_1^{(m)}(x) = 2.\mathbf{I}_c(x) \qquad \mathbf{I}_2^{(m)}(0) = 0 \tag{5.161.2}$$

i.e. in a two-conductor transmission line excited according to Eqns.(5.158), there exists only the common mode of propagation. As the phase voltages of the two conductors are equal at any point along the line, the two conductors connected in parallel can be regarded as an equivalent outward conductor with the earth as the return conductor. The return of current through the earth causes high attenuation and low velocity of propagation which makes this mode inefficient for both information and power transmission.

Physically, the common mode can be identified with a single phase line formed by the two conductors in the configuration of Fig.5.6-b.

(2) Excitation for differential mode only (Fig.5.6-c)

The two-conductor transmission line is excited such that

$$\mathbf{V}_1^{(p)}(0) = \mathbf{V}_d(0) = -\mathbf{V}_2^{(p)}(0) \tag{5.162}$$

In this case, the phase voltages and currents along the line are equal but have opposite phases:

$$\mathbf{V}_1^{(p)}(x) = \mathbf{V}_d(x) = -\mathbf{V}_2^{(p)}(x) \tag{5.163.1}$$

$$\mathbf{I}_1^{(p)}(x) = \mathbf{I}_d(x) = -\mathbf{I}_2^{(p)}(x) \tag{5.163.2}$$

Correspondingly, the modal voltages and currents are:

$$\mathbf{V}_1^{(m)}(x) = 0 \tag{5.164.1}$$

$$\mathbf{V}_2^{(m)}(x) = 2.\mathbf{V}_d(x) \tag{5.164.2}$$

$$\mathbf{I}_1^{(m)}(x) = 0 \tag{5.164.3}$$

$$\mathbf{I}_2^{(m)}(x) = 2.\mathbf{I}_d(x) \tag{5.164.4}$$

In this case, only the differential mode of propagation exists. It is characterised by an equivalent voltage between the two conductors and an equivalent current flowing outward in one conductor and returning through the other. The phase currents in the earth cancel and the earth return does not affect electromagnetic wave propagation. The two conductors can be regarded as a single phase isolated transmission line. Physically, the differential mode can be identified with a two-conductor transmission line in the configuration shown in Fig.5.6-d. In conclusion, it has been shown that for the particular choice of the transformation matrices [**S**] and [**Q**] defined by Eqns.(5.158), the natural modes of propagation can be defined by two isolated single phase transmission lines whose conductors represent linear combinations of the actual conductors of the two-conductor transmission line being considered. Generally, both differential and common modes coexist in two-conductor transmission lines.

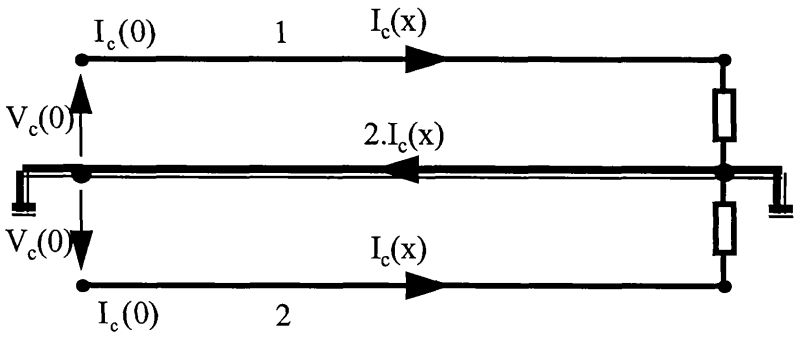

(a) Excitation for common mode only

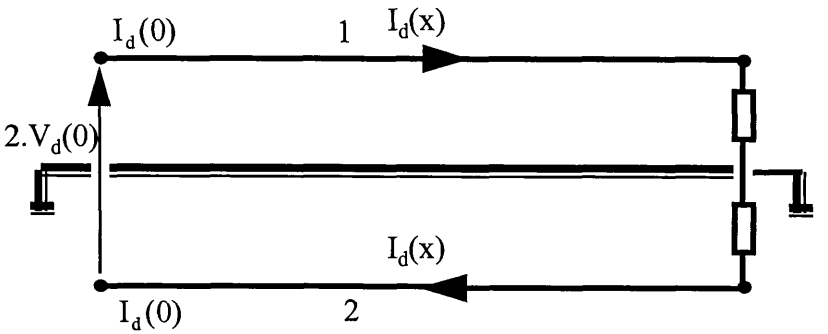

(c) Excitation for differential mode only

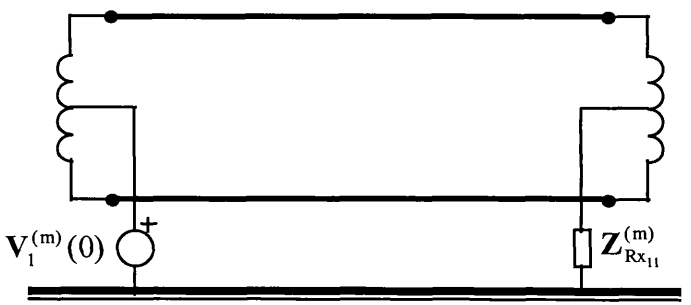

(b) Equivalent circuit of the common mode

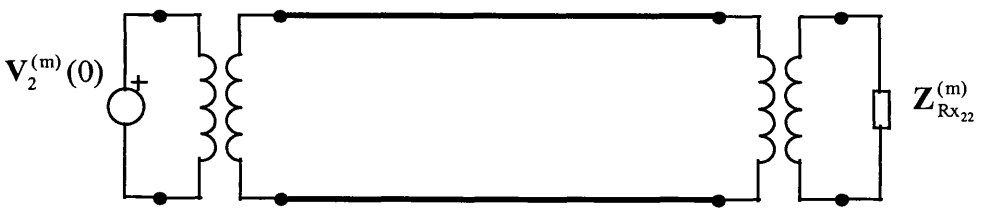

(d) Equivalent circuit of the differential mode

FIG. 5.6 Natural modes of propagation in a symmetrical two-conductor transmission line

The existence of propagation modes in two-conductor transmission lines was exploited long before the rigorous mathematical formulation was available, e.g. for multiplexing in communication lines. A similar principle is used on electrified railways for separation of traction and signalling currents.

5.4.2 Two-conductor transmission line terminations

Terminating networks for two-conductor transmission lines represent (2+1)-pole networks which can be described by nodal voltage or loop current analysis (Appendix B). For the particular case of two-conductor lines, the terminal-to-ground or node voltages and currents coincide with the terminal-to-terminal or mesh voltages and currents. This means that, unlike the general case of MTLs in two-conductor transmission line analysis, any of the above methods may be used. It also follows that the definite terminal admittance and the definite terminal impedance matrices of (2+1)-pole networks are related by simple inversion. Because of this relative simplicity, it is possible to express the elements of the terminal admittance/impedance matrix by the components of the terminating networks or their equivalent circuit. Table 5.7 contains expressions for the terminal admittance and impedance matrices for the most common star and delta equivalent circuit configurations. It is useful to derive the modal terminal admittance/impedances matrices for various terminating networks (Table 5.8). The derivations can be directly applied for track circuit analysis, and also allow some important qualitative conclusions to be made about the modal content and interaction for a two-conductor transmission line. In this respect, Table 5.9 contains useful generalised information. This table has been compiled in symbolic terms and reflects the properties of terminal admittance/impedance, reflection operator and input admittance/impedance matrices in the phase and modal domains. Examination of Table 5.9 leads to the following conclusion:

The modes in a two-conductor transmission line (including the terminating networks) are fully uncoupled and independent if and only if the terminating networks are 'modally' tuned. The latter requirement implies that a terminating network must be chosen in such a way that a special relationship exists between the elements of its phase terminal admittance/impedance matrix, in which the modal terminal admittance/impedance matrix is diagonal.

As an example, the condition of modal independence (modal 'tuning') in a terminating network defined with a delta equivalent circuit is given by the equation

$$\eta_1 . \mathbf{Y}^{\Delta}_{*_1} + \eta_2 . \mathbf{Y}^{\Delta}_{*_2} = (1-\eta_1).(1-\eta_2). \mathbf{Y}^{\Delta}_{*_{22}} \qquad (5.165)$$

The above concluding statement is also valid for the general MTL. For a symmetrical transmission line, the 'modal' tuning require the terminating networks to be symmetrical. This requirement is well known in practice. For example, it is a condition for the

elimination of interference between traction and the signalling currents in rail track circuits. However the 'modal' tuning has not been applied for more general cases for which it can have practical importance.

5.4.3 Non-uniform two-conductor transmission line analysis

The analysis procedure for non-uniform two-conductor transmission lines above conductive earth plane is illustrated in Fig.5.6. The non-uniform TL is terminated with transmitter and receiver networks and consists of a number of uniform TL sections with a number of intermediate discontinuities D(i), counted from the transmitter towards the receiver end. The analysis procedure consists of two stages:

(1) A step-by-step reduction of the overall non-uniform TL to a single uniform TL section. This reduction process is performed by subsequent substitution of the far right hand TL section by its input impedance, and continues until all the right hand sections of the non-uniform TL looking into the input terminals at the first discontinuity have been replaced with an equivalent TL section receiver impedance ($\mathbf{Z}^{(p)}_{Rx_{(i)}}$).

(2) Section-by-section solution of the overall non-uniform TL, starting with the near left hand uniform TL section and proceeding towards the receiver end. Each subsequent TL section is solved after the remaining parts of the overall TL have been substituted as follows:

- The left-hand part, looking from the TL section left-hand terminals back to the TL transmitter, with an equivalent transmitter (Tx_i) calculated from the Thevenin/Norton theorems for multiterminal networks;

- The right-hand part, looking from TL section right-hand terminals towards the TL receiver, with an equivalent receiver found during stage I of the analysis.

The above procedure can also be applied to the MTL, although there are some differences in the procedure, which must be performed purely mathematically using the matrix description of the discontinuities as derived in Sections 5.1.3, 5.2.4.1 and Appendix B. When two-conductor TLs are analysed, the relative simplicity of the terminating and intermediate discontinuity networks can be efficiently exploited by retaining the circuit description using lumped parameter networks with convenient circuit transformations. This enables the physical nature of the processes in a non-uniform TL to be maintained during analysis, even when the discontinuity networks are represented by equivalent circuits. Moreover, the mathematical description of the input admittance/impedance of a TL section can be easily described by an equivalent circuit. When the input admittance/impedance is that seen from the output terminals of an intermediate discontinuity, its lumped parameter equivalent circuit can be integrated with that of the

discontinuity. This gives a simplified structure after circuit transformation. The operation will be repeatedly used in the further analysis, and to facilitate it, a reference table covering the conversion various cases for input admittance/impedance matrix to equivalent circuit conversion has been complied (Fig. 5.7). The equivalent diagrams for the input admittance/impedance in Fig. 5.7 form another illustration of the coupling that occurs between modes when the matrices are not diagonal. The mutual coupling takes the form of an equivalent voltage or current source which is introduced into one of the modes, while being, function of the other.

TABLE 5.6: Modal analysis of a two-conductor transmission line

PROCEDURE OF MTL ANALYSIS	TWO-CONDUCTOR TRANSMISSION LINE (General case)	SYMMETRIC TWO-CONDUCTOR TRANSMISSION LINE
Determination of MTL primary parameters $\left[\mathbf{Z}^{(p)}\right]$ and $\left[\mathbf{Y}^{(p)}\right]$	$\left[\mathbf{Z}^{(p)}\right]=\begin{bmatrix}\mathbf{Z}_{11}^{(p)} & \mathbf{Z}_{12}^{(p)}\\ \mathbf{Z}_{12}^{(p)} & \mathbf{Z}_{22}^{(p)}\end{bmatrix}$ $\left[\mathbf{Y}^{(p)}\right]=\begin{bmatrix}\mathbf{Y}_{11}^{(p)} & \mathbf{Y}_{12}^{(p)}\\ \mathbf{Y}_{12}^{(p)} & \mathbf{Y}_{22}^{(p)}\end{bmatrix}$	$\left[\mathbf{Z}^{(p)}\right]=\begin{bmatrix}\mathbf{Z}_{11}^{(p)} & \mathbf{Z}_{12}^{(p)}\\ \mathbf{Z}_{12}^{(p)} & \mathbf{Z}_{11}^{(p)}\end{bmatrix}$ $\left[\mathbf{Y}^{(p)}\right]=\begin{bmatrix}\mathbf{Y}_{11}^{(p)} & \mathbf{Y}_{12}^{(p)}\\ \mathbf{Y}_{12}^{(p)} & \mathbf{Y}_{11}^{(p)}\end{bmatrix}$
Calculation of matrix $[\mathbf{P}]$ $[\mathbf{P}]=\left[\mathbf{Z}^{(p)}\right].\left[\mathbf{Y}^{(p)}\right]$	$[\mathbf{P}]=\begin{bmatrix}\mathbf{Z}_{11}^{(p)}.\mathbf{Y}_{11}^{(p)}+\mathbf{Z}_{12}^{(p)}.\mathbf{Y}_{12}^{(p)} & \mathbf{Z}_{11}^{(p)}.\mathbf{Y}_{12}^{(p)}+\mathbf{Z}_{12}^{(p)}.\mathbf{Y}_{22}^{(p)}\\ \mathbf{Z}_{12}^{(p)}.\mathbf{Y}_{11}^{(p)}+\mathbf{Z}_{22}^{(p)}.\mathbf{Y}_{12}^{(p)} & \mathbf{Z}_{12}^{(p)}.\mathbf{Y}_{12}^{(p)}+\mathbf{Z}_{22}^{(p)}.\mathbf{Y}_{22}^{(p)}\end{bmatrix}$	$[\mathbf{P}]=\begin{bmatrix}\mathbf{Z}_{11}^{(p)}.\mathbf{Y}_{11}^{(p)}+\mathbf{Z}_{12}^{(p)}.\mathbf{Y}_{12}^{(p)} & \mathbf{Z}_{11}^{(p)}.\mathbf{Y}_{12}^{(p)}+\mathbf{Z}_{12}^{(p)}.\mathbf{Y}_{11}^{(p)}\\ \mathbf{Z}_{12}^{(p)}.\mathbf{Y}_{11}^{(p)}+\mathbf{Z}_{11}^{(p)}.\mathbf{Y}_{12}^{(p)} & \mathbf{Z}_{12}^{(p)}.\mathbf{Y}_{12}^{(p)}+\mathbf{Z}_{11}^{(p)}.\mathbf{Y}_{11}^{(p)}\end{bmatrix}$
The eigenvalues of matrix $[\mathbf{P}]$ are calculated from the equation $\det\left([\mathbf{P}]-\lambda.[1]\right)=0$	$\lambda_{1,2}=\frac{1}{2}.\left[\mathbf{P}_{11}+\mathbf{P}_{22}\pm\sqrt{\left(\mathbf{P}_{11}-\mathbf{P}_{22}\right)^2+4.\mathbf{P}_{12}.\mathbf{P}_{21}}\right]$	$\lambda_{1,2}=\mathbf{P}_{11}\pm\mathbf{P}_{22}$
Calculation of the modal propagation constants	$\gamma_{1,2}=\sqrt{\lambda_{1,2}}$	$\gamma_{1,2}=\sqrt{\left(\mathbf{Z}_{11}^{(p)}\pm\mathbf{Z}_{12}^{(p)}\right).\left(\mathbf{Y}_{11}^{(p)}\pm\mathbf{Y}_{12}^{(p)}\right)}$
The elements of matrix $[\mathbf{S}]$ are determined from the systems of equations:	$\begin{vmatrix}\left(\mathbf{P}_{11}-\lambda_1\right).\mathbf{S}_{11}+\mathbf{P}_{12}.\mathbf{S}_{21}=0\\ \mathbf{P}_{21}.\mathbf{S}_{11}+\left(\mathbf{P}_{22}-\lambda_1\right).\mathbf{S}_{21}=0\end{vmatrix}$ $\begin{vmatrix}\left(\mathbf{P}_{11}-\lambda_2\right).\mathbf{S}_{12}+\mathbf{P}_{12}.\mathbf{S}_{22}=0\\ \mathbf{P}_{21}.\mathbf{S}_{12}+\left(\mathbf{S}_{22}-\lambda_2\right).\mathbf{S}_{22}=0\end{vmatrix}$	$\begin{vmatrix}\left(\mathbf{P}_{11}-\lambda_1\right).\mathbf{S}_{11}+\mathbf{P}_{12}.\mathbf{S}_{21}=0\\ \mathbf{P}_{21}.\mathbf{S}_{11}+\left(\mathbf{P}_{11}-\lambda_1\right).\mathbf{S}_{21}=0\end{vmatrix}$ $\begin{vmatrix}\left(\mathbf{P}_{11}-\lambda_2\right).\mathbf{S}_{12}+\mathbf{P}_{12}.\mathbf{S}_{22}=0\\ \mathbf{P}_{12}.\mathbf{S}_{12}+\left(\mathbf{P}_{11}-\lambda_2\right).\mathbf{S}_{22}=0\end{vmatrix}$
The voltage transformation matrix is defioned by the relations:	$\frac{\mathbf{S}_{11}}{\mathbf{S}_{21}}=-\frac{\mathbf{P}_{12}}{\mathbf{P}_{11}-\lambda_1}=-\frac{\mathbf{P}_{22}-\lambda_1}{\mathbf{P}_{21}}=\frac{1}{\eta_2}$ $\frac{\mathbf{S}_{12}}{\mathbf{S}_{22}}=-\frac{\mathbf{P}_{12}}{\mathbf{P}_{11}-\lambda_2}=-\frac{\mathbf{P}_{22}-\lambda_2}{\mathbf{P}_{21}}=\eta_1$	$\frac{\mathbf{S}_{11}}{\mathbf{S}_{21}}=\frac{1}{\eta_2}=1$ $\frac{\mathbf{S}_{12}}{\mathbf{S}_{22}}=\eta_1=-1$

TABLE 5.6: -continuation

PROCEDURE OF MTL ANALYSIS	TWO-CONDUCTOR TRANSMISSION LINE (General case)	SYMMETRIC TWO-CONDUCTOR TRANSMISSION LINE
Normalisation of matrix S Choosing $[\mathbf{D'}]=\frac{1}{(1-\eta_1.\eta_2)}.[1]$	$[\mathbf{S}]=\begin{bmatrix}1 & \eta_1\\ \eta_2 & 1\end{bmatrix}.\begin{bmatrix}\mathbf{D'}_{11} & \\ & \mathbf{D'}_{22}\end{bmatrix}=\begin{bmatrix}1 & \eta_1\\ \eta_2 & 1\end{bmatrix}.[\mathbf{D'}]$ $[\mathbf{S}]=\frac{1}{(1-\eta_1.\eta_2)}.\begin{bmatrix}1 & \eta_1\\ \eta_2 & 1\end{bmatrix}$	$[\mathbf{S}]=\begin{bmatrix}1 & -1\\ 1 & 1\end{bmatrix}.\begin{bmatrix}\mathbf{D'}_{11} & \\ & \mathbf{D'}_{22}\end{bmatrix}=\begin{bmatrix}1 & -1\\ 1 & 1\end{bmatrix}.[\mathbf{D'}]$ For $[\mathbf{D'}]=\frac{1}{2}.[1]$ $\quad [\mathbf{S}]=\frac{1}{2}.\begin{bmatrix}1 & -1\\ 1 & 1\end{bmatrix}$
The current transformation matrix $[\mathbf{Q}]$ can be found from the relation $[\mathbf{S}]^{-1}=[\mathbf{Q}]^{T}$	$[\mathbf{Q}]=\begin{bmatrix}1 & -\eta_2\\ -\eta_1 & 1\end{bmatrix}$	$[\mathbf{Q}]=\begin{bmatrix}1 & -1\\ 1 & 1\end{bmatrix}$
The inverses of the transformation matrices are:	$[\mathbf{S}]^{-1}=\begin{bmatrix}1 & -\eta_1\\ -\eta_2 & 1\end{bmatrix}$ $[\mathbf{Q}]^{-1}=\frac{1}{(1-\eta_1.\eta_2)}.\begin{bmatrix}1 & \eta_2\\ \eta_1 & 1\end{bmatrix}$	$[\mathbf{S}]^{-1}=\begin{bmatrix}1 & 1\\ -1 & 1\end{bmatrix}$ $[\mathbf{Q}]^{-1}=\frac{1}{2}.\begin{bmatrix}1 & 1\\ -1 & 1\end{bmatrix}$
The modal series impedance is calculated by: $[\mathbf{Z}^{(m)}]=[\mathbf{S}]^{-1}.[\mathbf{Z}^{(p)}].[\mathbf{Q}]$	$[\mathbf{Z}^{(m)}]=(1-\eta_1.\eta_2).\begin{bmatrix}\mathbf{Z}_{11}^{(p)}-\eta_1.\mathbf{Z}_{12}^{(p)} & \\ & \mathbf{Z}_{22}^{(p)}-\eta_2.\mathbf{Z}_{12}^{(p)}\end{bmatrix}$	$[\mathbf{Z}^{(m)}]=2.\begin{bmatrix}\mathbf{Z}_{11}^{(p)}+\mathbf{Z}_{12}^{(p)} & \\ & \mathbf{Z}_{22}^{(p)}-\mathbf{Z}_{12}^{(p)}\end{bmatrix}$
The modal shunt admittance is calculated by: $[\mathbf{Y}^{(m)}]=[\mathbf{Q}]^{-1}.[\mathbf{Y}^{(p)}].[\mathbf{S}]$	$[\mathbf{Y}^{(m)}]=\frac{1}{(1-\eta_1.\eta_2)}.\begin{bmatrix}\mathbf{Y}_{11}^{(p)}+\eta_2.\mathbf{Y}_{12}^{(p)} & \\ & \mathbf{Y}_{22}^{(p)}+\eta_1.\mathbf{Y}_{12}^{(p)}\end{bmatrix}$	$[\mathbf{Y}^{(m)}]=\frac{1}{2}.\begin{bmatrix}\mathbf{Y}_{11}^{(p)}+\mathbf{Y}_{12}^{(p)} & \\ & \mathbf{Y}_{22}^{(p)}-\mathbf{Y}_{12}^{(p)}\end{bmatrix}$

TABLE 5.6: -continuation

PROCEDURE OF MTL ANALYSIS	TWO-CONDUCTOR TRANSMISSION LINE (General case)	SYMMETRIC TWO-CONDUCTOR TRANSMISSION LINE
The modal characteristic impedance is calculated by: $\left[\mathbf{Z}_o^{(m)}\right]=\left[\gamma\right]^{-1}.\left[\mathbf{Z}^{(m)}\right]$	$\left[\mathbf{Z}_o^{(m)}\right]=\left(1-\eta_1.\eta_2\right).\begin{bmatrix}\dfrac{\mathbf{Z}_{11}^{(p)}-\eta_1.\mathbf{Z}_{12}^{(p)}}{\gamma_1} & \\ & \dfrac{\mathbf{Z}_{22}^{(p)}-\eta_2.\mathbf{Z}_{12}^{(p)}}{\gamma_2}\end{bmatrix}$	$\left[\mathbf{Z}_o^{(m)}\right]=2.\begin{bmatrix}\left(\dfrac{\mathbf{Z}_{11}^{(p)}+\mathbf{Z}_{12}^{(p)}}{\mathbf{Y}_{11}^{(p)}+\mathbf{Y}_{12}^{(p)}}\right)^{1/2} & \\ & \left(\dfrac{\mathbf{Z}_{11}^{(p)}-\mathbf{Z}_{12}^{(p)}}{\mathbf{Y}_{11}^{(p)}-\mathbf{Y}_{12}^{(p)}}\right)^{1/2}\end{bmatrix}$
The modal characteristic admittance is calculated by: $\left[\mathbf{Y}_o^{(m)}\right]=\left[\gamma\right]^{-1}.\left[\mathbf{Y}^{(m)}\right]$	$\left[\mathbf{Y}_o^{(m)}\right]=\dfrac{1}{\left(1-\eta_1.\eta_2\right)}.\begin{bmatrix}\dfrac{\mathbf{Y}_{11}^{(p)}+\eta_2.\mathbf{Y}_{12}^{(p)}}{\gamma_1} & \\ & \dfrac{\mathbf{Y}_{22}^{(p)}+\eta_1.\mathbf{Y}_{12}^{(p)}}{\gamma_2}\end{bmatrix}$	$\left[\mathbf{Y}_o^{(m)}\right]=\dfrac{1}{2}.\begin{bmatrix}\left(\dfrac{\mathbf{Y}_{11}^{(p)}+\mathbf{Y}_{12}^{(p)}}{\mathbf{Z}_{11}^{(p)}+\mathbf{Z}_{12}^{(p)}}\right)^{1/2} & \\ & \left(\dfrac{\mathbf{Y}_{11}^{(p)}-\mathbf{Y}_{12}^{(p)}}{\mathbf{Z}_{11}^{(p)}-\mathbf{Z}_{12}^{(p)}}\right)^{1/2}\end{bmatrix}$

TABLE 5.7 Two-conductor transmission line terminations

	Delta configuration	Star configuration
Termination network equivalent circuit	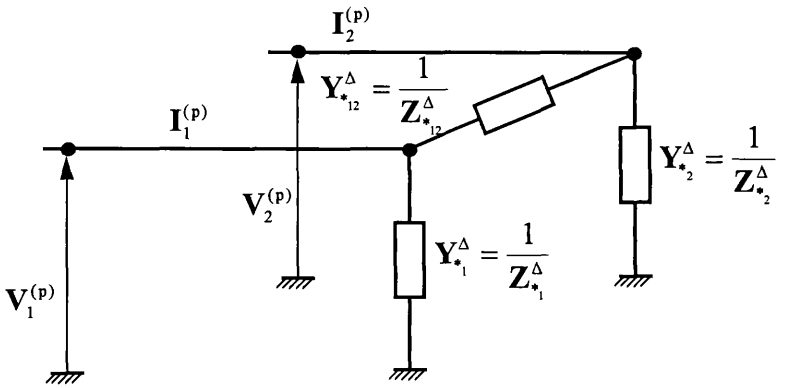	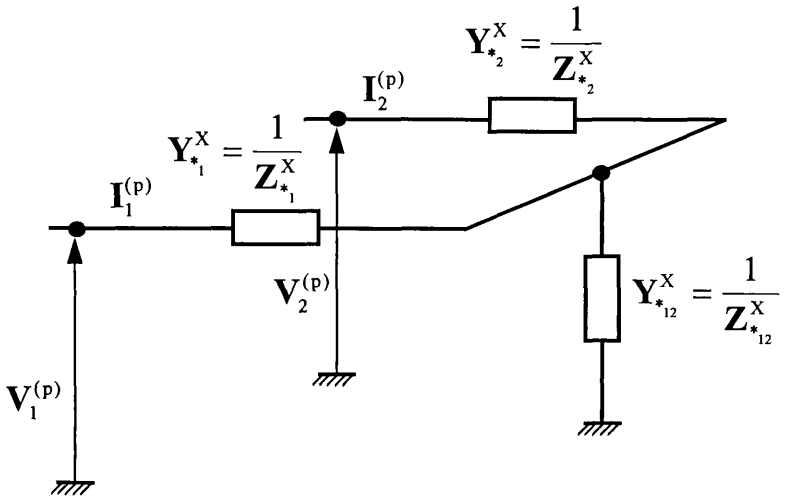
Definite terminal admittance matrix	$\left[\mathbf{Y}_{*}^{(p)}\right] = \begin{bmatrix} \mathbf{Y}_{*_1}^{\Delta} + \mathbf{Y}_{*_{12}}^{\Delta} & -\mathbf{Y}_{*_{12}}^{\Delta} \\ -\mathbf{Y}_{*_{12}}^{\Delta} & \mathbf{Y}_{*_2}^{\Delta} + \mathbf{Y}_{*_{12}}^{\Delta} \end{bmatrix}$	$\left[\mathbf{Y}_{*}^{(p)}\right] = \left(\sum \mathbf{Y}_{*}^{X}\right)^{-1} \cdot \begin{bmatrix} \mathbf{Y}_{*_1}^{X} \cdot \left(\mathbf{Y}_{*_2}^{X} + \mathbf{Y}_{*_{12}}^{X}\right) & -\mathbf{Y}_{*_1}^{X} \cdot \mathbf{Y}_{*_2}^{X} \\ -\mathbf{Y}_{*_1}^{X} \cdot \mathbf{Y}_{*_2}^{X} & \mathbf{Y}_{*_2}^{X} \cdot \left(\mathbf{Y}_{*_1}^{X} + \mathbf{Y}_{*_{12}}^{X}\right) \end{bmatrix}$ where $\sum \mathbf{Y}_{*}^{X} = \mathbf{Y}_{*_1}^{X} + \mathbf{Y}_{*_{12}}^{X} + \mathbf{Y}_{*_2}^{X}$
Definite terminal impedance matrix	$\left[\mathbf{Z}_{*}^{(p)}\right] = \left(\sum \mathbf{Z}_{*}^{\Delta}\right)^{-1} \cdot \begin{bmatrix} \mathbf{Z}_{*_1}^{\Delta} \cdot \left(\mathbf{Z}_{*_2}^{\Delta} + \mathbf{Z}_{*_{12}}^{\Delta}\right) & \mathbf{Z}_{*_1}^{\Delta} \cdot \mathbf{Z}_{*_2}^{\Delta} \\ \mathbf{Z}_{*_1}^{\Delta} \cdot \mathbf{Z}_{*_2}^{\Delta} & \mathbf{Z}_{*_2}^{\Delta} \cdot \left(\mathbf{Z}_{*_1}^{\Delta} + \mathbf{Z}_{*_{12}}^{\Delta}\right) \end{bmatrix}$ where $\sum \mathbf{Z}_{*}^{\Delta} = \mathbf{Z}_{*_1}^{\Delta} + \mathbf{Z}_{*_{12}}^{\Delta} + \mathbf{Z}_{*_2}^{\Delta}$	$\left[\mathbf{Z}_{*}^{(p)}\right] = \begin{bmatrix} \mathbf{Z}_{*_1}^{X} + \mathbf{Z}_{*_{12}}^{X} & \mathbf{Z}_{*_{12}}^{X} \\ \mathbf{Z}_{*_{12}}^{X} & \mathbf{Z}_{*_2}^{X} + \mathbf{Z}_{*_{12}}^{X} \end{bmatrix}$

Note: The subscript '*' substitutes 'Tx' or 'Rx'.
The superscript ' Δ ' refers to delta configuration parameters and ' X ' refers to star configuration parameters.

TABLE 5.8 Two-conductor transmission line terminating networks described in phase and modal quantities (see note on page 5-53)

Terminating network terminal admittance / impedance matrix	Modal transformation of the terminal admittance / impedance matrix Non-symmetric transmission line
Non-symmetric terminating network	$\left[\mathbf{Y}_{*}^{(m)}\right]=\begin{bmatrix}\mathbf{Y}_{*_{11}}^{(m)} & \mathbf{Y}_{*_{12}}^{(m)}\\ \mathbf{Y}_{*_{21}}^{(m)} & \mathbf{Y}_{*_{22}}^{(m)}\end{bmatrix}$ $\left[\mathbf{Z}_{*}^{(m)}\right]=\begin{bmatrix}\mathbf{Z}_{*_{11}}^{(m)} & \mathbf{Z}_{*_{12}}^{(m)}\\ \mathbf{Z}_{*_{21}}^{(m)} & \mathbf{Z}_{*_{22}}^{(m)}\end{bmatrix}$
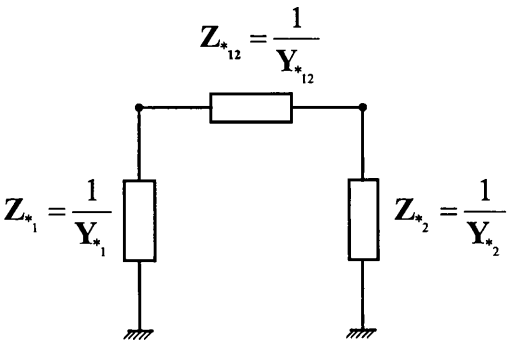	$\mathbf{Y}_{*_{11}}^{(m)}=\frac{\eta_2^2.\mathbf{Z}_{*_1}.\mathbf{Z}_{*_{12}}+(1-\eta_2)^2.\mathbf{Z}_{*_1}.\mathbf{Z}_{*_2}+\mathbf{Z}_{*_2}.\mathbf{Z}_{*_{12}}}{(1-\eta_1.\eta_2)^2.\mathbf{Z}_{*_1}.\mathbf{Z}_{*_{12}}.\mathbf{Z}_{*_2}}=\frac{\mathbf{Y}_{*_1}+(1-\eta_2)^2.\mathbf{Y}_{*_{12}}+\eta_2^2.\mathbf{Y}_{*_2}}{(1-\eta_1.\eta_2)^2}$
	$\mathbf{Y}_{*_{12}}^{(m)}=\mathbf{Y}_{*_{21}}^{(m)}=\frac{\eta_2.\mathbf{Z}_{*_1}.\mathbf{Z}_{*_{12}}-(1-\eta_1)(1-\eta_2).\mathbf{Z}_{*_1}.\mathbf{Z}_{*_2}+\eta_1.\mathbf{Z}_{*_2}.\mathbf{Z}_{*_{12}}}{(1-\eta_1.\eta_2)^2.\mathbf{Z}_{*_1}.\mathbf{Z}_{*_{12}}.\mathbf{Z}_{*_2}}=\frac{\eta_1.\mathbf{Y}_{*_1}-(1-\eta_1)(1-\eta_2).\mathbf{Y}_{*_{12}}+\eta_2.\mathbf{Y}_{*_2}}{(1-\eta_1.\eta_2)^2}$
	$\mathbf{Y}_{*_{22}}^{(m)}=\frac{\mathbf{Z}_{*_1}.\mathbf{Z}_{*_{12}}+(1-\eta_1)^2.\mathbf{Z}_{*_1}.\mathbf{Z}_{*_2}+\eta_1^2.\mathbf{Z}_{*_2}.\mathbf{Z}_{*_{12}}}{(1-\eta_1.\eta_2)^2.\mathbf{Z}_{*_1}.\mathbf{Z}_{*_{12}}.\mathbf{Z}_{*_2}}=\frac{\eta_1^2.\mathbf{Y}_{*_1}+(1-\eta_1)^2.\mathbf{Y}_{*_{12}}+\mathbf{Y}_{*_2}}{(1-\eta_1.\eta_2)^2}$
$\left[\mathbf{Y}_{*}^{(p)}\right]=\begin{bmatrix}\mathbf{Y}_{*_1}+\mathbf{Y}_{*_{12}} & -\mathbf{Y}_{*_{12}}\\ -\mathbf{Y}_{*_{12}} & \mathbf{Y}_{*_2}+\mathbf{Y}_{*_{12}}\end{bmatrix}$	$\mathbf{Z}_{*_{11}}^{(m)}=\frac{\eta_1^2.\mathbf{Z}_{*_2}.\mathbf{Z}_{*_{12}}+(1-\eta_1)^2.\mathbf{Z}_{*_1}.\mathbf{Z}_{*_2}+\mathbf{Z}_{*_1}.\mathbf{Z}_{*_{12}}}{\mathbf{Z}_{*_1}+\mathbf{Z}_{*_{12}}+\mathbf{Z}_{*_2}}=\frac{\eta_1^2.\mathbf{Y}_{*_1}+(1-\eta_1)^2.\mathbf{Y}_{*_{12}}+\mathbf{Y}_{*_2}}{\mathbf{Y}_{*_1}.\mathbf{Y}_{*_2}+\mathbf{Y}_{*_1}.\mathbf{Y}_{*_{12}}+\mathbf{Y}_{*_2}.\mathbf{Y}_{*_{12}}}$
$\left[\mathbf{Z}_{*}^{(p)}\right]=\frac{1}{\sum\mathbf{Z}_{*}}\begin{bmatrix}\mathbf{Z}_{*_1}.(\mathbf{Z}_{*_2}+\mathbf{Z}_{*_{12}}) & \mathbf{Z}_{*_1}.\mathbf{Z}_{*_2}\\ \mathbf{Z}_{*_1}.\mathbf{Z}_{*_2} & \mathbf{Z}_{*_2}.(\mathbf{Z}_{*_1}+\mathbf{Z}_{*_{12}})\end{bmatrix}$	$\mathbf{Z}_{*_{12}}^{(m)}=\mathbf{Z}_{*_{21}}^{(m)}=-\frac{\eta_1.\mathbf{Z}_{*_2}.\mathbf{Z}_{*_{12}}-(1-\eta_1)(1-\eta_2).\mathbf{Z}_{*_1}.\mathbf{Z}_{*_2}+\eta_2.\mathbf{Z}_{*_1}.\mathbf{Z}_{*_{12}}}{\mathbf{Z}_{*_1}+\mathbf{Z}_{*_{12}}+\mathbf{Z}_{*_2}}=-\frac{\eta_1.\mathbf{Y}_{*_1}-(1-\eta_1)(1-\eta_2).\mathbf{Y}_{*_{12}}+\eta_2.\mathbf{Y}_{*_2}}{\mathbf{Y}_{*_1}.\mathbf{Y}_{*_2}+\mathbf{Y}_{*_1}.\mathbf{Y}_{*_{12}}+\mathbf{Y}_{*_2}.\mathbf{Y}_{*_{12}}}$
$\sum\mathbf{Z}_{*}=\mathbf{Z}_{*_1}+\mathbf{Z}_{*_{12}}+\mathbf{Z}_{*_2}$	$\mathbf{Z}_{*_{22}}^{(m)}=\frac{\mathbf{Z}_{*_2}.\mathbf{Z}_{*_{12}}+(1-\eta_2)^2.\mathbf{Z}_{*_1}.\mathbf{Z}_{*_2}+\eta_2^2.\mathbf{Z}_{*_1}.\mathbf{Z}_{*_{12}}}{\mathbf{Z}_{*_1}+\mathbf{Z}_{*_{12}}+\mathbf{Z}_{*_2}}=\frac{\mathbf{Y}_{*_1}+(1-\eta_2)^2.\mathbf{Y}_{*_{12}}+\eta_2^2.\mathbf{Y}_{*_2}}{\mathbf{Y}_{*_1}.\mathbf{Y}_{*_2}+\mathbf{Y}_{*_1}.\mathbf{Y}_{*_{12}}+\mathbf{Y}_{*_2}.\mathbf{Y}_{*_{12}}}$

TABLE 5.8 Continuation

Terminating network terminal admittance / impedance matrix	Modal transformation of the terminal admittance / impedance matrix Non-symmetric transmission line
Symmetric terminating network	$\left[\mathbf{Y}_{*}^{(m)}\right]=\begin{bmatrix}\mathbf{Y}_{*_{11}}^{(m)} & \mathbf{Y}_{*_{12}}^{(m)}\\ \mathbf{Y}_{*_{21}}^{(m)} & \mathbf{Y}_{*_{22}}^{(m)}\end{bmatrix}$ $\left[\mathbf{Z}_{*}^{(m)}\right]=\begin{bmatrix}\mathbf{Z}_{*_{11}}^{(m)} & \mathbf{Z}_{*_{12}}^{(m)}\\ \mathbf{Z}_{*_{21}}^{(m)} & \mathbf{Z}_{*_{22}}^{(m)}\end{bmatrix}$
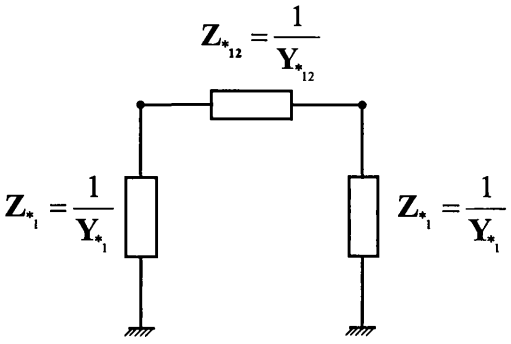	$\mathbf{Y}_{*_{11}}^{(m)}=\frac{(1-\eta_2)^2.\mathbf{Z}_{*_1}+(1+\eta_2^2).\mathbf{Z}_{*_{12}}}{(1-\eta_1.\eta_2)^2.\mathbf{Z}_{*_1}.\mathbf{Z}_{*_{12}}}=\frac{(1+\eta_2^2).\mathbf{Y}_{*_1}+(1-\eta_2)^2.\mathbf{Y}_{*_{12}}}{(1-\eta_1.\eta_2)^2}$ $\mathbf{Y}_{*_{12}}^{(m)}=\mathbf{Y}_{*_{21}}^{(m)}=\frac{(\eta_1+\eta_2).\mathbf{Z}_{*_{12}}-(1-\eta_1)(1-\eta_2).\mathbf{Z}_{*_1}}{(1-\eta_1.\eta_2)^2.\mathbf{Z}_{*_1}.\mathbf{Z}_{*_{12}}}=\frac{(\eta_1+\eta_2).\mathbf{Y}_{*_1}-(1-\eta_1)(1-\eta_2).\mathbf{Y}_{*_{12}}}{(1-\eta_1.\eta_2)^2}$ $\mathbf{Y}_{*_{22}}^{(m)}=\frac{(1-\eta_1)^2.\mathbf{Z}_{*_1}+(1+\eta_1^2).\mathbf{Z}_{*_{12}}}{(1-\eta_1.\eta_2)^2.\mathbf{Z}_{*_1}.\mathbf{Z}_{*_{12}}}=\frac{(1+\eta_1^2)..\mathbf{Y}_{*_1}+(1-\eta_1)^2.\mathbf{Y}_{*_{12}}}{(1-\eta_1.\eta_2)^2}$
$\left[\mathbf{Y}_{*}^{(p)}\right]=\begin{bmatrix}\mathbf{Y}_{*_1}+\mathbf{Y}_{*_{12}} & -\mathbf{Y}_{*_{12}}\\ -\mathbf{Y}_{*_{12}} & \mathbf{Y}_{*_1}+\mathbf{Y}_{*_{12}}\end{bmatrix}$	$\mathbf{Z}_{*_{11}}^{(m)}=\frac{\mathbf{Z}_{*_1}.\left((1+\eta_1^2).\mathbf{Z}_{*_{12}}+(1-\eta_1)^2.\mathbf{Z}_{*_1}^2\right)}{2.\mathbf{Z}_{*_1}+\mathbf{Z}_{*_{12}}}=\frac{(1+\eta_1^2).\mathbf{Y}_{*_1}+(1-\eta_1)^2.\mathbf{Y}_{*_{12}}}{\mathbf{Y}_{*_1}.\left(\mathbf{Y}_{*_1}+2.\mathbf{Y}_{*_{12}}\right)}$ $\mathbf{Z}_{*_{12}}^{(m)}=\mathbf{Z}_{*_{21}}^{(m)}=-\frac{\mathbf{Z}_{*_1}.\left((\eta_1+\eta_2).\mathbf{Z}_{*_{12}}-(1-\eta_1)(1-\eta_2).\mathbf{Z}_{*_1}\right)}{2.\mathbf{Z}_{*_1}+\mathbf{Z}_{*_{12}}}=-\frac{(\eta_1+\eta_2).\mathbf{Y}_{*_1}-(1-\eta_1)(1-\eta_2).\mathbf{Y}_{*_{12}}}{\mathbf{Y}_{*_1}.\left(\mathbf{Y}_{*_1}+2.\mathbf{Y}_{*_{12}}\right)}$ $\mathbf{Z}_{*_{22}}^{(m)}=\frac{\mathbf{Z}_{*_1}.\left((1+\eta_2^2).\mathbf{Z}_{*_{12}}+(1-\eta_2)^2.\mathbf{Z}_{*_1}\right)}{2.\mathbf{Z}_{*_1}+\mathbf{Z}_{*_{12}}}=\frac{(1+\eta_2^2).\mathbf{Y}_{*_1}+(1-\eta_2^2).\mathbf{Y}_{*_{12}}}{\mathbf{Y}_{*_1}.\left(\mathbf{Y}_{*_1}+2.\mathbf{Y}_{*_{12}}\right)}$
$\left[\mathbf{Z}_{*}^{(p)}\right]=\frac{1}{\sum\mathbf{Z}_{*}}\begin{bmatrix}\mathbf{Z}_{*_1}.\left(\mathbf{Z}_{*_2}+\mathbf{Z}_{*_{12}}\right) & \mathbf{Z}_{*_1}.\mathbf{Z}_{*_2}\\ \mathbf{Z}_{*_1}.\mathbf{Z}_{*_2} & \mathbf{Z}_{*_2}.\left(\mathbf{Z}_{*_2}+\mathbf{Z}_{*_{12}}\right)\end{bmatrix}$ $\sum\mathbf{Z}_{*}=\mathbf{Z}_{*_1}+\mathbf{Z}_{*_{12}}+\mathbf{Z}_{*_2}$	

TABLE 5.8 Continuation (see note on page 5-53)

Terminating network terminal admittance / impedance matrix	Modal transformation of the terminal admittance / impedance matrix Symmetric transmission line
Non-symmetric terminating network 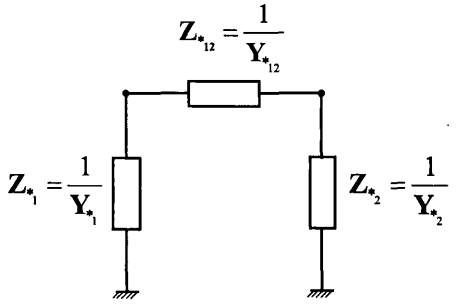 $\left[\mathbf{Y}_{*}^{(p)}\right]=\begin{bmatrix}\mathbf{Y}_{*_1}+\mathbf{Y}_{*_{12}} & -\mathbf{Y}_{*_{12}}\\ -\mathbf{Y}_{*_{12}} & \mathbf{Y}_{*_2}+\mathbf{Y}_{*_{12}}\end{bmatrix}$	$\left[\mathbf{Y}_{*}^{(m)}\right]=\frac{1}{4.\mathbf{Z}_{*_1}.\mathbf{Z}_{*_2}}\begin{bmatrix}\mathbf{Z}_{*_1}+\mathbf{Z}_{*_2} & \mathbf{Z}_{*_1}-\mathbf{Z}_{*_2}\\ \mathbf{Z}_{*_1}-\mathbf{Z}_{*_2} & \mathbf{Z}_{*_1}+4.\mathbf{Z}_{*_1}.\mathbf{Z}_{*_2}.\mathbf{Z}_{*_{12}}^{-1}+\mathbf{Z}_{*_2}\end{bmatrix}$ $\left[\mathbf{Y}_{*}^{(m)}\right]=\frac{1}{4}\begin{bmatrix}\mathbf{Y}_{*_1}+\mathbf{Y}_{*_2} & -\mathbf{Y}_{*_1}+\mathbf{Y}_{*_2}\\ -\mathbf{Y}_{*_1}+\mathbf{Y}_{*_2} & \mathbf{Y}_{*_1}+4.\mathbf{Y}_{*_{12}}+\mathbf{Y}_{*_2}\end{bmatrix}$ $\left[\mathbf{Z}_{*}^{(m)}\right]=\frac{1}{\mathbf{Z}_{*_1}+\mathbf{Z}_{*_{12}}+\mathbf{Z}_{*_2}}\begin{bmatrix}\mathbf{Z}_{*_1}.\mathbf{Z}_{*_{12}}+4.\mathbf{Z}_{*_1}.\mathbf{Z}_{*_2}+\mathbf{Z}_{*_2}.\mathbf{Z}_{*_{12}} & -\left(\mathbf{Z}_{*_1}-\mathbf{Z}_{*_2}\right).\mathbf{Z}_{*_{12}}\\ -\left(\mathbf{Z}_{*_1}-\mathbf{Z}_{*_2}\right).\mathbf{Z}_{*_{12}} & \left(\mathbf{Z}_{*_1}-\mathbf{Z}_{*_2}\right).\mathbf{Z}_{*_{12}}\end{bmatrix}$ $\left[\mathbf{Z}_{*}^{(m)}\right]=\frac{1}{\mathbf{Y}_{*_1}.\mathbf{Y}_{*_2}+\mathbf{Y}_{*_1}.\mathbf{Y}_{*_{12}}+\mathbf{Y}_{*_2}.\mathbf{Y}_{*_{12}}}.\begin{bmatrix}\mathbf{Y}_{*_1}+4\mathbf{Y}_{*_{12}}+\mathbf{Y}_{*_2} & \mathbf{Y}_{*_1}-\mathbf{Y}_{*_2}\\ \mathbf{Y}_{*_1}-\mathbf{Y}_{*_2} & \mathbf{Y}_{*_1}+\mathbf{Y}_{*_2}\end{bmatrix}$
Symmetric terminating network 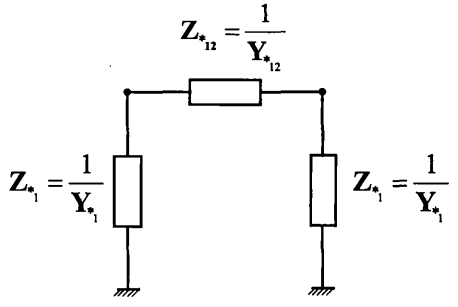 $\left[\mathbf{Y}_{*}^{(p)}\right]=\begin{bmatrix}\mathbf{Y}_{*_1}+\mathbf{Y}_{*_{12}} & -\mathbf{Y}_{*_{12}}\\ -\mathbf{Y}_{*_{12}} & \mathbf{Y}_{*_1}+\mathbf{Y}_{*_{12}}\end{bmatrix}$	$\left[\mathbf{Y}_{*}^{(m)}\right]=\frac{1}{2.\mathbf{Z}_{*_1}.\mathbf{Z}_{*_{12}}}\begin{bmatrix}\mathbf{Z}_{*_{12}} & 0\\ 0 & 2.\mathbf{Z}_{*_1}+\mathbf{Z}_{*_{12}}\end{bmatrix}$ $\left[\mathbf{Y}_{*}^{(m)}\right]=\frac{1}{2}\begin{bmatrix}\mathbf{Y}_{*_1} & 0\\ 0 & \mathbf{Y}_{*_1}+2.\mathbf{Y}_{*_{12}}\end{bmatrix}$ $\left[\mathbf{Z}_{*}^{(m)}\right]=\frac{2.\mathbf{Z}_{*_1}}{2.\mathbf{Z}_{*_1}+\mathbf{Z}_{*_{12}}}\begin{bmatrix}2.\mathbf{Z}_{*_1}+\mathbf{Z}_{*_{12}} & 0\\ 0 & \mathbf{Z}_{*_{12}}\end{bmatrix}$ $\left[\mathbf{Z}_{*}^{(m)}\right]=\begin{bmatrix}2.\mathbf{Y}_{*_1}^{-1} & 0\\ 0 & 2.\left(\mathbf{Y}_{*_1}+2.\mathbf{Y}_{*12}\right)^{-1}\end{bmatrix}$

TABLE 5.8 Continuation (see note on page 5-53)

Terminating network terminal admittance / impedance matrix	Modal transformation of the terminal admittance / impedance matrix	
	Non-symmetric transmission line	Symmetric transmission line
$\mathbf{Y}_{*_{12}} = 0$ 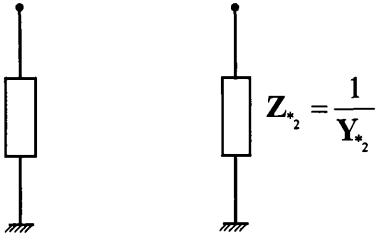 $\mathbf{Z}_{*_1} = \frac{1}{\mathbf{Y}_{*_1}}$ $\mathbf{Z}_{*_2} = \frac{1}{\mathbf{Y}_{*_2}}$ $\left[\mathbf{Y}_{*}^{(p)}\right] = \begin{bmatrix} \mathbf{Y}_{*_1} & 0 \\ 0 & \mathbf{Y}_{*_2} \end{bmatrix}$ $\left[\mathbf{Z}_{*}^{(p)}\right] = \begin{bmatrix} \mathbf{Z}_{*_1} & 0 \\ 0 & \mathbf{Z}_{*_2} \end{bmatrix}$	$\left[\mathbf{Y}_{*}^{(m)}\right] = \frac{1}{\left(1-\eta_1.\eta_2\right)^2}\begin{bmatrix} \mathbf{Y}_{*_1} + \eta_2^2.\mathbf{Y}_{*_2} & \eta_1.\mathbf{Y}_{*_1} + \eta_2.\mathbf{Y}_{*_2} \\ \eta_1.\mathbf{Y}_{*_1} + \eta_2.\mathbf{Y}_{*_2} & \eta_1^2.\mathbf{Y}_{*_1} + \mathbf{Y}_{*_2} \end{bmatrix}$ $\left[\mathbf{Y}_{*}^{(m)}\right] = \frac{1}{\left(1-\eta_1.\eta_2\right)^2.\mathbf{Z}_{*_1}.\mathbf{Z}_{*_{12}}}\begin{bmatrix} \eta_2^2.\mathbf{Z}_{*_1} + \mathbf{Z}_{*_2} & \eta_1.\mathbf{Z}_{*_2} + \eta_2.\mathbf{Z}_{*_1} \\ \eta_1.\mathbf{Z}_{*_2} + \eta_2.\mathbf{Z}_{*_1} & \mathbf{Z}_{*_1} + \eta_1^2.\mathbf{Z}_{*_2} \end{bmatrix}$ $\left[\mathbf{Z}_{*}^{(m)}\right] = \frac{1}{\mathbf{Y}_{*_1}.\mathbf{Y}_{*_2}}\begin{bmatrix} \eta_1^2.\mathbf{Y}_{*_1} + \mathbf{Y}_{*_2} & -\left(\eta_1.\mathbf{Y}_{*_1} + \eta_2.\mathbf{Y}_{*_2}\right) \\ -\left(\eta_1.\mathbf{Y}_{*_1} + \eta_2.\mathbf{Y}_{*_2}\right) & \mathbf{Y}_{*_1} + \eta_2^2.\mathbf{Y}_{*_2} \end{bmatrix}$ $\left[\mathbf{Z}_{*}^{(m)}\right] = \begin{bmatrix} \mathbf{Z}_{*_1} + \eta_1^2.\mathbf{Z}_{*_2} & -\left(\eta_1.\mathbf{Z}_{*_2} + \eta_2.\mathbf{Z}_{*_1}\right) \\ -\left(\eta_1.\mathbf{Z}_{*_2} + \eta_2.\mathbf{Z}_{*_1}\right) & \eta_2^2.\mathbf{Z}_{*_1} + \mathbf{Z}_{*_1} \end{bmatrix}$	$\left[\mathbf{Y}_{*}^{(m)}\right] = \frac{1}{4}\begin{bmatrix} \mathbf{Y}_{*_1} + \mathbf{Y}_{*_2} & -\mathbf{Y}_{*_1} + \mathbf{Y}_{*_2} \\ -\mathbf{Y}_{*_1} + \mathbf{Y}_{*_2} & \mathbf{Y}_{*_1} + \mathbf{Y}_{*_2} \end{bmatrix}$ $\left[\mathbf{Y}_{*}^{(m)}\right] = \frac{1}{4.\mathbf{Z}_{*_1}.\mathbf{Z}_{*_2}}\begin{bmatrix} \mathbf{Z}_{*_1} + \mathbf{Z}_{*_2} & \mathbf{Z}_{*_1} - \mathbf{Z}_{*_2} \\ \mathbf{Z}_{*_1} - \mathbf{Z}_{*_2} & \mathbf{Z}_{*_1} + \mathbf{Z}_{*_2} \end{bmatrix}$ $\left[\mathbf{Z}_{*}^{(m)}\right] = \frac{1}{\mathbf{Y}_{*_1}.\mathbf{Y}_{*_2}}\begin{bmatrix} \mathbf{Y}_{*_1} + \mathbf{Y}_{*_2} & \mathbf{Y}_{*_1} - \mathbf{Y}_{*_2} \\ \mathbf{Y}_{*_1} - \mathbf{Y}_{*_2} & \mathbf{Y}_{*_1} + \mathbf{Y}_{*_2} \end{bmatrix}$ $\left[\mathbf{Z}_{*}^{(m)}\right] = \begin{bmatrix} \mathbf{Z}_{*_1} + \mathbf{Z}_{*_2} & -\left(\mathbf{Z}_{*_1} - \mathbf{Z}_{*_2}\right) \\ -\left(\mathbf{Z}_{*_1} - \mathbf{Z}_{*_2}\right) & \mathbf{Z}_{*_1} + \mathbf{Z}_{*_2} \end{bmatrix}$
$\mathbf{Y}_{*_{12}} = 0$ 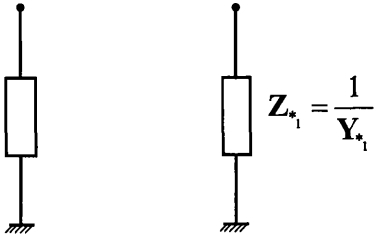 $\mathbf{Z}_{*_1} = \frac{1}{\mathbf{Y}_{*_1}}$ $\mathbf{Z}_{*_1} = \frac{1}{\mathbf{Y}_{*_1}}$ $\left[\mathbf{Y}_{*}^{(p)}\right] = \begin{bmatrix} \mathbf{Y}_{*_1} & 0 \\ 0 & \mathbf{Y}_{*_1} \end{bmatrix}$ $\left[\mathbf{Z}_{*}^{(p)}\right] = \begin{bmatrix} \mathbf{Z}_{*_1} & 0 \\ 0 & \mathbf{Z}_{*_1} \end{bmatrix}$	$\left[\mathbf{Y}_{*}^{(m)}\right] = \frac{\mathbf{Y}_{*_1}}{\left(1-\eta_1.\eta_2\right)^2}\begin{bmatrix} 1+\eta_2^2 & \eta_1+\eta_2 \\ \eta_1+\eta_2 & 1+\eta_1^2 \end{bmatrix}$ $\left[\mathbf{Y}_{*}^{(m)}\right] = \frac{1}{\left(1-\eta_1.\eta_2\right)^2.\mathbf{Z}_{*_1}}\begin{bmatrix} 1+\eta_2^2 & \eta_1+\eta_2 \\ \eta_1+\eta_2 & 1+\eta_1^2 \end{bmatrix}$ $\left[\mathbf{Z}_{*}^{(m)}\right] = \frac{1}{\mathbf{Y}_{*_1}}\begin{bmatrix} 1+\eta_1^2 & -\left(\eta_1+\eta_2\right) \\ -\left(\eta_1+\eta_2\right) & 1+\eta_2^2 \end{bmatrix}$ $\left[\mathbf{Z}_{*}^{(m)}\right] = \mathbf{Z}_{*_1}.\begin{bmatrix} 1+\eta_1^2 & -\left(\eta_1+\eta_2\right) \\ -\left(\eta_1+\eta_2\right) & 1+\eta_2^2 \end{bmatrix}$	$\left[\mathbf{Y}_{*}^{(m)}\right] = \frac{\mathbf{Y}_{*_1}}{2}\begin{bmatrix} 1 & 0 \\ 0 & 1 \end{bmatrix}$ $\left[\mathbf{Y}_{*}^{(m)}\right] = \frac{1}{2.\mathbf{Z}_{*_1}}\begin{bmatrix} 1 & 0 \\ 0 & 1 \end{bmatrix}$ $\left[\mathbf{Z}_{*}^{(m)}\right] = \frac{2}{\mathbf{Y}_{*_1}}\begin{bmatrix} 1 & 0 \\ 0 & 1 \end{bmatrix}$ $\left[\mathbf{Z}_{*}^{(m)}\right] = 2.\mathbf{Z}_{*_1}.\begin{bmatrix} 1 & 0 \\ 0 & 1 \end{bmatrix}$

TABLE 5.8 Continuation (see note on page 5-53)

Terminating network	Terminal admittance / impedance matrix	Modal transformation of the terminal admittance / impedance matrix	
		Non-symmetric transmission line	Symmetric transm.line
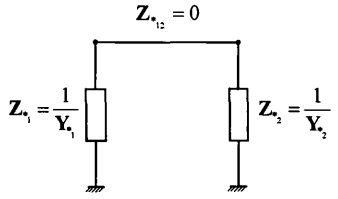	$[Z_{\bullet}^{(p)}] = \frac{Z_{\bullet_1}.Z_{\bullet_2}}{Z_{\bullet_1}+Z_{\bullet_2}}.\begin{bmatrix}1 & 1\\ 1 & 1\end{bmatrix}$	$[Z_{\bullet}^{(m)}] = \frac{1}{Y_{\bullet_1}+Y_{\bullet_2}}.\begin{bmatrix}(1-\eta_1)^2 & (1-\eta_1)(1-\eta_2)\\ (1-\eta_1)(1-\eta_2) & (1-\eta_2)^2\end{bmatrix}$ $[Z_{\bullet}^{(m)}] = \frac{Z_{\bullet_1}.Z_{\bullet_2}}{Z_{\bullet_1}+Z_{\bullet_2}}.\begin{bmatrix}(1-\eta_1)^2 & (1-\eta_1)(1-\eta_2)\\ (1-\eta_1)(1-\eta_2) & (1-\eta_2)^2\end{bmatrix}$	$[Z_{\bullet}^{(m)}] = \frac{1}{Y_{\bullet_1}.Y_{\bullet_2}}\begin{bmatrix}4 & 0\\ 0 & 0\end{bmatrix}$ $[Z_{\bullet}^{(m)}] = \frac{Z_{\bullet_1}.Z_{\bullet_2}}{Z_{\bullet_1}+Z_{\bullet_2}}.\begin{bmatrix}4 & 0\\ 0 & 0\end{bmatrix}$
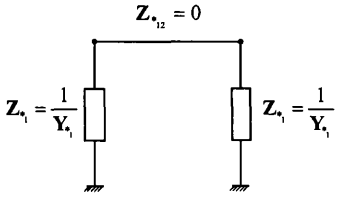	$[Y_{\bullet}^{(p)}] = \frac{1}{2}.Z_{\bullet_1}\begin{bmatrix}1 & 1\\ 1 & 1\end{bmatrix}$	$[Z_{\bullet}^{(m)}] = \frac{1}{2.Y_{\bullet_1}}.\begin{bmatrix}(1-\eta_1)^2 & (1-\eta_1)(1-\eta_2)\\ (1-\eta_1)(1-\eta_2) & (1-\eta_2)^2\end{bmatrix}$ $[Z_{\bullet}^{(m)}] = \frac{Z_{\bullet_1}}{2}.\begin{bmatrix}(1-\eta_1)^2 & (1-\eta_1)(1-\eta_2)\\ (1-\eta_1)(1-\eta_2) & (1-\eta_2)^2\end{bmatrix}$	$[Z_{\bullet}^{(m)}] = \frac{1}{Y_{\bullet_1}}.\begin{bmatrix}2 & 0\\ 0 & 0\end{bmatrix}$ $[Z_{\bullet}^{(m)}] = Z_{\bullet_1}.\begin{bmatrix}2 & 0\\ 0 & 0\end{bmatrix}$
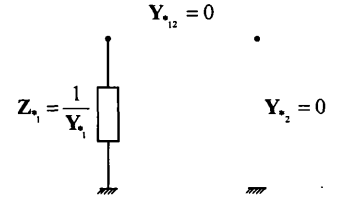	$[Y_{\bullet}^{(p)}] = \begin{bmatrix}Y_{\bullet_1} & 0\\ 0 & 0\end{bmatrix}$	$[Y_{\bullet}^{(m)}] = \frac{Y_{\bullet_1}}{(1-\eta_1\eta_2)^2}\begin{bmatrix}1 & \eta_1\\ \eta_1 & \eta_1^2\end{bmatrix}$	$[Y_{\bullet}^{(m)}] = \frac{Y_{\bullet_1}}{4}\begin{bmatrix}1 & -1\\ -1 & 1\end{bmatrix}$
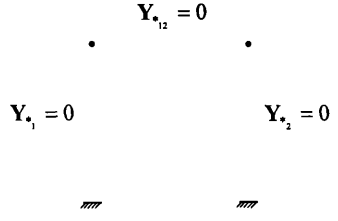	$[Y_{\bullet}^{(p)}] = \begin{bmatrix}0 & 0\\ 0 & 0\end{bmatrix}$	$[Y_{\bullet}^{(m)}] = \begin{bmatrix}0 & 0\\ 0 & 0\end{bmatrix}$	$[Y_{\bullet}^{(m)}] = \begin{bmatrix}0 & 0\\ 0 & 0\end{bmatrix}$

TABLE 5.8 Continuation (see note on page 5-53)

Terminating network	Terminal admittance / impedance matrix	Modal transformation of the terminal admittance / impedance matrix	
		Non-symmetric transmission line	Symmetric transm.line
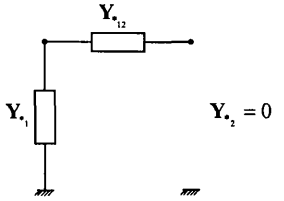 $\left[\mathbf{Y}_{\bullet}^{(p)}\right] = \begin{bmatrix} \mathbf{Y}_{\bullet 1} + \mathbf{Y}_{\bullet 12} & -\mathbf{Y}_{\bullet 12} \\ -\mathbf{Y}_{\bullet 12} & \mathbf{Y}_{\bullet 12} \end{bmatrix}$	$\left[\mathbf{Y}_{\bullet}^{(m)}\right] = \frac{1}{(1-\eta_1.\eta_2)^2}.\begin{bmatrix} \mathbf{Y}_{\bullet 1} + (1-\eta_2)^2.\mathbf{Y}_{\bullet 12} & \eta_1.\mathbf{Y}_{\bullet 1} - (1-\eta_1)(1-\eta_2).\mathbf{Y}_{\bullet 12} \\ \eta_1.\mathbf{Y}_{\bullet 1} - (1-\eta_1)(1-\eta_2).\mathbf{Y}_{\bullet 12} & \eta_1^2.\mathbf{Y}_{\bullet 1} + (1-\eta_1)^2.\mathbf{Y}_{\bullet 12} \end{bmatrix}$ $\left[\mathbf{Y}_{\bullet}^{(m)}\right] = \frac{1}{\mathbf{Y}_{\bullet 1}.\mathbf{Y}_{\bullet 12}}.\begin{bmatrix} \eta_1^2.\mathbf{Y}_{\bullet 1} + (1-\eta_1)^2.\mathbf{Y}_{\bullet 12} & -(\eta_1.\mathbf{Y}_{\bullet 1} - (1-\eta_1)(1-\eta_2).\mathbf{Y}_{\bullet 12}) \\ -(\eta_1.\mathbf{Y}_{\bullet 1} - (1-\eta_1)(1-\eta_2).\mathbf{Y}_{\bullet 12}) & \mathbf{Y}_{\bullet 1} + (1-\eta_2)^2.\mathbf{Y}_{\bullet 12} \end{bmatrix}$	$\left[\mathbf{Y}_{\bullet}^{(m)}\right] = \frac{1}{4}\begin{bmatrix} \mathbf{Y}_{\bullet 1} & -\mathbf{Y}_{\bullet 1} \\ -\mathbf{Y}_{\bullet 1} & \mathbf{Y}_{\bullet 1} + 4\mathbf{Y}_{\bullet 12} \end{bmatrix}$ $\left[\mathbf{Z}_{\bullet}^{(m)}\right] = \frac{1}{\mathbf{Y}_{\bullet 1}.\mathbf{Y}_{\bullet 12}}.\begin{bmatrix} \mathbf{Y}_{\bullet 1} + 4\mathbf{Y}_{\bullet 12} & \mathbf{Y}_{\bullet 1} \\ \mathbf{Y}_{\bullet 1} & \mathbf{Y}_{\bullet 1} \end{bmatrix}$
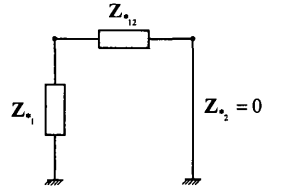	$\left[\mathbf{Z}_{\bullet}^{(p)}\right] = \begin{bmatrix} \mathbf{Z}_{\bullet 1}.\mathbf{Z}_{\bullet 12}.(\mathbf{Z}_{\bullet 1} + \mathbf{Z}_{\bullet 12})^{-1} & 0 \\ 0 & 0 \end{bmatrix}$	$\left[\mathbf{Z}_{\bullet}^{(m)}\right] = \frac{1}{\mathbf{Y}_{\bullet 1} + \mathbf{Y}_{\bullet 12}}.\begin{bmatrix} 1 & -\eta_2 \\ -\eta_2 & \eta_2^2 \end{bmatrix}$ $\left[\mathbf{Z}_{\bullet}^{(m)}\right] = \frac{\mathbf{Z}_{\bullet 1}.\mathbf{Z}_{\bullet 12}}{\mathbf{Z}_{\bullet 1} + \mathbf{Z}_{\bullet 12}}.\begin{bmatrix} 1 & -\eta_2 \\ -\eta_2 & \eta_2^2 \end{bmatrix}$	$\left[\mathbf{Z}_{\bullet}^{(m)}\right] = \frac{1}{\mathbf{Y}_{\bullet 1} + \mathbf{Y}_{\bullet 12}}.\begin{bmatrix} 1 & -1 \\ -1 & 1 \end{bmatrix}$ $\left[\mathbf{Z}_{\bullet}^{(m)}\right] = \frac{\mathbf{Z}_{\bullet 1}.\mathbf{Z}_{\bullet 12}}{\mathbf{Z}_{\bullet 1} + \mathbf{Z}_{\bullet 12}}.\begin{bmatrix} 1 & -1 \\ -1 & 1 \end{bmatrix}$
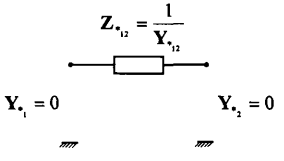	$\left[\mathbf{Y}_{\bullet}^{(p)}\right] = \mathbf{Y}_{\bullet 12}\begin{bmatrix} 1 & -1 \\ -1 & 1 \end{bmatrix}$	$\left[\mathbf{Y}_{\bullet}^{(m)}\right] = \frac{\mathbf{Y}_{\bullet 12}}{(1-\eta_1\eta_2)^2}\begin{bmatrix} (1-\eta_2)^2 & -(1-\eta_1).(1-\eta_2) \\ -(1-\eta_1).(1-\eta_2) & (1-\eta_1)^2 \end{bmatrix}$	$\left[\mathbf{Y}_{\bullet}^{(m)}\right] = \begin{bmatrix} 0 & 0 \\ 0 & \mathbf{Y}_{\bullet 12} \end{bmatrix}$
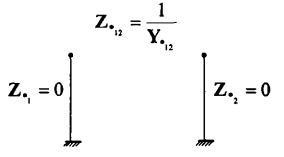	$\left[\mathbf{Z}_{\bullet}^{(p)}\right] = \begin{bmatrix} 0 & 0 \\ 0 & 0 \end{bmatrix}$	$\left[\mathbf{Z}_{\bullet}^{(m)}\right] = \begin{bmatrix} 0 & 0 \\ 0 & 0 \end{bmatrix}$	$\left[\mathbf{Z}_{\bullet}^{(m)}\right] = \begin{bmatrix} 0 & 0 \\ 0 & 0 \end{bmatrix}$

TABLE 5.9 Terminal admittance matrix, terminal impedance matrix, reflection operators and input impedance of a two-conductor transmssion line

Phase domain			Modal domain		
Transmission line termination					
Quan-tity	Symmetric, 'modally' tuned	Other	Quan-tity	Symmetric, 'modally' tuned	Other
$[Z_*^{(p)}]$ $[Y_*^{(p)}]$	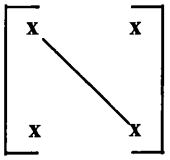	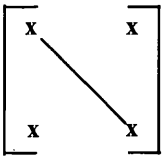	$[Z_*^{(m)}]$ $[Y_*^{(m)}]$	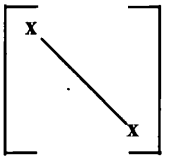	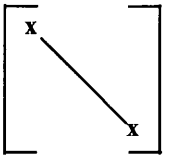
$[K_V^{(p)}]$ $[K_I^{(p)}]$	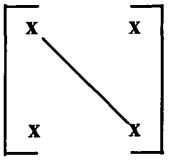	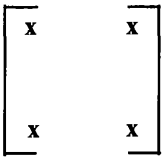	$[K_V^{(m)}]$ $[K_I^{(m)}]$	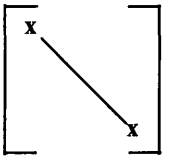	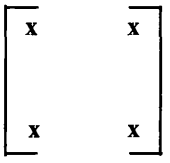
$[Z_{inp}^{(p)}]$ $[Y_{inp}^{(p)}]$	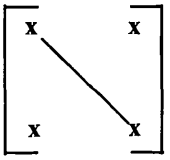	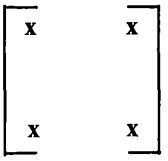	$[Z_{inp}^{(m)}]$ $[Y_{inp}^{(m)}]$	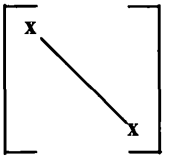	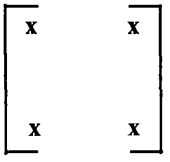
	Symmetric	Non-symmetric		Symmetric	Non-symmetric
Transmission line					

Note: Subscript '*' substitutes 'Tx' or 'Rx'

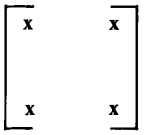 Rectangular, non-symmetric, non-diagonal matrix

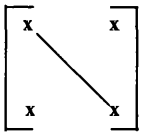 Symmetric matrix

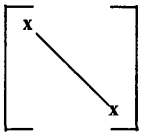 Diagonal matrix

FIGURE 5.7 Equivalent circuit representation of two-conductor input impedance /admittance

	Phase quantities			
	General case		'Modal' tuning	
	Delta	Star	Delta	Star
$[\mathbf{Y}_{inp}^{(p)}]$	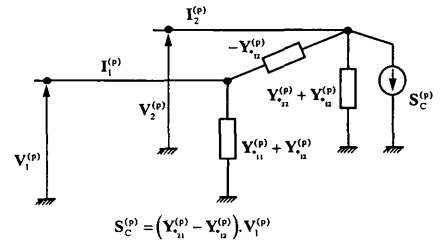	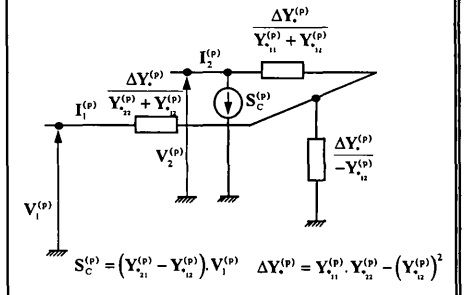	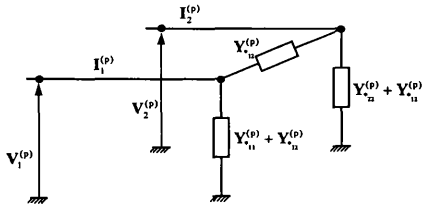	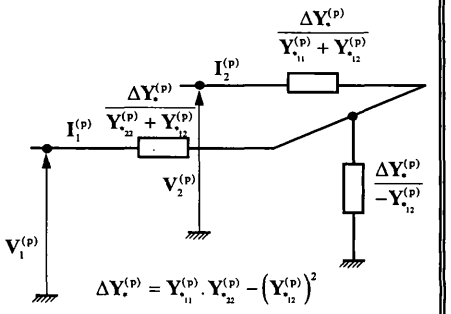
$[\mathbf{Z}_{inp}^{(p)}]$	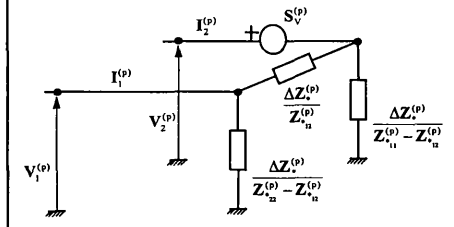	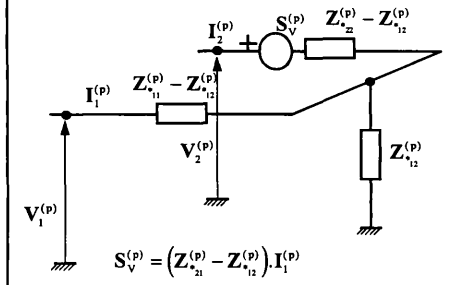	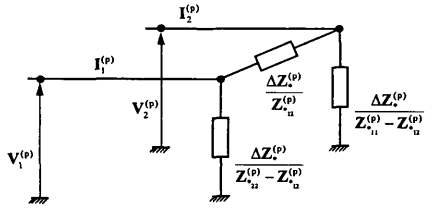	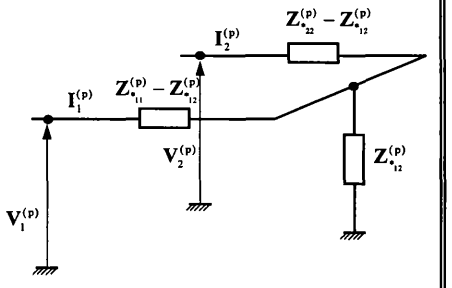

Note: The subscript '*' substitutes 'Tx', 'Rx' or 'inp'.

FIGURE 5.7 Continuation

	Modal quantities			
	General case		'Modal' tuning	
	Delta	Star	Delta	Star
$[\mathbf{Y}_{inp}^{(m)}]$	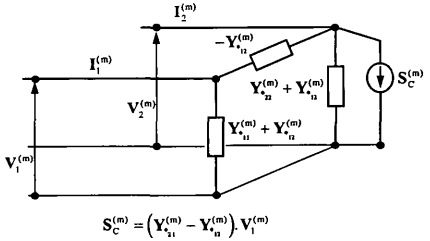	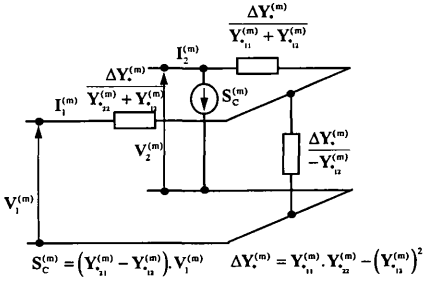	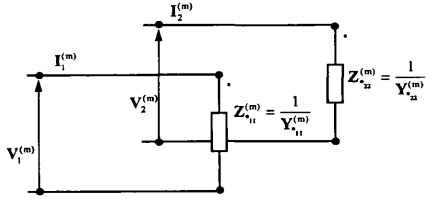	
$[\mathbf{Z}_{inp}^{(m)}]$	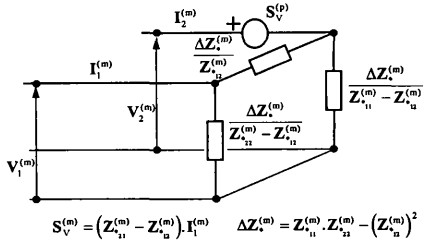	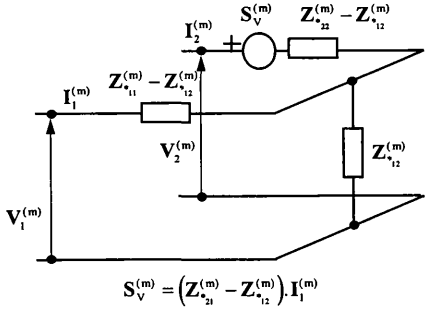		

Note: The subscript '*' substitutes 'Tx', 'Rx' or 'inp'.

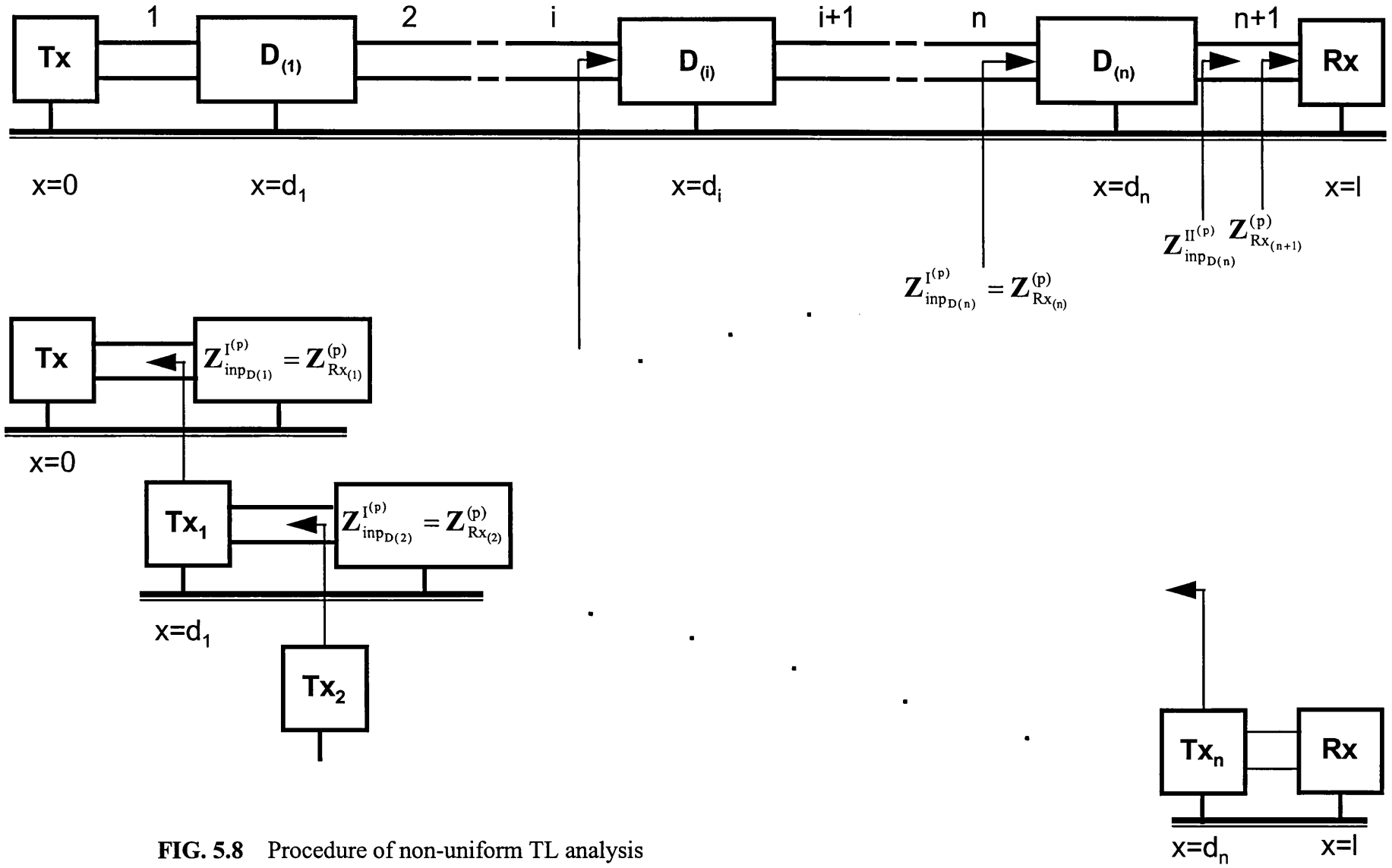

FIG. 5.8 Procedure of non-uniform TL analysis

Chapter 6

DEVELOPMENT OF A COMPUTER PROGRAM FOR TRACK CIRCUIT ANALYSIS AND DESIGN (TCADP)

The objective of this chapter is to present the development process and the structure of the software tool for track circuit analysis and design. Firstly, consideration is given to the requirements which such a specialised computer tool should implement, and particularly, to the specific track circuit related requirements. These considerations form the basis on which the method of computer implementation of the track circuit model is chosen. Justification is given for the choice of a purpose built software program. Further TCADP general structure is presented and the main building blocks and their operation explained in more details. The facilities provided by the TCADP and the procedure of using them are illustrated by modelling and simulation of an existing track circuit. In this way this chapter provides the background information necessary for the practical application of TCADP. Finally, the philosophy of validation of the track circuit computer model is explained.

6.1 CHOICE OF OPTION FOR THE DEVELOPMENT OF COMPUTER TRACK CIRCUIT SIMULATOR

The physical and functional models and the mathematical techniques presented in the previous chapters constitute a sufficient background for the implementation of a realistic and versatile track circuit computer model. Different approaches can be adopted and the choice of the most suitable one can only be decided in the context of its intended application. The analysis of the particular track circuit related requirements identifies the specific features which the required track circuit simulation tool should incorporate and allow to estimate which approach is most advantageous in achieving the necessary specification.

6.1.1 Requirements for the design of track circuit simulation tool

Designers of modern jointless AF track circuits need engineering tools which would enable them to perform the tasks of track circuit analysis and design.

Track circuit analysis consists in the evaluation of track circuit performance for any specified set of design parameters, operating conditions and environmental factors. This involves solution of the track circuit as an electric network in terms of some representative physical parameters, i.e. voltages, currents, impedances, etc. as well as the computation of specific coefficients characterising the track circuit performance for the

particular operating mode. The track circuit simulator should enable easy access to various output physical and derived variables and should allow to set different values of design parameters or specify different operating conditions.

The track circuit analysis includes as well the task of establishing how a particular parameter or external effect affects track circuit performance. Hence, the TCADP should be able to perform repeated simulations and derive the required relationship from the results of these simulations.

The problem of track circuit design consists in defining the set of track circuit parameters which would ensure that the track circuit operates according to the required functional algorithm. This problem can be reduced to the multiple solution of the problem of track circuit analysis, performed in a specifically ordered way. The aim is to accomplish a directed search through the multidimensional space defined by the constraints on the design parameters for a set of parameters which will guarantee the specified track circuit functionality and performance. To achieve this, the basic simulation tool has to be upgraded with additional facilities, based on a suitable optimisation method, which enable control of the search for the optimum design solution.

In addition, it is desirable that a fully developed track circuit simulation tool enables the investigation of track circuit operation under transient excitation as well as electromagnetic interference from various sources.

As far as the TCADP application is concerned the following requirements apply:

- versatility of application to various track circuit designs with minimum individual adjustment of the model,
- convenience in specifying and changing the conditions of simulation,
- convenience in entering the input data and inspecting the output results,
- well documented computer programs to allow possible modifications.

Table 6.1 gives an appreciation of the different types of simulations that are required to investigate various track circuit conditions. Some of the simulations may require different models and it may not prove efficient to incorporate all types of simulations within the same program. Instead, TCADP can be built as a set of computer programs, each specialised for a particular type of simulation. An alternative is for some types of simulations to use suitable professional simulation software.

The above considerations lead to the conclusion that a fully developed TCADP will have a layered structure and it would be most efficient to develop it stage by stage. The first step, achieved in the present research work, is the design of TCADP basic configuration, namely that part which performs track circuit analysis. It is supplemented by special

TABLE 6.1 Types of simulations necessary for the investigation of track circuit operation under various operating and environmental conditions

TC status / Type of simulation	TC excitation	External excitation		Design parameters		Operating conditions			Environm. factors		Application
	Steady state	Steady state	Transient	Steady state	Static varying	Static	Static varying	Dynamically changing	Steady state	Varying	
TC steady state solution	✓			✓		✓			✓		Static TC performance analysis Adjustments
		✓									
Multiple track circuit steady state solutions	✓			✓	✓	✓	✓		✓	✓	Frequency / parameter scans, Dynamic TC performance, Definition of worst/best scenarios
		✓									
Frequency domain solution with steady state excitation	✓			✓		✓		✓	✓		Investigation of coding and modulation techniques Investigation of the effect of EMI
		✓									
Time domain solution with steady state excitation	✓			✓		✓		✓			Investigation of dynamic track circuit performance
		✓									
Time domain solution with transient excitation			✓							✓	Investigation of the effect of EMI

subroutines for solving particular design optimisation problems. It is considered that the development of TCADP upper layer which is supposed to solve the general problem of track circuit design, should be based on the experience gained from the extensive application of TCADP basic configuration.

6.1.2 Possible approaches to the implementation of a track circuit computer model

The background for the modelling of track circuits provided by Chapters 3, 4 and 5 can be used for the implementation of a computer track circuit model on the basis of either of the following modelling techniques:

6.1.2.1 Analytical modelling

This approach is based on the derivation of analytical expressions of track circuit performance coefficients and other derived variables describing different aspects of track circuit performance. These expressions are written in terms of track circuit design parameters and other parameters defining the particular track circuit operating conditions. Track circuit performance can then be determined by computation of the analytical expressions for the desired values of the arguments. The difficulty is that such expressions have to be individually derived for each operating mode. On the other hand, the jointless audio frequency track circuits are complex systems and the analytical expressions describing their performance take the form of complicated mathematical functions of multiple variables which are difficult and sometimes impossible to visualise. The conventional methods of mathematical analysis are not practical but the investigation of the complex analytical functions can be done on computer.

The design of track circuits using this computer modelling approach involves optimisation of a set of mathematical expressions with respect to a number of optimisation parameters (track circuit design parameters) and according to a set of restrictions. Essentially this is a non-linear optimisation problem. It provides a fundamental solution of the complex problem of track circuit design which, despite some difficulties in finding a suitable optimisation algorithm, can be efficient when using the computer computational power.

The restrictions of the analytical approach are:

- A high proportion of the modelling, namely the derivation of the analytical expressions is done 'by hand';
- High complexity both in deriving the analytical expressions and in performing the computer solution and optimisation.;
- The track circuit model is highly abstract.

This method has been efficiently applied to DC and AC track circuits in [G-9]. The applicability of the method for audio-frequency track circuits with a current receiver has been demonstrated in [G-12, G-13].

6.1.2.2 Physical modelling

This approach is based on the implementation of a computer image of the real physical model in which each track circuit physical component i.e. tuning capacitor, adjustment resistor, impedance bond, section of rail track, etc. is represented by an appropriate physical model of the component. Each component can be modelled at either 'element' or 'system' level.

The 'element' level of modelling implies representation in terms of the basic passive or active electric circuit elements. The advantage of this approach is that it gives the greatest level of detail and access to every single element of the model. In general, this representation is always possible, but in some cases it may lead to unjustified complexity.

The 'system' level of modelling refers to a representation of a component in terms of equations relating the terminal voltages and currents. This approach gives a concise and exact description. The internal structure is not relevant and the user has access only to the terminals.

The choice of 'element' or 'system' level modelling should be based on a careful consideration of what level of detail is required and which elements need to be accessible for the purpose of track circuit investigation. The optimum compromise between detail and complexity has to be determined for each individual track circuit component. For instance, a transmission line may be modelled by a series connection of an adequate number of T- or π- lumped parameter networks, each representing an electrical equivalent of an incremental section of the transmission line or, alternatively, it can be described by an analytical relation between the voltages and currents at the two terminations. The first approach is more convenient for modelling short sections of transmission lines, such as the sections of rail track used for tuning of track circuit terminations. It is not suitable for modelling long sections of transmission lines, in which cases, the 'system' level modelling is more appropriate.

The approach based on physical modelling involves the computer implementation of a suitable solution technique. Once the model is set up and validated, it can be used to simulate the operation of the system for any specified set of values of the defining parameters. The system performance can be then assessed indirectly from the results of the system simulations. The difficulty in applying this technique is in determining the

range of simulations which must be carried out in order to derive confident conclusions about the system behaviour.

Some simulation tools are based on professional electric circuit simulation packages [6-1, 6-2, 6-3], whilst others use specially-designed computer models [2-23, 6-4].

In relation to this project particular consideration has been given to the Electromagnetic Transients Simulation Program (EMTDC) created by Manitoba HVDC Research centre [6-5]. Although developed specifically for power systems modelling it is applicable to any electric circuit network. From the input data, specified in a input data file with fixed format, the model of the electric circuit is assembled in the form of a node admittance matrix. The solution of the electric network is based on the solution of the system of nodal voltage equations which gives the values of all node voltages and branch currents.

EMTDC operates in the time domain and all lumped parameter components and transmission line sections are modelled by suitable time domain equivalent representations. The resistors are time invariant while the inductors and the capacitors are represented by a resistor in parallel to a current source. The EMTDC has the following important features which are particularly relevant to the track circuit modelling:

- Time-domain simulation with steady state or transient excitation;
- All electric circuit parameters are easily accessible by the user during the course of the simulation;
- Possibility for reconfiguration of the network during simulation by using control switches;
- All node voltages and branch currents are accessible as outputs. There is possibility for implementation of 'meters' through which any physical or derived variable can be calculated and output;
- Ability to automatically run multiple simulations on the same time domain model changing one or more variables to search for optimum response;
- Set of subroutines for calculation of transmission line parameters, transformer parameters, etc.;
- Possibility to control the run of the simulation by a user written dynamics simulation subroutine (DSDYN);
- Accessible source code.

Regarding the suitability of EMTDC for track circuit simulations it was felt that this program was particularly suitable for simulation of transient excitation, as originally intended, but was not as suitable for investigation of the steady state operation. A particular disadvantage of the program is that extreme care should be taken in specifying some variables, such as the initial conditions of simulation, the parameters of the branches with small resistance and the simulation time step, etc., as these can very easily cause

unstable numerical solution. It was therefore decided to concentrate the efforts in developing a purpose built simulation tool which gives freedom in implementing the computer model and best suited simulation features.

In conclusion, both approaches have their advantages and disadvantages but the optimum solution seems to be the combination of universally applicable facilities for electric circuit description and problem solving with purpose-developed software for solving the specific problem of track circuit design and optimisation.

6.2 COMPUTER IMPLEMENTATION OF TRACK CIRCUIT MODEL

6.2.1 Structure of the computer model. Model building blocks.

The track circuit computer model has a modular structure and is built as a cascade connection of model building modules, each representing a (n+1)- or (2n+1)-pole networks (Fig.6.1 and Appendix B). The modular structure is very advantageous in enabling an easy assembly of different configurations.

In general, the building modules correspond to the separate pieces of equipment connected to the rails as well as sections of rail track. The model modules describing sections of rail track, except those with special purpose e.g. short sections of rails used for tuning of track circuit terminations, are universally applicable to all types of track circuits. However, the modules representing various components of the track circuit equipment are application specific. As a result it is unavoidable that the track circuit model should be individually assembled for each particular application. This is done once and the effort necessary to create the computer code is minimised to the highest extent. This is achieved by describing each type of module with its own subroutine. The interface connection between the modules is made through the specification of the values of the subroutine variables The computer code describing the model represents a list of 'CALL SUBROUTINE ...' commands in the order in which the modules are connected.

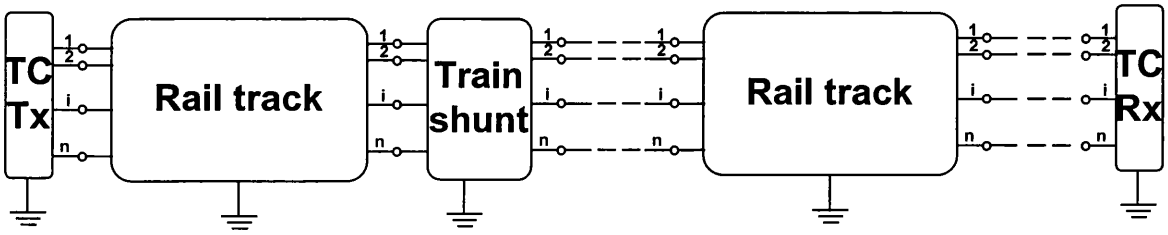

FIG.6.1 Structure of track circuit computer model

The specific model building modules of the various components of track circuit equipment are mostly described as lumped parameter networks. In some instances it is

TAB.6.2 Components of FS 2000 track circuit computer model

Ref. No	Modelling module	Universal	Application specific	Method of modelling
1	Long section of rail track	✓		Transmission line
2	Long section of rail track occupied by a vehicle	✓		Transmission line with a discontinuity (train shunt)
3	Short section of rail track (Track Circuit Termination)		✓	Lumped parameter network with series resistance and inductance equivalent to those of the short section of rail track
4	Short section of rail track (between the two termination bonds)		✓	
5	Long section of cable (between trackside equipment and equipment room)	✓		Transmission line
6	Tail cable	✓		Lumped resistance and inductance equivalent to those of the section of cable
7	Termination bond		✓	Lumped resistance and inductance
8	Tuning unit capacitor		✓	Lumped resistance and capacitance
9	Tuning unit transformer		✓	Equivalent circuit of a transformer derived from the parameters of the Short circuit and Open circuit tests
10	Track circuit transmitter		✓	Equivalent Thevenin Tx
11	Track circuit receiver		✓	Equivalent Rx

convenient to integrate a lumped parameter network module with a module of a short section of rail track. Table 6.2 contains a list of the modelling modules necessary for the assembly of FS 2000 track circuit computer model.

Transmission line models, both for long and short sections, are defined in terms of the transmission line primary parameters. During each simulation run of the program their values are calculated for the current frequency, using interpolation curves of rail track parameters derived on the basis of experimental results. To simulate shunted track

circuits, alternative short and long rail track section modules are implemented which incorporate a static or dynamically moving train shunt.

It should be noted that the model building modules of FS 2000 track circuit components described in Table 6.2 refer to modelling a track circuit on a non-electrified railway line. In this case the rail track can be represented by a two-conductor transmission line and it is most convenient to take advantage of the relative simplicity of the 'element' level modelling as applied to the lumped parameter track circuit components. When investigating the problem of electrical interferences or the operation of track circuits on electrified railway lines all lumped parameter networks have to be described in terms of (n+1)- or (2n+1)-terminal networks. This can be done by extending the systems of two equations describing a two-port network to systems of n equation written in matrix form. Analytically, the model will then represent a cascade connection of matrices which will operate only in terms of the terminal and intermediate voltages and currents. However, when an internal component is of interest for the investigation, it would still be possible to 'access' it using the equations relating the voltage and the current in this element with the terminal voltages and currents.

6.2.2 Method and procedure of solution of track circuit computer model

The solution procedure of the implemented physical track circuit computer model is based on the idea of the solution method described in Section 5.4.3. It includes two stages: forward and backward solution.

The forward solution consists of consecutive reductions of the whole track circuit network to a simpler circuit by successively replacing parts of the network by simpler equivalent circuits. This process starts with the calculation of the equivalent impedances seen looking from the track circuit terminations into the adjacent track circuits and continues towards the track circuit transmitter until a simple one loop equivalent circuit is obtained. This circuit is then solved to determine the value of the current in the track circuit transmitter.

The second stage of the solution procedure consists in defining the currents and the voltages in all track circuit components from a knowledge of the current in track circuit transmitter. This is done in consecutive steps, each consisting in backward substitution of an equivalent circuit with the real circuit and solving that circuit to obtain the voltages and currents in its components.

The electric circuit reduction carried out on the first stage of the solution procedure is implemented in two parallel computational channels. One is based on the Thevenin (or Norton) theorem and the other is based on the substitution theorem. The results of the two computations are compared at several check points of the track circuit to ensure that the

computations are correct. After successful debugging and testing of the program one of the channels can be removed.

In addition two parallel computational branches are implemented - one referring to the unoccupied state of the track circuit, and the other - to a shunted track circuit. Switching between the two algorithms is achieved by 'shunt' flags. A 'shunt' flag is assigned to each particular section of the track circuit network which is being reduced in one calculation step.

After the full track circuit solution the program calculates some derivative variables which are of particular interest for the analysis of track circuit performance such as track circuit transfer impedance, performance coefficients, transfer coefficients of electrical separating joints and other variables as necessary.

6.3 CONFIGURATION AND OPERATION OF THE PROGRAM FOR TRACK CIRCUIT ANALYSIS AND DESIGN

6.3.1 General structure

A concept for the general structure of TCADP is shown in Fig.6.2. It has a task-oriented, modular structure consisting of two groups of modules: a core group of processing and control modules and an input-output periphery.

The input provides a user-friendly facility for describing the TC electric network, specifying the problem to be solved and transferring the input data to the main program through input dialogue and/or input data files.

The output includes storing the required output results into files in a form suitable for graphical processing and two- or three-dimensional representation of the output data.

The main part of TCADP is the central group of problem solving modules: 'TC solver', 'Simulation control' and 'Task control logic'. Fig.6.2 shows a layered graphical representation of these modules, reflecting the real organisation of the program and the interaction between the modules.

6.3.1.1 'TC solver' module

This is the basic building module which provides solution of the TC model and definition of the TC performance for a specified track circuit status. The module includes a TC model, a sub-module for assembly of the configuration required for the simulation and a subroutine for solution of the specified TC electric network. This module was essentially described in more details in Section 6.2. To complete its description with reference to FS 2000 track circuit it can be noted that the 'TC solver' module is based on the following subroutines:

- SBCIN - Subroutine for calculation of the Thevenin equivalent of the cable transmission line connecting the trackside equipment to the equipment room;
- SBZTB - Subroutine for modelling and solution of the termination bond section of FS 2000 track circuit;
- SBZTT - Subroutine for modelling and solution of the track circuit termination section of FS 2000 track circuit;
- SBZTL - Subroutine for modelling and solution of the rail track between TC transmitting and receiving ends.

The use of these subroutines makes the programming code more efficient but more importantly, it enables the track circuit model to be structured as a modular structure. This is essential for reducing the necessary adjustments when the tool is to be used for the simulation of a different type of track circuit.

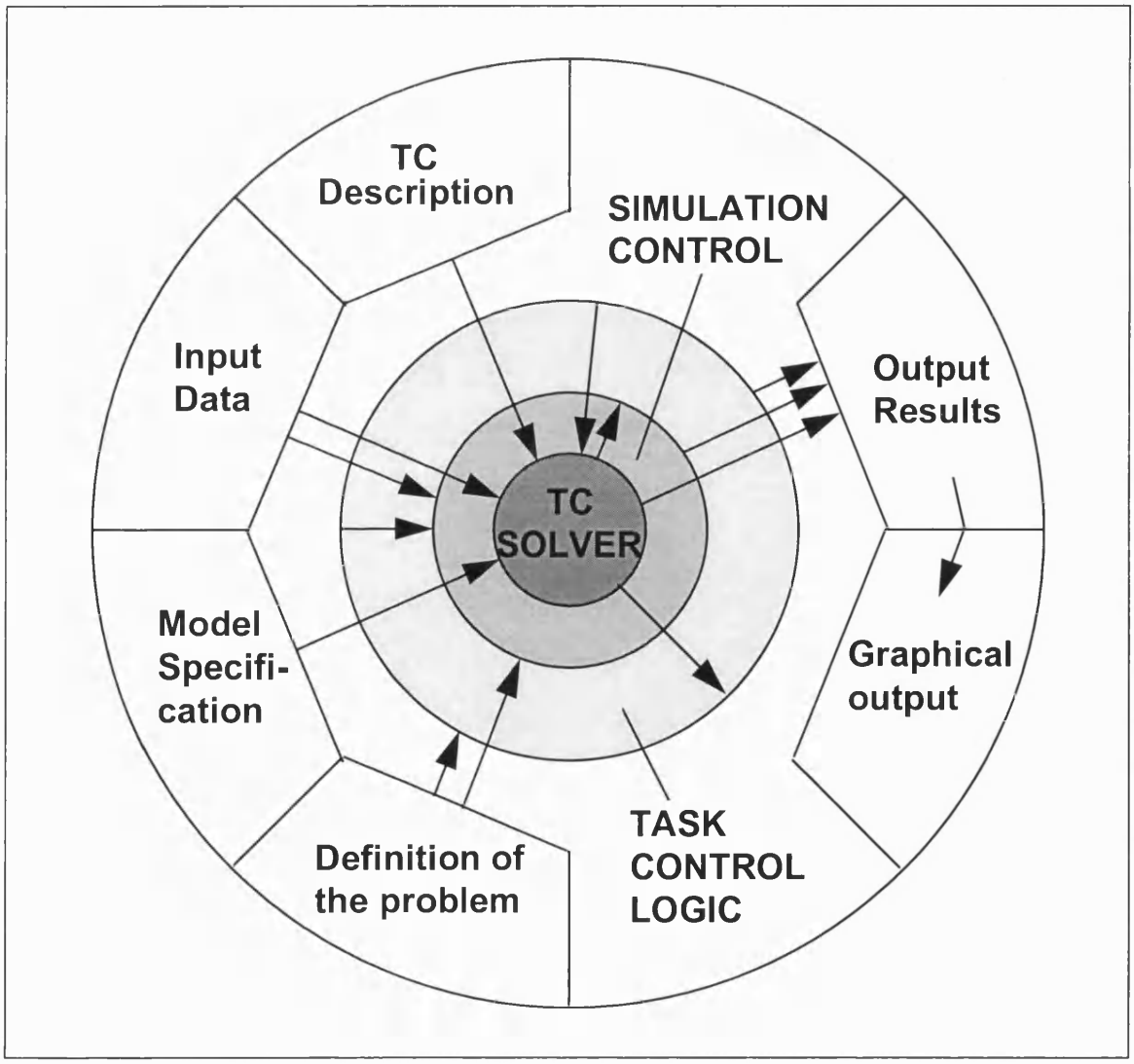

FIG.6.2 TCADP general structure

6.3.1.2 'Simulation control' module

When applying TCADP for the investigation of TC dynamic performance, a number of successive solutions of the specified track circuit model would be required. Moreover, different track circuit model might need to be used in each simulation (e.g. as a train moves along a track circuit). The control of the dynamic simulation is performed by the second layer module which controls the cycle of multiple runs of the TC solver, reassembles the model or the configuration, reassigns the input data for each new run and stores the output results from each run. This module controls as well the so called 'parameter variation' simulations. Such simulations can be requested either directly by the user who specifies the conditions of parameter variation or performed as part of an optimisation procedure. In the second case the conditions of parameter variation are received from the upper layer.

6.3.1.3 'Task control logic' module

The problem of defining the worst or best scenario of operation and the optimisation of track circuit design involves multiple runs of the 'TC solver'. However, in this case, especially if optimisation of the TC design is concerned, the control logic performing the control of the cycle or nested cycles is much more complicated. It should perform a specifically directed search through the track circuit definition area following a specific optimisation strategy. The other main function of this module is the processing of the results according to the specified minimisation or optimisation criterion.

The choice of the appropriate optimisation strategy is difficult in view of the complexity and non-linearity of the optimisation function and the multiple variables involved. For such complex functions and for computer applications, direct search methods are more appropriate than the methods which use the function values as well as gradient calculation such as Hooke and Jeeves's, Nelder and Mead's, etc., described in [6-6]. Direct search methods do not require computation of gradients and involve only circuit analysis techniques. They rely on error function evaluation in order to search for a point with a lower function value.

6.3.2 Facilities of the CAE tool for track circuit computer simulation

TCADP provides the following facilities for the simulation and investigation of track circuits:

6.3.2.1 Choice of track circuit configuration

Depending on the purpose of the simulation the user has the option to use either a simplified or a full track circuit model. The simplified TC model consists of a single

track circuit, the adjacent rail track at both TC ends being substituted by equivalent impedances. This model can be used in most cases, especially when multiple runs are concerned. When the purpose of the simulation is to investigate the track circuit terminations, ESJ operation under train shunt conditions or proximity effects between adjacent track circuits the full model has to be used.

6.3.2.2 Static/dynamic simulation of track circuit operation under various conditions

The track circuit simulator allows to perform TC simulations under the following operating conditions:

- Unoccupied track circuit, unoccupied adjacent track circuits;
- Unoccupied track circuit, occupied adjacent track circuit with static train shunt at any location or dynamically moving train shunt;
- Dynamically moving train shunt along three consecutive track circuits or any specified length of track within these track circuits;
- Two adjacent track circuits occupied with either static train shunts at any location or with one static and one dynamically moving shunt;
- Static train shunts at any specified location (for modelling individual train axles).

6.3.2.3 Frequency and/or parameter variation

The simulation tool allows to investigate track circuit performance as function of a number of design parameters such as:

- Tx and Rx internal impedances,
- Track circuit length,
- Rail track parameters,
- Distance between the track circuit and the equipment room,
- Frequency.

The range and step of parameter variation are specified by the user. When necessary, variation of other parameters can be incorporated.

6.3.2.4 Parameter optimisation

The simulation tool includes a specific module which calculates the optimum length of track circuit terminations as function of track circuit length and the length of the cables connecting the trackside equipment to the equipment room. In principle, any other optimisation problems can be solved but the optimisation strategy has to be applied by the user. The development of the 'Task control logic' module will enable the optimisation process to be performed automatically.

6.3.2.5 Multiple run feature

For some simulations, e.g. dynamic track circuit operation, it is not possible to perform simultaneous variation of the frequency or a parameter. In such cases the multiple run feature can be used which enables to repeat the simulation for a different value of a parameter or the frequency.

6.3.2.6 Short/detailed solution

Apart of the detailed track circuit solution, TCADP provides qualitative measure of track circuit performance in terms of different track circuit performance coefficients and other derived variables and may indicate the range of parameters for which the required performance is not ensured.

6.3.2.7 User guidance

During the execution of the computer program the user is given comprehensive guidance as to what possible configurations and simulation conditions he may specify as well as indication of execution time errors.

6.3.3 TCADP operational characteristics

TCADP is developed using FORTRAN 77 programming language. The programming code consists of 2800 lines which include defined functions, subroutines and detailed commentaries. The main program is supported by 5 major subroutines. The execution time for a single run of the program on a 486, 133 MHz personal computer is between 3 and 4 seconds. The execution time of more complex dynamic simulations depends on the number of runs required.

6.4 APPLICATION OF TCADP FOR TRACK CIRCUIT SIMULATION

The basic version TCADP is developed with reference to the FS 2000 track circuit. When versions for the other track circuit designs are developed, the application of TCADP will be straightforward. However, if the tool is to be used in its present state of development for the simulation of a different track circuit type, some adaptation work is necessary. The volume of this work is not big but it requires a good knowledge of the program structure and the methods of building up and solving the track circuit model. This is necessary in order to provide a correct interface between the universal and the application specific modules.

The adaptation work which is required has two aspects - preparation of the input data and reassembling the model of the new track circuit.

6.4.1 Preparation of input data

The preparation of the input data for running the track circuit simulator includes preparation of a schematic diagram, an input data file and input data to be entered during the start up dialogue.

6.4.1.1 Schematic diagram and notation

The first requirement for the application of the software tool for simulation of track circuit operation is to produce a clear schematic diagram of the track circuit. The purpose of the diagram is not only for visualisation of the track circuit model. It proves invaluable throughout the modelling and simulation stages, forms the basis on which the track circuit model is built up, and is the key to which everything else is referenced. There is no particular format in which the schematic diagram should be presented. It is important that it is drawn to show all the track circuit components and the way they are connected to the running rails with the level of detail which the user requires. It is recommended that the diagram includes at least the two adjacent track circuits. This configuration can then form the basis of the full track circuit model.

The schematic diagram should define the notation system providing a unique identification of the main physical variables in terms of which the track circuit model is set up. Indeed, the most easy and unambiguous way to define the notation system is to indicate the variables on the diagram. They should include:

- All currents, voltages and impedances which are of interest for the simulation and should be accessible to the user;
- All equivalent input impedances and energy sources which will be used in the solution procedure;
- All components of track circuit equipment with indication of the track circuit they belong to;
- Division of the track circuit configuration into a number of sections on the basis of functional and/or modelling consideration and their unique identification;
- Unique name identifications of all track circuit sections' lengths and other dimensions as necessary;
- Unique name identifications of the 'shunt' flags and shunt positions assigned to each track circuit section;
- Identification of one direction of travel as '1' and the other as '0';
- Definition of any other variables and any other useful information.

Fig.6.3 shows the schematic diagram of FS 2000 track circuit used in the application of TCADP and gives an illustration of the above requirements.

The system of notation is application specific.

6.4.1.2 Input data file

The input data file is of fixed format and contains the values of the basic track circuit design parameters. When read from the file these values are assigned to the corresponding variables and used as default values but can easily be changed through the input dialogue. The input data file is also application specific as it reflects the particular track circuit design.

An input data file for the FS 2000 track circuit is shown in Table 6.3. It refers to track circuit type YL. Every track circuit type has its individual input data file.

A separate input data file is required for the simulation of static train shunt operation. It specifies the position of train shunt(s) in terms of track circuit section 'shunt' flag and train shunt position within the section(s).

6.4.1.3 Input dialogue

Some input data which are more likely to change from one simulation to another are specified during the input dialogue. These are:

- Use of the full or simple track circuit model;
- Simulation of unoccupied or shunted track circuit;
- Lengths of the cables connecting the trackside equipment to the equipment room;
- Variation of frequency and if 'Yes' - the range and the step of variation;
- Variation of parameter and if 'Yes' - the range and the step of variation;
- Name of input data file;
- Specification of the conditions for simulation of track circuit shunt operation;
- Is another run required and if so - new input file name.

6.4.2 Assembling of track circuit model

It has already been pointed out that the track circuit model has modular structure, based on several subroutines, some of which are universally applicable and some are application specific. The adjustment of the model for the simulation of a new type of track circuit would require writing one or more subroutines, each describing a characteristic part of the track circuit. These application specific subroutines can be produced using the available subroutines as templates for their style and interface to the main program to be uniform with those adopted in the basic version of TCADP.

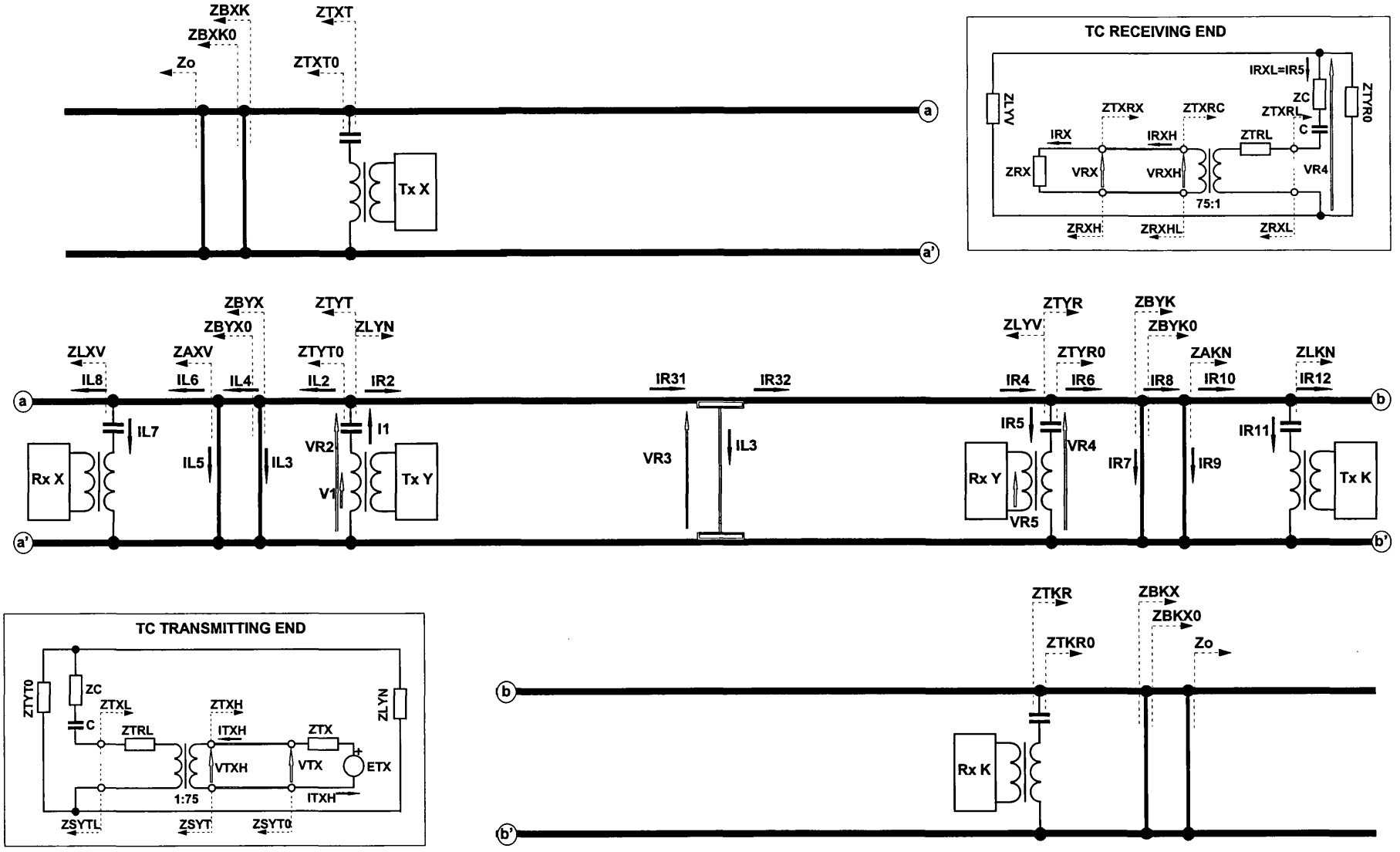

FIG.6.3 Schematic diagram of three consecutive FS 2000 track circuits with indication of currents, voltages and equivalent input impedances

TABLE.6.3 Input data file for FS 2000 track circuit (YL type)

Termination bond (TB) parameters **RTB** = 3.10E-03	**LTB** = 1.4E-06			
Tx/Rx tuning unit connecting cables - resistance and inductance **RC** = 6.20E-03	**LC** = 1.32E-06			
TU transformer impedance referred to the low side **RTRL** = 6.00E-03	**LTRL** = 1.00E-06			
Transformer ratio Low side (rail track) / High side (Tx or Rx) **RATIO** = 0.01333				
Tx and Rx TU capacitors (TC Y) **CTUYT** = 73.00E-06	**CTUYR** = 73.00E-06			
Tx resistance and Tx output voltage **RTX** = 8.00	**ETXRX** = 80.00			
Rx internal resistance, energisation and de-energisation levels **RRX** = 30.00	**IUP** = 24.00E-03	**IDOWN** = 21.50E-03		
Lengths of TB (Tx end), TCT (Tx end), TC, TCT (Rx end) and TB (Rx end) - TC Y **TBLYX** = 0.75	**TTLYT** = 7.08	**LY** = 300.00	**TTLYR** = 7.08	**TBLYK** = 0.75
Tx and Rx tuning unit capacitors (TC X) **CTUXT** = 87.00E-06	**CTUXR** = 87.00E-06			
Lengths of TB (Tx end), TCT (Tx end), TC, TCT (Rx end) -TC X **TBLXK** = 0.75	**TTLXT** = 7.08	**LX** = 300.00	**TTLXR** = 7.08	
Tx and Rx TU capacitors (TC K) **CTUKT** = 118.00E-06	**CTUKR** = 118.00R-06			
Lengths of TB (Tx end), TCT (Tx end), LK, TCT (Rx end) - TC K **TTLKT** = 6.96	**LK** = 300.00	**TTLKR** = 6.96	**TBLKX** = 0.75	
Parameters of the cable connecting the trackside equipment to the equipment room **CABLER** = 16.3E-03	**CABLEL** = 0.64E-06	**CABLEG** = 1.00E-09	**CABLEC** = 0.10E-09	
Frequency of TC Y **FREQ** = 5520.00				

6.5 VALIDATION OF TRACK CIRCUIT MODEL

6.5.1 Validation strategy

The validation strategy includes two methods complementing each other. The first method is carried out throughout the development of the track circuit model and its computer implementation and consists in the validation of any single step of this process. It is applied to the individual model components and the individual aspects of the model building process through a continuous analysis and monitoring of their accuracy and correctness. The purpose of this activity is not only to gain confidence that the model is correct and will produce realistic results but also, to get a good knowledge and a measure of how well the track circuit model maps the real system. This knowledge is essential for the further use of the model - it enables to correctly interpret the simulation results and forms the background for further improvement of the model.

The second method involves validation of the overall model to ensure that the individual model elements are correctly integrated and interact in the expected way. This validation method requires the model to be tested and the results to be compared with results which are known to be correct, e.g. obtained by experimental measurements of the real track circuit. However, testing and validating all aspects of the model would require carrying out extensive experiments involving track circuit operation under various operating conditions which is difficult to achieve in real conditions. It has therefore been decided to model an established track circuit, with widespread use and well known specification and performance in various operating conditions. The availability of a defined point of reference and good understanding of what simulation results are to be expected is even more beneficial. It enables during the testing and validation of the model to concentrate on the model itself and interpret the results from point of view of the model design rather than not being able to separate the effect of the modelling approximations, inaccuracies, etc. from the specific phenomena being simulated.

6.5.2 Validation on element level

The element level validation has been carried out in parallel with the model development by using the following validation techniques:

- Careful choice of models for the individual track circuit components based on analysis of their applicability;
- Analysis and verification of the impact of the inaccuracies of model parameters and those resulting from the approximations and simplifying assumptions made, etc.;
- Use of well proven solution methods;

- Checking the solution procedure and proving its correctness;
- Extensive testing and verification of the computer program to prove its correctness.

The implementation of the above techniques has been an inherent part of the modelling process and has been referred to along with the presentation of the various model development stages. Here, the main conclusions regarding the validation at element level will be summarised.

6.5.2.1 Choice of models for track circuit components

The track circuit model has a simple modular structure. The individual components are modelled using well proven models, namely those of a transmission line and electric circuits with lumped parameter elements. These models are exact and do not introduce any approximations. The precision of the models depends only on the correctness of the model parameters.

In some cases, the models have been suitably approximated for the sake of simplification. For instance, a short section of rail track has been modelled by equivalent T-networks with lumped parameters representing rail track resistance and inductance and neglecting rail track conductance and capacitance as negligible. Another example is the modelling of tuning unit transformer with an equivalent circuit in which the magnetising inductance and the core loss resistance have been neglected as being much higher that the other elements. In both cases, the effects of the approximations have been proved insignificant by comparing results obtained using the precise and the approximated models.

6.5.2.2 Correctness of model parameters

The parameters of the track circuit components connected to the rails are correct as they have been either provided by the manufacturer (i.e. termination bonds, tuning unit capacitors, dimensions of tuning unit areas, cables between track and equipment room, transmitter and receiver) or measured (i.e. tuning unit transformer).

As far as the parameters describing rail track as a transmission line are concerned, a different approach applies. When referring to rail track parameters in general, without reference to a particular railway line, it is correct to define them not in terms of particular values, but rather, in terms of parameter ranges. This is justified as well by the fact that the parameters of a particular track vary themselves and the correct track circuit performance has to be ensured for the whole range of rail track parameters. Therefore, the aim was to define some average parameters with some realistic range of variation. These data have been obtained on the basis of a compilation of experimental data. To account for the effect of the frequency, averaged experimental data have been interpolated in the relevant frequency range and used in the computer program for the calculation of rail

track resistance, inductance, conductance and capacitance for the desired frequency. Being based on experiment, the data used should as well incorporate the effect of non-linearity.

This approach has been found fully acceptable for the setting of the track circuit model and has produced very satisfactory validation results. However, it does not exclude the necessity of defining the rail track parameters as accurately as possible when the simulation tool is to be used for a particular application, especially a non-conventional rail track.

6.5.2.3 Solution method and correctness of the solution

The solution of the developed track circuit model is based on well proven fundamental methods of solution of electric networks: the Kirchoff's laws, Thevenin theorem and the substitution theorem. These solution methods do not involve inverting matrices and do not involve any risk of numerical computational problems. The solution of the model is done in two alternative ways and the results are then being compared to eliminate any mistakes. In addition, the results obtained by solving the track circuit model for a few particular cases have been compared with results obtained by solving the model on Mathcad.

6.5.2.4 Correctness of the computer program

The correctness of the computer code has been proved by extensive debugging and testing of all possible paths of the program. The main program module 'Track circuit solver', performing the solution of the model is built on computational redundancy with multiple check points. All stages of the development of the program and the introduction of new features is documented. The program has a detailed flow-chart which enables to visualise the simulation control, setting of flags, initial conditions, etc. and is invaluable for future program modifications.

6.5.3 Validation on system level

The validation of the overall simulation tool has been carried out through the following validation steps:

- Reassurance that the simulation program works the way it was intended to work according to the specified simulation conditions;
- Qualitative analysis of the simulation results for different types of simulations to ensure that the results are sound, the values are within the expected range, the conclusions drawn from the results of the simulations are logically expected;
- Using TCADP for modelling and simulation of a track circuit for which detailed knowledge of its design, parameters and performance is available and detailed

quantitative comparison of the results obtained by simulation with the preliminary known performance characteristics for various operational situations;

- Asking 'experts in the field' to review the model and simulation results.

Each of the above steps has given positive result and has helped in acquiring confidence that the developed track circuit model is correct. The most convincing among the above validation techniques was the application of TCADP for the simulation of the well established FS 2000 track circuit, manufactured by Westinghouse Signals Limited, the results of which, together with their analysis are presented in the next chapter.

Chapter 7

APPLICATION OF TCADP FOR TRACK CIRCUIT SIMULATION, PERFORMANCE ANALYSIS AND OPTIMISATION

The objective of this chapter is to demonstrate the use of the program for track circuit analysis and design and the applicability of its facilities for analysis and optimisation of track circuit performance. Without providing an exhaustive track circuit performance analysis the simulations aim to cover various aspects of track circuit design and operation. All simulations are done for the FS 2000 (metro version) track circuit. The simulation results are then analysed, the purpose of this analysis being to establish whether they conform with the preliminary known facts of track circuit design and operation, and on this basis draw conclusions about the validity of the track circuit computer model.

7.1 PROGRAMME AND ORGANISATION OF TRACK CIRCUIT SIMULATIONS

It has become clear that track circuits are open systems and their performance is susceptible to a large number of external changing environmental factors. In addition, jointless audio-frequency track circuits are complex systems and their design and performance involves a number of design parameters. Thus, in general, the investigation of track circuit performance requires a large number of simulations, for various conditions and, sometimes multiple varying parameters. In order to keep track of the large number of produced results and be able to analyse them in the right perspective, it is essential that the simulations are carried out according to a preliminary defined programme (Table 7-1) setting out clearly the purpose and the conditions of each simulation and the form or the required output results. The results or series of results have to be analysed in due course as the conclusions made may affect the way other simulations are performed or may call for different kind of simulations. As a result the preliminary program is being updated and appended as the track circuit investigation advances. It is important that the results of the simulations are presented in a clear graphical form and are kept in a well organised and documented way so as to allow easy access for reference and comparison. This includes the consistent use of a general system of notations.

The notation used in this chapter is defined in Fig. 6-17. The meaning of each curve in the graphs is indicated in the corresponding legend. When a secondary axis is used the names of the variables referred to that axis are explicitly indicated on it.

TABLE 7.1 Programme for track circuit analysis

Ref. No	Operating mode	Conditions of simulation	Output results	Aim of the simulation
1.1	Unoccupied	Frequency sweep	Representative for the TC analysis currents, voltages, impedances and admittances	Understand and demonstrate the tuning of TC terminations
1.2	Unoccupied	Frequency sweep	Compound graphs of the characteristics of the consecutive track circuit used on the same track	Estimate the allocation of frequencies to consecutive track circuits and possible interference effects.
2.	Unoccupied	Track circuit operating frequency	Performance coefficients	Estimation of TC performance in 'unoccupied' operating mode
3.1	Unoccupied	Frequency sweep & variation of rail track parameters within the expected range	Input impedances of the series and parallel tuned circuits at track circuit terminations Current in track circuit receiver Track circuit transfer impedance	Demonstrate the effect of rail track parameter variation on TC resonant characteristics and the level of track circuit operating signal.
3.2	Unoccupied	Frequency sweep and TC length variation from Lmin to Lmax	Input impedances of the series and parallel tuned circuits at track circuit terminations Current in track circuit receiver Track circuit transfer impedance Coefficients of track circuit performance	Demonstrate the effect of TC length on TC resonant characteristics and the level of track circuit operating signal. Find the maximum TC length which satisfies the performance coefficient for unoccupied TC.

TABLE 7.1 Continuation

3.3	Unoccupied	Variation of track circuit transmitter and receiver impedances	Input impedances of the series and parallel tuned circuits at track circuit terminations Current in track circuit receiver Track circuit transfer impedance Coefficients of track circuit performance	Demonstrate the effect of TC transmitter and receiver impedance on TC resonant characteristics and the level of track circuit operating signal. Find the maximum TC length which satisfies the performance coefficient for unoccupied TC.
3.4	Unoccupied	Train shunt on an adjacent track circuit close to TC Tx or Rx end. Variation of the values of train shunt resistance.	TC receiver current Currents in TC tuning units representative impedances Track circuit transfer impedance	Investigate the effect of a train shunt on an adjacent track circuit. Establish possible pre- and post-shunting areas and effect of train shunt resistance on their length.
3.5	Unoccupied	Variation of parameters and environmental effects	Current in TC receiver Track circuit transfer impedance Coefficients of performance	Establish the combination of TC parameters and environmental factors resulting in a worst scenario for unshunted operation.
4.1	Occupied	Train shunt moving along the track circuit from the receiving to the transmitting end.	Current in TC receiver Track circuit transfer impedance Coefficients of train shunt performance in shunt operation	Demonstrate the track circuit performance under shunt operation. Establish the position of minimum train shunt sensitivity.

TABLE 7.1 Continuation

4.2	Occupied	Static/moving train shunt in track circuit termination areas	Current in track circuit Tx and Rx tuning units and in TC receiver Representative impedances	Demonstrate the track circuit performance under train shunt in track circuit termination area.
4.3	Occupied	Train shunt in different position and frequency sweep	Coefficients of train shunt performance in shunt operation	Establish possible zones with no shunt sensitivity or overlapping zones.
4.4	Occupied	Variation of track circuit length	Input impedances of the series and parallel tuned circuits at track circuit terminations Track circuit transfer impedance Current in track circuit receiver Coefficients of track circuit performance	Demonstrate the effect of the various parameters on TC resonant characteristics and the level of track circuit operating signal. Establish the maximum track circuit length for which train detection is ensured.
4.5	Occupied	Variation of rail track parameters		
4.6	Occupied	Variation of Tx and Rx impedances		
4.7	Occupied	Variation of the value of train shunt resistance	Current in TC receiver	Establish the maximum value of train shunt resistance which can be detected by the track circuit.
4.8	Occupied	Train shunt on an adjacent track circuit	Current in TC receiver Currents in Tx and Rx tuning units Coefficients of track circuit performance in shunted operation	Establish possible effect of a second train shunt on an adjacent track circuit resulting in a reduction of train shunt sensitivity
4.9	Occupied	Variation of parameters and environmental	Current in TC receiver Track circuit transfer impedance Coefficients of performance	Establish the combination of TC parameters and environmental factors resulting in a worst scenario.

7.2 SIMULATION RESULTS

7.2.1 Complete track circuit solution

A complete track circuit solution involves the computation of all defined electric variables describing the track circuit electric network for a particular set of operating conditions. As well as the definition of the currents, voltages, impedances and admittances at every point of the track circuit, the complete solution involves the definition of some derived variables such as input impedances, equivalent impedances, equivalent energy sources, transfer impedances and coefficients characterising the track circuit performance.

An illustration of a complete solution of FS 2000 track circuit for the 'unoccupied' operating mode is shown in Figures 7.1 to 7.14. Even though not all the variables shown in the graphs may seem to be immediately required for the analysis of the track circuit performance, their computation may prove useful for reference in further analysis, moreover their computation does not require any additional computational effort. The full solution allows a more in-depth understanding of track circuit operation.

7.2.2 Tuning of track circuit terminations

The frequency sweep simulations (Figures 7.1 to 7.14) give a perfect illustration of the tuning of track circuit terminations and allows an estimation of its efficiency.

Tuning of track circuit terminations is necessary to deliver a sufficiently high operating signal into the rails and in the TC receiver, as well as to help confine the operating signal within the track circuit boundaries. The tuning capacitors in conjunction with the inductance of short sections of rails make the circuit seen from Tx output or Rx input appear as a series tuned circuit. On the other hand, seen from the rails the Tx and the Rx track circuit terminations appear to be tuned in parallel resonance at the operating frequency.

All currents in track circuit transmitting end (Fig.7-1) and in the receiving end (Fig.7-3) have well expressed resonance characteristics. In particular, the currents flowing in the Tx tuning unit (I1), in the rails at the transmitting end (IR2) and in the Tx TC termination (IL2) as well as the current in the receiver (IR5) are perfectly centred around the track circuit operating frequency of 5520 Hz. For the other currents it can be observed that the further they are from the tuning unit the more their resonance frequency is displaced from the operating frequency. This is due to the effect of other reactive components, and predominantly, the inductance of the rails.

Conditions of simulation

Track circuit type	Y, Long track circuit
Frequency	5520 Hz
Operating mode	Unoccupied
Track circuit model	Full

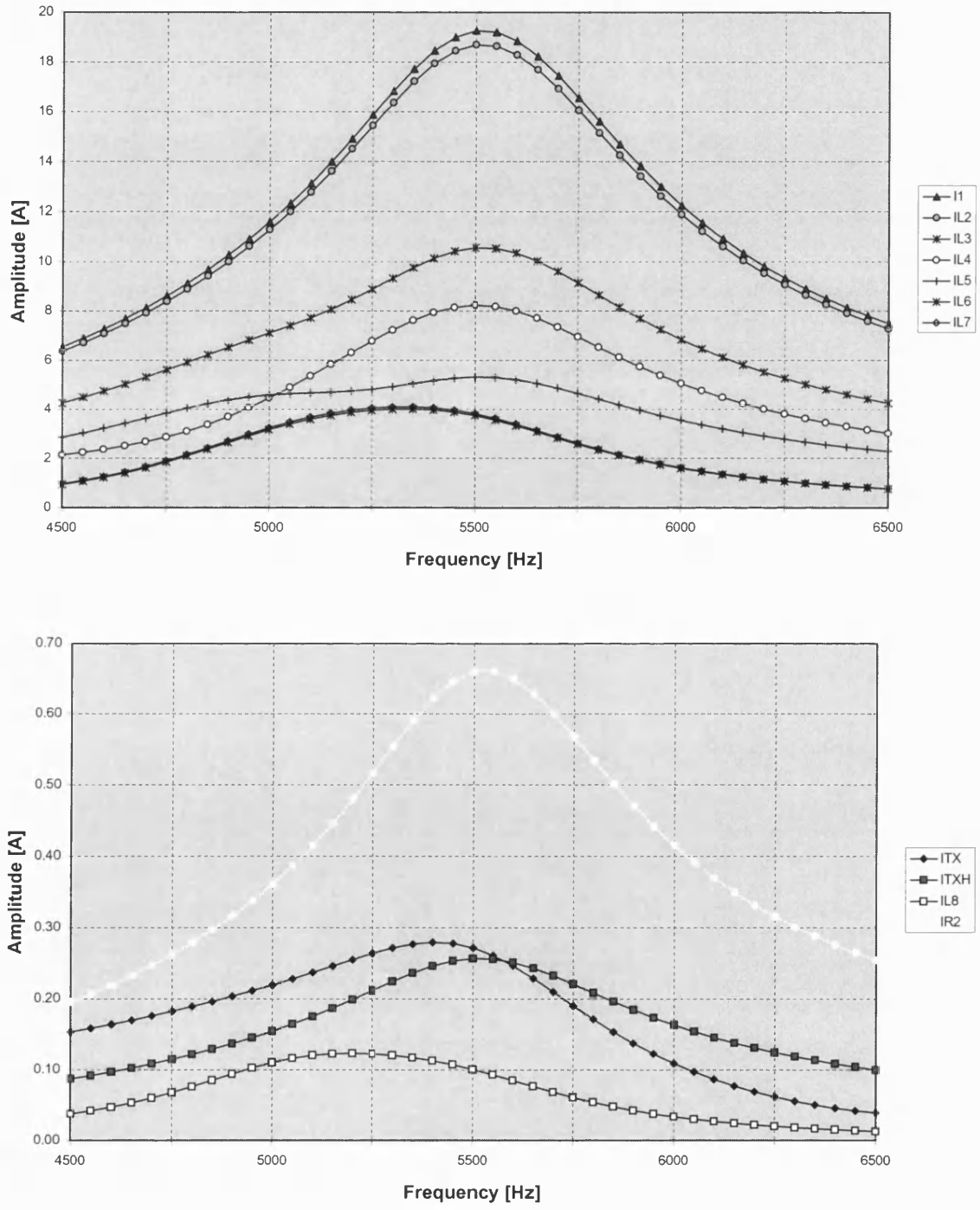

FIG.7.1 Amplitudes of currents in track circuit transmitting end as function of frequency

Conditions of simulation

Track circuit type	Y, Long track circuit
Frequency	5520 Hz
Operating mode	Unoccupied
Track circuit model	Full

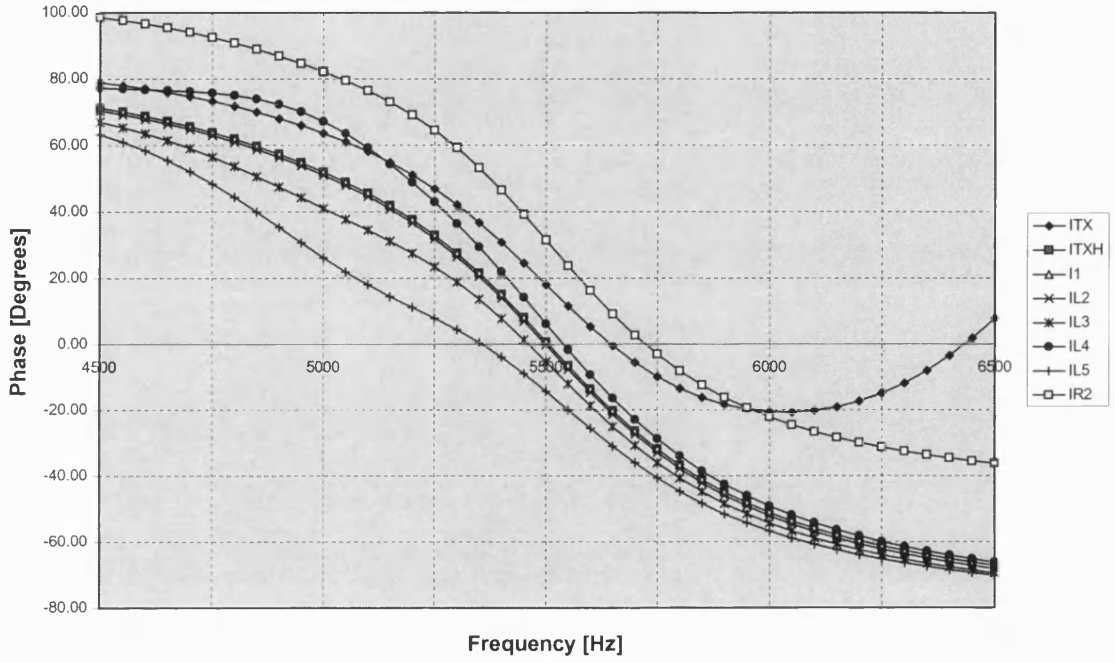

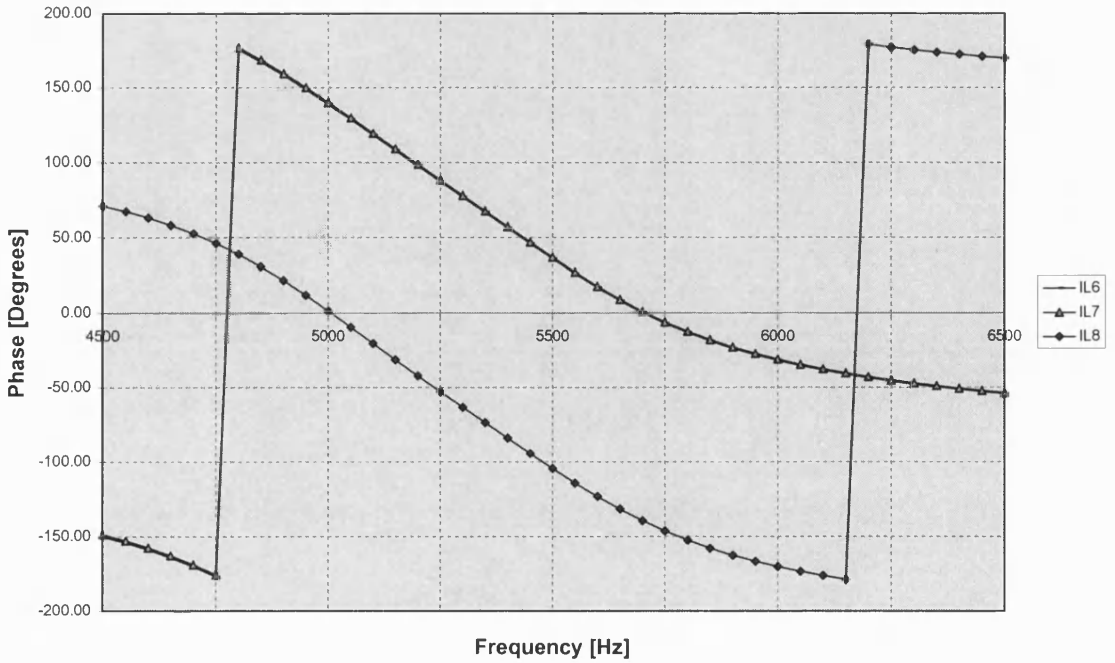

FIG.7.2 Phases of currents in track circuit transmitting end as function of frequency

Conditions of simulation

Track circuit type	Y, Long track circuit
Frequency	5520 Hz
Operating mode	Unoccupied
Track circuit model	Full

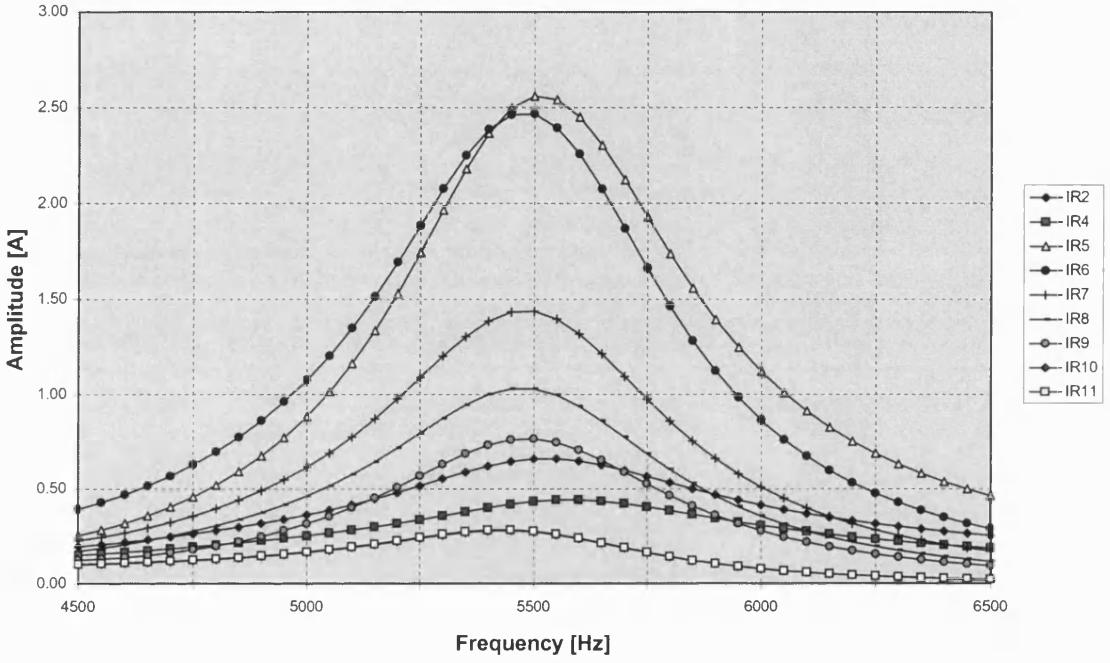

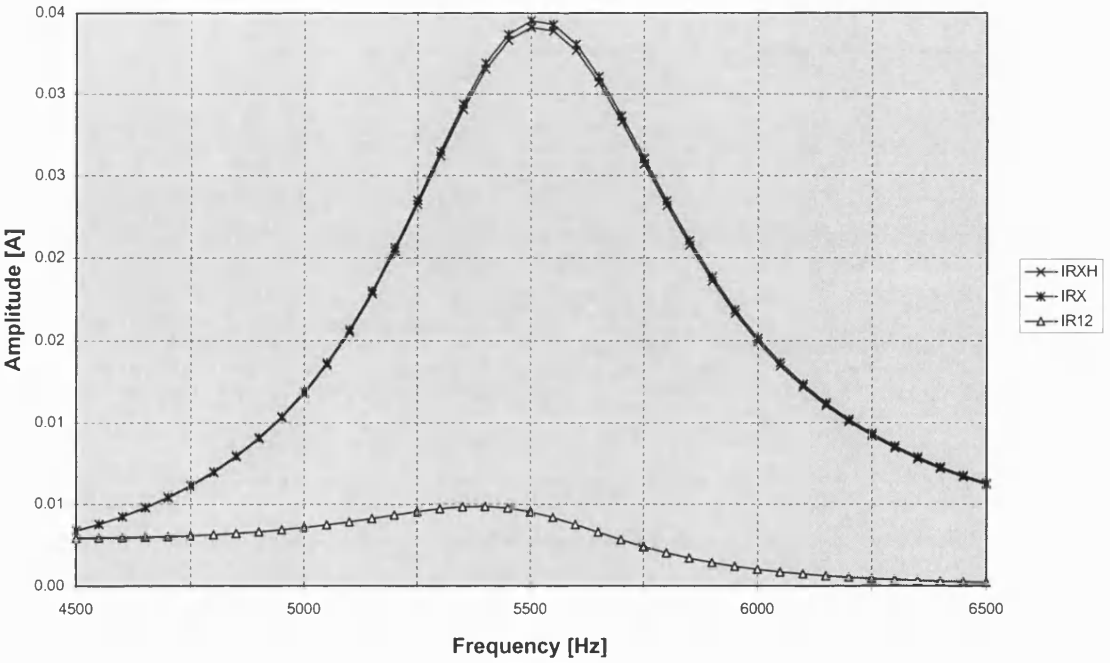

FIG.7.3 Amplitudes of currents in track circuit receiving end as function of frequency

Conditions of simulation

Track circuit type	Y, Long track circuit
Frequency	5520 Hz
Operating mode	Unoccupied
Track circuit model	Full

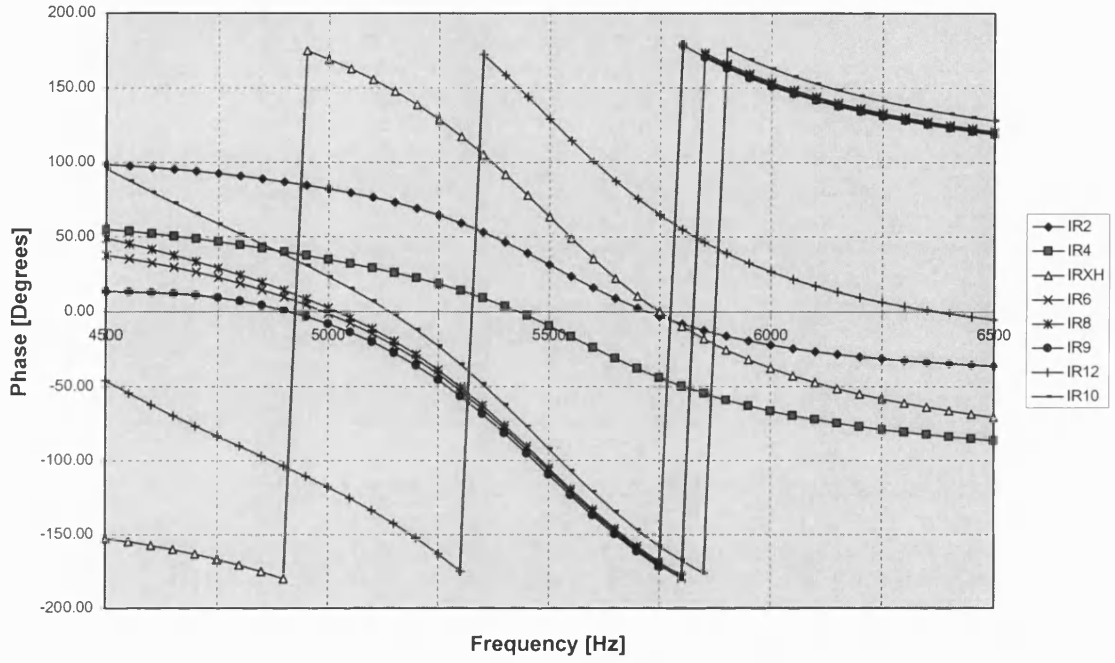

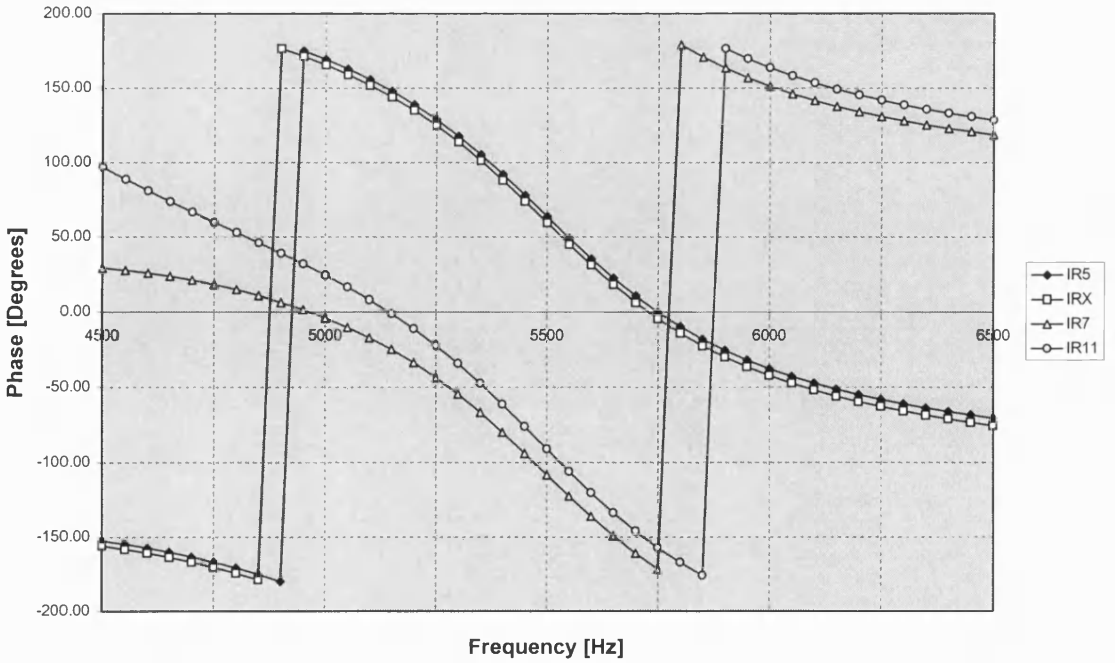

FIG.7.4 Phases of currents in track circuit receiving end as function of frequency

Conditions of simulation

Track circuit type	Y, Long track circuit
Frequency	5520 Hz
Operating mode	Unoccupied
Track circuit model	Full

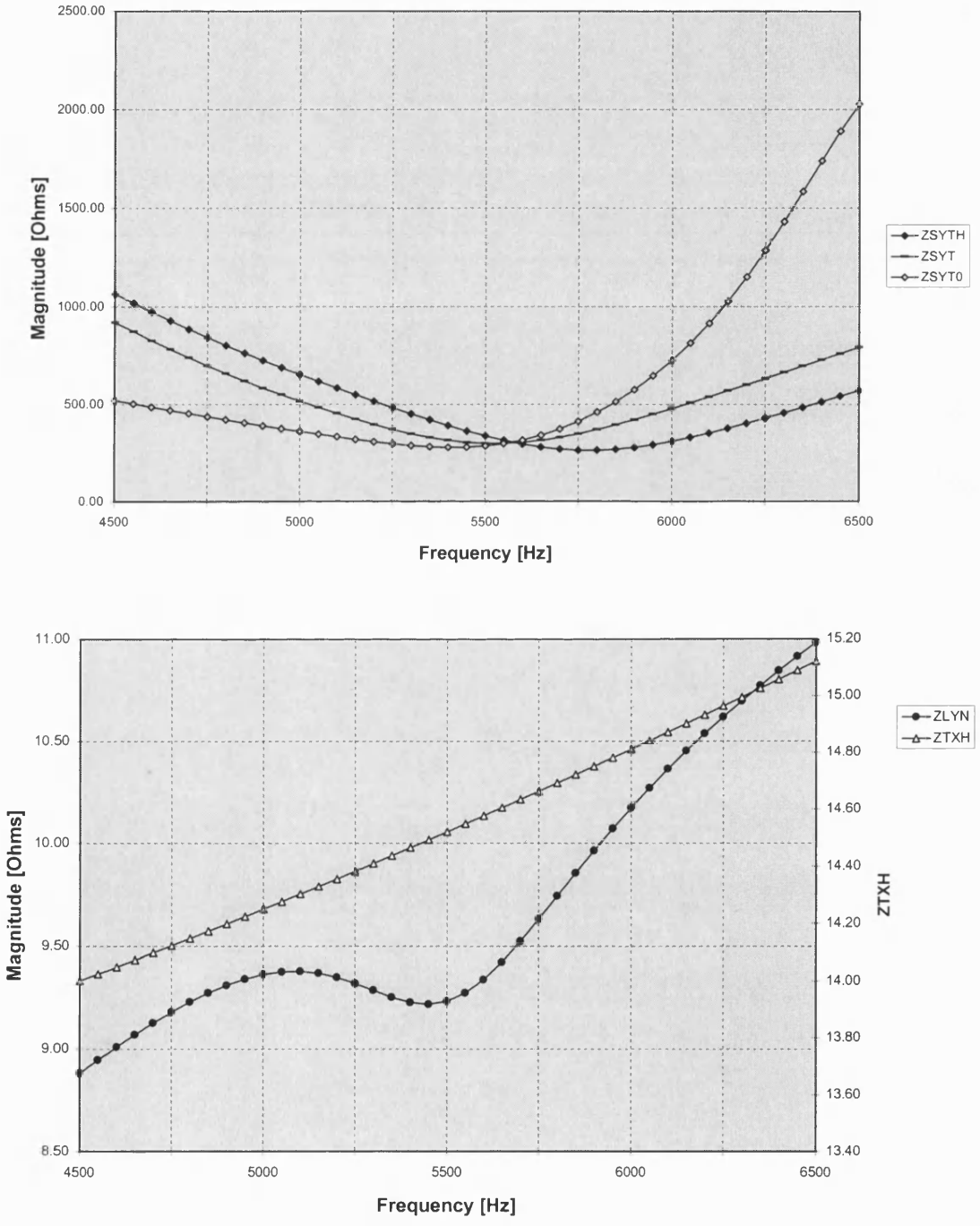

FIG.7.5 Magnitudes of impedances in track circuit transmitting end as function of frequency

Conditions of simulation

Track circuit type	Y, Long track circuit
Frequency	5520 Hz
Operating mode	Unoccupied
Track circuit model	Full

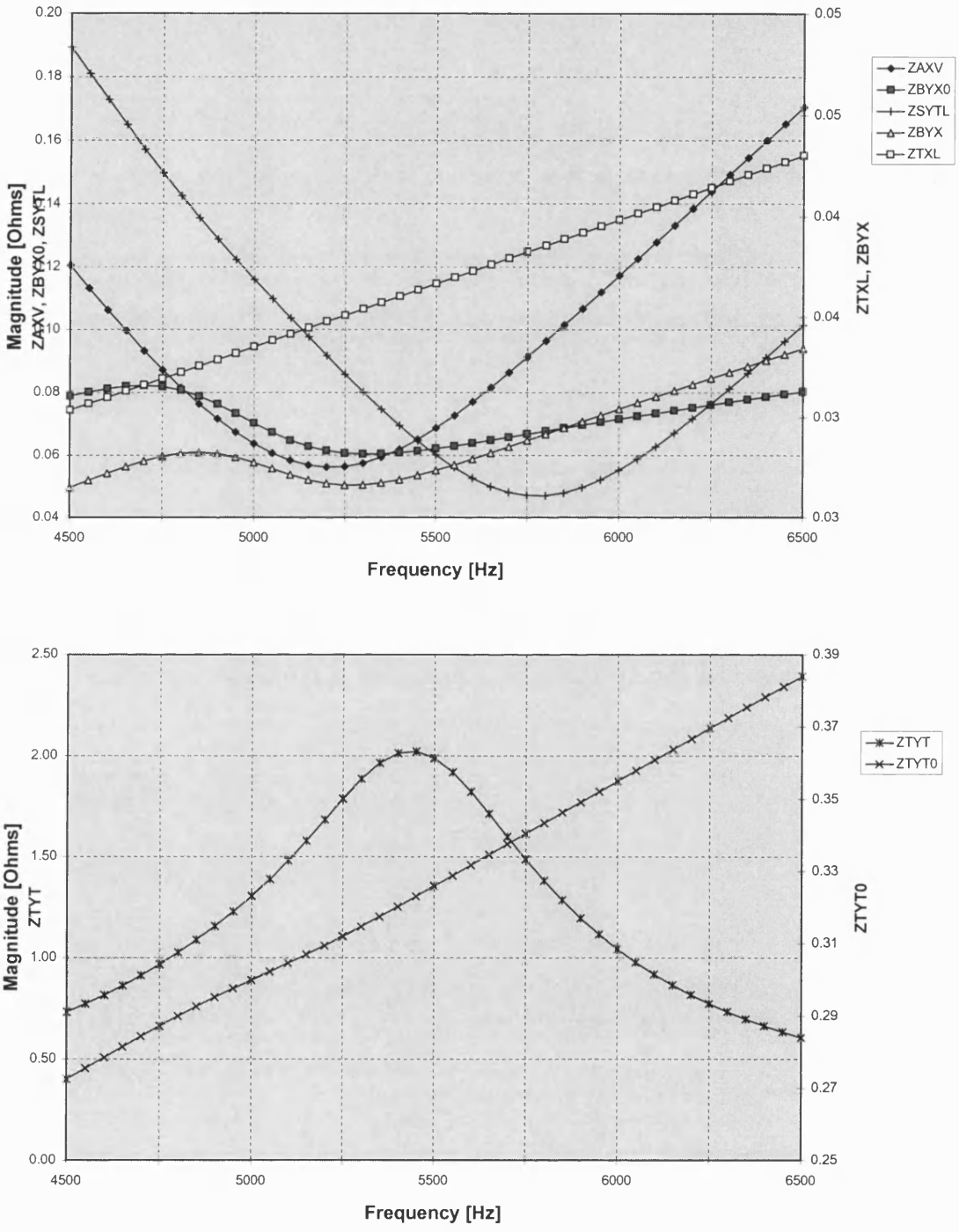

FIG.7.6 Magnitudes of impedances in track circuit transmitting end as function of frequency

Conditions of simulation

Track circuit type	Y, Long track circuit
Frequency	5520 Hz
Operating mode	Unoccupied
Track circuit model	Full

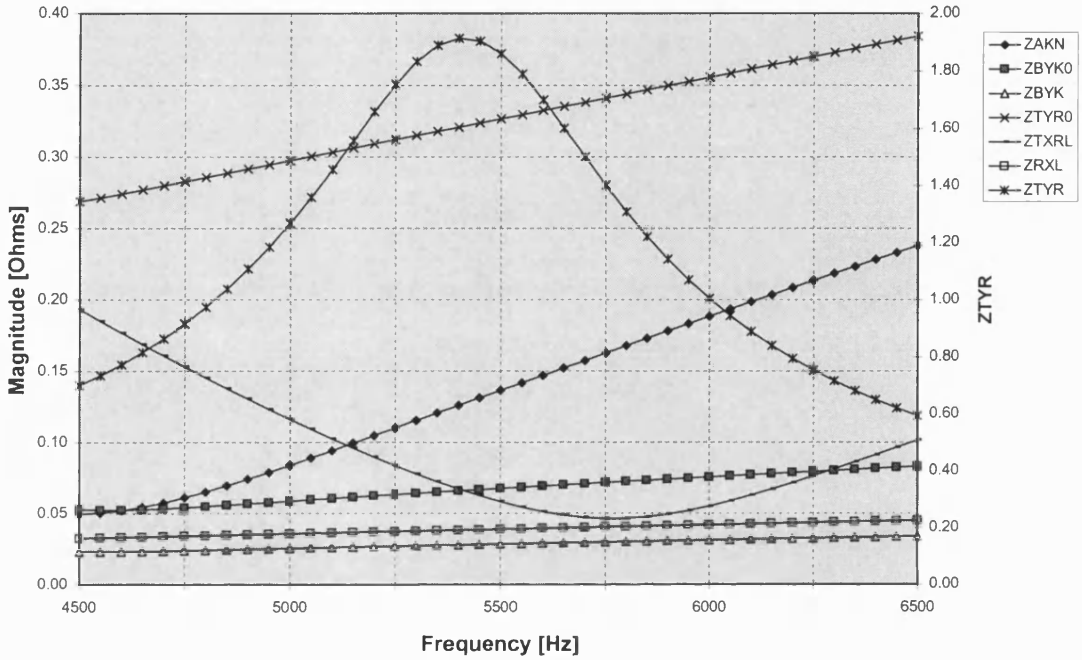

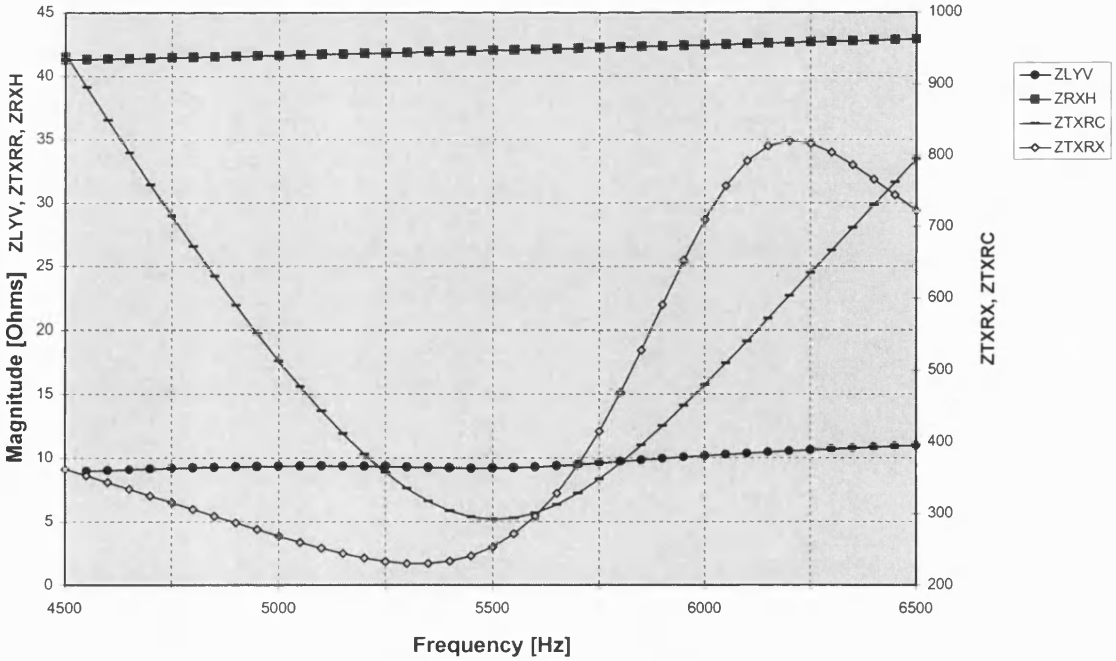

FIG.7.7 Magnitudes of impedances in track circuit receiving end as function of frequency

Conditions of simulation

Track circuit type	Y, Long track circuit
Frequency	5520 Hz
Operating mode	Unoccupied
Track circuit model	Full

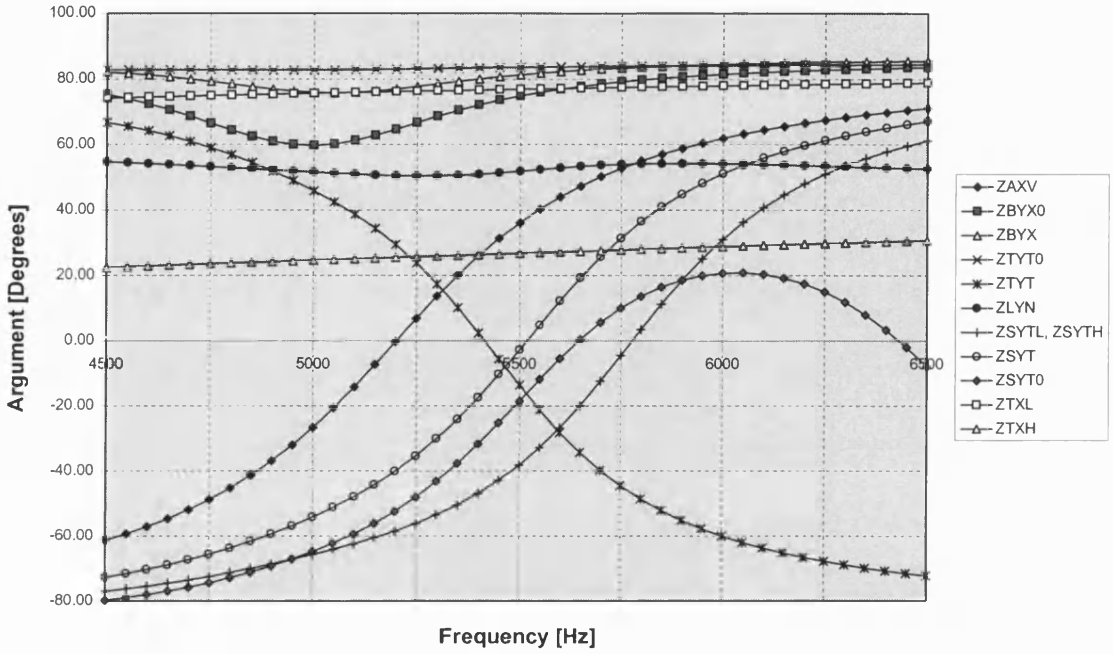

FIG.7.8 Arguments of impedances in track circuit transmitting end as function of frequency

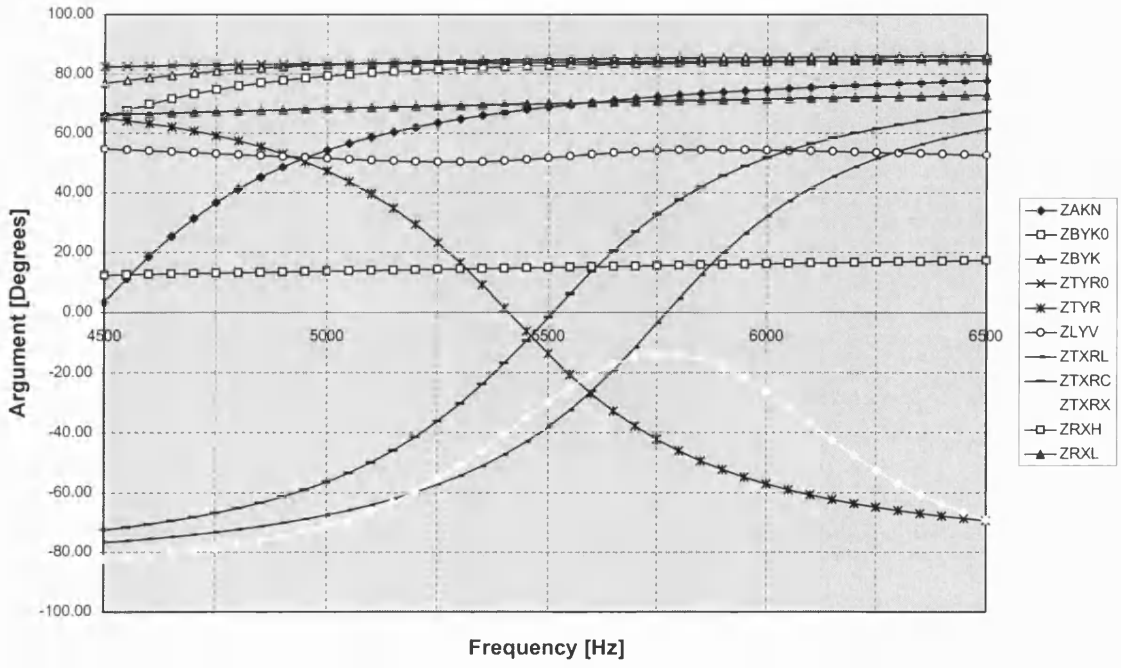

FIG.7.9 Arguments of impedances in track circuit receiving end as function of frequency

Conditions of simulation

Track circuit type	Y, Long track circuit
Frequency	5520 Hz
Operating mode	Unoccupied
Track circuit model	Full

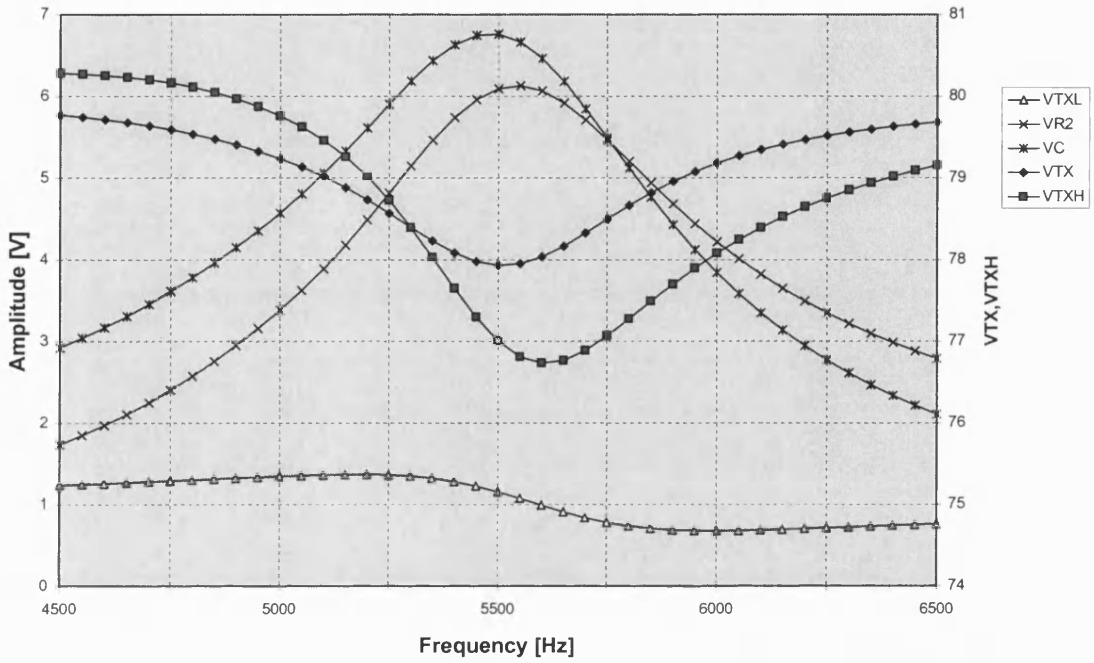

FIG.7.10 Amplitudes of voltages in track circuit transmitting end as function of frequency

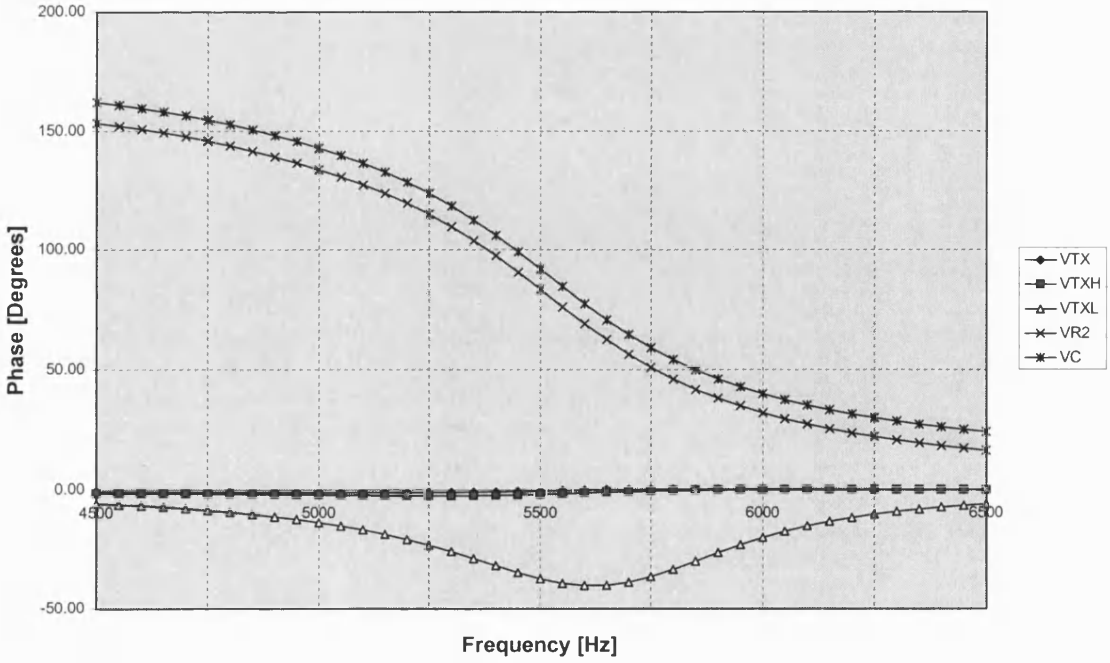

FIG.7.11 Phases of voltages in track circuit transmitting end as function of frequency

Conditions of simulation

Track circuit type	Y, Long track circuit
Frequency	5520 Hz
Operating mode	Unoccupied
Track circuit model	Full

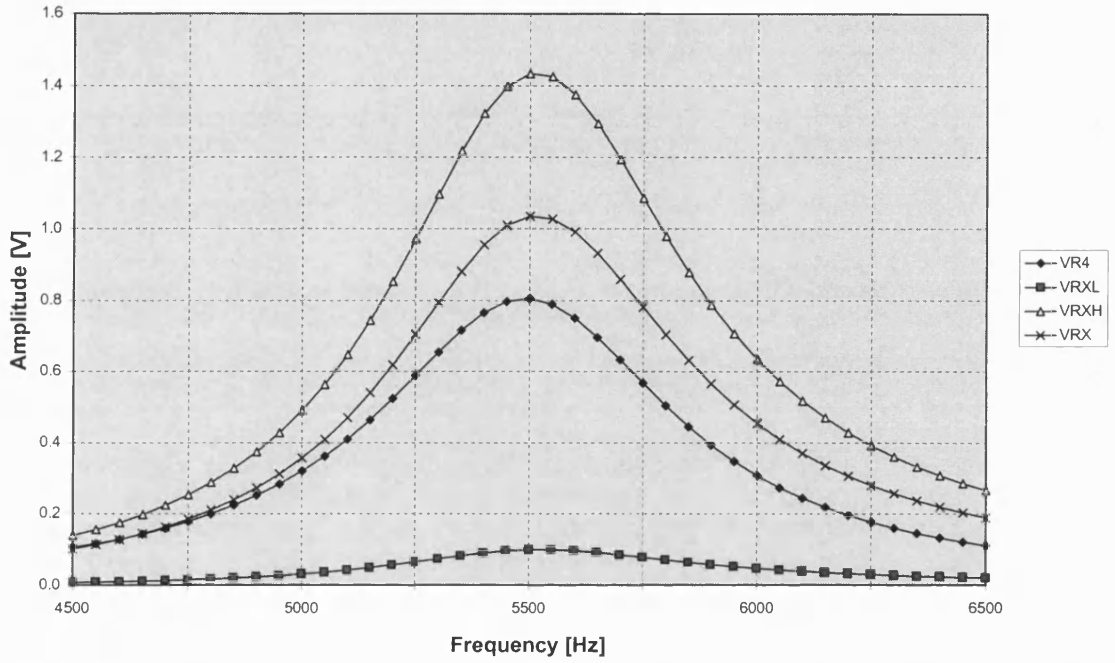

FIG.7.12 Amplitudes of voltages in track circuit receiving end as function of frequency

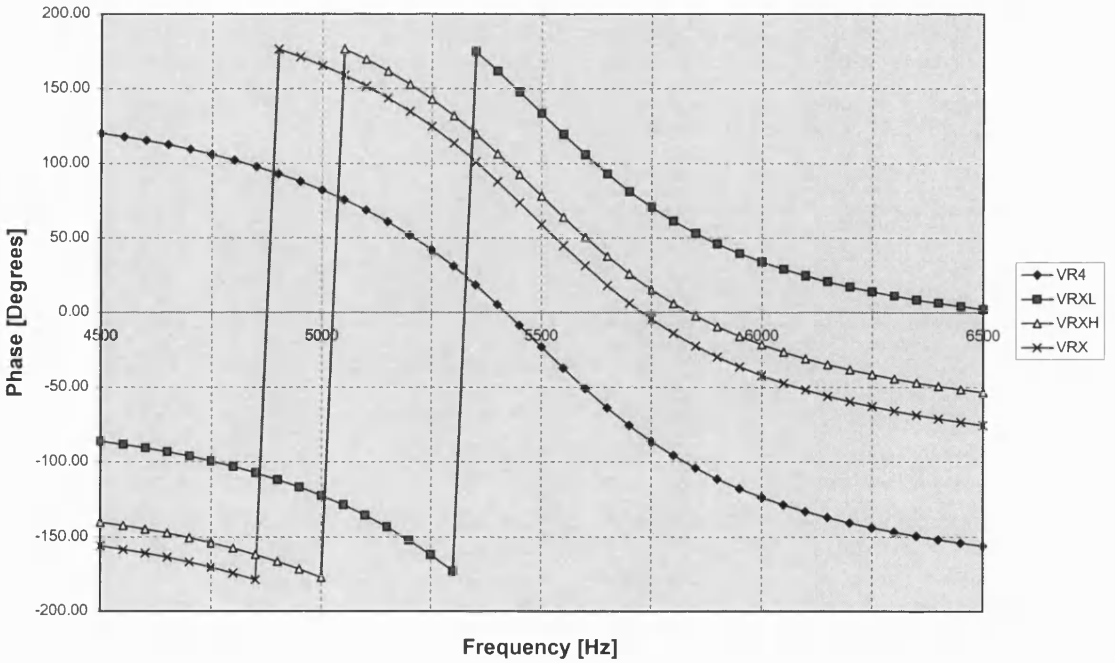

FIG.7.13 Arguments of voltages in track circuit receiving end as function of frequency

Conditions of simulation - Frequency sweep from 3500 to 6500 Hz

Track circuit type	Y, Long track circuit (300 m)
Opearting frequency	5520 Hz
Operating mode	Unoccupied
Track circuit model	Full

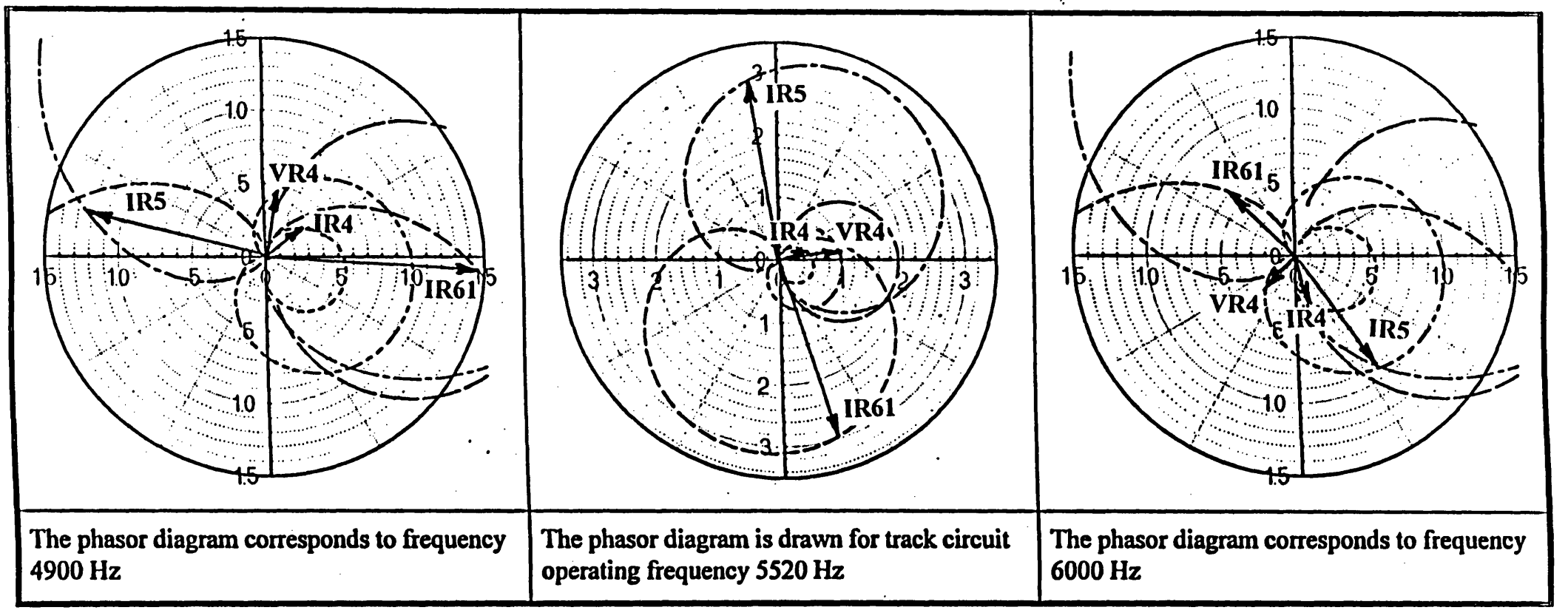

The phasor diagram corresponds to frequency 4900 Hz	The phasor diagram is drawn for track circuit operating frequency 5520 Hz	The phasor diagram corresponds to frequency 6000 Hz

FIG.14 Tuning of track circuit receiving end

The series resonant tuning is confirmed by the graphs of the magnitude and argument of ZSYT - the impedance seen from the output of TC Tx. Fig.7.5 shows that ZSYT magnitude has a minimum at around 5520 Hz and in Fig.7.8 its argument crosses the zero-axis at the same frequency.

The voltage of TC Tx referred to the secondary of TU transformer is 1.17V (rms) while the voltage across the rails at the points of connection of Tx TU is about 6.2V. This gives a quality factor Q of 5.2 which agrees with the Q-factor indicated in FS2000 Specification (Ref.[2-19]).

The parallel resonance tuning of TC termination at the receiving end is illustrated by the graphs of the magnitude and the argument of ZTYR - the impedance of TC receiving termination seen looking from the points of connection of the Rx tuning unit. The graph in Fig.7.7 shows a parallel resonance characteristic with resonance frequency around 5420 Hz and the graph in Fig.7.9 indicates that its argument becomes zero at the same frequency. The resonance frequency is lower than the track circuit operating frequency but still delivers the required resonance effect. The amplitude of the current in the rails at the receiving end (IR4) is 0.45A (Fig.7.3) while the amplitudes of the current in the Rx end tuning unit (IR5) and the current in the rails flowing towards the Rx end termination bonds (IR6) are correspondingly 2.6A and 2.45A - almost six times higher than IR4. The high current IR5 produces a considerable voltage at the input of TC receiver. Fig.7.4 confirms the expected phase relationship between IR5 and IR6 of 180 degrees at the resonance frequency.

The typical parallel resonance relationships between the currents and voltages in the resonance circuit are very clearly seen from the phasor diagrams drawn on the polar plots in Fig.7.14.

7.2.3 Track circuit separation

Figures 7-1 and 7 -3 showing the distribution of currents in the track circuit transmitting and receiving end allow to make conclusions about the ability of FS 2000 electrical separating joints to confine track circuit operating signal within the track circuit boundaries. In the transmitting end the current flowing in the Tx tuning unit divides into two currents: the current flowing into the track circuit IR2 and the current flowing towards the Tx end termination bonds IL2. The relationship between IR2 and IL2 is governed by the ZLYN and ZTYT0 which at the resonance frequency are 9.25Ω (Fig.7.5) and 0.32Ω (Fig.7.6). The currents IR2 and IL2 are accordingly 0.66A and 18.7A. Current IL2 Further inspection of the graphs in Fig.7.1 shows that current IL2 closes mainly through the two terminating bonds (|IL3| = 10.5A, |IL3| = 5.3A) but a small part of it

closes through the tuning unit of the adjacent track circuit (|IL7| = 3.8A). The current entering the rails of the adjacent track circuit IL8 is insignificant (|IL8| = 0.1A).

The above figures show that by providing a low impedance path for the current the ESJs contain the Tx current with its own track circuit. However, this is at the expense of the 'useful' signal transmitted into the track circuit being considerably low. The value of the current of TxY flowing through RxX (IL7) obtained by simulation was higher than expected but was confirmed by FS2000 designers. These results indicate how the efficiency of the ESJs can be improved further. If an improvement is to be undertaken this may affect the spacing of track circuit operating frequencies shown in Fig.7.16.

Another illustration of track circuit separation properties of the ESJs is given in Fig.7.18. The graphs in this figure allow to compare the amplitudes of the currents in the transmitter of an Y track circuit and the adjacent receiver of a K track circuit.

7.2.4 Track circuit termination length

The length of the track circuit termination is an important parameter of the series and parallel resonance tuning. This is illustrated in Fig.7.19 showing the tuning of the transmitting end for various values of track circuit termination length. For the particular track circuit modelled in this example the best tuning is achieved for TCT length of about 5.0 - 5.25 m. For lower values of TCT length the resonance is shifted towards higher frequencies, for lower values the resonant peak is split into two, giving a wider resonant characteristic.

By running an optimisation subroutine the following optimum values of the track circuit termination lengths have been found:

	TCT length		
Track circuit type	X	Y	K
Long track circuit	7.08	7.08	6.95
Short track circuit	5.2	5.42	4.9

The above values are in very good agreement with the values indicated by the manufacturer in [2-15], namely 6 to 8 m for long TCs and 4 to 6 m for short TCs.

7.2.5 Maximum and minimum track circuit lengths

The maximum track circuit length is restricted by the losses in the rail track transmission line. Fig.7.21 represents the amplitude of the current in TC receiver as function of track

Conditions of simulation

	Fig.7.15	Fig.7.16
Track circuit type	Y, Long TC	X,Y,K, Long TCs
Frequency	5520 Hz	5040, 5520, 4320 Hz
Operating mode	Unoccupied	
Track circuit model	Full	

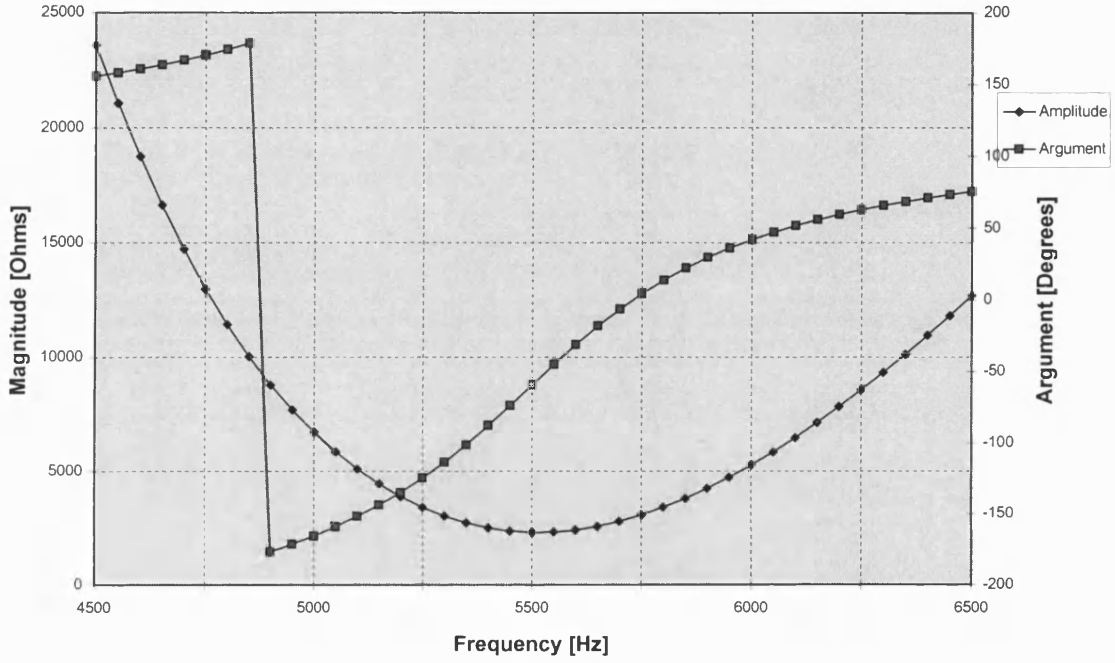

FIG.7.15 Track circuit transfer impedance

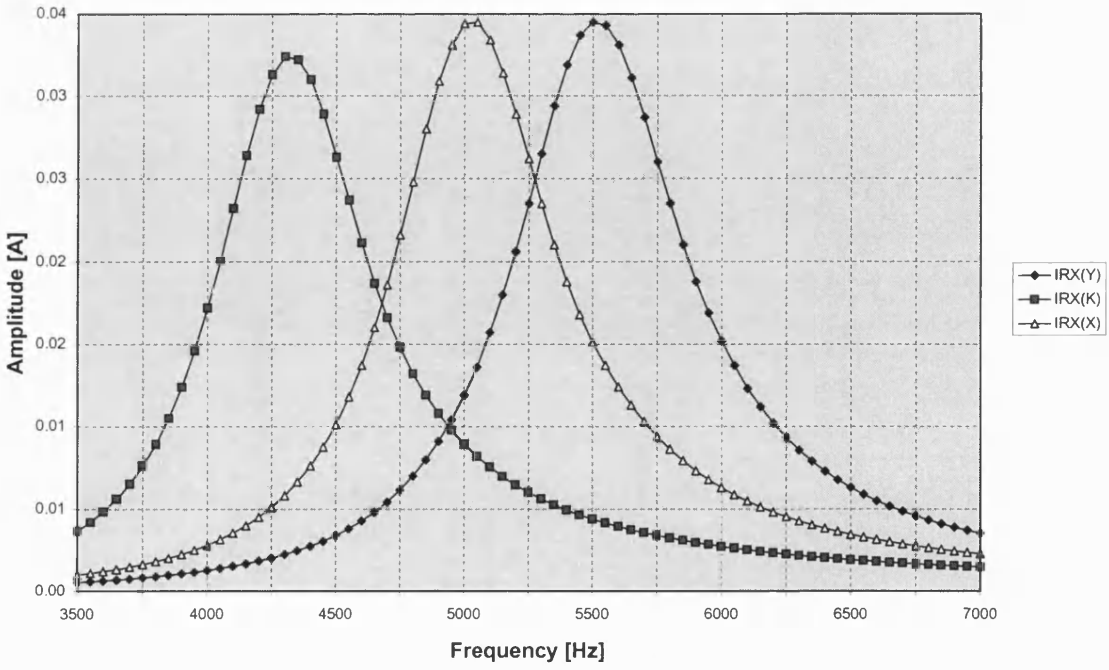

FIG.7.16 Track circuit receiver currents in three consecutive track circuits

Conditions of simulation

Track circuit type	Y, Long track circuit
Frequency	5520 Hz
Operating mode	Unoccupied
Track circuit model	Full

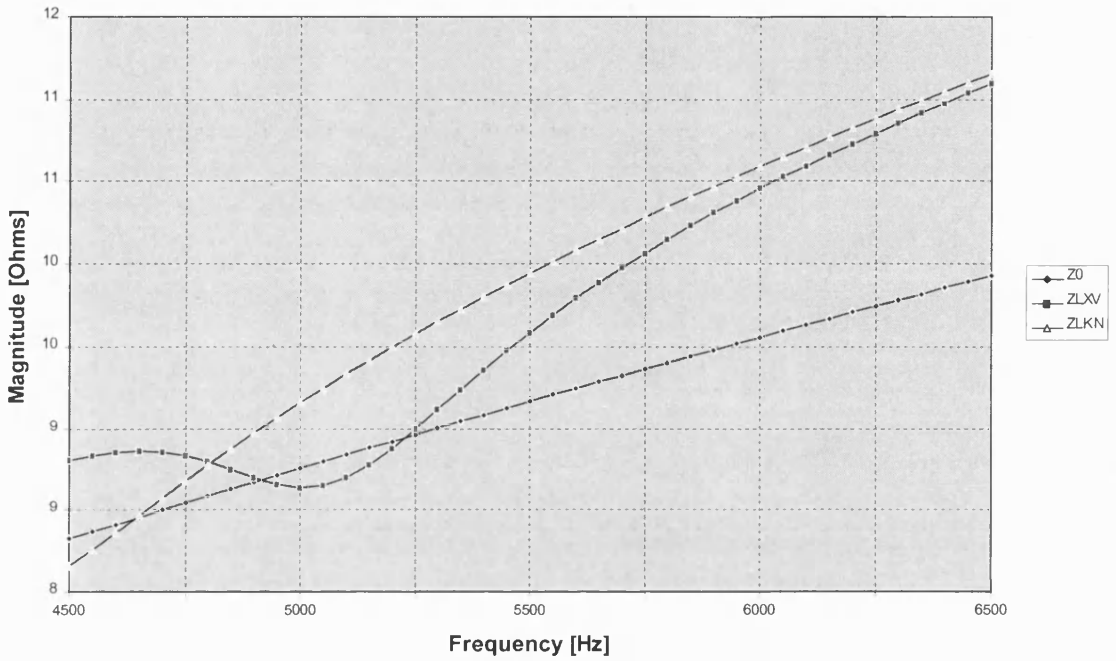

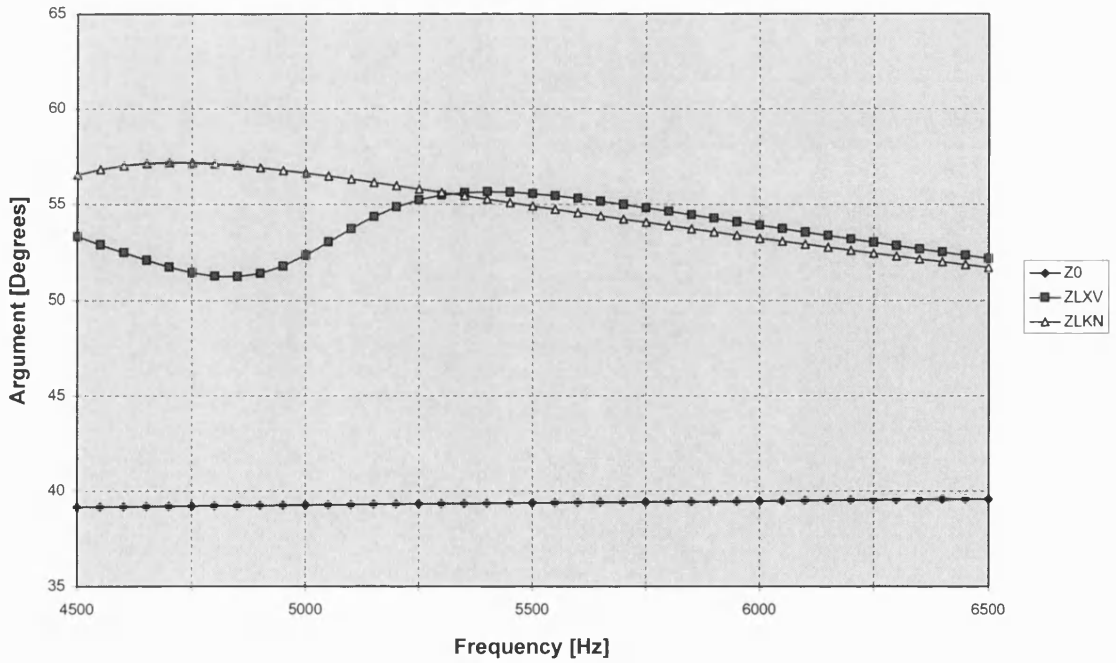

FIG.7.17 Comparison of rail track characteristic impedance (Z0) with the impedances seen looking into adjacent track circuits

Conditions of simulation	Fig.7.18	Fig.7.19
Track circuit type	YL (300m) and KL (300 m)	YS (50 m)
Operating frequency	5520 Hz and 4320 Hz	5520 Hz
Operating mode	Unoccupied	
Track circuit model	Full	

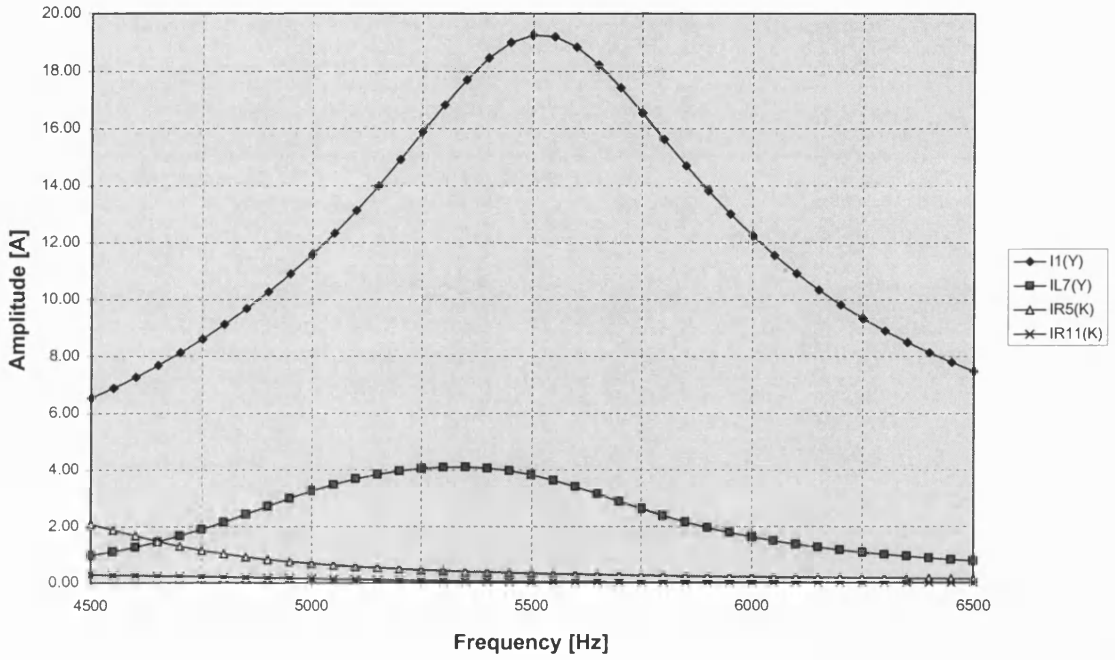

FIG.7.18 Comparison of the currents of two adjacent track circuits in the adjacent TUs

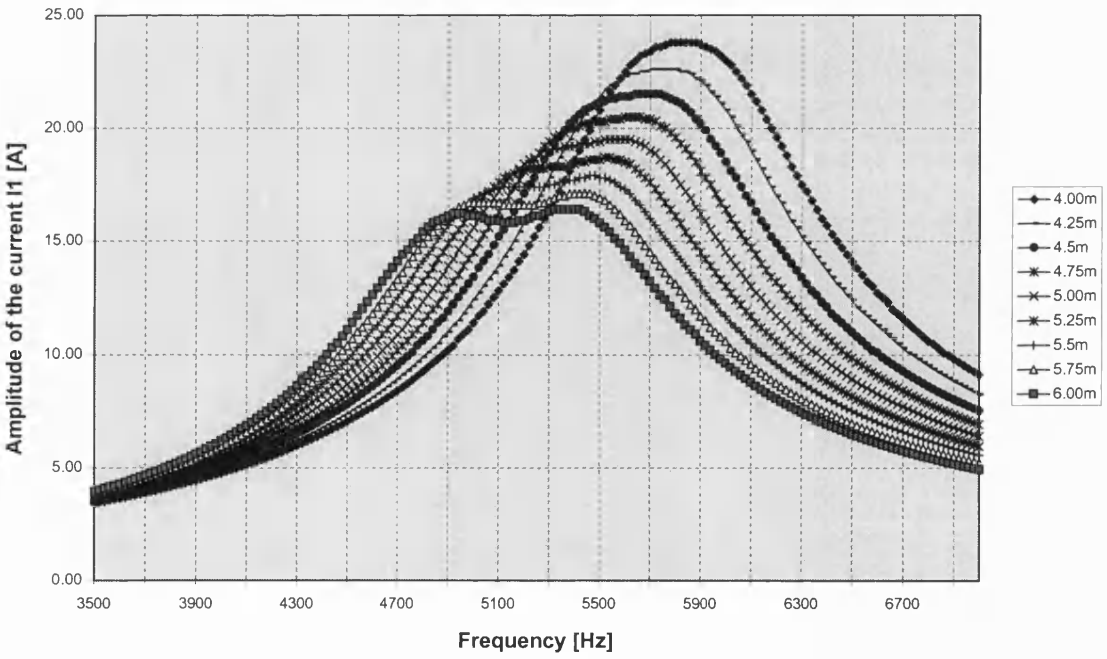

FIG.7.19 Effect of track circuit termination length on the tuning of the terminations

circuit length and shows that the maximum length of long track circuits is 400 m. This figure agrees with the maximum TC length given by the manufacturer.

The minimum length which a track circuit can have is defined by the conditions of resonance tuning. This is particularly expressed in short track circuits (40 - 100 m) where due to being very close to each other, the tuning units of the transmitting and receiving end may interfere. The 3D graph in Fig.7.22 refers to short track circuits and shows the tuning of TC transmitting tuning unit as function of track circuit length. It is clearly seen that the higher the length, the better the tuning while for track circuit lengths of about 40 m the resonance peak starts splitting and no satisfactory tuning can be provided. For track circuit lengths below 40 m the tuning is absolutely distorted. The figure of track circuit minimum length for short track circuits is in agreement with the figure provided by the manufacturer.

7.2.6 Effect of the distance to the equipment room

The investigation of the effect of the length of the cables connecting the trackside tuning units with the transmitters and receivers installed in a remote equipment room is illustrated in Figures 7.20, 7.35 and 7.36 With the increase of the distance to the tuning unit the current in track circuit receiver reduces but remains well above the receiver's energisation level. This is explained not as much with increase of the transfer impedance of the cable transmission line but rather with its effect on the tuning of track circuit terminations. To obtain optimum tuning it is advisable to adjust the tuning according to the distance to the equipment room. This is shown by the graphs in Fig.7.36 which have been produced by an optimisation subroutine. Smoother curves could be produced by using a smaller incremental step for the distance to the equipment room.

7.2.7 Effect of transmitter and receiver impedances

The impedances of the transmitter and receiver of FS 2000 track circuit can be regarded as purely active, so the investigation of their effect has been based on variation of the value of Tx and Rx resistance. This does not affect the tuning of track circuit termination, so the effect of increasing Tx or Rx resistance is expressed only in a slight reduction of the level of the signal. An illustrative graph is shown in Fig.7.23.

Contrary to the unoccupied track circuit condition the effect of the Tx and Rx impedances on track circuit operation in shunted and broken rail operating modes is much more complex. The magnitudes and the arguments of the Tx and Rx impedances as well as the relationship between them strongly affects the worst case scenarios. When a track circuit is required to detect broken rails the choice of Tx and Rx impedances is a matter of optimisation.

Conditions of simulation	Fig.7.20	Fig.7.21
Track circuit type	YL, 300m	YL, TC length varies
Operating frequency	5520 Hz	
Operating mode	Unoccupied	
TC parameters	Variation of the distance to the equipment. room	YL, TC length varies
Track circuit model	Full	

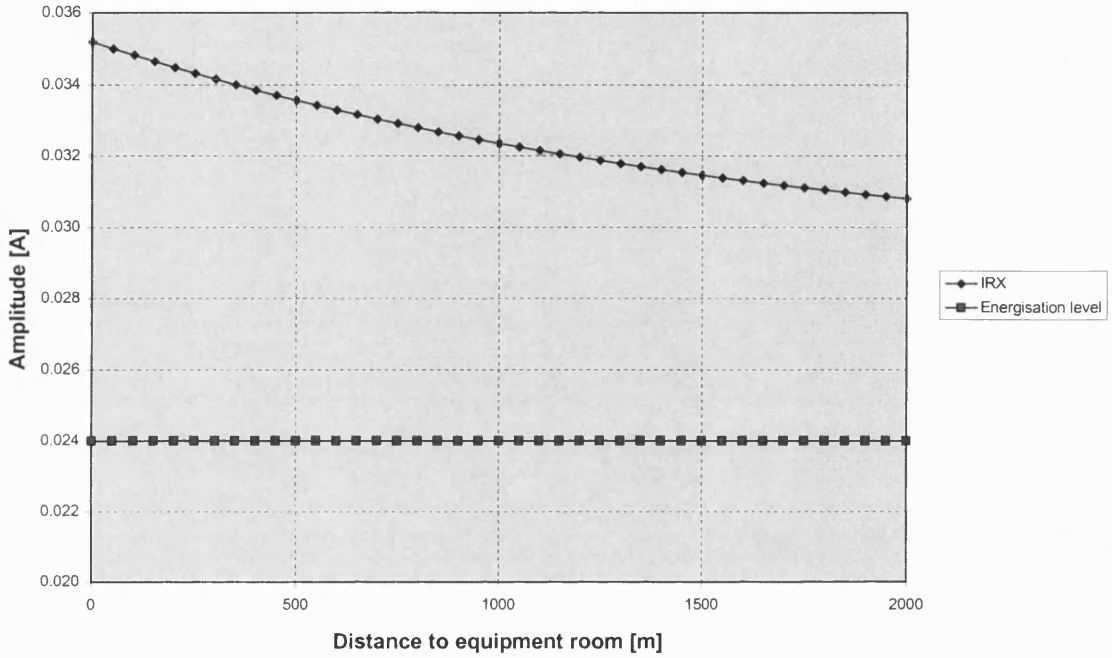

FIG.7.20 Current in track circuit receiver as function of the distance to the equipment room

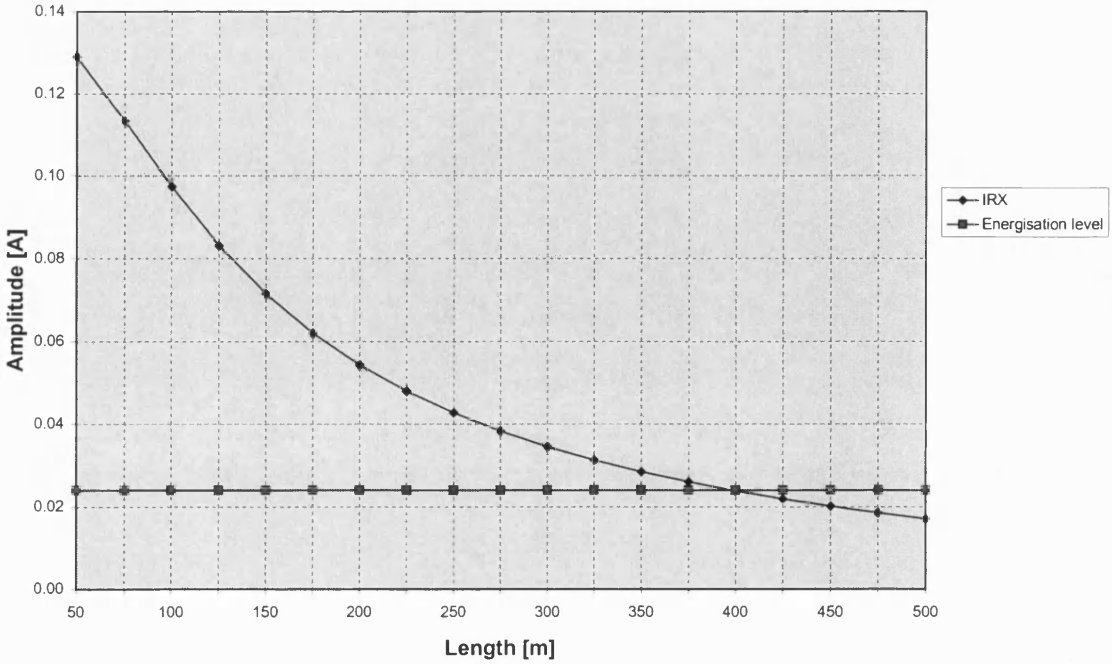

FIG 7.21 Current in track circuit receiver as function of track circuit length

Conditions of simulation	Fig.7.22	Fig.7.23
Track circuit type	YS, TC length varies	YL, 300 m
Operating frequency	5520 Hz	
Operating mode	Unoccupied	
TC parameters	Variation of TC length	Variation of Rx resistance
Track circuit model	Full	

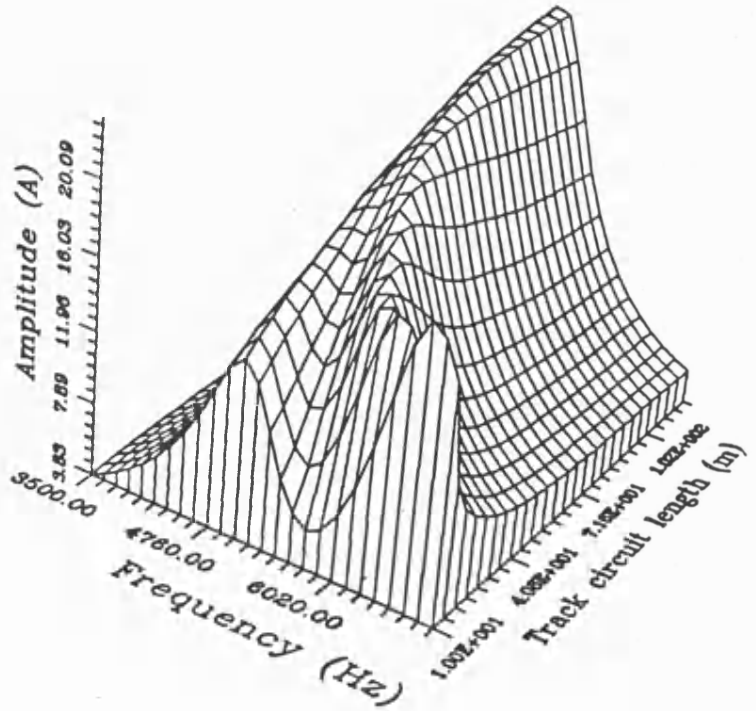

FIG.7.22 Effect of track circuit length on track circuit tuning - Current in Tx tuning unit as function of TC length

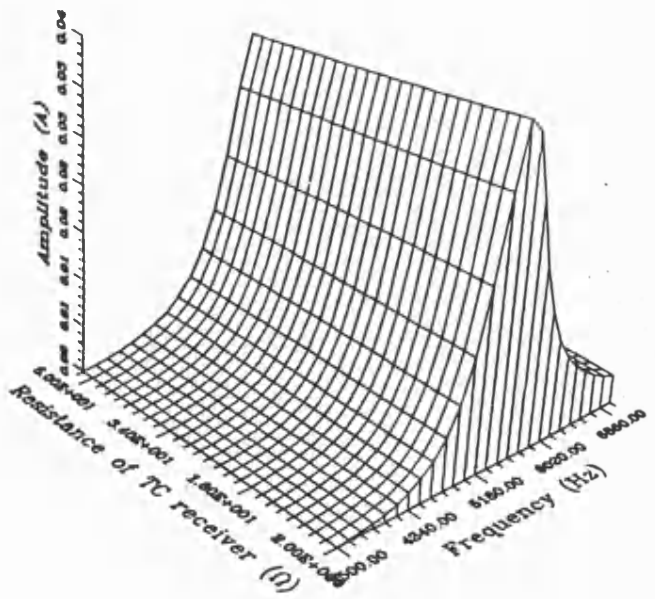

FIG.7.23 Amplitude of the current in TC receiver as function of Rx resistance

7.2.8 Effect of rail track parameters

The investigation of the effect of the rail track primary parameters is necessary for two reasons. On one side, the designers must satisfy themselves that the track circuit operates correctly in all operating modes for the complete range of variation of rail track parameters or alternatively, for each operating mode, establish the set of parameters corresponding to the worst case scenario and check that the track circuit still operates correctly for those particular sets of parameters. On the other hand, the investigation of the effect of rail track parameters forms the basis for the necessary site adjustments which is particularly relevant for non traditional rail track structures, rail track in tunnels, viaducts, etc.

Some representative 3D graphs illustrating the effect of rail track parameters on track circuit operation in unoccupied mode are shown in Figures 7.24 to 7.27.

The effect of an increased rail track resistance (Fig.7.24) is to reduce the level of track circuit operating signal due to increased losses in the rail track transmission line. The change in phase is barely visible.

Rail track conductance is strongly affected by the weather conditions and varies within a very wide range, from a few mS/m to several hundred mS/m. As for the rail resistance, the effect on the phase is negligible. The effect on the level of the track circuit operating signal however is substantial and it must be ensured that the track circuit will operate correctly even for the highest expected value of rail track conductance (Fig.7.25).

Rail track inductance has the most substantial effect on the track circuit operation as it forms part of the tuning of track circuit terminations. The graph of the current in track circuit receiver as function of the frequency and the rail track inductance (Fig.7.26) shows that with the increase of the inductance there is a clear shift of the resonance frequency towards the lower frequency. Although it is not very apparent from this graph at the operating frequency of the track circuit the amplitude of the current has a peak. It corresponds to the value of rail track inductance which provides the best tuning of track circuit terminations (about 1.2 μH/m).

The effect of rail-to rail capacitance is shown in Fig.7.27 representing the magnitude of the track circuit transfer impedance as function of the frequency and the capacitance. The magnitude of the transfer impedance being the lowest at the track circuit operating frequency decreases with the increase of the capacitance but there is no visible phase change.

It must be noted that the above mentioned 3D graphs are theoretical, in that they do not account for the correlation between the two variables which is due to the fact that the rail track parameters are themselves frequency dependent.

Conditions of simulation	Fig.7.24
Track circuit type	YL,
Operating frequency	5520 Hz. Freq. varies between 3.5 and 7.0 kHz
Operating mode	Unoccupied
TC parameters	Variation of rail track resistance
Track circuit model	Full

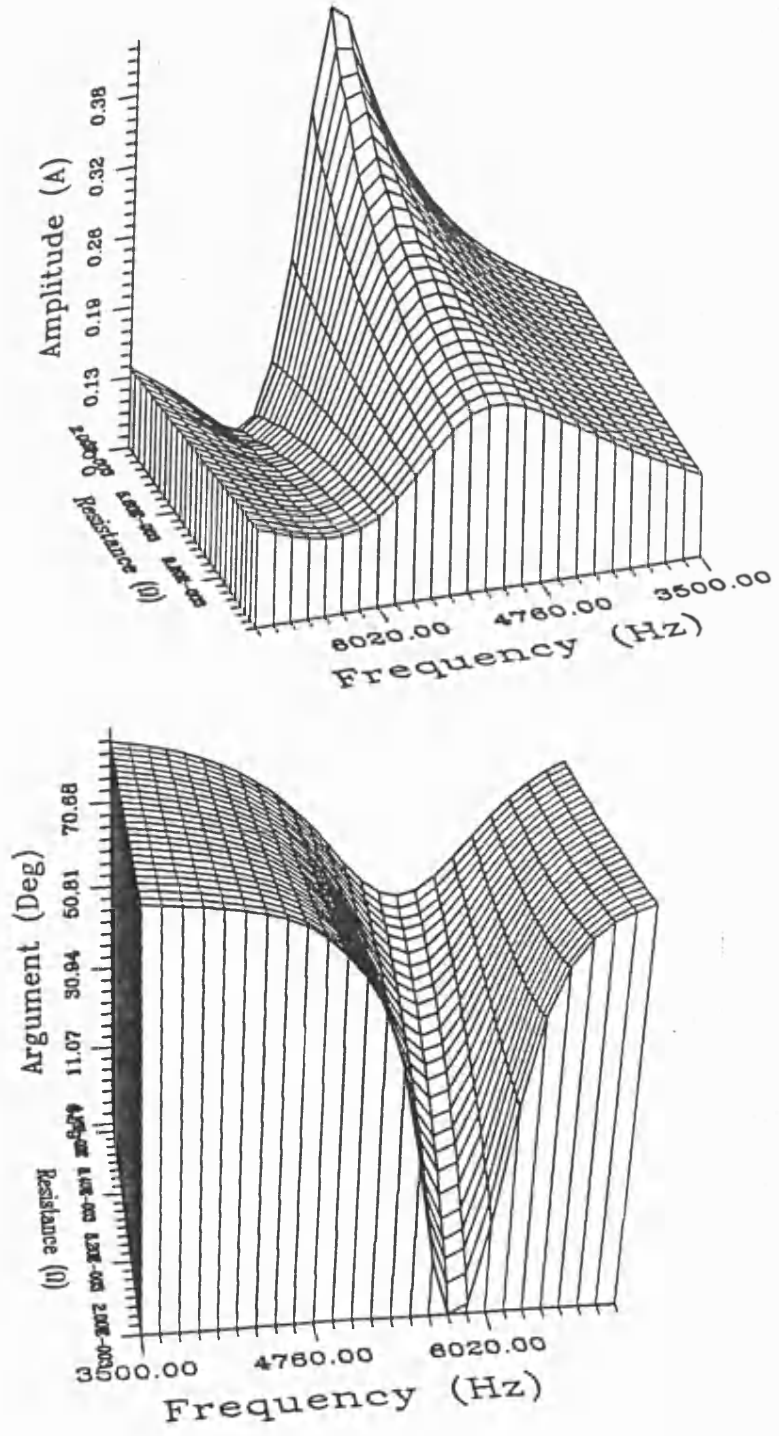

FIG.7.24 Current in track circuit transmitter as function of frequency and rail track resistance

Conditions of simulation	Fig 7.25
Track circuit type	YL, 300 m long
Operating frequency	5520 Hz. Freq. varies between 3.5 and 7.0 kHz
Operating mode	Unoccupied
TC parameters	Variation of rail track conductance
Track circuit model	Full

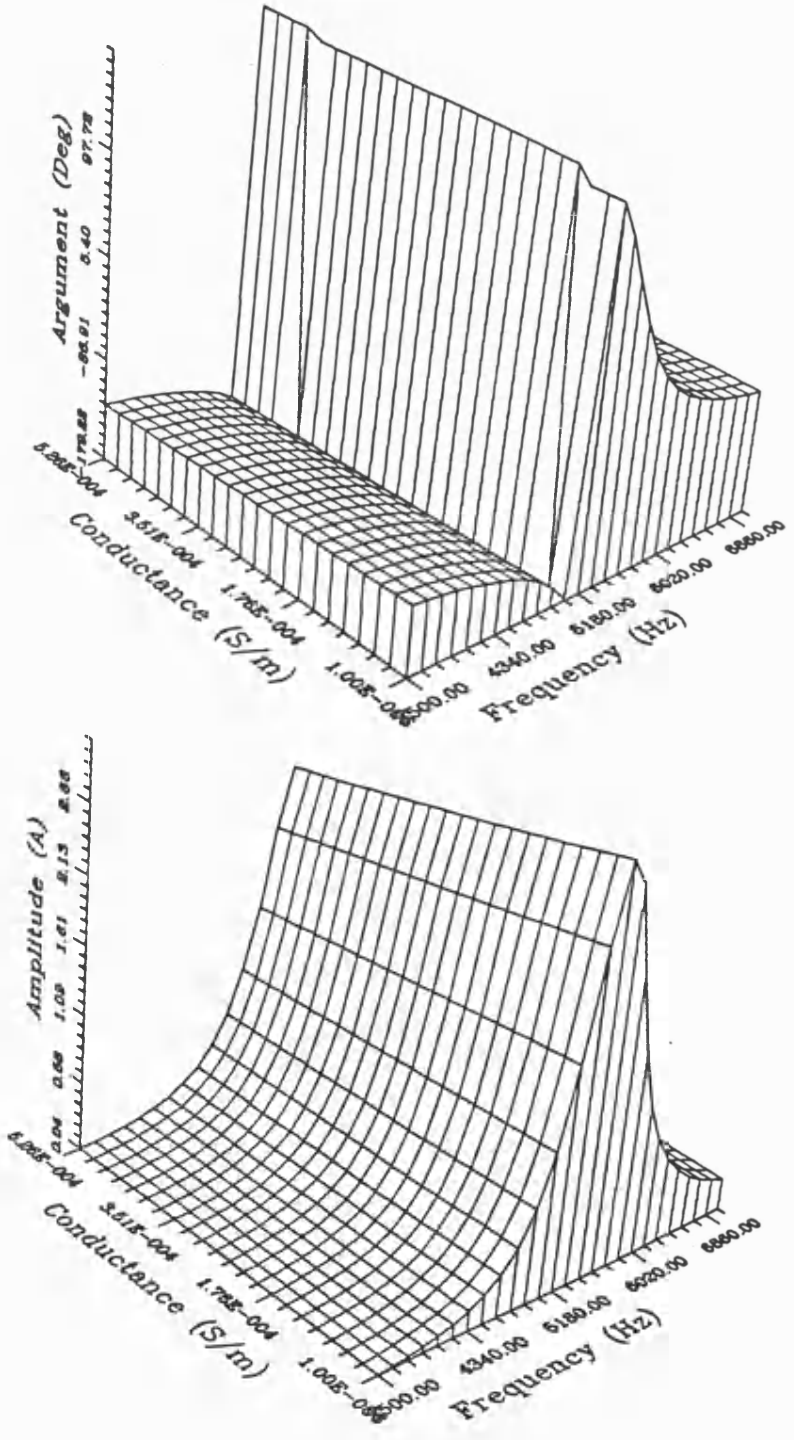

FIG.7.25 Current in track circuit receiver tuning unit as function of frequency and rail track conductance

Conditions of simulation	Fig 7.26	Fig.7.27
Track circuit type	YL, 300 m long	
Operating frequency	5520 Hz, Freq. varies between 3.5 and 7.0 kHz	
Operating mode	Unoccupied	
TC parameters	Variation of rail track inductance	Variation of rail track capacitance
Track circuit model	Full	

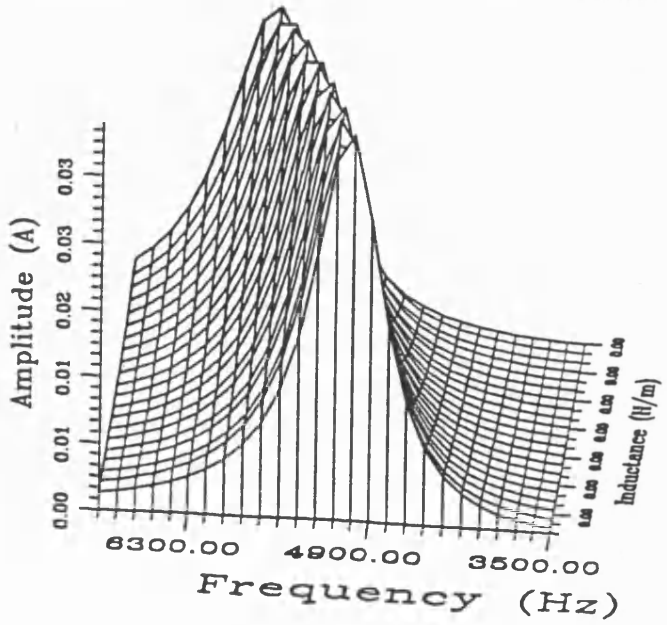

FIG.7.26 Current in track circuit receiver as function of frequency and rail track innductance

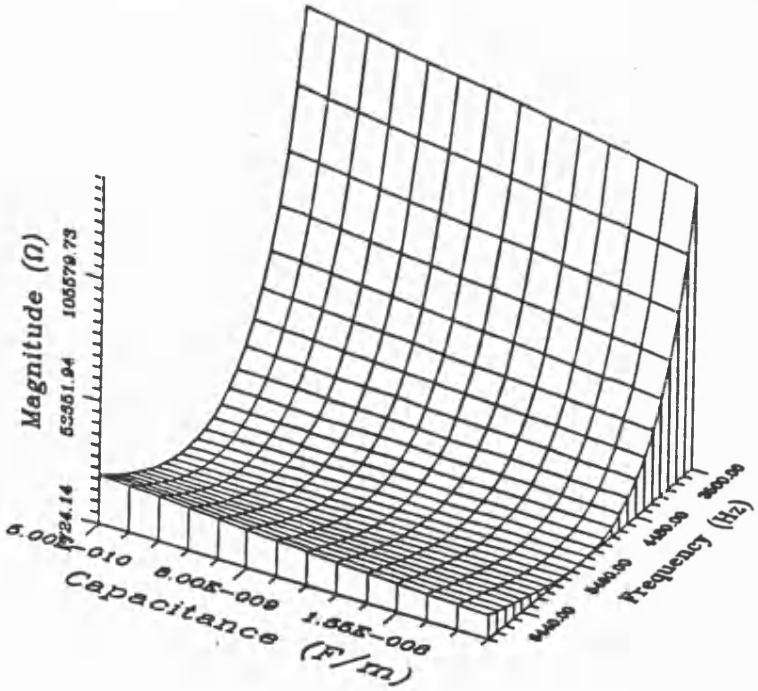

FIG.7.27 Magnitude of track circuit transfer impedance as function of frequency and rail track capacitance

7.2.9 Investigation of track circuit performance under train shunt conditions

The computer tool for track circuit simulation provides good facilities for an in-depth investigation of track circuit operating in train detection operating mode. The basis of the investigation is the full track circuit solution for a moving train shunt. As FS 2000 track circuit are jointless it can be expected that the zone of train shunt influence extends beyond the track circuit physical length. To establish the exact zone of train shunt influence simulations have been carried out to obtain a full track circuit solution for a train shunt moving along three consecutive track circuits K, Y and X, in the direction from TC K to TC X (Figures 7.28 to 7.29). The position of the train shunt is defined with respect of TC K receiving end. For better understanding of the graphs thin lines indicate the positions of the tuning units and the termination bonds. The graphs of the currents in the transmitting end indicate a steady increase starting when the train enters the track circuit at the receiving end and then a sharp fall in the transmitting end as the train shunts the transmitter. After the train leaves the track circuit it continues to affect the transmitting end currents by drawing a higher current from the transmitter, after which the currents steadily reach their normal values for the unshunted track circuit. The graphs of the currents in the track circuit receiving end clearly illustrate the effect of train detection. It is expressed in a sharp drop of the amplitude of the current in track circuit receiver when the train enters the track circuit and a sharp increase to its normal value for unoccupied condition when the train leaves the track circuit in the transmitting end. While the shunt moves along the track circuit the amplitude of the current in the receiver is well below the de-energisation level with a minimum and two maximums. The maxima are located at short distances from track circuit tuning units, and the minimum is towards the middle of the track circuit. The two maximums characterise the positions in which the track circuit has the worst train shunt sensitivity. The same behaviour is seen on the graph of track circuit transfer impedance in Fig.7.31. The train shunt sensitivity is a complex function of the magnitudes and arguments of the input impedances of track circuit terminations seen looking from the rail track as well as on the relationship between these impedances. This train shunt sensitivity characteristic agrees with the results of the mathematical analysis of shunt operation described in [8] for input impedances of track circuit terminations with negative arguments and medium value of the magnitude. In this simulation the values of the input impedances at track circuit terminations are as follows: $ZTYT = 1.94e^{-j15^{\circ}}$, $ZTYR = 1.82e^{-j15^{\circ}}$.

The graphs in Figures 7.28, Fig.7.29 and 7.31-a have been produced for the following steps of advancing the train shunt: in the track circuit - 15.0 m, between the termination bonds -0.05 m and in the track circuit termination areas - 0.25 m. These steps are quite small and allow to produce very accurate train shunt graphs except in the areas of track circuit terminations. The reason is that the different steps of advancing the train shunt

Conditions of simulation	Fig 7.28
Track circuit type	Three TCs - XL,YL,KL each 300 m long
Operating frequency	XL - 4800 Hz, YL -5520 Hz, KL - 4320 Hz
Operating mode	Train moving along KL, YL and XL
Train shunt step	TB area - 0.05m, TU area - 0.25m, TC length area - 15m
Train shunt resistance	0.3 Ω
Track circuit model	Full

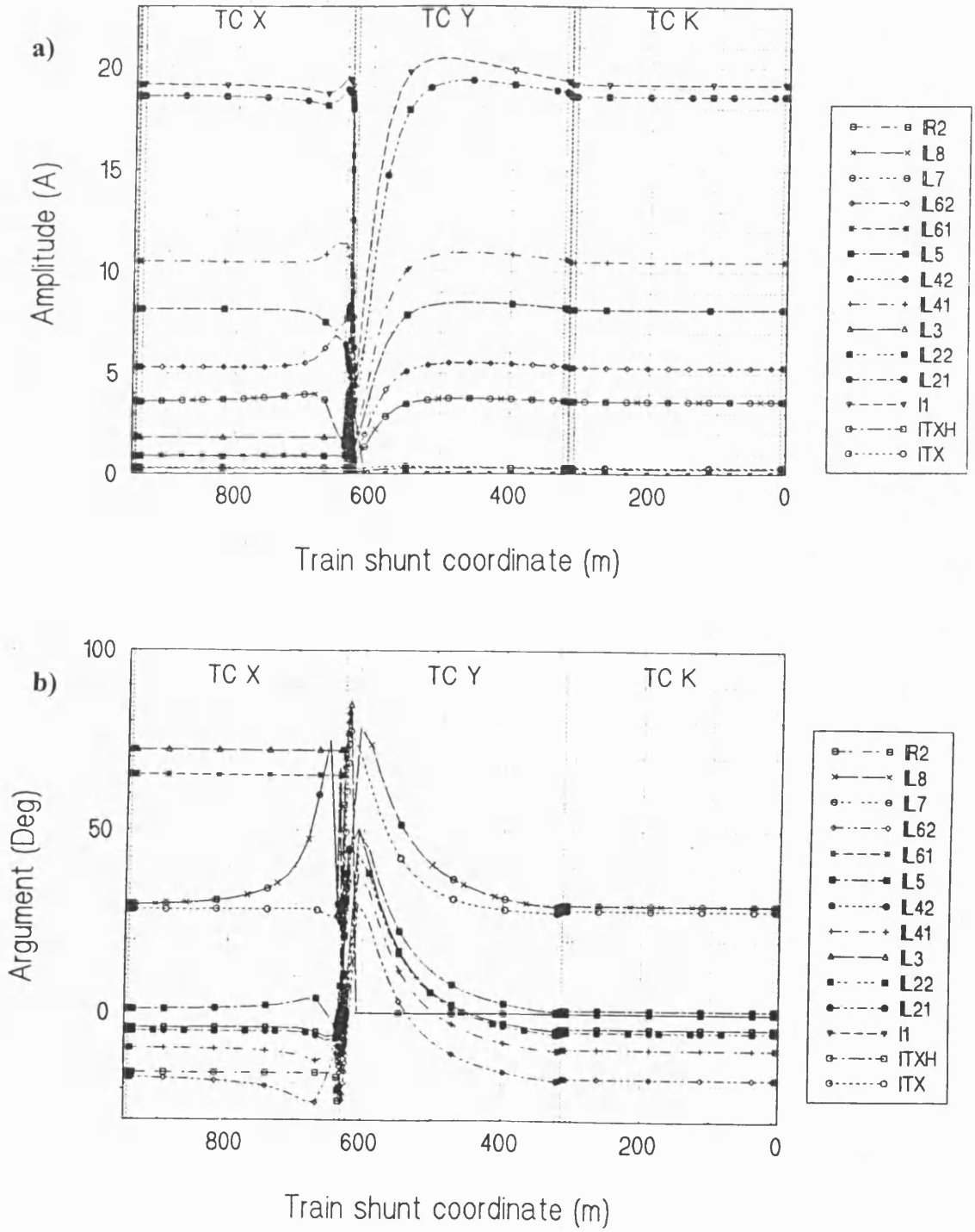

FIG.7.28 Currents in TC transmitting end as function of train shunt position

Conditions of simulation	Fig 7.29
Track circuit type	Three TCs- XL,YL,KL each 300 m long
Operating frequency	XL - 4800 Hz, YL -5520 Hz, KL - 4320 Hz
Operating mode	Train moving along KL, YL and XL
Train shunt step	TB area - 0.05m, TU area - 0.25m, TC length area - 15m
Train shunt resistance	0.3 Ω
Track circuit model	Full

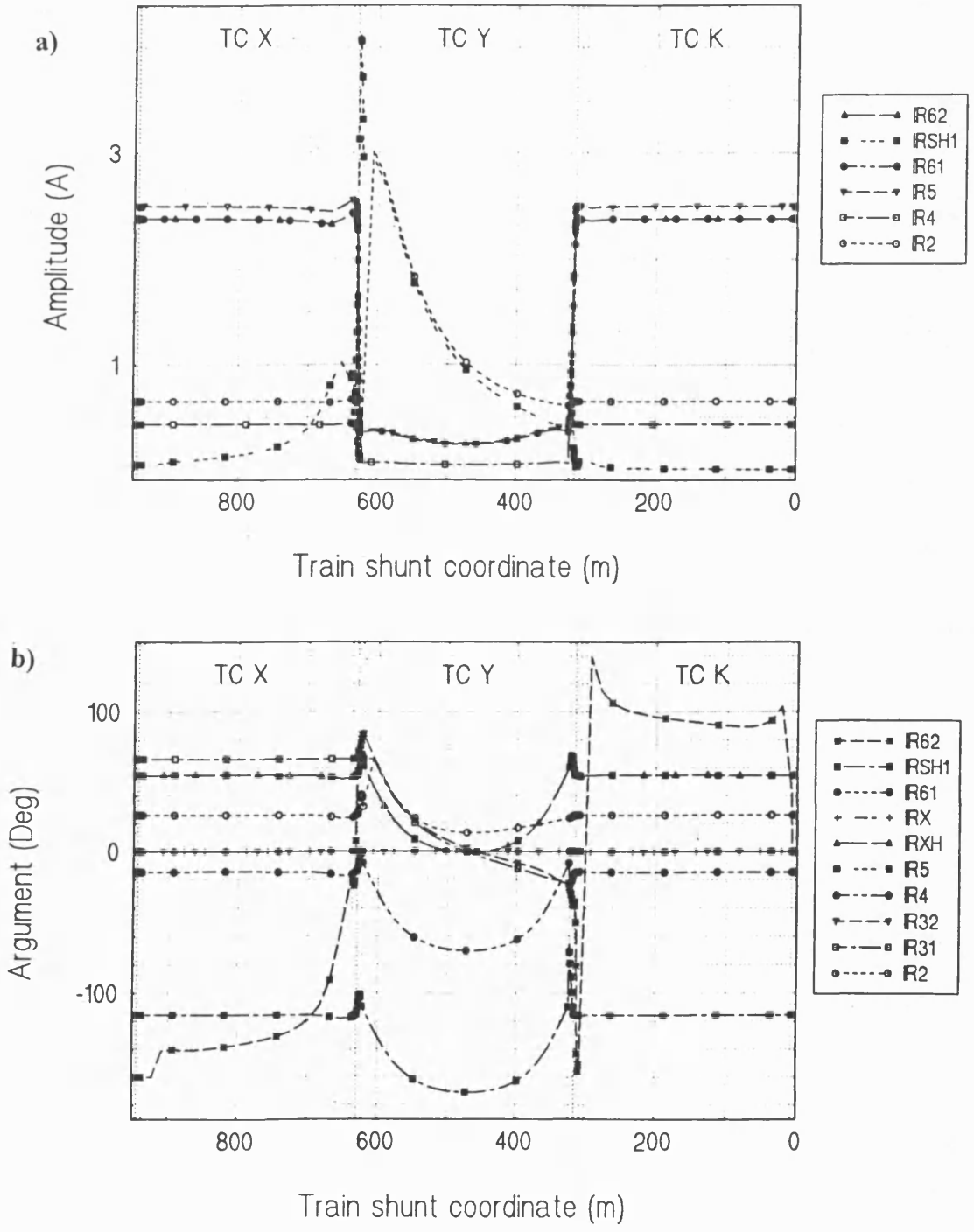

FIG.7.29 Currents in TC receiving end as function of train shunt position

Conditions of simulation	Fig 7.30
Track circuit type	Three TCs - XL,YL,KL each 300 m long
Operating frequency	XL - 4800 Hz, YL -5520 Hz, KL - 4320 Hz
Operating mode	Last 30m of KL, TB area and first 30 m of YL
Train shunt step	0.1 m
Train shunt resistance	0.3 Ω
Track circuit model	Full

a)

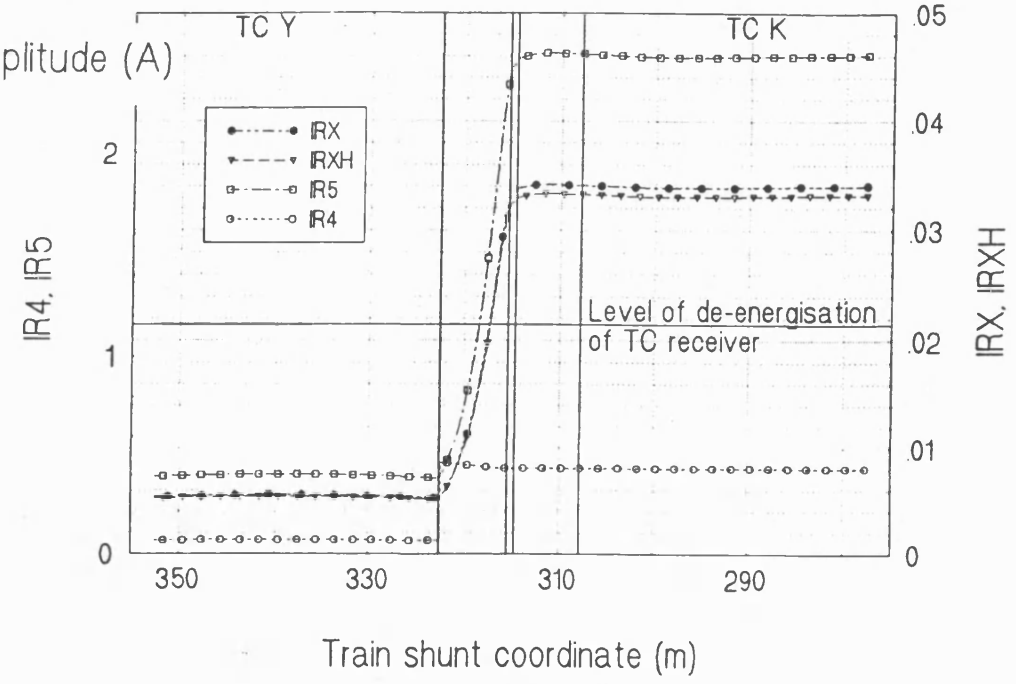

b)

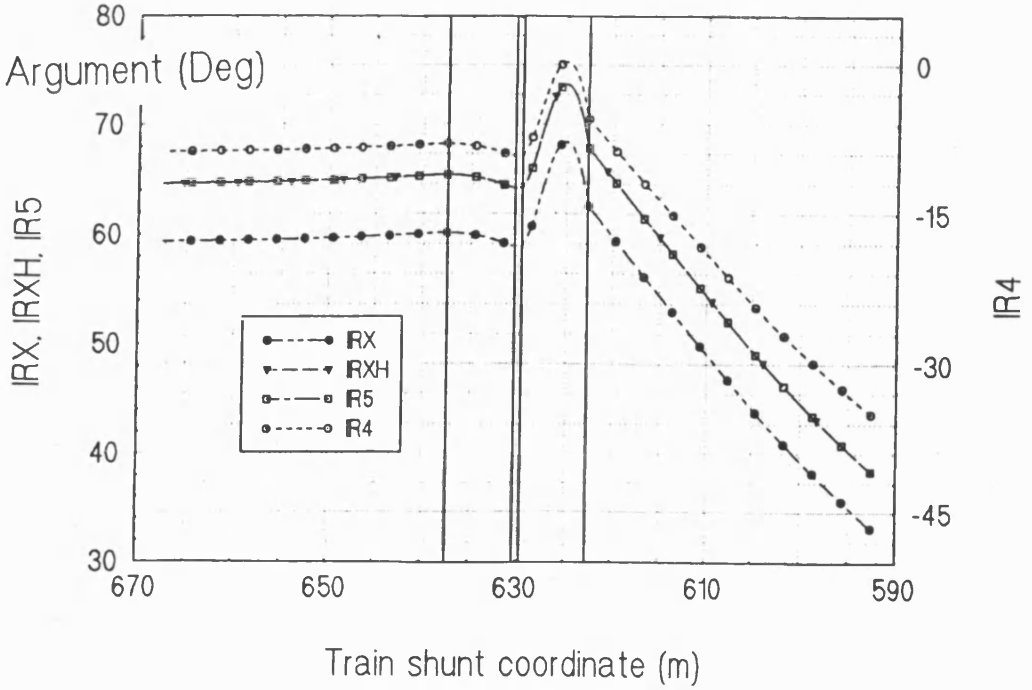

FIG.7.30 Currents in TC receiving end as function of train shunt position

Conditions of simulation	Fig 7.31 -a	Fig.7.31-b
Track circuit type	Three TCs- XL,YL,KL each 300 m long	
Operating frequency	XL - 4800 Hz, YL -5520 Hz, KL - 4320 Hz	
Operating mode	Train moving along KL, YL and XL	Last 30m of KL, TB area and first 30m of YL
Train shunt resistance	0.3 Ω	
Train shunt step	TB area - 0.05m, TU area - 0.25m, TC length area - 15m	0.1m throughout
Track circuit model	Full	

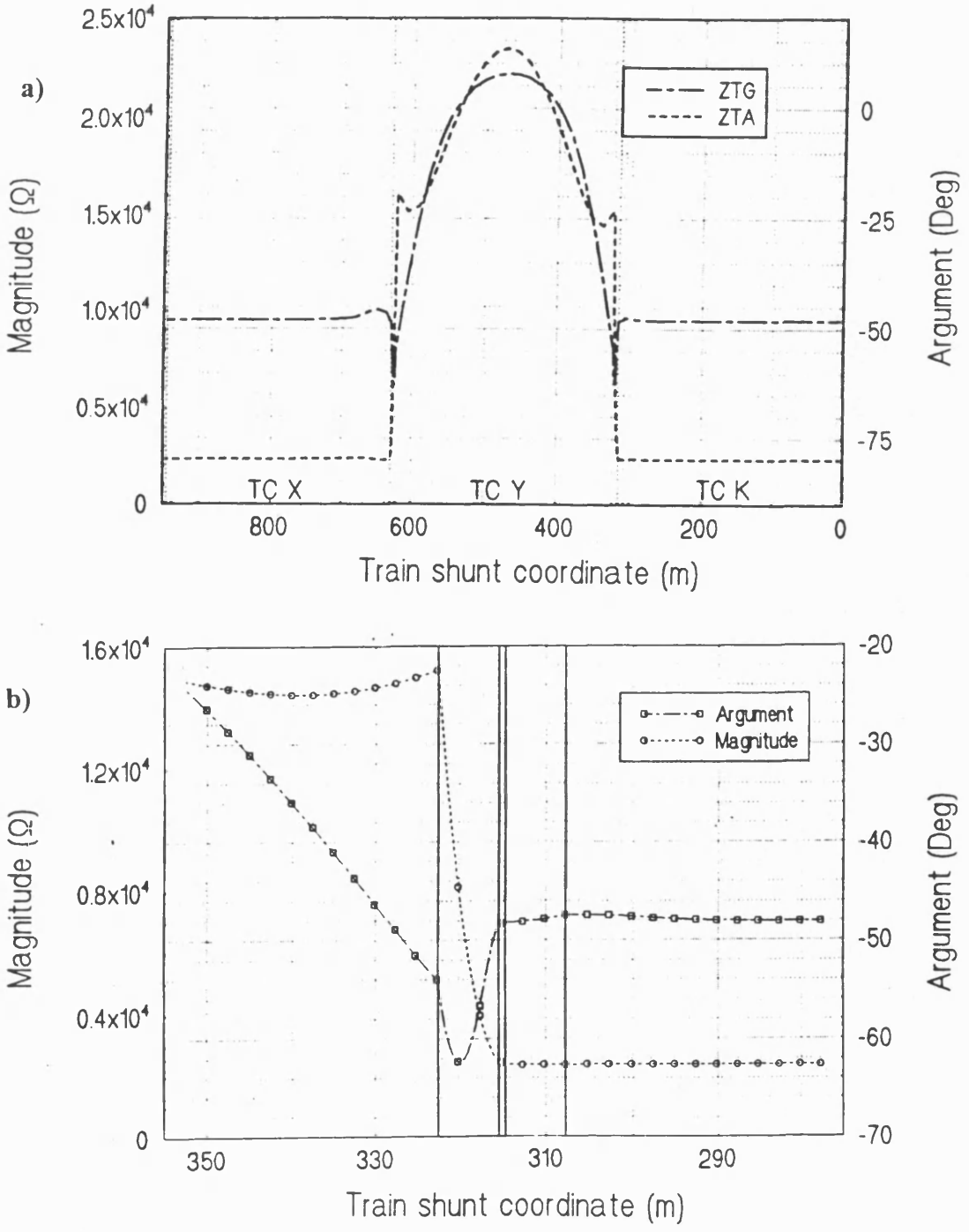

FIG.7.31 TC transfer impedance as function of train shunt position

Conditions of simulation	Fig 7.32
Track circuit type	Two TCs - XL,YL each 300 m long
Operating frequency	XL - 4800 Hz, YL -5520 Hz
Operating mode	Train moving along the Rx end of YL and the Tx end of XL
Train shunt resistance	0.3Ω
Train shunt step	0.1m throughout
Track circuit model	Full

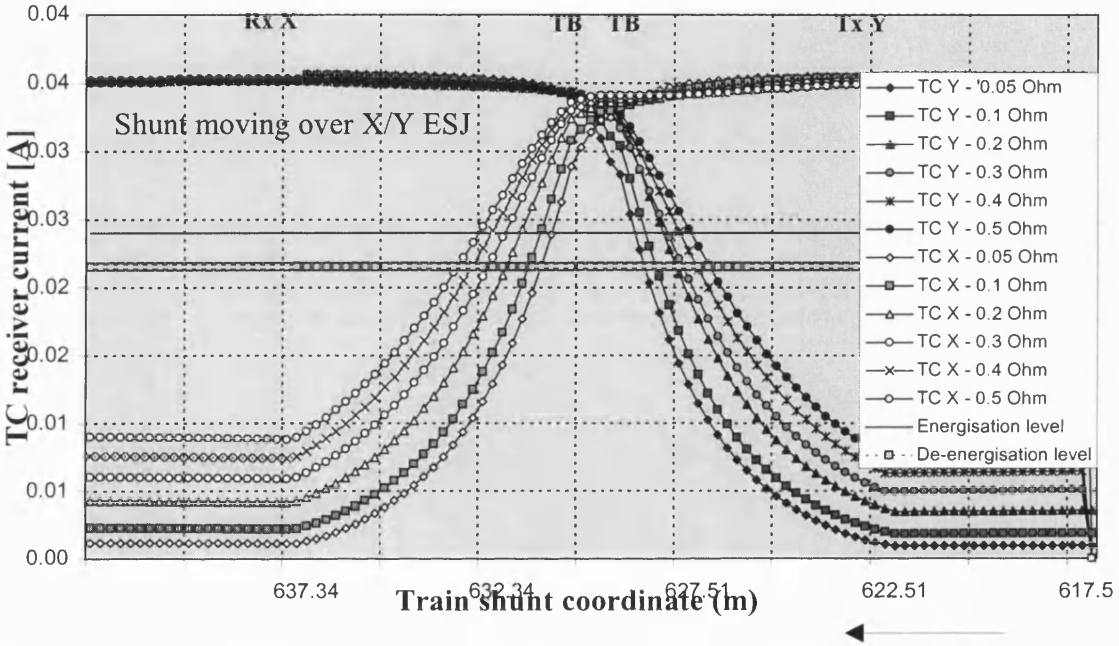

FIG.7.32 Train detection in X/Y ESJ area - Amplitudes of XL and YL receiver currents

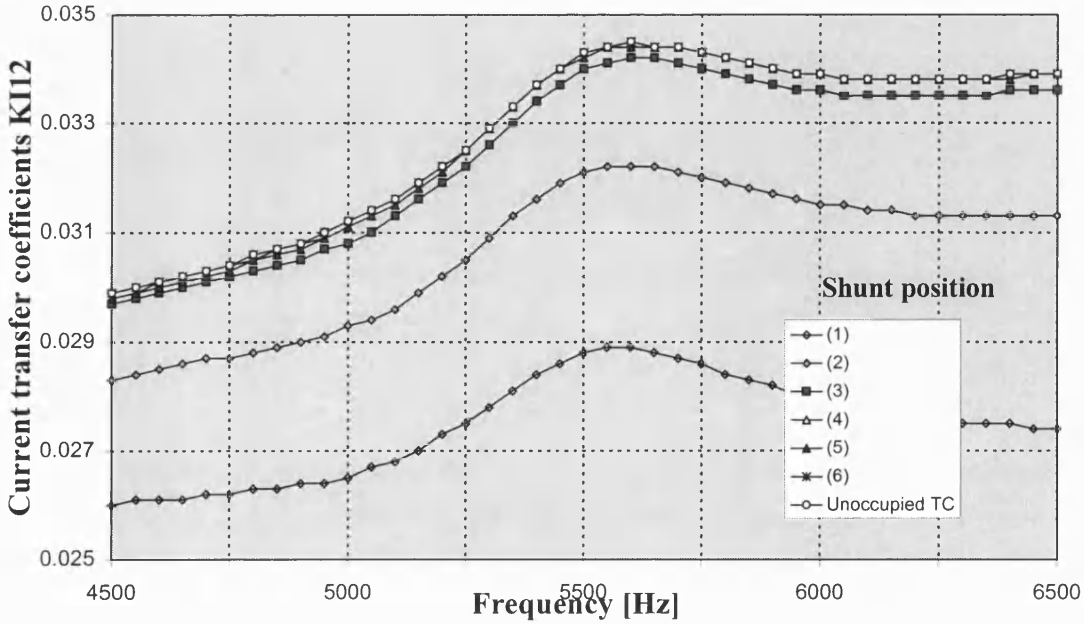

FIG.7.33-a Parameters of X/Y ESJ model (Conditions of simulation on page 7-35)

Conditions of simulation	Fig 7.33 -a, b,c
Track circuit type	Two TCs - XL,YL each 300 m long
Operating frequency	XL - 4800 Hz, YL -5520 Hz
Operating mode	Static train shunt at 6 different positions as shown in Fig.7.34
Train shunt resistance	0.3 Ω
Train shunt step	0.1m
Varying parameter	Frequency varying from 4500 to 6500 Hz
Track circuit model	Full

b)

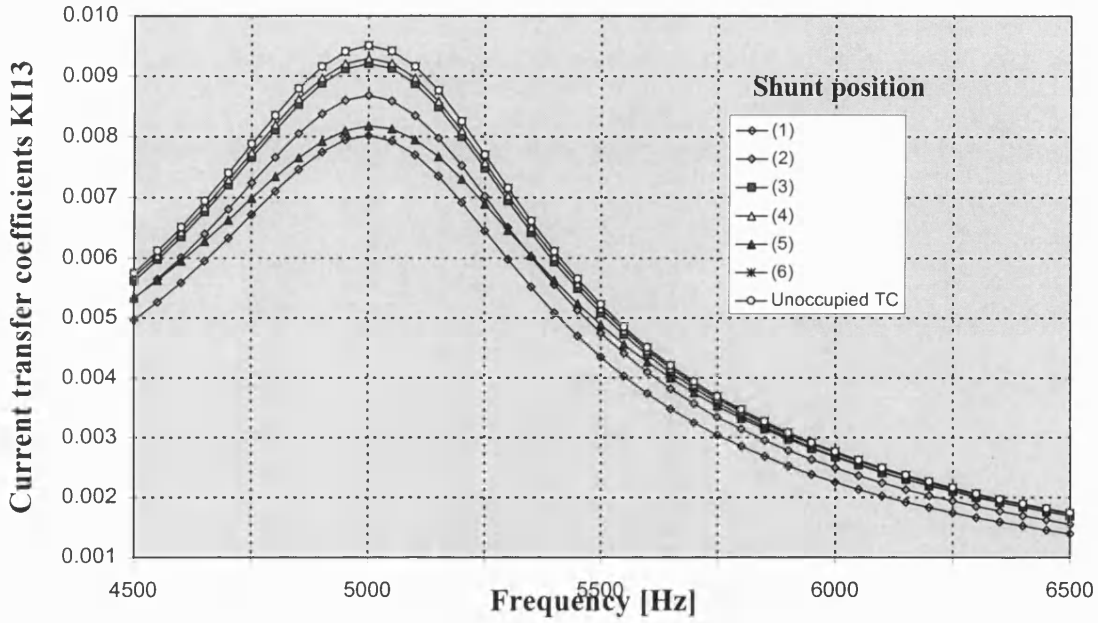

c)

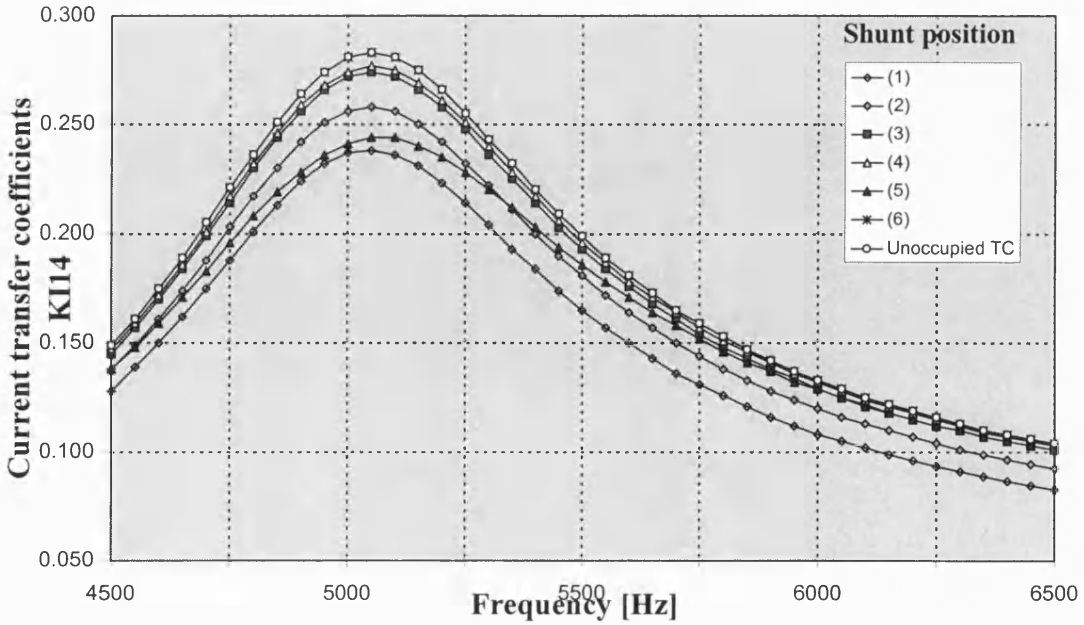

FIG.7.33 Parameters of X/Y ESJ model

cause distortion of the graphs at the boundaries between the sections with different values of the step. Therefore, for track circuit termination areas more accurate graphs have been produced using the same step of advancing the train shunt throughout the area of simulation. Examples of such graphs are shown in Figs.7.30 and 7.31-b. Such graphs are particularly useful for the investigation of ESJs and their operation in the presence of train shunt. By running suitably chosen simulations one can define the 'dead' zone in which a train shunt remains undetected by either of the track circuits and establish how the length of this zone is affected by various parameters. An example is shown in Fig.7.32 which illustrates the fact that the higher the train shunt resistance, the wider the 'dead' zone is. For the standard train shunt resistance of 0.3 Ohm the width of the dead zone is 4.16 m which is in good agreement with the specified figure of 2 - 4 m.

The graphs in Fig.7.33-a, b and c represent the transfer characteristics of an ESJ described as a four port network (Section 3.2.4). The coefficients KI12, KI13 and KI14 are shown at six positions of the train shunt as indicated on Fig.7-34. The shunt effect is well expressed for KI12 (Fig.7.33-a). With shunt in position (1) the value of the signal transmitted from the receiver into the TC greatly reduces. In position (2) it is still considerably reduced, while in position (3) and onwards it is only negligibly smaller than the value in unshunted operation irrespective of train shunt position. Transfer coefficients KI13 and KI14 reduce negligibly in value.

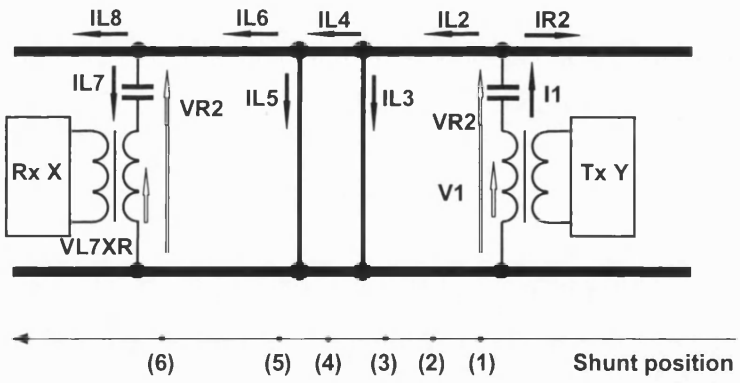

FIG.7.34 ESJ between track circuits X and Y with positions of shunt operation simulations

7.2.10 Optimisation of track circuit design

In its present form the CAE tool allows to solve some particular optimisation problems such as:

- Determination of the optimum length of track circuit termination area as function of the distance to the equipment room (for track circuit with centrally located equipment)

Conditions of simulation	Fig 7.35	Fig.7.36
Track circuit type		XS, YS, KS
Operating frequency		5040, 5520, 4320 Hz
Operating mode	Unoccupied	
Varying parameters	Tx end cable length TCT length	Tx end cable length
Track circuit model	Full	

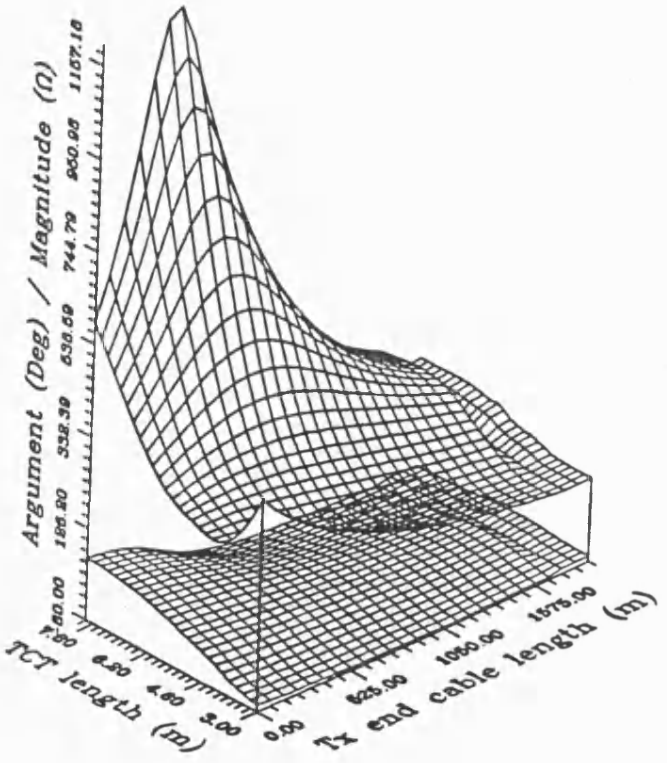

FIG.7.35 Input impedance ZSYT as function of track circuit termination length and distance to equipment room

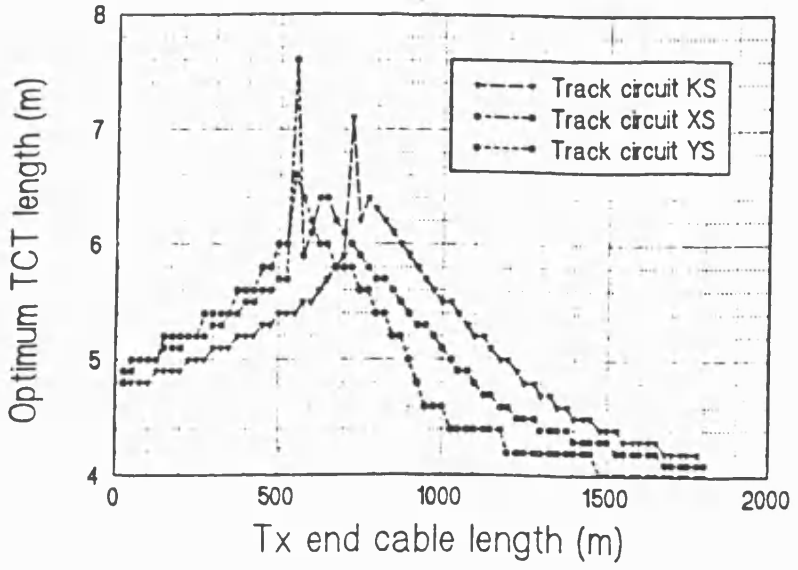

FIG.7.36 Optimum values of track circuit termination lengths for track circuits types XS, YS and KS

- Determination of track circuit minimum and maximum lengths, etc.

However, the user must himself define the set of simulations necessary for the definition of the optimum parameter, control the run of these simulations, store and process the output results, i.e. perform the functions which will eventually be carried out by the 'Task Control Logic' layer of TCADP. Illustration of these facilities is shown in Figs.7.35 and 7.36

7.3 CONCLUSIONS REGARDING THE VALIDATION OF THE TRACK CIRCUIT MODEL

All results obtained from the simulations of FS 2000 track circuits have confirmed the expected track circuit performance, showing very good agreement with the specific values and design parameters indicated by the manufacturer in [2-19]. A set of simulation results have been acknowledged as well by a track circuit design engineer of the manufacturing company. They compare well with other FS 2000 simulation results produced using the professional simulation software package SABER [6-2], [6-3]. This, together with the positive outcome from the other validation techniques described in Chapter 6 gives enough confidence to consider the model on which TCADP is based enough accurate and versatile as it is required for investigation of real problems related to the application of jointless track circuits. Although the model has been developed specifically for the FS 2000 track circuit, by applying correctly the suggested modelling technique accurate models for any other jointless TC can be created.

Chapter 8

CONCLUSION

8.1 CONCLUDING REMARKS

The traditional method of track circuit design is by continuous development based on good engineering judgement and the trial-and-error technique complemented by experimental measurements. This method although satisfactory for the DC and power AC track circuits does not necessarily lead to an optimum design and is not efficient when modern audio-frequency jointless track circuits are concerned. In particular, the lack of physical insulation between adjacent track circuits affects the design in two ways. On one side the functional algorithm of AF JTCs is more complex than that of jointed TCs, as it takes over the essential functions of the insulating block joints. On the other hand, because the adjacent track circuits are physically and functionally interrelated, they must be designed as a system of jointless track circuits rather than a single track circuit. Correspondingly, their design is much more complex, involving a higher number of design parameters which are difficult to optimise using traditional techniques. Hence, there is a need for a systematic approach to jointless track circuit design. Recognising this need, the aim of the present research work was to develop new methodology and new design tools to enable systematic track circuit investigation, design and optimisation.

The methodology presented in this thesis provides a directed design procedure which takes account of the specific track circuit function and design requirements and ensures that the design process will be conducted in such a way as to yield an optimum design which fully meets the design specification. The practical application of this systematic design approach requires versatile tools enabling exact track circuit solutions and performance assessment for various values of the design parameters and varying operating and environmental conditions. Very often, experimental measurements are the only way to check track circuit design and obtain reliable results about track circuit performance or solve interference and other problems related to track circuit application. The use of experiments is however very restricted as they are difficult to conduct especially on operational railways. The present research work has adopted an efficient and economic alternative, namely to use modern computer based simulation methods. Despite the availability of professional electric circuit simulation software it was decided to develop *instead* a purpose built, track circuit oriented simulation tool. This approach has lead to a more efficient, tailor made track circuit model, but more importantly, it has also enabled special facilities necessary to perform the procedures of systematic track circuit investigation and design to be implemented.

The development of the methodology and software tools for track circuit design has necessitated and leads to an innovative modelling approach consisting of the following stages. Firstly, track circuits are analysed from two different aspects - functionality and physical structure to reveal their specific features. The results of this analysis are then used to derive two separate track circuit models - a functional model representing an abstract mathematical definition of the track circuit functional algorithm, and a physical model which is a mathematical description of the track circuit as a physical system in the form of an electric network. At the next stage of the modelling process the functional and the physical models are integrated into one track circuit model in which the mathematical relationships defining the requirements of the function algorithm are expressed in terms of the real physical design parameters. Finally, this integrated model is implemented and solved in a computer program.

The track circuit functional model provides the methodological background for track circuit design and optimisation. It introduces appropriate categories of variables (input operating effects, environmental effects and design parameters) which enable a full definition of the track circuit status and express the TC function. On this basis the problem of track circuit design and optimisation can be then formulated mathematically as a non-linear optimisation problem and an appropriate solution strategy can be defined. The development of the functional model has lead to the following methodological concepts:

- The track circuit functional algorithm cannot be referred to a single operating point but must be ensured for a defined operating range. This requirement has been implemented by introducing an appropriate region of definition of track circuit operating conditions and conducting the search for the design solution over the whole definition area.

- Track circuits are open systems and their operation can be influenced by a number of environmental factors. This is accounted for by including the vector of TC environmental effects as a parameter of the design process.

- To achieve the requirement for fail-safe operation the design parameters of track circuit equipment are introduced as a particular type of input effect. Each has a specified region of definition and the functional algorithm monitors that the values of the design parameters are within the specified ranges.

- The TC functional model introduces the concept of decomposition of the functional algorithm into several operating modes

- The TC functional model introduces quantitative measures of track circuit performance in the form of performance criteria. These enable the worst case scenarios, defining the borders of track circuit operating range to be determined.

- In addition, the functional model of jointless track circuits justifies the need to model and investigate AF JTC as a system of track circuits and to amend the track circuit functional algorithm with specific functions taking into account the functionality of ESJs.

The physical model identifies track circuits as multiconductor transmission lines over lossy ground with lumped parameter discontinuity networks. This is a very general and powerful model which could be applied for the modelling of track circuits in all practical applications. Although in the present work the model has been applied for the most simple case of non-electrified railways it can be easily extended and applied to the modelling of track circuits in areas with third rail DC or AC overhead electrification. The model allows different track circuit configurations to be accommodated and various interference problems to be studied. The difficulty in setting up this model for more complicated configurations is the definition of multiconductor line primary parameters in the form of the series impedance and shunt admittance matrices [**Z**] and [**Y**].

The track circuit physical model is supported by an appropriate mathematical technique and solution procedure which are universally applicable, irrespective of the number of conductors and discontinuities. Two solution methods have been considered in detail - MTL analysis in the phase domain and in the modal domain based on the theory of natural modes. The analysis includes the definition of general systems of notation and sets of matrix variables necessary for describing and solving the sections of multiconductor transmission line and the discontinuities, derivation of formulae and equations which are best suited for track circuit analysis. The analysis has concluded that, in general, a full solution of MTL networks in the modal domain is not possible. This is due to the impossibility of modal decoupling of the termination and intermediate discontinuities. In the same time, the analysis has recognised the definite advantages of applying the theory of natural modes for the solution of the sections of multiconductor transmission line. Despite the necessity of carrying phase-to-modal and modal-to-phase transformations at each interface to a discontinuity this method simplifies the solution and allows access to the real physical components of the termination and intermediate discontinuity networks. In addition, modal analysis provides an insight and a deep understanding of the processes of coupling of the natural modes and is particularly useful in the investigation of the broken rail detection operating mode.

The mathematical derivations on which the MTL analysis is based have been used to compile a number of tables containing the most useful for the TC analysis formulae, circuit and analytical representations including a table detailing step-by-step the

procedure of modal analysis of a two-conductor transmission line. These tables form a useful handbook for the mathematical description and solution of track circuit models in its own right.

The mathematical formulation of the TC physical model is completed by a simple but universal procedure for solving non-uniform MTLs. It includes a forward procedure of step-by-step reduction of the whole network to a single uniform MTL section, solution of this section and backwards sequential solution of each discontinuity and uniform MTL section.

The implementation of the track circuit model into a computer program enables an exact and complete solution of the track circuit to be obtained, including currents, voltages, impedances, etc. at any branch and node of the electric circuit and at any point along the rails. The computer program allows various static and dynamically changing operating conditions to be simulated, the effect of various parameters and track circuit performance to be measured. The provision of this facility already constitutes an invaluable help to designers of AF JTCs, especially when more complex configurations are concerned. In principle, this could have been achieved, with higher or lesser success and efficiency with any professional software program for modelling and solving electric circuits. The objective of this research work was to develop not simply a computer program for solving track circuit electric networks but rather a specialised tool offering facilities for the investigation of track circuits and the solution of various track circuit related problems. To achieve this objective the track circuit solver subroutine was designed as the inner layer of a three layered computer program (TCADP) structured in such a way as to provide tailor-made facilities for track circuit investigation and optimisation. The middle layer implements the control of dynamic simulations as well as investigations of the effect of various parameters on track circuit design. The upper layer is the most track circuit specific part of the program and implements the logic, enabling definition of worst case scenarios and different particular or general optimisation problems.

In the computer implementation of the track circuit model an attempt has been made to ensure the maximum possible degree of modularity so as to minimise the effort necessary for adjustment of the model to a different type of track circuit. In its present form TCADP requires the user to have a good knowledge of the structure and operation of the computer program as adjustment of the program for a different type of track circuit would require modification of the program code. This is inevitable for a software tool which is open to the user for further adjustments, extensions and upgrading.

The track circuit model has been validated by extensive testing and application of TCADP for the investigation of an established and well known track circuit. The results of the simulations of track circuit operation under various operating conditions have

demonstrated very good agreement with the preliminary known track circuit specification and performance. This fact, in conjunction with other validation techniques proves the correctness of the track circuit model and the viability of the modelling method and solution procedure. Furthermore, some unknown and 'unexpected' results have been obtained which have been confirmed by track circuit design engineer. These results indicate ways of improving the track circuit design and confirm the usefulness of the software tool.

8.2 MAIN ACHIEVEMENTS

The main achievements of the present research work can be summarised as follows:

- The research work provides a methodological basis for a systematic study of track circuit performance and systematic solution of a wide range of track circuit related problems, such as design, optimisation, investigation of interference, etc.

- The proposed methodology for track circuit studies is supported by a versatile and efficient software tool enabling track circuit operation to be simulated for any specified set of design parameters, operating conditions and environmental effects and specific operations to be performed allowing the proposed methodology for the solution of various track circuit problems to be implemented.

- Development and validation of a track circuit model using an original modelling procedure combining abstract functional modelling and physical electric network modelling with subsequent synthesis of the two models into one complete track circuit model.

- Development of a track circuit functional model based on application of formal methods which provides a systematic understanding of the complex problem of track circuit design and draws a general frame in which any track circuit related problem can be placed, analysed and expressed with the level of detail required by the application.

- Development of a general track circuit physical model in the form of a non-uniform multiconductor transmission line, allowing any track circuit configuration and layout, and if necessary interfering environment, to be accommodated without restriction on the complexity of the electric network which has to be modelled.

- Application of the theory of natural modes in MTLs for the modelling and analysis of track circuits. Derivation and compilation of a mathematical formulae, equivalent circuit representations, etc. in a form suitable for direct application to track circuit analysis.

- Development of a universal solution procedure for analysis of non-uniform MTLs

8.3 FURTHER WORK

As indicated earlier the present research work provides a methodological background for track circuit analysis, design and optimisation in the form of an abstract, formally defined track circuit functional model. This model can be used for the formulation and systematic solution of various track circuit related problems. On this basis the development of this research work can be continued and extended without restriction on the type of track circuit application.

In parallel to that, the computer track circuit simulation tool developed on the basis of the proposed methodology is designed as an open system envisaging the necessity for further development. Its application and validation proved its viability, but on other side, they indicated the need for its further extension and refinement. Its future application would require further development, both horizontally and vertically.

The horizontal development would be necessary for:

- Adjustment of the track circuit model to different track circuit types i.e. modelling different ESJs and different track circuit layouts - central feeding with two receiving ends, layouts for points and crossing areas, track circuits on parallel tracks, different bonding arrangements
- Extension of the model to allow for simulation of track circuits on electrified railway lines
- Extension of the model to enable the simulation of additional operating conditions i.e. broken rail detection, shunt operation with broken rail, unbalance of the traction return currents, different types of interferences, etc.

The vertical development would involve:

- Further development of the 'Simulation control logic' layer to enable the simulation of more complex scenarios of dynamic operation or the investigation of the complex effect of a higher number of design parameters.
- Further development of the 'Task control logic layer' of TCADP to enable the solution of more general optimisation problems, involving a higher number of design parameters, specification of various design criteria and a fully automated search for the optimum set of design parameters.

In the long term, it is essential for the further development of the software simulation tool that it is applied for the solution of real problems. This would stimulate its further extension and improvement and would indicate appropriate paths for developing a versatile and user-friendly simulation tool for the solution of practical track circuit related problems.

Chapter 9

REFERENCES

9.1 GENERAL REFERENCES

G-1 JOHNK, C.T.A., Engineering Electromagnetic Fields and Waves, John Wiley & Sons, New York, 1988

G-2 PIPES,L., Matrix methods for engineers, Printice-Hall, Inc., Englewood Cliffs, N.J., 1963

G-3 FIDLER, J.K., NIGHTINGALE, C., Computer aided circuit design, Thomas Nelson and Sons Ltd., Hong Kong, 1978

G-4 KALLER, M.I., SCBOLEV, U.V., BOGDANOV ,A.G., Theory of Linear Electric Networks in Railway Signalling and Communications, Editor 'Transport', Moscow, 1987

G-5 CHIPMAN, R.A., Theory and Problems of Transmission Lines, McGraw-Hill Book Company, New York, 1868

G-6 BICKFORD, J.P., MULLINEUX, N., REED, J.R. Computation of power system transients, Peter Peregrinus Ltd, 1976

G-7 NOCK, O.S., Railway Signalling, A&C Black, London, 1980

G-8 European Railway Signalling, A&C Black, London1995

G-9 BRILEEV, A.M., KRAVTZOV, U.A., SHISHLIAKOV, A.V.,
Theory, Design and Operation of Track Circuits, Publishing house 'Transport', Second edition, Moscow 1978

G-10 KOTLIARENKO, N.F., SHISHLIAKOV, A.V, SOBOLEV,U.V., SKRIPIN, I.Z., SHISHLIAKOV, V.A., Railway Signalling and Control, Editor 'Transport', Third edition, Moscow 1983

G-11 Prof. POUPE, Zabezpecovaci Technica v Zeleznicni Doprave, (Railway Signalling Systems) - Part II, Railway Publishing House, Prague 1991

G-12 IANCU, O.D., Computer-aided Design of Non-insulated Track Circuits, Rail International, Vol. 5, No. 6, June 1974, pp.423-436

G-13 IANCU, O.D., Non-insulated Track Circuits with Direct-coupled Receiver: Analysis Relations, Method of Calculation, Rail International, Vol. 7, No. 11, November 1976, pp. 638-645

G-14 WEDEPOHL, L.M., Application of Matrix Methods to the Solution of Travewlling-Wave Phenomena in Polyphase Systems, IEE Proceedings, Vol. 110, No.12, Dec. 1963, pp. 2200-2212

G-15 GALLOWAY, R.H., SHORROCKS, W.B., WEDEPOHL,L.M., Calculation of Electrical Parameters for Short and Long Polyphase Transmission Lines, IEE Proceedings, Vol. 111, No. 12, Dec. 1964, pp. 2051-2059

9.2 REFERENCES USED IN CHAPTER 2

2-1 GROSE, B.H., Jointless Track Circuits and Electrified Railways, Proceedings of the Institution of Railway Signal Engineers, 1972/73, pp. 110-133

2-2 BROWN, C., A Review of Jointless Track Circuits, Proceedings of the Institution of Railway Signal Engineers, 7 Feb.1985, London

2-3 Problems and Techniques in the Use of Audio-frequency Track Circuits, Railway System Controls, Vol. 6, No. 1, May 1975, pp. 22-25

2-4 FRIELINGHAUS, K.H., Contingencies in the Design of the Audio Track Circuit, Rail Engineering International, Vol. 4, No. 4, May 1974, pp. 182-188

2-5 HILL, R.J., Train Position Detection and Track-train Data Transmission using Audio Frequency Track Circuits, Journal of Electrical and Electronics Engineering, Australia, Vol. 5, No. 4, Dec. 1985, pp. 267-277

2-6 SEWELL,T., Evolution of Electronics in Railway Signalling from the Track Circuit Standpoint, IEEE Vehicular Technology Conference, Boulder CO, 21-23 May 1985, pp. 292-298

2-7 Track Circuit separators for Alternating Current Track Circuit Arrangements of Railway Installations, Patent Publication 1 087 427, Published 18 Oct. 1967

2-8 Audio Frequency (AF) Track Circuits with Electric Separation Joint for All-Welded Tracks, SIEMENS Publication ES Bs 2-2530-805-101, March 1969

2-9 HUEMMER, K., Interference-free Track Vacancy Detection, International Conference on Railways in the Electronic Age, London, 17-20 Nov. 1981

2-10 Jointless Audio Frequency Track Circuits Gl S 9/15, SIEMENS Publication F 6532/105.101

2-11 Safety for the Rail Services. Track Vacancy Detection with the FTG S Remote-fed and Coded Audio-frequency Track Circuit, SIEMENS Publication A19100-V100-B607-X-7600

2-12 CZEHOWSKY, J., Die neue Gleisfreimeldung FTG S 917 (The New Train Detection Device FTG S 917), Signal + Draht, Vol. 74, No 7/8, !982, pp.151-160

2-13 FTG S Remote Fed and Coded Jointless Audio Frequency Track Circuit with Electrically Divided Sections, SIEMENS Publication A25090-A532-A108-1-7600

2-14 FS2500 Jointless Track Circuit - Mainline Version, Technical Manual, Westinghouse Brake and Signal Ltd., Issue 2, Oct.1984

2-15 Metro Jointless Track Circuit FS 2500, Westinghouse Signals, Publication P130600, Issue 1, Aug. 1985

2-16 Track Circuit, Westinghouse Brake and Signal Company Ltd., UK Patent Application GB 2 153 571 A, Published 21 Aug. 1985

2-17 BROWN, C.R., HOLLANDS, R.D. and BARTON,.D., Continuous Automatic Train Control and Safety Systems using Microprocessors, International Conference on Electric railway Systems for a New Century, London,

22-25 Sept. 1987

2-18 GAFFNEY, P., HARRIS, F.W., Signalling for Mass Transit railway - the Hong Kong Experience, Proceedings of the Institution of Railway Signal Engineers, 1988/1989, pp. 20-40

2-19 FS2500 Jointless Track Circuit - Metro Version, Technical Manual, Westinghouse Brake and Signal Ltd., Issue 7, Sept.1989

2-20 FS 2600 Track Circuit System,
Westinghouse Data Sheet, Part 8, 8.12, Issue 2, 1993

2-21 GROSE, B.H., Jointless Track Circuit for Electrified Lines, Rail Engineering International, Vol.3, No.5, June 1973, pp. 221-227

2-22 MOOREY, E., Towards the Universal Jointless Track Circuit,
Railway Gazette International, Vol. 134, No. 9, Sept. 1978, pp.654-657

2-23 MILLER, G.D.,Traction Cross-Bonds and AC Track Circuits,
Railway Gazette International, Vol. 136, No. 12, Dec. 1980, pp.1052-1053

2-24 ROSE, J., Traction Immunity for New Circuit
International Railway Journal, Vol. 21, No.3, March 1981, pp. 32/34/36

2-25 Audio Frequency Jointless Track Circuit TI 21, ADtranz Publication, Feb. 1997

2-26 TI 21 Audio Frequency Track Circuits,
RAILTRACK, Railway Group Standard GK/RC0761, Issue 1, June 1996

2-27 SCHULMEYER, H.L., Höherfrequenter isolierstoßfreier Gleisstromkreis FME L 20/80 (Highfrequency Track Circuit without Insulating Joints),
Signal + Draht, Vol. 73, No. 7/8, 1981, pp.186-190

2-28 Jointless High Frequency AC Track Circuit Model FME L20/80,
SEL Publication MAC 03230-13-1e, 1981

2-29 UEBEL, H., Track Monitoring and Automatic Block for Lines Carrying Low Traffic Volumes, International Conference on Electric Railway systems for a New Century, London, 22-25 Sept. 1987, pp. 337-340

2-30 UEBEL, H., KNIGHT, A.C., New German Developments in the Field of Train Detection, IEE Proceedings, Part B, Vol. 134, No.3 ,May 1987, pp.167-175

2-31 WEBER, O., High Speed Traffic Signalling, Rail Engineering - The Way Ahead: International Conference to Mark the 150th Anniversary of Passenger railways, London, 22-26 Sept. 1975, pp. 176-182

2-32 Circuit de Voie sans Joints Universel (Track Circuit without Insulating Jonts),
CSEE Publication FER-F-7-c, June 1977

2-33 GROCE-SPINELLI, J.F., Universal Jointless Track Circuit, Letters, Railway Gazette International, March 1979, p.245

2-34 AUDINOT, P., Track-to-Cab Transmission, 25th Annual Meeting of JUREMA, Zagreb, Yugoslavia, 1980, Zagreb Rad Jurema, Vol. 25, Part 5, 1980, pp. 135-137

2-35 Rétiveau, R., La Signalisation Ferroviaire (Railway Signalling), Presses de L'Ecole Nationale des Ponts and des Chaussées, Paris, 1987, pp.102-115

2-36 UM 71 - All Purpose Jointless Track Circuit with Electric Separation Joints, CSEE Transport Publication, 1993

2-37 The 'ASTER' System of Track Circuits without insulating Block Joints for Non-Electrified Lines, British Rail Specification BR 13448, II edition, Feb. 1968

2-38 Audio Frequency Overlay Circuits can be User in Subways, Railway Signalling and Communications, June 1965, pp.21-23

2-39 AF-200 W wayside Detection and Cab Signalling System, WABCO Technical description 6005

2-40 AF 1000 W Audiofrequency Track Circuit, ANSALDO TRANSPORTI Publication 3.5.4.1, Sept. 1994

2-41 High Frequency Track Circuits for railroads Interrelated at Switches and Crossovers, US Patent 3 524 054, Patented 11 Aug. 1970

2-42 Track Circuit Controls Signals, Railway System Controls, Aug.1972, pp.30-32

2-43 Implications of Modern Transit signalling Concepts for Mainline Railroad Operation, Railway System Controls, Vol. 6, No. 1, Jan. 1975, pp.22-26

2-44 Jointless High Frequency Track Circuit Systems for Railroads, US Patent 4 053 128, Patented 11 Oct. 1977

2-45 HOELSCHER, J., RUDICH, R., Compatibility of rate-Coded Audio Frequency Track Circuits with Chopper Propulsion Drive in Transit Systems, International Conference on Railways in the Electronic Age, London, 17-20 Nov. 1981, pp.128-136

2-46 HOLMSTROM, R., LONG, L., GIGNON, R. Assuring Compatibility of rapid Transit propulsion and Signalling Systems, 32nd IEEE Vehicular Technology Conference, San Diego, California, 23-26 May 1982

2-47 Dual Code Track Circuit, GRS Publication, Folder 282, July 1983

2-48 BOLLINGER, W., WELCO Working on BARTD Signaling, Railway Signaling and Communications, Dec.1967, pp. 18-22

2-49 Signaling System for Determining the Presence of a Train Vehicle, US Patent 3 526 378, Patented 1 Sept. 1970

2-50 BART Track Circuit Description

2-51 FRIEDLANDER, G.D., BART's Hardware - from Bolts to Computers, IEEE Spectrum, Vol. 9, No. 10, Oct.1972, pp.60-72

2-52 BART Needs a Reliable Track Circuit, Railway Gazette International, Vol. 6, No. 9, Sept. 1978, pp. 631-632

2-53 Jointless Track Circuit Metro Type CVCM 75, ALSTHOM-ATLANTIQUE Publication SIG C 2375

2-54 Jointless Track Circuit Metro Type CVCM 75, Description ALSTHOM-ATLANTIQUE Publication

2-55 STRATTON, D.H., Reed Jointless Track Circuits to be Installed on Electrified

Lines, Railway Gazette International, Vol.134, No. 9, Sept. 1978, pp.656-657

2-56 STRATTON, D.H., The Reed Jointless Track Circuit, National Conference Publication, Institution of Engineers Australia, No.79/2, Electrical Energy Conference, Brisbane, 17-18 May 1979, pp.41-44

2-57 Reed Jointless Track Circuits, Track Circuit Manual, Southern region, Part 6, Issued by the Signalling and Telecommunications Engineering Department of British Rail, Oct.1986

9.3 REFERENCES USED IN CHAPTER 4

4-1 MACENTEE, J.A., Railway Track as a Short Transmission Line, M.Sc. Thesis, University of Birmingham, 1972

4-2 HOPKINS, P.R.G., Crosstalk between Track Circuits on Adjacent Roads of a Railway System, M.Phil. Thesis, University of Brunel, April 1981

4-3 FRICKE, H., FORM, P., Application of Communication Techniques to a Future System of Train and Line protection, Cybernetics and Electronics on the Railways, Vol. III, No. 4, April 1966, pp. 166-203

4-4 FRICKE, H., Sensitivity of Response and Resolving power of Non-Insulated Track Circuits for the Counting of Axles and Vehicles of Trains, Cybernetics and Electronics on the Railways, Vol. V, No. 7-8, July-August 1968, pp. 261-270

4-5 MELLITT,B. Data Transmission Characteristics of Railway Track, Electronics Letters, Vol. 9, No. 23, 15 Nov. 1973, pp. 550-551

4-6 FISCHER, A.J., Track, Track Circuits and Traction, International Conference on Electric Railway Systems for a New Century, London, 22-25 Sept.1987 (London: IEE 1987), pp.184-188

4-7 IANCU, O.D., Dependenta de Frecventa Parametrilor Primari ai Circuitelor de Cale (Frequency Dependency of Track Circuit Primary parameters), Revista Cailor Ferate Romane, No. 2, 1972, pp. 63-69

4-8 LITTER, G.E., The Harmonic Performance of a High Voltage AC Electric Railway System with Single and Multiple Train Loading, Railways in the Electronic Age, IEE Conference, Publication No.203, pp.105-110

9.4 REFERENCES USED IN CHAPTER 5

5-1 CRISTINA, S., D'AMORE, M., Effect of Reflection Waves on Polyphase Non-uniform Power Line Carrier Channels: a New Propagation Matrix Model, IEEE Transactions on Power Apparatus and Systems, Vol. PAS-100, No.4, April 1981, pp. 1685-1692

5-2 PIPES,L., Matrix Methods for Engineers, Printice Hall, Inc., Englewwod Cliffs, N.J., 1963

9.5 REFERENCES USED IN CHAPTER 6

6-1 HILL,R.J., BEROVA,M.L., CARPENTER,D.C., MEECHAM, G.J.W., International Conference on Automation Signalling performance Equipment Control and Telecommunications ASPECT 1991, 7-9 Oct. 1991, London

6-2 HILL, R.J., COLES, P.C., A Model for Railway Track Circuit Operation Using Electric Power Transmission Simulation Software, Proceedings of the 27th University Power Engineering Conference, Bath, 1992, pp.123-126

6-3 HILL, R.J., COLES, P.C., A User-friendly Simulator for Modelling Audio Frequency Track Circuit Operation, Proceedings of the 1993 IEEE/ASME Joint Railroad Conference, 1993, pp.77-86

6-4 DETH, F.V., The SNCF New Approach to Track Circuits, Proceedings of the Institution of Railway Signal Engineers, 1992/93, pp.52-69

6-5 EMTDC User Manual, Manitoba HVDC Research Centre, Nov. 1988

6-6 FIDLER, J.K., NIGHTINGALE, C., Computer Aided Circuit Design, Thomas Nelson and Sons Ltd., Hong Kong, 1978

9.6 REFERENCES USED IN APPENDIX A

A-1 TRUEBLOOD, H.M., WASCHEK, G., Investigation of Rail Impedances, AIEE Transactions, Vol. 53, 1934, pp. 1771-1780

A-2 STANEK, E.K., CATALTEPE, T., WIITANEN, D.O., Phenomena that Affect the Calculation of the Inductance and Resistance of Mine Track/Trolley systems, Proceedings 1984 IEEE Industry Applications Society Annual Meeting, Chicago IL, 30 Sept. - 4 Oct. 1984, (New York: IEEE 1984), pp. 100-106

A-3 HILL, R.J., CARPENTER, D.C., Determination of Rail Internal Impedance for Electric Railway Traction System Simulation, IEE Proceedings, Part B: Electric Power Applications, Vol.138, No. 6, November 1991, pp.311-321

A-4 HOLMSTROM, F.R., Conductive Interference in Rapid Transit Signalling Systems, Vol. I: Theory and Data; Final Report, UMTA-MA-06-0153-85-5, DOT-TSC-UMTA-85-21, November 1985

A-5 CARPENTER, D.C., HILL,R.J., Rail Impedance Modelling for DC-fed Railway Traction Simulation, Proceedings IASTED International Symposium on Applied Modelling and , Simulation, Lugano, Switzerland, June 18-21, 1990, pp.105-108

A-6 CARPENTER, D.C., HILL, R.J., Modelling of Nonlinear Rail Impedance in AC Traction Power Systems, IEE Transactions on Power Delivery, Vol. 6, No. 4, October 1995, pp. 1755-1761

A-7 HOLMSTROM, F.R., The Model of Conductive Interference in Rapid Transit Signaling Systems; IEEE Transactions on Industry Applications, Vol. IA-22, No. 4, July/August 1986

A-8 Mutual Design of Overhead Transmission Lines and Railroad Communications

and Signal Systems; Final Report, EPRI EL-3301, Project 1902-1, October 1983

A-9 CARPENTER, D.C., HILL,R.J., The Effect of Magnetic saturation, Hysteresis and Eddy Currents on Rail Track Impedance, Proceedings of 1989 IEEE/ASME Joint Railroad Conference, Philadelphia, PA, April 25-27, 1989, New York, IEEE, pp.73-79

A-10 TYLAVSKY, D.J., KULKARMI, A.Y., Inductance Calculations for Earth-return Trolley Systems, Proceedings of 1988 IEEE Industry Applications Society Annual Meeting, Pittsburgh PA, 2-7 October 1988 (New York: IEEE 1988), 2, pp. 1216-1223

A-11 FIGURNOV, E.P., Rail track impedance in the AC traction supply system, Elektritchestvo, No. 7, 1989, pp.17-22

A-12 CARSON, J.R., Wave Propagation in Overhead Wires with Ground Return, System Technical Journal, Vol. 5, October 1926, pp. 539-556

A-13 PERZ, M.C., RAGHUVEER, M.R., Generalized Derivation of Fields and Impedance Correction Factors of Lossy Transmission Lines, Part I - Lossy Conductors above Lossless Ground, Part II - Lossy Conductors above Lossy Ground, IEEE Transactions on Power Apparatus and Systems, Vol. PAS-93, Nov./Dec. 1974, pp. 1827-1841

A-14 POLLACZEK, F., Sur le Champ Produit par un Conducteur Simple Infmiment Long Parcouru par un Courant Alternatif (On the Problem of the Field Produced by an Infinitely Long Wire Carrying Alternating Current), Revue Generale de l'Electricité, 30 May 1931, pp. 851-967

A-15 WISE, W.H., Effect of Ground Permeability on Ground Return Circuits, Bell System Technical Journal, Vol. 10, 1931, pp. 472-484

A-16 WISE, W.H., Propagation of high-frequency currents in ground return circuits, Proceedings of the Institute of Radio Engineers, Vol. 22, No. 4, April 1934, pp. 522-527

A-17 RUDENBERG, R., Fundamental Considerations on Ground Currents, Electrical Engineering, Jan. 1945

A-18 GARY, C., Approche Complète de la Propagation Multifière en Haute Frequence par Utilisation des Matrices Complexes (Complete Approach to Multiconductor Propagation at High Frequency with Complex Matrices), EdF Bulletin de la Direction des Etudes et Recherches, Serie B, No. 3/4, 1976, pp. 5-20

A-19 DERI, A., TEVAN, G., SEMLYEN, A., CASTANHEIRA, A., The Complex Ground Return Plane, a Simplified Approach for Homogeneous and Multi-layer Earth Return, IEEE Transactions on Power Apparatus and Systems, Vol.PAS-100, No. 8, Aug. 1981, pp. 3686-3693

A-20 MULLINEUX, N., REED, J.R., Calculation of Electrical Parameters for Short and Long Polyphase Transmission Lines, Proceedings of IEE, Vol. 112, No. 4, 1965, pp.741

A-21 WEDEPOHL, L.M., WASLEY, R.G., Wave Propagation in Multiconductor Overhead Lines. Calculation of Series Impedance for Multilayer Earth,

Proceedings of IEE, Vol. 113, No. 4, April 1966, pp. 627-632

A-22 AMETANI, A., Stratified Earth Effects on Wave Propagation - Frequency Dependent Parameters, IEEE PES Winter Meeting, New York, 27 Jan.-1 Feb. 1974, (New York: IEEE 1974), pp.1233-1239

A-23 WEDEPOHL, L.M., EFTHYMIADIS, A.E., Wave Propagation in Transmission Lines over Lossy Ground: a New, Complete Field Solution, Proceedings of IEE, Vol. 125, No. 6, June 1978, pp. 505-510

A-24 EFTHYMIADIS, A.E., WEDEPOHL, L.M., Propagation Characteristics of Infinitely-Long Single-Conductor Lines by the Complete Field Solution Method, Proceedings of IEE, Vol. 125, No. 6, June 1978, pp.511-517

A-25 KAIDANOV, F.G., KOSTENKO, M.V., PEREL'MAN, L.S., Precise Determination of the Transmission Line Constants and Analysis of the Telegraph Equations for the Example of a Two-conductor Transmission Line, Electrichestvo, No. 3, 1965, pp.15-21, (English Translation in Electrical Technoly, No. 2, 1965, pp. 179-198

A-26 KOSTENKO, M.V., Electromagnetic Wave Propagation in Multiconductor Transmission Lines, Electrichestvo, No. 11, 1960, pp. 9-12

A-27 KUESTER, E.F.,CHANG, D.C., PLATE, S.W., Electromagnetic Wave Propagation along Horizontal Wire Systems in or Near a Layered Earth, Electromagnetics, Vol. 1, July-Sept. 1981, pp. 243-266

A-28 WAIT, J.R., Excitation of an Ensemble of Parallel Cables by an External Dipole over a Layered Ground, Arch. Elek. Ubertragungstech., No. 31, 489-493

A-29 OLSEN, R.G., PANKASKIE, T.A., On the Exact, Carson and Image Theories for Wires at or Above the Earth's Surface, IEEE Transactions on Power Apparatus and Systems, Vol. PAS-102, No. 4, April 1983, pp.769-778

A-30 Electric Traction Power Supply, Proceedings of Omsk Institute of Railway Engineers, Vol.104, Part 1, Omsk, 1969

A-31 WAGNER, C.F., EVANS, R.D., Symmetrical Components as Applied to the Analysis of Unbalanced Electrical Circuits, McGraw-Hill, Inc. 1933

A-32 WAIT, J.R., Excitation of a Coaxial Cable or Wire Inductor Located over the Ground by a Dipole Radiator, AEU, Band 31, 1977, pp. 121-127

A-33 WAIT, J.R., Electromagnetic Waves in Stratified Media, Second edition, Pergamon Press, New York, 1970

A-34 HILL, R.J., CARPENTER, D.C., TASAR, T., Railway Track Admittance, Earth-Leakage Effects and Track Circuit Operation, 1989 IEEE/ASME Joint Railroad Conference, Philadelphia, April 1989, pp.55-62

A-35 MAYHAN, R.J., BAILEY, R.E., An Indirect Measurement of the Effect Dielectric Constant and Loss Tangent of Typical Concrete Roadways, IEEE Transactions on Antennas and Propagation, Vol. AP-23, No.4, July 1975, pp. 565-569

A-36 HILL, R.J., CARPENTER, D.C., Rail Track Transmission Line Distributed Impedance and Admittance: Theoretical Modelling and Experimental Results, IEEE Transactions on Vehicular Technology, Vol. 42, No. 2, May 1993, pp. 225-

Appendix A

THE RAIL TRACK AS A TWO-CONDUCTOR TRANSMISSION LINE OVER LOSSY GROUND

This Appendix contains a critical review of the methods of determination of the rail track parameters in terms of the series impedance and shunt admittance matrices introduced in Chapter 4. A symmetrical rail-track geometry is adopted, with the assumptions that $\mathbf{Z}_{11} = \mathbf{Z}_{22}$ and $\mathbf{Y}_{11} = \mathbf{Y}_{22}$.

A.1 SERIES IMPEDANCE

A first approximation to the series impedance model is to regard the earth as a conductor parallel to the rails and located at some depth under the ground surface. The series self-impedance of the rail-ground loop can then be assumed to be

$$\mathbf{Z}_{ii} = \mathbf{Z}_r + \mathbf{Z}_e - 2\mathbf{Z}_{r-e} \tag{A.1}$$

where $\mathbf{Z}_r$ and $\mathbf{Z}_e$ are the conductor components of the line self-impedance which account for the conductor resistance and self-reactance, and the component $\mathbf{Z}_{r-e}$ (termed the separation component) represents the mutual inductive impedance between the two conductors. A common approach in electrical power engineering is to divide the self-impedance of a current-carrying conductor into internal and external parts. The internal component accounts for the conductor resistance and the inductance contribution due to varying magnetic flux within the conductor. The external component arises from the effects of the magnetic field outside the conductor. By applying these considerations to the $\mathbf{Z}_r$ term, the self-impedance of the rail-ground return loop can be further decomposed as follows:

$$\mathbf{Z}_{ii} = \mathbf{Z}_{r_{int}} + \mathbf{Z}_{r_{ext}} + \mathbf{Z}_e - 2\mathbf{Z}_{r-e} \tag{A.2}$$

The terms $\mathbf{Z}_{r_{ext}}$ and $\mathbf{Z}_{r-e_{ext}} = -2.\mathbf{Z}_{r-e}$ can be combined since they are both effects of the external magnetic flux linking the conductor, i.e.

$$\mathbf{Z}_{ii_{ext}} = \mathbf{Z}_{r_{ext}} + \mathbf{Z}_{r-e_{ext}} \tag{A.3}$$

In the above model, the term $\mathbf{Z}_e$ has been introduced artificially and is not physically separable from the total circuit series impedance. It can be derived only after the characteristics and location of the equivalent ground-return conductor have been specified. It is therefore convenient to add this term to the external line impedance to yield a modified term for the external impedance ($\mathbf{Z}'_{ii_{ext}}$) as

$$\mathbf{Z}'_{ii_{ext}} = \mathbf{Z}_{ii_{ext}} + \mathbf{Z}_e \tag{A.4}$$

This then accounts for the earth return effect. Finally, the series self-impedance can be expressed as

$$\mathbf{Z}_{ii} = \mathbf{Z}_{r_{int}} + \mathbf{Z}'_{ii_{ext}} \tag{A.5}$$

where the index 'i' has been introduced for consistency with the matrix component notation. The series mutual impedances between the two rail-ground return loops have only external components and can be expressed as

$$\mathbf{Z}_{ij} = \mathbf{Z}'_{ij_{ext}} \tag{A.6}$$

where $\mathbf{Z}'_{ij_{ext}}$ denotes the mutual impedance between the two rail conductors accounting for the effect of the earth-return path. In matrix notation, the series impedance matrix [**Z**] can be represented as the sum of a diagonal internal impedance matrix and a modified external impedance matrix:

$$[\mathbf{Z}] = [\mathbf{Z}_{int}] + [\mathbf{Z}'_{ext}] \tag{A.7}$$

This approach of analyzing rail track series impedance, first applied by Trueblood and Waschek [A-1], makes possible the simplification of further analysis by splitting the [**Z**] matrix into components which depend on different factors and account for different phenomena.

A.1.1 Internal impedance

A.1.1.1 Characteristics of rail as an electric conductor

The internal impedance includes the resistance and the contribution to the reactance due to the magnetic flux confined within the conductor. Both components depend on the distribution of current within the conductor, which is in turn determined by the following factors:

A.1.1.1.1 *Electrical and magnetic properties of the rail material*

The electrical and magnetic parameters of the rails are generally not completely specified by the manufacturer as they are intended for the mechanical support of rail vehicles rather than electrical conductors.

The electrical properties of rail steel are defined in terms of its electrical conductivity (σ_r) which is a function of temperature. The values of σ_r quoted in Table A.1 show that rail steel may be regarded as a typical conductor but with far lower conductivity than the materials traditionally used for conductors such as copper and aluminum.

TABLE A.1 Rail steel conductivity

Reference	σ	Comment
[G-9]	$4.76 \cdot 10^6$	Flat-bottom rail steel
[A-2]	$4.46 \cdot 10^6$	Rail steel
[A-3]	$4.44 \cdot 10^6$	Flat-bottom rail steel
	$4.95 \cdot 10^6$	Bull -Head rail steel
	$8.85 \cdot 10^6$	Conductor rail steel
[A-4]	$4.79 \cdot 10^6$	Rail steel
[G-1]	$3.72 \cdot 10^6$	Aluminium
	$5.80 \cdot 10^6$	Copper

The magnetic properties of rail steel are determined by the presence of ferromagnetic material. Ferromagnetic materials are characterized by:

- Hysteresis **B-H** loops, present with periodical excitation, implying that cyclical changes in magnetic field intensity **H** will lead to cyclical variations of magnetic flux density **B** lagging the changes in **H**.

- Magnetisation curves which saturate at relatively low values of applied magnetic field intensity.

The fundamental magnetic characteristic of the material is represented by the absolute magnetic permeability (μ) which is defined as the ratio of flux density **B** to magnetic field strength **H** :

$$\mu = \mu_o . \mu_r = \frac{\mathbf{B}}{\mathbf{H}} \ (\text{H/m}) \tag{A.8}$$

•where μ_o is the magnetic permeability of free space and μ_r is the relative magnetic permeability of the material. In terms of the magnetic permeability, the above properties of rail ferromagnetic material can be summarized as:

- $\mu > \mu_o \ \ (\mu_r > 1)$ (A.9)

- μ has a complex value ($\hat{\mu}$) which accounts for the phase lag between **B** and **H**, i.e.

$$\hat{\mu} = \frac{B_o . \exp(j\omega t - \theta)}{H_o . \exp(j\omega t)} = \frac{B_o}{H_o} \exp(-j\varphi) = \mu' - j\mu'' \tag{A.10}$$

- $\hat{\mu}$ = f(H), i.e. the **B-H** relationship is nonlinear. (A.11)

- μ is frequency dependent

- μ is temperature dependent.

The specialised literature contains references to various methods for determination of μ. Aiming at the determination of rail series impedance as a function of frequency and excitation current, Hill and Carpenter [A-3, A-5, A-6] found equivalent complex permeability values which account for hysteresis and saturation effects in rail steel. The resulting curves were obtained using a combined approach which included:

- An experimental determination of the rail material **B-H** loops, with subsequent spectral analysis to quantify the distortion effects due to hysteresis and saturation.

- A FDM technique to model and solve the diffusion equation for the magnetic field strength, accounting for the effects of hysteresis and saturation.

The magnitude of the effective permeability was then calculated from the effective skin depth found by solving the diffusion equation, while the phase angle was determined from the loss factor.

Instead of investigating μ directly, Holmstrom [A-7] proposed a method for the calculation of the μ/σ ratio which was then in turn used for the calculation of rail internal impedance. The method was based on experimentally measured internal impedance values. Analytically calculation of external impedance produced very good accuracy.

A.1.1.1.2 *Rail cross-section shape*

For their mechanical purpose, rails have a specific cross-section shape which is characterized by a very irregular geometry. There are two main variations of rail cross-section in general use. These are known as 'Bull Head' and 'Flat Bottom' rail. The irregular geometry of rail contributes to setting up a specific current and flux density pattern inside the rail, during AC excitation. Because of the irregular cross-section, an exact solution of the diffusion equation to find these distributions can be obtained only by numerical techniques.

A widely used approach to model the rail shape is to approximate the cross section by an equivalent solid circular conductor [G-9, 4-1, 4-2, A-3, A-8, A-9]. This allows the application of analytic and series solutions, available for the current distribution and series impedance of cylindrical conductors.

For AC excitation, the circular approximation is based on determination of the equivalent perimeter. This is justified for high frequencies when, due to the redistribution of the current inside the conductor, only a thin layer on the surface of the conductor carries current. During excitation with DC currents or AC currents at very low frequency, the conductor resistance is governed by the complete cross-section. Hence the cross-sectional

area must be used as the basis for the determination of the equivalent circular conductor radius.

To achieve higher accuracy in the calculation of the internal inductance, Hill and Carpenter evaluated the effective radius of the rail by numerical computation of the geometric mean distance (GMD). The GMD is of the irregularly shaped rail, measured from itself, and interpreted in the form of a circular conductor equivalent [A-3]. The technique was proposed for cases when the skin depth is significant compared with the conductor dimensions and using the method, the GMD was found to be about 11 cm for typical flat-bottom rail.
A similar value (10.18 cm) was obtained by Holmstrom [A-7]. His method involved processing experimental data for rail internal impedance, and curve fitting the results to an analytical expression for the total rail inductance.

A.1.1.1.3 *Current (magnetic field) excitation*

Rails are used as conductors in two independent electrical systems, operating with currents of different magnitude and frequency: the traction supply system and the signalling system.

Approximate values of the traction return current are:

- for DC traction systems, up to 3 kA total (representing 1.8 MW at 600 V)
- for low (16⅔ or 25 Hz) or industrial (50 or 60 Hz) AC traction systems, 240 A total (representing 12 MW at 25 kV).

These values can increase during high traffic density, on steep track sections or during faults, when current magnitude in one rail can almost double.

The frequency of signalling current in the rails depends on the exact type of track circuit. Both DC and AC (power frequency, between 25 - 125 Hz or audio-frequency, between 0.2 - 300 kHz) track circuits are in use. The magnitude of the signalling current is generally about 1-2A, except for high-voltage pulse track circuits where it could reach peak value of 180 V.

The above considerations demonstrate the necessity to consider the effect of rail magnetic permeability on the series impedance for the two excitation cases:

- Alternating magnetisation with small excitation and continuous DC field superposition, and
- Alternating magnetisation with high excitation.

In the first case, the working point on the **B-H** curve is shifted from the origin, whilst the **B-H** trajectory represents a small Rayleigh loop whose tip is on the initial magnetisation

curve. The small hysteresis loop area indicates that the hysteresis loss is relatively small. In the second case, severe distortions may occur if the excitation approaches the area of maximum permeability.

A.1.1.2 Factors accounting for rail series internal impedance

When modelling the rail internal impedance, it is expedient to consider two groups of factors: those which are inherent to all current carrying conductors and those which are due to the ferromagnetic properties of rail material.

The first group of factors includes:

- DC resistance as determined by rail electrical conductivity
- Skin effect, manifesting itself during AC excitation and resulting in a decrease of effective current-carrying cross-section, and hence an increase of the series resistance and a reduction in the internal reactance.

The second group of factors includes:

- Increase of the internal flux with DC excitation, and hence increase of the DC internal inductance with a factor of μ_r times (since $L_{DC} = \mu_o.\mu_r / 8\pi$).
- Introduction of additional power losses due to specific ferromagnetic material phenomena, such as:

(a) Hysteresis energy losses during cyclic magnetisation: these losses are determined by the coercive field strength (loop width) and by the excitation (loop height) in addition to the frequency; the hysteresis loss becomes less important at high frequencies.

(b) Other losses due to magnetic resonance, relaxation processes and after-effects which are important at very high frequencies.

- Increase of the skin effect through decrease of the skin depth, which depends on the magnetic permeability; equivalently, this effect may be described as the increase in the power losses due to the skin effect. The eddy current losses depend primarily on the resistivity and the conductor thickness, and increase with the square of frequency. The effect of eddy current losses is reflected in the **B-H** loop shape, since the loop is enlarged in proportion to the resulting joule-heat losses.

Further modification of the skin effect due to the non-linear B-H relationship in the saturation region; consequently, the magnetic flux distribution is modified near the surface of the conductor, leading to an increase in the power loss and a fall in the resistance.

A.1.1.3 Calculation of rail series internal impedance

The accurate determination of rail series internal impedance requires the creation of an analytical model of the rail as an electric conductor. The model should then incorporate all the factors that have an impact on the series impedance. However, in view of the complicated rail shape and the non-linear **B-H** relationship, such a model will not have a straightforward analytical solution. The solution can be achieved only by applying numerical techniques with reasonable approximations to control the subsequent loss of accuracy.

An analytical model for the internal impedance of a solid homogeneous, isotropic, circular, non-ferrous conductor (μ =const) is described in [G-5]. The differential equation describing the internal impedance is obtained by applying Faraday's law to a rectangular path in the radial plane of the conductor. The solution of the equation gives an expression for current density, from which the rail internal impedance can be derived (Table A.2) With some approximations, this model can be used to describe the skin effect in rail. The main approximation relates to the substitution of an equivalent circular conductor for the rail cross-section. If the considerations of Section A.1.1.1.2 are taken into account during the modelling, the loss of accuracy will be minimized.

For practical calculations of rail series internal impedance, the exact solution in terms of Bessel functions may be approximated by simpler expressions. However, for some conditions, the approximate model of a rail as an equivalent circular conductor is oversimplified and thus there will be errors in determining the internal impedance from the model. In support of this statement, Holmstrom has shown [A-7] with experimental data that the behaviour of the impedance components as a function of frequency does not in general conform with the prediction of the equivalent circular conductor model. However, the model can be useful at audio frequencies where the hysteresis effect is not significant and the internal impedance is a small fraction of the total rail series self-impedance.

For a more accurate determination of the internal impedance, it is necessary to quantify the effect of the irregular cross-section in addition to the second group of factors of Section A.1.1.2.

A.1.1.3.1 *Rail shape effect*

It can be shown by calculation that above a critical frequency, the skin depth becomes comparable with certain rail cross-section dimensions, such as the web thickness and base edge height. At such locations, the small conductor thickness can cause an important additional power loss. The resulting loss of accuracy when treating the rail as an equivalent circular conductor can be compensated by introducing a correction rail shape effect coefficient, defined as:

TABLE A.2 Calculation of rail internal impedance

Ref.	Formulae for the calculation of $\mathbf{Z}_{int}\ (\Omega/m)$	Comment
[A-8]	$\mathbf{Z}_{int} = \frac{\gamma}{u\sigma}.\frac{I_0(\gamma r)}{I_1(\gamma r)}$ where $\gamma = \sqrt{j\omega\mu\sigma}$	Exact solution
[A-10]	$\mathbf{Z}_{int_{lf}} = \frac{1}{\pi r^2\sigma} + j\omega\frac{\mu}{8\pi}$ $\quad \mathbf{Z}_{int_{hf}} = \frac{1}{u\sigma\delta}(1+j)$ $\quad \mathbf{Z}_{int} = \sqrt{R_{lf}^2 + X_{lf}^2}$	Approximation for low frequencis ($r/\delta < 0.7$) and for high frequencies ($r/\delta > 4.95$)
[A-4]	$\mathbf{Z}_{int} = \frac{1}{4\pi r^2\sigma} + \sqrt{\frac{\mu}{\pi}}.\frac{1}{2\sqrt{\sigma}r}.\sqrt{f}.(1+j)$	Valid for $r/\delta > 2$
[G-9]	$\mathbf{Z}_{int} = \frac{\sqrt{2}}{u\sigma\delta}.(1+j.k_0)$; $\quad k_0 = 0.6 - 0.87$	Newman's formula for strong magnetic fields and high frequencies
[A-11]	$\mathbf{Z}_{int} = \frac{\sqrt{2}}{u\sigma\delta}.(k_1 + jk_0.k_2)$ where for for H>1.2 kA/m $k_1 = k_2 = 1$ and 0<H<1.2 kA/m $k_1 = 0.76\sqrt{1+0.423.H^3}$ and $k_2 = \sqrt{1+0.766(1.2-H)^2}$	Adjustment of Newman's formula for any magnetic field strength by the coefficients K_1 and K_2 obtained by curve fitting of experimental data.
[A-3]	$\mathbf{Z}_{int} = \frac{\gamma}{u\sigma}.\frac{I_0(\gamma r)}{I_1(\gamma r)}$ where $\gamma = \sqrt{j\omega\hat{\mu}\sigma}$, $\hat{\mu} = \mu.\exp(-j\theta/2)$, $\hat{\delta} = \delta.\exp(-j\theta/2)$ $\mathbf{Z}_{int_{lf}} = \frac{1}{\pi r^2\sigma}\left[\left(1 + \frac{r^2}{4\delta^2}\sin\theta + \frac{r^4}{48\delta^2}\cos(2\theta)\right) + j\left(\frac{r^2}{4\delta^2}\cos\theta - \frac{r^4}{48\delta^2}\sin(2\theta)\right)\right]$ $\mathbf{Z}_{int_{hf}} = \frac{1}{\pi r^2\sigma}\left\{\left[\frac{1}{4} + \sqrt{2}\cos\left(\frac{\pi}{4} - \frac{\theta}{2}\right)\right].\left(\frac{r}{2\delta} + \frac{3\delta}{32r}\right) + j\left[\sqrt{2}\sin\left(\frac{\pi}{4} - \frac{\theta}{2}\right)\right].\left(\frac{r}{2\delta} + \frac{3\delta}{32r}\right)\right\}$	Exact solution in which hysteresis and eddy current losses are taken into account through the effective value of the complex permeability Low frequncy solution for $r \ll \delta$ High frequency solution for $r \gg \delta$

$$K_s = \frac{Z'_{int.r}}{Z'_{int.c}} \qquad (A.12)$$

where $Z'_{int.r}$ and $Z'_{int.c}$ are the internal impedances of the rail and its equivalent conductor, ignoring hysteresis effect contributions to the internal impedance. This coefficient can be defined experimentally by using the test equipment described by Hill and Carpenter [A-5, A-6] (Fig.A.1). The apparatus was constructed for the measurement of the absolute internal impedance of an isolated rail (the test conductor), after calibration to zero internal impedance using a hollow reference conductor of identical shape to the rail. The required internal impedances $Z'_{int.r}$ and $Z'_{int.c}$ can be obtained with only two measurements, performed on the test and reference conductors with rail shape and circular cross sectional area. All conductors are copper or aluminum so as to exclude the effect of hysteresis.

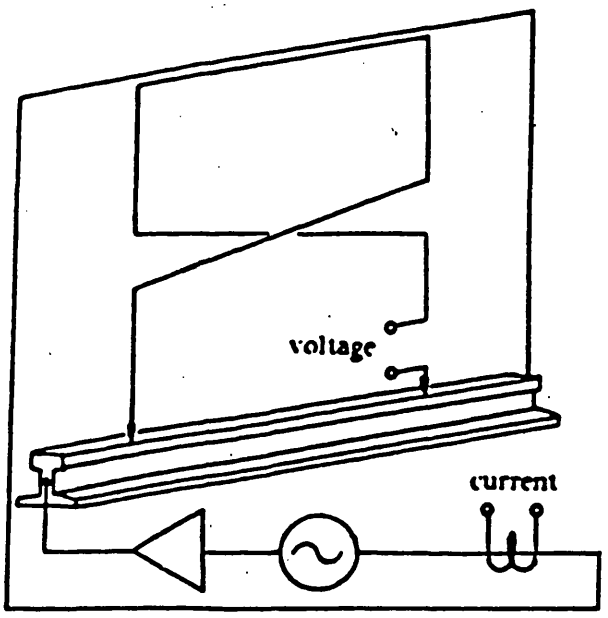

FIG.A.1 Experimental arrangement for the measurement of rail internal impedance

A.1.1.3.2 *Hysteresis and saturation loss effect*

The determination of the hysteresis and saturation loss effect is not well covered in the literature. Figurnov [A-11] has reported the adjustment of a linear model to account for hysteresis by experimentally obtaining correction coefficients.

A more fundamental approach to the problem is presented in several recent papers by Hill and Carpenter [A-3, A-5, A-6, A-9]. As with other researchers, they adopted an approximate equivalent circular conductor model made of non-ferrous material as the basis of their rail impedance model. They then approached realistic rail behaviour by introducing hysteresis and saturation loss effects by adopting an effective value of

magnetic permeability determined as discussed in Section A.1.1.1.1. The analytical model was then validated by Finite Element Modelling (FEM) and experimentation.

A.1.2 External impedance

As outlined in Section A.3, the external series impedance has two components. The first is determined by the geometry of the system - the height and horizontal separation of the conductors. The second can be regarded as a correction term accounting for the effect of the lossy ground return path.

The ground affects the external impedance mainly through its finite conductivity which in turn depends on the substrata geological structure and moisture content which varies with frequency and depth. The ground permittivity is thought to have a lesser significance than the conductivity, while the permeability is important only in ferrous geological regions.

A.1.2.1 Theoretical models of external impedance for a transmission system with lossy ground return

The problem of the determination of series external impedance for a system of parallel conductors suspended horizontally above the ground has been extensively and thoroughly investigated since the beginning of the century. The first fundamental work was that of Carson (1926) [A-12] who considered wave propagation in an infinitely long wire parallel to a plane homogeneous semi-infinite earth. By introducing a number of simplifying assumptions (TEM propagation, infinitely thin conductor, relative permittivities and permeabilities of air and ground equal to unity) and applying Maxwell's equations with some circuit concepts, he derived the following expressions for the external self and mutual impedances (rewritten in the SI units):

$$Z_{ii} = j\omega \frac{\mu_o}{2\pi}.\ln\frac{2H_i}{r_i} + \omega\frac{\mu}{\pi}.J_s \quad , \qquad \mu = \mu_o \tag{A.13.1}$$

$$Z_{ij} = j\omega \frac{\mu_o}{2\pi}.\ln\frac{D'_{ij}}{D_{ij}} + \omega\frac{\mu}{\pi}.J_m \quad , \qquad \mu = \mu_o \tag{A.13.2}$$

where J_s and J_m are the ground correction terms given by

$$J_s = P_s + jQ_s = \int_o^\infty \frac{j.e^{-2h\lambda}}{\lambda + \sqrt{\lambda + j\omega\mu\sigma}}d\lambda \tag{A.13.3}$$

$$J_m = P_m + jQ_m = \int_o^\infty \frac{j.e^{-(H_i+H_j)\lambda}}{\lambda + \sqrt{\lambda + j\omega\mu\sigma}}\cos(\lambda D_{ij}).d\lambda \tag{A.13.4}$$

The first terms in the expressions for Z_{ii} and Z_{ij} correspond to the external impedances as defined by the geometry of the system (with reference to Fig.A.2), using the concept of image conductors in conjunction with a perfectly conducting ground [A-13]. The second terms are the correction terms which take into account the effect of the finite earth

conductivity. They are complex quantities whose real parts represent the eddy current losses in the ground and whose imaginary parts represent the energy stored in the secondary field in the ground and air. Carson developed asymptotic expansions for the infinite integrals J_s and J_m as a rapidly converging infinite series. The Carson formulae account only for the finite conductivity of the earth. The quasi-static analysis is valid only at low frequencies where the polarization currents in the ground can be neglected.

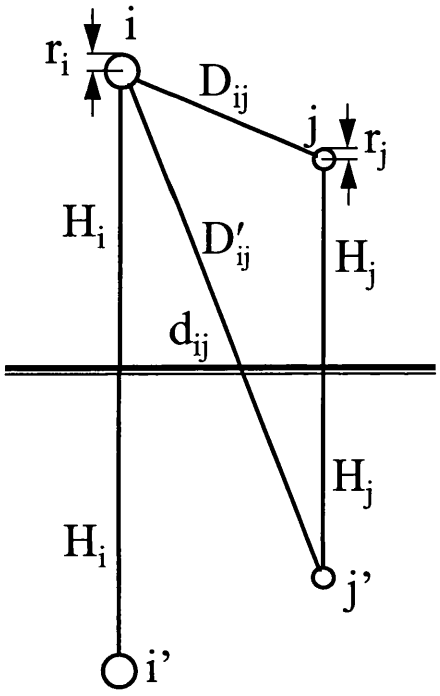

FIG.A.2 Geometry of two conductors and their image conductors

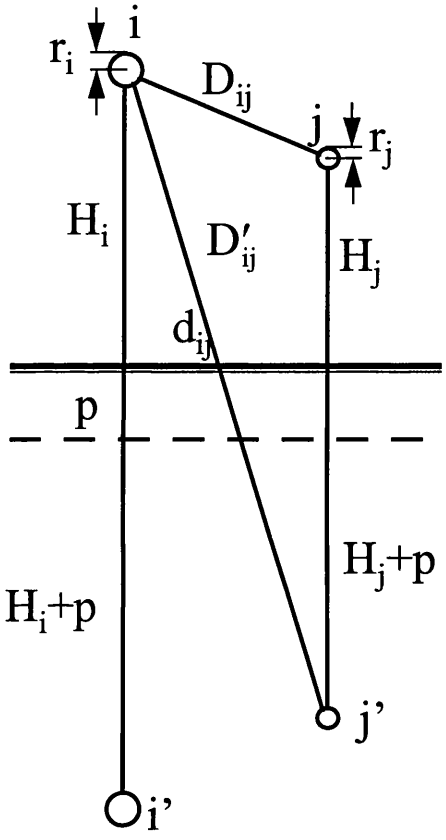

FIG.A.3 Geometry of two conductors for the model of complex penetration depth

Another work based on the same simplifying assumptions is that of Pollaczek (1931) [A-14] who obtained alternative expressions for the self and mutual impedances, whilst extending their validity to both aerial and underground conductors. He showed that in the case of an infinitely long conductor in the air, the earth can be equivalently represented by a cylindrical surface of almost arbitrary shape in which ground eddy currents flow. Wise (1931) has revised the work of Carson and extended the analysis of correction terms to include the effect of a relative magnetic permeability greater than unity [A-15]. In another work [A-16], he removed the restrictions of low frequency and relative earth permittivity being equal to unity, and developed alternative correction terms that take into account the

displacement currents in the ground. Introducing the concept of equivalent depth of return (D_e), the self and mutual impedance become

$$Z_{ii} = \frac{\omega\mu_o}{8} + j\frac{\omega\mu_o}{2\pi}\ln\frac{D_e}{r_i} \quad \text{(A.14.1)}$$

$$Z_{ij} = \frac{\omega\mu_o}{8} + j\frac{\omega\mu_o}{2\pi}\ln\frac{D_e}{D_{ij}} \quad \text{(A.14.2)}$$

$$D_e = 385.878\sqrt{\rho / f} \quad \text{(A.14.3)}$$

Rudenberg (1945) [A-17] derived an alternative formula for the equivalent depth of return:

$$D_e = 399.6\sqrt{\rho / f} \quad \text{(A.15)}$$

on the basis of an approximate expression given for the distribution of electric current inside the earth. A further development of the concept was suggested by Dubanton (1976) [A-18]. He formulated the idea that the return currents in the ground are concentrated on a fictitious plane, parallel to the ground surface and located at a complex penetration depth p, where $p = 1/\sqrt{j\mu\omega\sigma}$ (Fig.A.3). This idea was given a theoretical justification by Deri et al [A-19] who used it to derive simple formulae for the external impedance Their results were consistent with Carson's formulae and were applicable to a multi-layer earth. With the development of computer-based numerical techniques, new solutions involving numerical methods for the calculation of the definite integrals in the correction term expressions have been proposed (Perz and Raghuveer (1974) [A-13], Mullineux and Reed (1965) [A-20]). Both solutions are similar to those of Carson and lead to a numerical derivation of the field and correction factors. The first assumes non-unity ground μ_r and ε_r but the second assumes non-unity only for μ_r.

The next step towards obtaining a more realistic solution was to remove the restriction about the homogeneous earth. A non-homogeneous earth can be modelled either as a series of parallel layers, each characterized with its own conductivity, permittivity and permeability, or with a continuously varying conductivity, permittivity and permeability as functions of depth. Using the double-integral transform technique proposed in [A-20], Wedepohl and Wesley [A-21] derived infinite integral expressions for the self and mutual impedances of conductors over a two-layered earth.

Their solution can be extended to include the effects of displacement currents. The numerical results which they provided show that for stratified cases, considerable differences from the homogeneous case may occur when the resistivities of the layers differ by a factor of 10. Using comparative graphs, they showed that the homogeneous earth model can give accurate results only at very high frequencies, when the return currents are confined to the upper layer. Thus consideration should be given to the ratio of

layers resistivity, and the first layer depth. Stratified earth effects have also been extensively investigated by Ametani [A-22], who applied a three-layer earth model. His conclusion was that significant differences in the frequency-dependency of the impedance for homogeneous and three-layered earth may occur at low frequencies but they are negligible at frequencies higher than 1 MHz. His results illustrate the effect of the resistivity profile which can substantially affect the frequency dependency. He also concluded that the ferromagnetic layers can introduce a noticeable difference compared with the homogeneous case. The above quasi-static theories are all based on low-frequency approximations. More rigorous exact field solution in the sense that it satisfies the electromagnetic uniqueness theorems can also be obtained. A significant achievement in this direction is represented by the work of Wedepohl and Efthymiadis [A-23], who solved the problem of wave propagation in multiconductor power systems above a homogeneous, lossy ground. The analysis is general, without restriction on the values of the conductivities, permittivities and permeabilities of the two media comprising the system. The technique considers the field as the sum of a complementary pair of TM and TE waves rather than the approximate TEM wave considered in the quasi-static theories. The appropriate field continuity equalities were satisfied at the ground surface and conductor surface boundaries, from which expressions for all field components in the two media were obtained. In reference [A-24], the same authors used the exact solution to establish the effect of various parameters on the wave propagation characteristics and to quantify the range of validity for Carson's method. Comparison of the numerical results obtained by each methods confirmed that Carson's corrections are valid for medium and low ground resistivities at power frequency. Differences were found, however, for high ground resistivities above 1 kHz. Other solutions have been found for different physical systems [A-25, A26]. According to Kuester [A-27], the most general solution of the problem, valid for an arbitrary number of wires and a multi-layered earth, was given by Wait [A-28].

A.1.2.2 Applicability of the analytical models to rail track

The above methods for the determination of the external impedance of a set of parallel conductors have a direct application in various problems concerned with power transmission systems, such as the prediction of mutual electromagnetic interference between power and communication lines. Experience with the application of the models has confirmed their usefulness. However, there is no reported application of the models for the determination of rail track external impedance. The irregular shape of the rail and its location at the air-ground interface make the optimum choice of calculation method for this application difficult. Thus the simplifying assumptions governing each method must be examined carefully before the suitability of the technique is assessed.

Olsen and Pankaskie [A-29] give an account of the simplifying assumptions on which the quasi-static analyses of Carson and other similar work are based. The following assumptions are considered:

- Conductor height from ground is much greater than conductor radius
- Distance between conductors is much smaller than the free space wavelength
- Phase constant of the ground is much smaller than phase constant of free space
- Attenuation constant of ground is much smaller than phase constant of ground.

The authors have stressed the fact that the first and last assumptions do not hold for rails, so Carson's equations are not applicable for rail track. The last assumption is critical since decreased contact resistance between rail and ground will affect the relative values of attenuation and phase constants. This will be especially apparent in wet conditions due to the presence of ballast beneath the rail. A realistic model of rail track external impedance must be obtained by experimental methods, and there is no completely satisfactory theory which accounts for the finite radius of the conductor laid on the surface of the earth.

A.1.2.3 Calculation of rail series external impedance

Because of the lack of an exact theoretical model, the most reasonable approach to determine the rail series external impedance is to adopt one of the conveniently available solutions, and then to verify the extent it differs from experimental data. Brileev et al.[G-9, G-10] have adopted Pollaczek's formulae for conductors laying on the surface of the ground:

$$L_{ext} = \left(1 + 2\ln\frac{2}{\gamma r_r\sqrt{4\pi\sigma\omega}} - j\frac{\pi}{2}\right).10^{-7} \quad \text{(H/m)} \qquad \text{(A.16.1)}$$

$$M = \left(1 + 2\ln\frac{2}{\gamma(b - r_r)\sqrt{4\pi\sigma\omega}} - j\frac{\pi}{2}\right).10^{-7} \quad \text{(H/m)} \qquad \text{(A.16.2)}$$

where γ is the Euler constant (γ = 1.7811)

r_r is the equivalent radius of the rail calculated on the basis of perimeter (cm)

b is the distance between the rail axes (cm) and

σ is the ground conductivity in CGS(m) units (1 abS/cm=10^{-11} S/m).

Measurements conducted to check the validity of these formulae gave between 5 and 10% difference in the magnitude and phase of the rail loop impedance compared with the computed values.

Figurnov [A-11], in a model of the AC traction power supply, calculated the rail external impedance using the equivalent depth of return method, by the formula

$$D_e = \frac{c}{2\sqrt{\omega\sigma\mu_o}} \quad \text{(m)} \qquad \text{(A.17)}$$

In equation (A.16), the coefficient c is determined to provide the best agreement with experimental measurements. A typical value at 50 Hz is c = 3.695. The earth-return component of resistance is also required, and may be calculated by Shalimov's method [A-30], which gives value of 0,048 Ω/m for conductors suspended not more than 10m above the earth. The value is in good agreement with that obtained by Wagner and Evans [A-31], of 0.049 Ω/m.

Taflove et al [A-8] were concerned with the analysis of the inductive and ground-current coupling effects between power transmission and railroad signalling and communications lines. For the calculation of rail external impedance, they referred to Wait's work [A-32, A-33] which gave a closed-form solution for the self and mutual impedances of a current-carrying conductor located at the interface of the air-ground media:

$$Z_{ii_{ext}} = \frac{j\omega\mu_o}{\pi\left(\gamma_g^2 - \gamma_o^2\right).r_r^2}\left(1 - \gamma_g.r_r K_1\left(\gamma_g.r_r\right)\right) \quad (\Omega/m) \qquad (A.18.1)$$

$$Z_{ij} = \frac{j\omega\mu_o}{\pi\left(\gamma_g^2 - \gamma_o^2\right).(d_2 - d_1)^2}\left(1 - \gamma_g.|d_1 - d_2|.K_1\left(\gamma_g|d_1 - d_2|\right)\right) \quad (\Omega/m) \qquad (A.18.2)$$

where r_r is the equivalent radius of the rail (m)

$\gamma_o = j\omega\sqrt{\mu_o\varepsilon_o}$ is the free-space propagation constant (m^{-1})

$\gamma = j\omega\sqrt{\mu_o\varepsilon_g}$ is the propagation constant in the earth medium (m^{-1})

d_1, d_2 are the horizontal separation of rails 1 and 2 from the origin and

K_1 is the modified Bessel function of the second kind, of order one, with complex argument.

Although no numerical results were given the authors claimed that the experimental verification had been successful. The experiment was based on short circuit and open circuit measurements of the magnitude and phase of the input impedance, with subsequent calculation to obtain the primary and secondary line parameters. The experiment was performed with differential (rail-to-rail) and common (rails-to-ground) excitation so that from the 4 measured complex quantities the 4 unknown components in the **Z** and **Y** matrices can be determined if the track is assumed to be symmetrical. Due to the impossibility in providing a real short circuit for the common mode test the short-circuit rails-to-ground input impedance was estimated to be one quarter that of the short circuit differential mode input impedance.

Hill and Carpenter [A-36] considered the problem of the determination of rail series external impedance in a number of ways, including:

- Theoretical modelling based on Bickford's formulae [G-6] for a two-layer earth. To test the accuracy of this model, it was applied to several earth conductivity cases including the two limiting cases of a perfect conductor and a perfect insulator, a homogeneous ground and a two layer ground.
- Application of the Finite Element Method (FEM) to the electromagnetic analysis of rail track. This technique provides higher accuracy since it takes into account both rail shape and rail proximity effects.
- A triple-short-circuit experimental test to determine the mutual impedances, with prior knowledge of the self impedance values.The results gave good general agreement between the theory, experiment and numerical modelling. However, some discrepancies were observed which were explained by deficiencies in the Bickford model.

A.2 SHUNT ADMITTANCE

The shunt admittance properties of rail track arise from the effects of the transverse rail-to-rail and rail-to-ground leakage currents flowing as a result of imperfect insulation and finite permittivity in the track substructure. The shunt admittance is variable, depending on the local geological structure and environmental conditions.

A.2.1 Physical model of rail track shunt admittance

Rail track shunt admittance arises from the presence of two conductors at the interface between two half-space regions. The upper region is a homogeneous dielectric (air), and the lower is an inhomogeneous medium comprising several layers with different physical, chemical and electrical properties. The exact calculation of rail track conductance and susceptance requires knowledge of the conductivity and permittivity of the lower half space as functions of frequency and depth, taking account of their temperature and moisture content dependencies. To estimate equivalent parameter values for the rail trackbed electrical admittance model, the data and measurement techniques developed in geoscience can be utilised. McEntee [4-1] and Hopkins [4-2] have used empirical equations and data for the ground resistivity, taking into account the material structure, frequency, water content and temperature. The procedure can also be carried out for the permittivity as function of the frequency and water content, although corresponding experimental measurement results are not available at low frequencies. It is necessary to adopt an effective value for the relative permittivity which accounts for the area and the thickness of the soil layers. More accurate models take account of depth variations in conductivity and permittivity.

Hill et al [A-34] have applied a well established technique for determination of the conductivity as function of depth, involving measurement of the apparent resistance of the

ground and finding a best fit solution of the Laplace equation for the potential throughout the medium. Using the method, a two-layer conductivity model, satisfactory for low frequencies, has been found. The problem of variation of electric permittivity with depth has been approached by determining an effective constant value for the dielectric constant for the whole lower substance half-space [A-35]. It is based on experimental measurement and a simple capacitive model of the shunt admittance between two wires on the surface of the earth.

The complete model of rail track admittance must take into account the conductive leakage and displacement current paths which pass through areas with different conductivity and permittivity. The rails and metallic fastenings also may exhibit electronic conductivity properties, while ties, ballast and the ground, which always have some moisture content, can be regarded as electrolytes with ionic conductivity. Thus electrochemical processes take place at the electrode-electrolyte interfaces, causing double layers and polarisation of the electrodes. A detailed qualitative description of rail track as electrochemical system is given by Brileev in [G-9]. His model is illustrated with an equivalent diagram of rail track admittance in terms of a rail-to-rail track insulation impedance (Fig.A.4). The diagram shows that the insulation impedance (or shunt admittance) depends on both the impedances of the electrolytes (purely resistive and independent of frequency) and the impedances of the electronic-ionic conductivity interfaces. The latter include a capacitive component and depend on the intensity of the electrochemical processes taking place at the interfaces. These processes are influenced mainly by the moisture content, the temperature, the voltage between rails, the chemical composition of impregnating oils and the ballast pollution. A similar model is presented by Iancu [4-7].

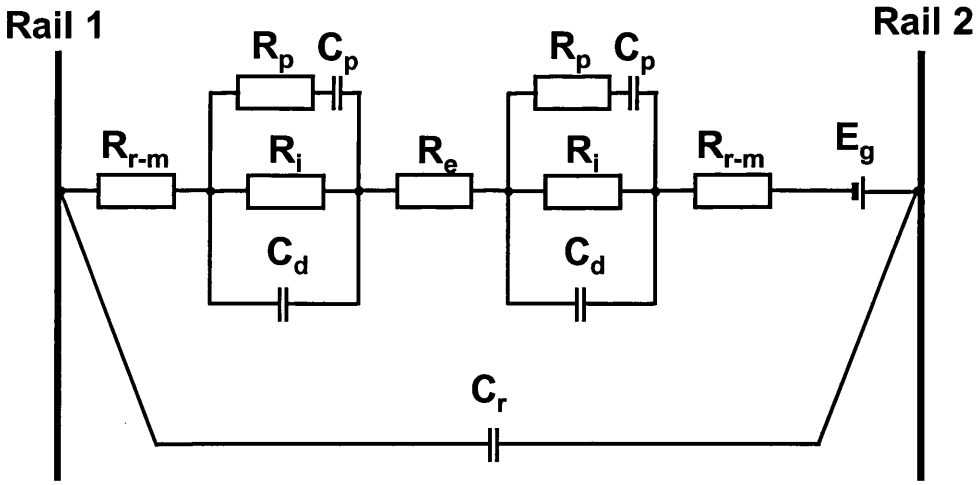

FIG.A.4 Model of rail track conductance

A.2.2 Determination of rail shunt admittance

Most studies requiring values for rail track admittance utilise the equivalent shunt admittance as measured between the rails [G-9, 4-1, 4-2, 4-5]. The values quoted (Fig.3.4c-d) are in general experimentally measured, and refer to the total equivalent shunt admittance. In cases where the self and mutual admittance terms are required separately, the equivalent shunt admittance values have been apportioned between self and mutual values [4-6, A-9]. In reference [4-6], the shunt admittance is represented with three components (Fig.A.5-a), but no justification is given. In reference [G-9], the admittance is divided into self and mutual conductance components, as shown in Fig.A.5-b, on the basis of an experimentally obtained value of the relation between mutual and self conductances, and assuming symmetrical rail track.

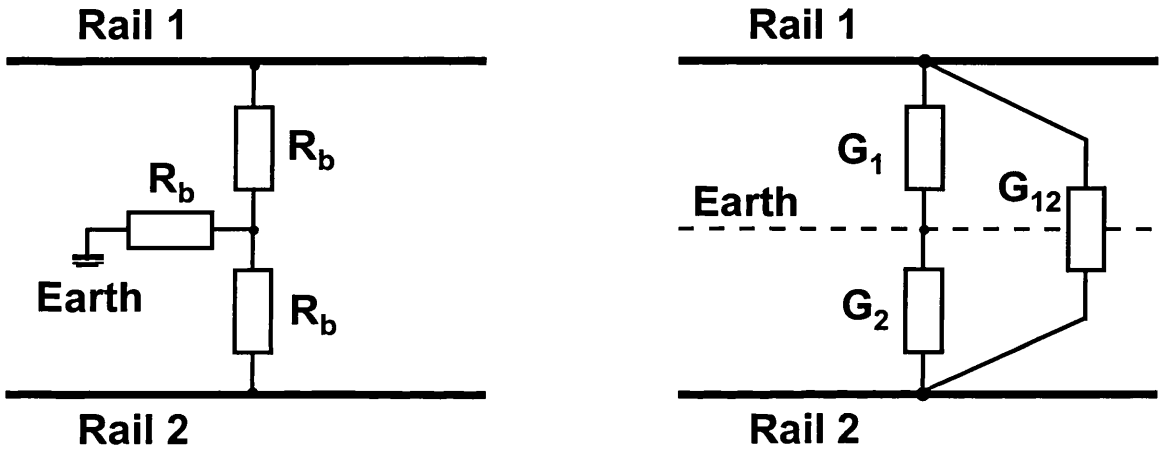

(a) Fischeer's model of rail track conductance ([4-6])

(b) Brileev's model of rail track conductance ([G-9])

FIG.A.5 Circuit models of rail track conductance

A first approximation for the mutual capacitance is that of the capacitance of two parallel cylindrical conductors above (Eqn. A.18) [4-1] or laid on (Eqn. A.19) a homogeneous ground with constant relative permittivity [A-34]. Expressions for the capacitances are

$$C = \frac{\pi\varepsilon_r}{2.\ln\dfrac{8h.\tanh(\pi D/4H)}{\pi D}} \text{ (F/m)} \qquad \text{(A.19)}$$

$$C_{12} = \frac{2\pi\varepsilon_o\varepsilon_r}{(1+\varepsilon_r).\ln[(S-D)/D]} \text{ (F/m)} \qquad \text{(A.20)}$$

An attempt to determine the shunt admittance in terms of the components of the [Y] matrix has been made by Hill and Carpenter [A-36] who modelled a third-rail track configuration. To take into consideration the irregular rail and trackbed geometry they applied numerical modelling using FEM, verified by experimental measurement. The

ground was modelled by a four-layer conductivity variation and good agreement with measured conductance values was achieved. The susceptance model is based on a constant effective permittivity with depth. Supporting experimental measurements of capacitance are based on the independence of the series impedance and shunt admittance for a short section of track and include a discontinuous rail test which monitors the leakage currents, and a direct inter-rail admittance test.

Appendix B

OUTLINE OF MULTIPOLE NETWORK THEORY

B.1 M - POLE NETWORKS

B.1.1 Basic definitions. Node and loop analysis of multipoles.

A multipole (m-pole) is a network element which has m accessible terminals (Fig.B.1). Each terminal 'i' is associated with a terminal current $\mathbf{I}_{t_i}$ and a terminal voltage $\mathbf{V}_{t_i}$. The positive current direction convention is as shown in Fig.B.1, and the voltages are referred to a common reference point. The description of the multipole network has been introduced by Shekel [B-1], and is based on the following two fundamental properties:

(1) The sum of the terminal currents is identically zero

$$\sum_{i=1}^{m} \mathbf{I}_{t_i} = 0 \qquad \text{(B.1)}$$

(This postulate is equivalent to Kirchhoff's current law).

(2) The currents remain unchanged if each terminal voltage $\mathbf{V}_{t_i}$ is replaced by $\mathbf{V}_{t_i} + \delta$, where δ is an arbitrary constant. This property implies that the common reference point of zero potential may be chosen arbitrarily.

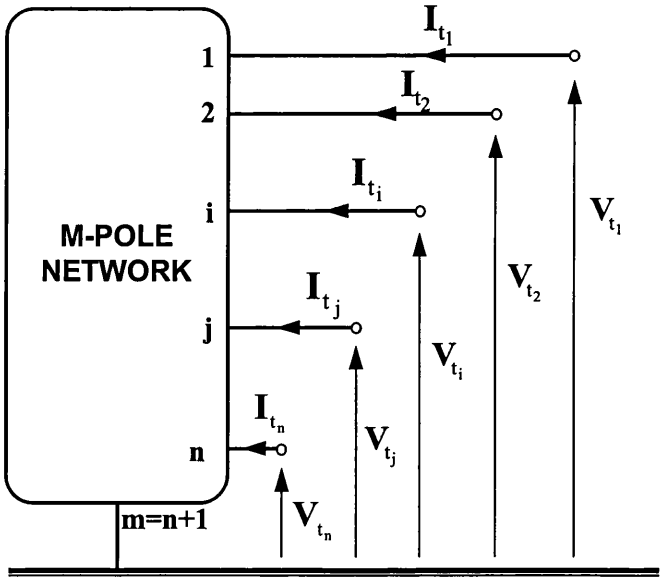

FIG.B.1 A multipole (multiterminal network) described in terms of terminal node voltages and terminal currents

The external behaviour of a passive multipole network can be described by an indefinite terminal admittance matrix $[\mathbf{Y}'_t]$ defined by the equation

$$[\mathbf{I}_t] = [\mathbf{Y}'_t].[\mathbf{V}_t] \tag{B.2}$$

From Eqn.(B.2), the current at the i-th terminal can be expressed as:

$$\mathbf{I}_{t_i} = \sum_{j=1}^{m} \mathbf{Y}'_{t_{ij}} . \mathbf{V}_{t_j} \tag{B.3}$$

Hence the terminal admittance coefficients may be evaluated as

$$\mathbf{Y}'_{t_{ij}} = \mathbf{I}_{t_i} / \mathbf{V}_{t_j} \tag{B.4}$$

subject to the condition that all terminal voltages, other than the j-th are zero.

If the multipole is active e.g. if it contains internal sources, it may be described by the matrix equation

$$[\mathbf{I}_t] = [\mathbf{Y}'_t].[\mathbf{V}_t] + [\tilde{\mathbf{I}}_t] \tag{B.5}$$

where $[\tilde{\mathbf{I}}_t]$ is a column-matrix of constants which are independent of the terminal voltages and currents. The elements of $[\tilde{\mathbf{I}}_t]$ are the currents in the terminals which flow as response to the internal sources when all terminals of the multipole are grounded. By virtue of property (1) these currents are constrained by

$$\sum_{i=1}^{m} \tilde{\mathbf{I}}_{t_i} = 0 \tag{B.6}$$

Alternatively, a passive multipole can be described by its terminal impedance coefficients which form an indefinite terminal impedance matrix $[\mathcal{Z}'_t]$. This matrix is based on loop analysis of the multipole, and is defined by the equation

$$[\mathcal{V}_t] = [\mathcal{Z}'_t].[I_t] \tag{B.7}$$

where $[\mathcal{V}_t]$ is the column-matrix of the loop voltages e.g. the potential differences between two adjacent terminals and $[I_t]$ is the column-matrix of the loop currents, taken as entering one terminal and leaving by the adjacent terminal (Fig.B.2).

The following properties hold for the loop analysis of multipoles:

(3) The sum of the loop potentials is zero and

(4) The loop potentials depend only on the differences between the loop currents, rather than their absolute values.

The terminal impedance coefficients can be defined from Eqn.(B.7) as

$$\mathcal{Z}'_{t_{ij}} = \mathcal{V}_{t_i} / I_{t_j} \tag{B.8}$$

subject to the condition that all terminals except the j-th are open-circuit.

For an active multipole, Eqn.(B.7) may be extended to account for the internal energy sources:

$$[\mathcal{V}_t] = [\mathcal{Z}'_t]\cdot[I_t] + [\tilde{\mathcal{V}}_t] \tag{B.9}$$

where $[\tilde{\mathcal{V}}_t]$ is the column matrix of constants which are independent of $[\mathcal{V}_t]$ and $[I_t]$, and equal the loop voltages when all terminals are open circuit.

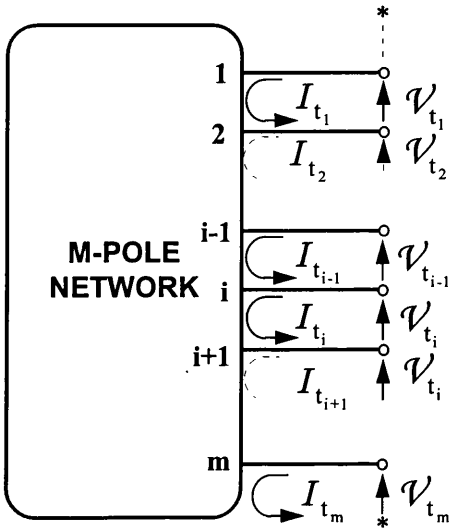

FIG.B.2 A m-pole (multipole or multiterminal network) described in terms of terminal-to-terminal voltages and mesh currents

The indefinite admittance $[\mathbf{Y}'_t]$ and impedance $[\mathcal{Z}'_t]$ matrices possess the following properties:

The sum of the components in each column vanishes, that is,

$$\sum_{i=1}^{n} \mathbf{Y}'_{t_{ij}} = 0 \qquad \text{for all } j = 1,2\,..n \tag{B.10.1}$$

$$\sum_{i=1}^{n} \mathcal{Z}'_{t_{ij}} = 0 \qquad \text{for all } j = 1,2\,..n \tag{B.10.2}$$

The sum of the components in each row vanishes, that is,

$$\sum_{j=1}^{n} \mathbf{Y}'_{t_{ij}} = 0 \qquad \text{for all } i = 1,2\,..n \tag{B.11.1}$$

$$\sum_{j=1}^{n} \mathcal{Z}'_{t_{ij}} = 0 \qquad \text{for all } i = 1,2\,..n \tag{B.11.2}$$

Proof of these properties is given in Reference [B-2].

From the above, it follows that both $[\mathbf{Y}'_t]$ and $[\mathcal{Z}'_t]$ matrices are singular and cannot be inverted. Physically, this means that in nodal analysis, the terminal currents of the multipole depend only on the differences of the terminal voltages rather than their absolute values and in loop analysis, the loop potentials depend only on the difference between two adjacent loop currents, rather than their absolute values.

From Eqn.(B.2) or (B.5), if according to property (2) of the multipoles the value of δ is chosen such that

$$\delta = -\mathbf{V}_{t_n} \tag{B.12}$$

then the voltage at the m-th terminal becomes zero and it may be regarded as the reference point for all other terminal voltages. Moreover, the last m-th column of the $[\mathbf{Y}'_t]$ matrix can be deleted without causing any changes in the matrix equations (B.2) and (B.5). The last row, used for the definition of the current at the m-th terminal, can also be deleted since this current can be evaluated from property (1). The matrix $[\mathbf{Y}_t]$ obtained after the last (or, in principle, any other) row and column have been struck out is then nonsingular, or definite, and may be inverted for use in the equation:

$$[\mathbf{V}_t] = [\mathbf{Y}_t]^{-1}.[\mathbf{I}_t] = [\mathbf{Z}_t].[\mathbf{I}_t] \tag{B.13}$$

Similarly, a definite impedance matrix can be obtained by assuming the m-th loop current to be zero and solving for the m-th loop voltage from the sum of the other loop voltages. This strikes the m-th row and column from $[\mathcal{Z}'_t]$, giving a definite invertable terminal impedance matrix $[\mathcal{Z}'_t]$ with the following equation:

$$[I_t] = [\mathcal{Z}_t]^{-1}.[\mathcal{V}_t] = [\mathcal{Y}_t].[\mathcal{V}_t] \tag{B.14}$$

Using the definite terminal admittance/impedance matrix the equations describing multipole networks can be rewritten as follows:[1]

$$[\mathbf{I}_t] = [\mathbf{Y}_t].[\mathbf{V}_t] \tag{B.15.1}$$

$$[\mathbf{I}_t] = [\mathbf{Y}_t].[\mathbf{V}_t] + [\tilde{\mathbf{I}}_t] \tag{B.15.2}$$

$$[\mathcal{V}_t] = [\mathcal{Z}_t].[I_t] \tag{B.16.1}$$

$$[\mathcal{V}_t] = [\mathcal{Z}_t].[I_t] + [\tilde{\mathcal{V}}_t] \tag{B.16.2}$$

In the above equations the definite matrices $[\mathbf{Y}_t]$ and $[\mathcal{Z}_t]$ are of order (n,n) and all column matrices are of order (1,n), where n = m-1. The multipoles described by their definite admittance or impedance matrix will be referred to as (n+1)-poles rather than m-

[1]It should be remembered that the voltage and current variables in Eqns.(B.1) to (B.6), (B.10.1), (B.11.1), (B.13), (B.15.1) and (B.15.2) differ from those in Eqns.(B.7) to (B.9), (B.10.2), (B.11.2), (B.14), (B.16.1) and (B.16.2). In the former case, they are terminal currents and terminal-to-reference voltages; in the latter case, they are loop currents and loop potentials.

poles. This notation recalls that one of the multipole terminals is used as the common 'earth' reference point.

The terminal impedance and the terminal admittance matrices are related to each other but are not connected by a simple matrix inversion. The conversion between them is treated in detail in Ref.[B-3].

B.1.2 Norton and Thevenin Theorems for multipole networks

A multipole network is an interconnection of multipoles which may be joined together in series or in parallel. A parallel combination of two multipoles represents a direct generalization of the parallel combination of two 2-pole networks. The admittance coefficients of the parallel combination are the sums of the corresponding admittance coefficients of the component multiples.

A generalisation of Norton's theorem for active multiples can be readily obtained from the above definition. According to Eqn.B.15.2 any active multipole **M** can be represented as a parallel combination of a passive multipole **P** and a current source multipole **C** (Fig.B.3). The passive multipole **P** is derived from the active multipole by short-circuiting all internal voltage sources and open-circuiting the current sources and is characterised by the definite terminal admittance matrix $[\mathbf{Y}_t]$. The current source multipole **C** is defined by

$$[\mathbf{J}_t] = -[\tilde{\mathbf{I}}_t] \tag{B.17}$$

the positive sense of $[\mathbf{J}_t]$ being chosen as indicated on Fig.B.3. Substituting this notation into Eqn.B.15.2 gives the analytical expression of the generalised Norton's theorem:

$$[\mathbf{I}_t] = [\mathbf{Y}_t].[\mathbf{V}_t] - [\mathbf{J}_t] \tag{B.18}$$

From Eqn.B.15.2 the terminal voltages can be expressed as follows:

$$[\mathbf{V}_t] = [\mathbf{Y}_t]^{-1}.\left([\mathbf{I}_t] - [\tilde{\mathbf{I}}_t] \right) = [\mathbf{Y}_t]^{-1}.[\mathbf{I}_t] - [\mathbf{Y}_t]^{-1}.[\tilde{\mathbf{I}}_t] \tag{B.19}$$

In the above equation the term $[\mathbf{Y}_t]^{-1}.[\mathbf{I}_t]$ can be regarded as the voltages at the terminals when all sources inside the multipole are deactivated, while the term $-[\mathbf{Y}_t]^{-1}.[\tilde{\mathbf{I}}_t]$ represents the response to the internal sources when all multipole terminals are open-circuited. This term can be regarded as defining an equivalent 2n-pole voltage source $[\mathbf{E}_t]$ with positive sence as shown on Fig.B.4. Introducing the notation

$$[\mathbf{E}_t] = -[\mathbf{Y}_t]^{-1}.[\tilde{\mathbf{I}}_t] \tag{B.20}$$

into Eqn.(B.18) yields

$$[\mathbf{V}_t] = [\mathbf{Y}_t]^{-1}.[\mathbf{I}_t] + [\mathbf{E}_t] \tag{B.21}$$

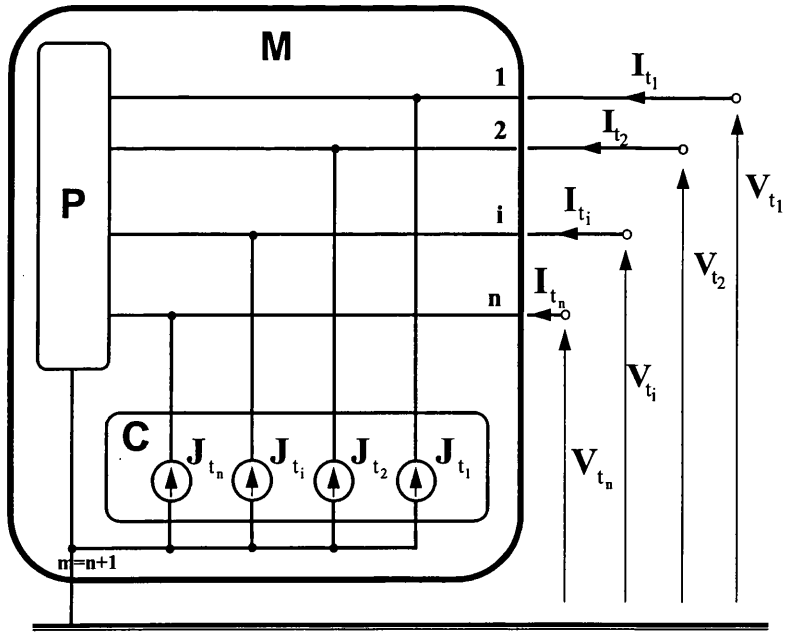

FIG.B.3 Norton's equivalent diagram of an active multipole network

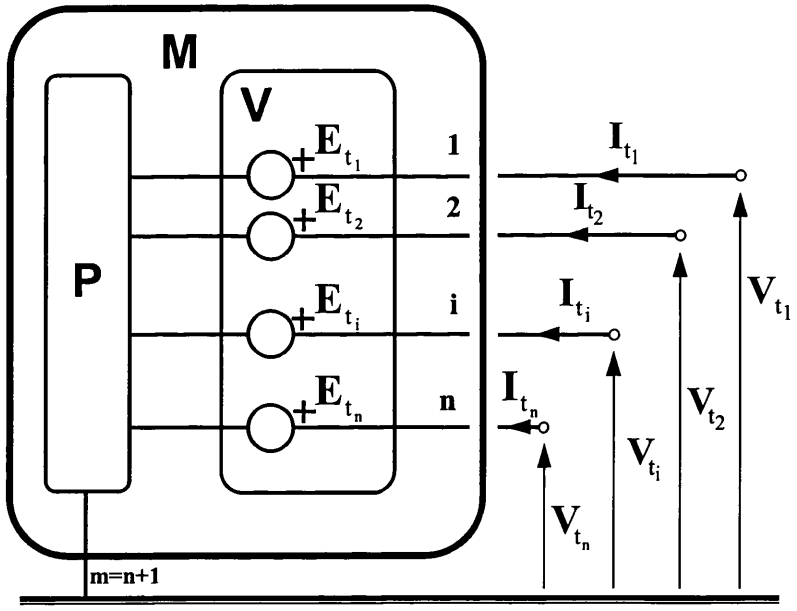

FIG.B.4 Thevenin's equvalent diagram of an active multipole network

It states that any active m-pole **M** is equivalent to a passive multipole **P**, in series with a 2m-pole voltage source network **V** (Fig.B.4). The passive multipole **P** is identical to that in Norton's theorem. The multiterminal voltage source network **V** is defined by the matrix $[\mathbf{E}_t]$ where $\mathbf{E}_{t_i}$ is the voltages of the i-th terminal when all terminals of **M** are open-circuited.

B.2 2N+1 - POLE NETWORKS

The (2n+1)-pole networks are a particular case of multiterminal networks which are of special interest to the present work (Fig.B.5-a). They can also be regarded as a generalisation of the common two-port network shown in Fig.B.5-b. These are multipoles having two groups of poles with n terminals in each group and the (n+1)-th pole is adopted as a common reference point. Such multipoles can be described by the methods outlined in Section B.1, for instance by Eqn.B.15.1. However, it is the definition of their transfer properties from one of the groups of terminals designated as input to the other group designated as output which is of particular interest. This involves defining the relationships between the terminal voltages and currents of the input port $\left[\mathbf{V}_{2t}^{I}\right]$ and $\left[\mathbf{I}_{2t}^{I}\right]$ and those of the output port $\left[\mathbf{V}_{2t}^{II}\right]$ and $\left[\mathbf{I}_{2t}^{II}\right]$. One way of doing this is by rearranging the 2n equations of the matrix equation (B.15.1) in such a way as to obtain an equation of the form

$$\begin{bmatrix}\left[\mathbf{I}_{2t}^{I}\right]\\ \left[\mathbf{I}_{2t}^{II}\right]\end{bmatrix}=\begin{bmatrix}\left[\mathbf{Y}_{2t}^{I,I}\right] & \left[\mathbf{Y}_{2t}^{I,II}\right]\\ \left[\mathbf{Y}_{2t}^{II.,I}\right] & \left[\mathbf{Y}_{2t}^{II,II}\right]\end{bmatrix}\cdot\begin{bmatrix}\left[\mathbf{V}_{2t}^{I}\right]\\ \left[\mathbf{V}_{2t}^{II}\right]\end{bmatrix}=\left[\mathbf{Y}_{2t}\right]\cdot\begin{bmatrix}\left[\mathbf{V}_{2t}^{I}\right]\\ \left[\mathbf{V}_{2t}^{II}\right]\end{bmatrix} \tag{B.22}$$

The coefficients of the other matrix transfer equations shown in Table B.1. can be derived in a similar way.

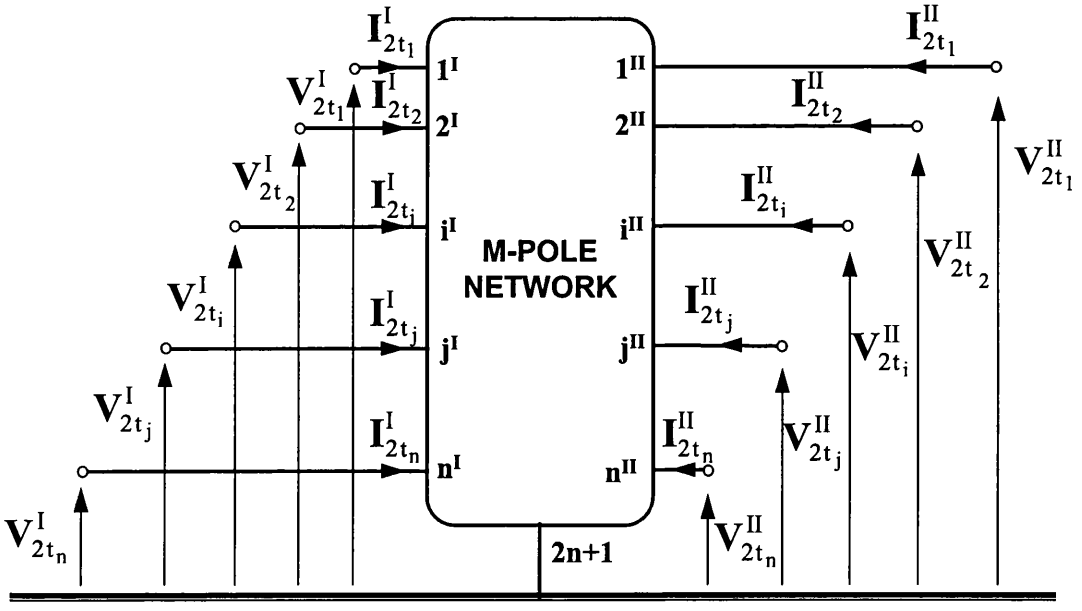

FIG.B.5-a A two-port multipole network described in terms of terminal node voltages and currents

TABLE B.1: (2n+1)-pole network transfer eqations

Open circuit impedance parameters
$\begin{bmatrix} [\mathbf{V}_{2t}^{I}] \\ [\mathbf{V}_{2t}^{II}] \end{bmatrix} = \begin{bmatrix} [\mathbf{Z}_{2t}^{I,I}] & [\mathbf{Z}_{2t}^{I,II}] \\ [\mathbf{Z}_{2t}^{II,I}] & [\mathbf{Z}_{2t}^{II,II}] \end{bmatrix} \cdot \begin{bmatrix} [\mathbf{I}_{2t}^{I}] \\ [\mathbf{I}_{2t}^{II}] \end{bmatrix} = \begin{bmatrix} \mathbf{Z}_{2t} \end{bmatrix} \cdot \begin{bmatrix} [\mathbf{I}_{2t}^{I}] \\ [\mathbf{I}_{2t}^{II}] \end{bmatrix}$
Short circuit admittance parameters
$\begin{bmatrix} [\mathbf{I}_{2t}^{I}] \\ [\mathbf{I}_{2t}^{II}] \end{bmatrix} = \begin{bmatrix} [\mathbf{Y}_{2t}^{I,I}] & [\mathbf{Y}_{2t}^{I,II}] \\ [\mathbf{Y}_{2t}^{II,I}] & [\mathbf{Y}_{2t}^{II,II}] \end{bmatrix} \cdot \begin{bmatrix} [\mathbf{V}_{2t}^{I}] \\ [\mathbf{V}_{2t}^{II}] \end{bmatrix} = \begin{bmatrix} \mathbf{Y}_{2t} \end{bmatrix} \cdot \begin{bmatrix} [\mathbf{V}_{2t}^{I}] \\ [\mathbf{V}_{2t}^{II}] \end{bmatrix}$
Transmission (chain or ABCD) parameters
$\begin{bmatrix} [\mathbf{V}_{2t}^{I}] \\ [\mathbf{I}_{2t}^{II}] \end{bmatrix} = \begin{bmatrix} [\mathcal{A}_{2t}] & [\mathcal{B}_{2t}] \\ [C_{2t}] & [\mathcal{D}_{2t}] \end{bmatrix} \cdot \begin{bmatrix} [\mathbf{V}_{2t}^{II}] \\ -[\mathbf{I}_{2t}^{II}] \end{bmatrix} = \begin{bmatrix} \mathbf{T}_{2t} \end{bmatrix} \cdot \begin{bmatrix} [\mathbf{V}_{2t}^{II}] \\ -[\mathbf{I}_{2t}^{II}] \end{bmatrix}$
Inverse transmission parameters
$\begin{bmatrix} [\mathbf{V}_{2t}^{II}] \\ [\mathbf{I}_{2t}^{II}] \end{bmatrix} = \begin{bmatrix} [\widetilde{\mathcal{A}}_{2t}] & [\widetilde{\mathcal{B}}_{2t}] \\ [\widetilde{C}_{2t}] & [\widetilde{\mathcal{D}}_{2t}] \end{bmatrix} \cdot \begin{bmatrix} [\mathbf{V}_{2t}^{I}] \\ -[\mathbf{I}_{2t}^{I}] \end{bmatrix} = \begin{bmatrix} \mathbf{B}_{2t} \end{bmatrix} \cdot \begin{bmatrix} [\mathbf{V}_{2t}^{I}] \\ -[\mathbf{I}_{2t}^{I}] \end{bmatrix}$
Hybrid parameters
$\begin{bmatrix} [\mathbf{V}_{2t}^{I}] \\ [\mathbf{I}_{2t}^{II}] \end{bmatrix} = \begin{bmatrix} [\mathbf{H}_{2t}^{I,I}] & [\mathbf{H}_{2t}^{I,II}] \\ [\mathbf{H}_{2t}^{II,I}] & [\mathbf{H}_{2t}^{II,II}] \end{bmatrix} \cdot \begin{bmatrix} [\mathbf{I}_{2t}^{I}] \\ [\mathbf{V}_{2t}^{II}] \end{bmatrix} = \begin{bmatrix} \mathbf{H}_{2t} \end{bmatrix} \cdot \begin{bmatrix} [\mathbf{I}_{2t}^{I}] \\ [\mathbf{V}_{2t}^{II}] \end{bmatrix}$
Inverse hybrid parameters
$\begin{bmatrix} [\mathbf{I}_{2t}^{I}] \\ [\mathbf{V}_{2t}^{II}] \end{bmatrix} = \begin{bmatrix} [\mathbf{G}_{2t}^{I,I}] & [\mathbf{G}_{2t}^{I,II}] \\ [\mathbf{G}_{2t}^{II,I}] & [\mathbf{G}_{2t}^{II,II}] \end{bmatrix} \cdot \begin{bmatrix} [\mathbf{V}_{2t}^{I}] \\ [\mathbf{I}_{2t}^{II}] \end{bmatrix} = \begin{bmatrix} \mathbf{G}_{2t} \end{bmatrix} \cdot \begin{bmatrix} [\mathbf{V}_{2t}^{I}] \\ [\mathbf{I}_{2t}^{II}] \end{bmatrix}$

$[\mathbf{V}_{2t}^{I}]$, $[\mathbf{I}_{2t}^{I}]$, $[\mathbf{V}_{2t}^{II}]$ and $[\mathbf{I}_{2t}^{I}]$ are (1,n)-order matrices of the terminal voltages and currents of portI and port II correspondingly, with positive directions as shown in Fig.B.5-a.

$[\mathbf{Z}_{2t}]$, $[\mathbf{Y}_{2t}]$, $[\mathrm{T}_{2t}]$, $[\mathbf{B}_{2t}]$, $[\mathbf{H}_{2t}]$ and $[\mathbf{G}_{2t}]$ are (n,n)-order matrices.

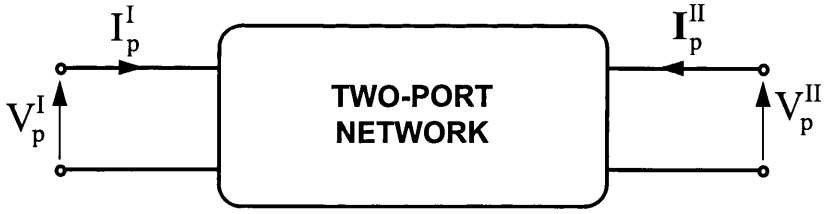

FIG.5.B-b Two-port network

In particular applications concerned with the transmission of energy or signals from one port to the other, as is the case in transmission line discontinuities, it is most convenient to use the transmission parameter form. The transmission matrix $[\mathbf{T}_{2t}]$ can be determined by two methods:

(1) Find the $[\mathbf{Z}_{2t}]$, $[\mathbf{Y}_{2t}]$, $[\mathbf{H}_{2t}]$ or $[\mathbf{G}_{2t}]$ matrix using the appropriate number of short-circuit and open-circuit tests, followed by the conversion formulae $([\mathbf{Z}_{2t}],[\mathbf{Y}_{2t}],[\mathbf{H}_{2t}],[\mathbf{G}_{2t}]) \Rightarrow [\mathbf{T}_{2t}]$ to calculate the matrix $[\mathbf{T}_{2t}]$.

(2) Use the node voltages or loop currents method to define a system of 2n equations, and rearrange the equations in the form of the transmission matrix $[\mathbf{T}_{2t}]$

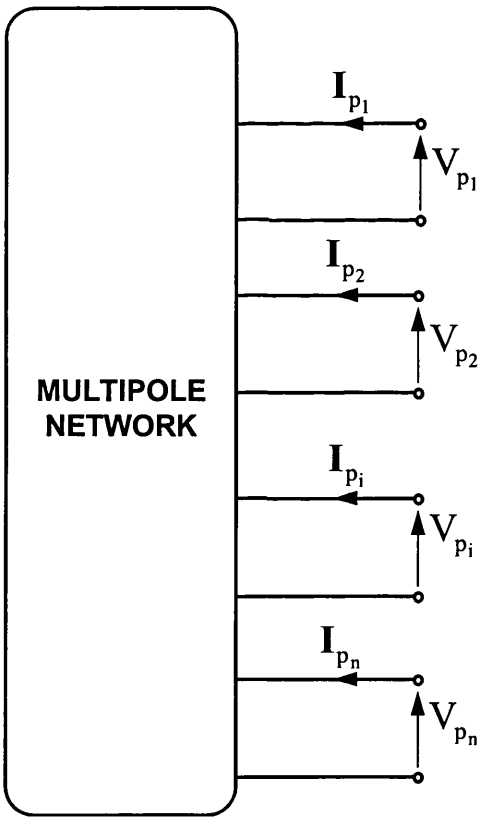

FIG.B.6 Multiport network

B.3 N-PORT NETWORKS

An n-port or multiport is a network having n accessible terminal pairs or ports. A pair of terminals may be called a port only if the current entering one terminal equals the current leaving the other terminal at all times. Each port has an associated port voltage $\mathbf{V}_{p_i}$ and a port current $\mathbf{I}_{p_i}$ with positive direction as shown in Fig.B.6.

One common method of describing multiports is in terms of the relationships between the port voltages and the port currents. These relationships can be analytically expressed by the matrix equations:

$$\left[\mathbf{V}_p\right] = \left[\mathbf{Z}_p\right].\left[\mathbf{I}_p\right] \tag{B.23}$$

$$\left[\mathbf{I}_p\right] = \left[\mathbf{Y}_p\right].\left[\mathbf{V}_p\right] \tag{B.24}$$

where $\left[\mathbf{V}_p\right]$ and $\left[\mathbf{I}_p\right]$ are the column matrices of the port voltages and port currents, $\left[\mathbf{Z}_p\right]$ is the open-circuit impedance matrix and $\left[\mathbf{Y}_p\right]$ is the the short-circuit admittance matrix. From Eqns.(B.23) and (B.24), it follows that, provided that they are not singular, the $\left[\mathbf{Z}_p\right]$ and $\left[\mathbf{Y}_p\right]$ matrices are related by matrix inversion

$$\left[\mathbf{Z}_p\right] = \left[\mathbf{Y}_p\right]^{-1} \tag{B.25}$$

The open-circuit impedance coefficients parameters $\mathbf{Z}_{p_{ij}}$ are defined as

$$\mathbf{Z}_{p_{ij}} = \mathbf{V}_{p_i} / \mathbf{I}_{p_j} \tag{B.26}$$

subject to the condition that all other port currents except that of the i-th port are zero (the ports are open-circuited).

Similarly, the short-circuit admittance parameters $\mathbf{Y}_{p_{ij}}$ are defined as

$$\mathbf{Y}_{p_{ij}} = \mathbf{I}_{p_i} / \mathbf{V}_{p_j} \tag{B.27}$$

subject to the condition that all other port voltages except that at the j-th port are zero, i.e. they are short circuited.

Eqns.(B.29) and (B.30) describe a passive multiport. Multiports containing internal sources of energy can be described by applying the superposition principle which yields the equation

$$\left[\mathbf{I}_p\right] = \left[\mathbf{Y}_p\right].\left[\mathbf{V}_p\right] + \left[\tilde{\mathbf{I}}_p\right] \tag{B.28}$$

where $\left[\mathbf{Y}_p\right]$ is the short-circuit admittance matrix of the n-port determined when all internal sources are reduced to zero (the current sources are replaced by open-circuits, and the voltage sources by short-circuits). The column matrix $\left[\tilde{\mathbf{I}}_p\right]$ represents the contribution

to the port currents $[\mathbf{I}_p]$ caused by the internal independent sources acting alone (that is under the condition $[\mathbf{V}_p]=[\mathbf{0}]$). Thus the $[\tilde{\mathbf{I}}_p]$ matrix may be interpreted as the value assumed by $[\mathbf{I}_p]$ when the ports are short-circuited which causes $[\mathbf{V}_p]$ to vanish. Hence, the original n-port network with internal independent sources is equivalent to a source-free n-port network, in parallel with n independent current sources placed at the ports. The values of these current sources are equal to the short-circuit port currents of the original network. For the direction of the current sources $[\mathbf{J}_p]$ adopted in Fig.B.7-a

$$[\mathbf{J}_p]=-[\tilde{\mathbf{I}}_p] \tag{B.29}$$

and the Norton equivalent diagram is expressed by the equation

$$[\mathbf{I}_p]=[\mathbf{Y}_p].[\mathbf{V}_p]-[\mathbf{J}_p] \tag{B.30}$$

Alternatively, an active multiport network can be represented with a Thevenin equivalent diagram as follows:

$$[\mathbf{I}_p]=[\mathbf{Y}_p].([\mathbf{V}_p]+[\mathbf{E}_p]) \tag{B.31}$$

where

$$[\mathbf{E}_p]=[\mathbf{Y}_p]^{-1}.[\tilde{\mathbf{I}}_p]=-[\mathbf{Y}_p]^{-1}.[\mathbf{J}_p] \tag{B.32}$$

and is defined by the the port voltages of the n-port network when all n port are open circuited (Fig.B-7-b).

B.4. 2N-PORT NETWORKS

2n-port networks are multiport networks having two groups of ports, with n ports in each (Fig.B.8). This type of multiport networks is essentially a multiport network whose ports have been partitioned into two groups. As such, they can be described by Eqn.(B.29) (or alternatively with Eqn.(B.30)) in which $[\mathbf{V}_p]$ and $[\mathbf{I}_p]$ are column vectors of (1,2n)-order and the $[\mathbf{Z}_p]$ and $[\mathbf{Y}_p]$ matrices are of (2n,2n)-order. Rearranging Eqn.(B.29) in such a way that the first n elements of the column matrices correspond to the ports in the first group of ports and the other n to those in the second group of ports, and correspondingly partitioning the [Z] matrix yields the equation

group of ports and the other n to those in the second group of ports, and correspondingly partitioning the [Z] matrix yields the equation

$$\begin{bmatrix}[\mathbf{V}_{2p}^{I}]\\ [\mathbf{V}_{2p}^{II}]\end{bmatrix}=\begin{bmatrix}[\mathbf{Z}_{2p}^{I,I}] & [\mathbf{Z}_{2p}^{I,II}]\\ [\mathbf{Z}_{2p}^{II.,I}] & [\mathbf{Z}_{2p}^{II,II}]\end{bmatrix}.\begin{bmatrix}[\mathbf{I}_{2p}^{I}]\\ [\mathbf{I}_{2p}^{II}]\end{bmatrix}=[\mathbf{Z}_{2p}].\begin{bmatrix}[\mathbf{I}_{2p}^{I}]\\ [\mathbf{I}_{2p}^{II}]\end{bmatrix} \tag{B.34}$$

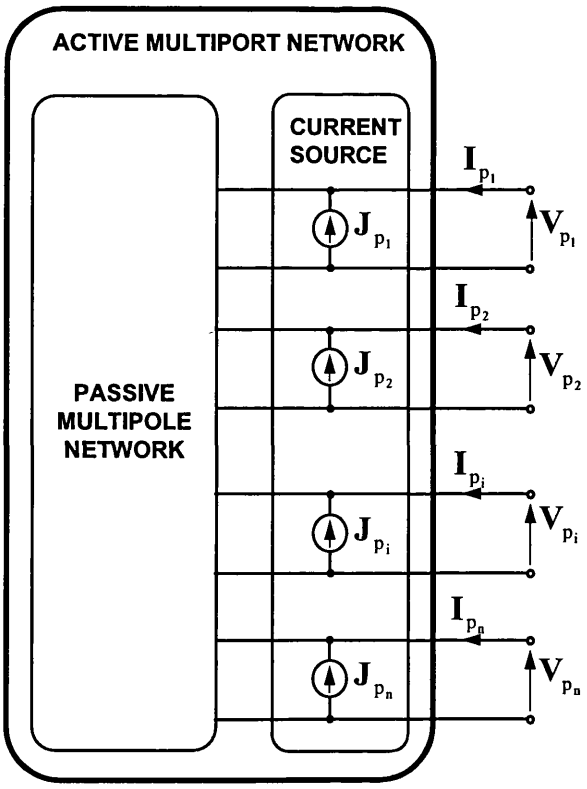

FIG.B.7-a Norton equivalent diagram of a multiport network

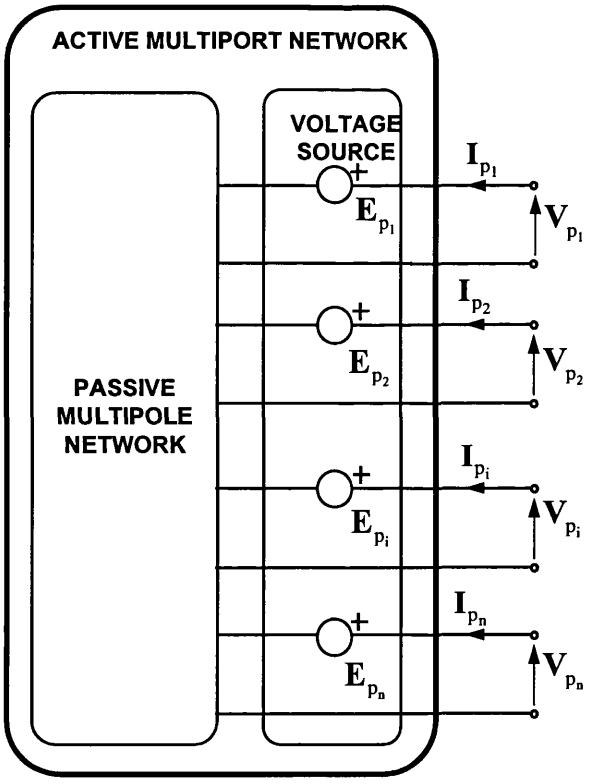

FIG.B.7-b Thevenin equivalent diagram of a multiport network

Eqn.(B.40) coincides in form with Eqn.(B.23) from Table B.1, except the subscript '2p' is used instead of '2t', which implies that the voltages and the currents refer to the ports of the 2n-port network rather than the terminals of the $(2 \times n + 1)$-pole network. In general, substituting the subscript '2t' with '2p' (i.e. considering port instead of terminal), all the Eqns.in Table B.1 apply to the description of 2n-port networks. For the transmission line application, the most convenient formulation uses the transmission parameters. The transmission matrix $[\mathbf{T}_{2p}]$ can be determined using the procedure for the determination of matrix $[\mathbf{T}_{2p}]$ given in Section B.2 with the usual substitution of 'port' for 'terminal'.

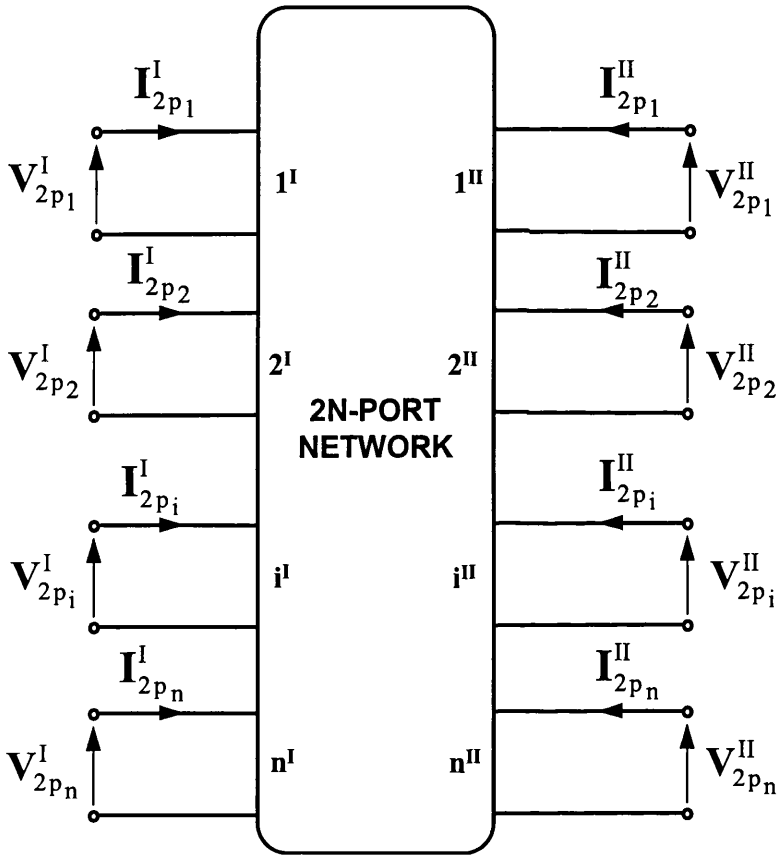

FIG.B.8 2n-port network

Appendix C

MATRIX HYPERBOLIC FUNCTIONS

The matrix hyperbolic functions of [A] are defined by the same expressions as the scalar hyperbolic functions, except that the argument is the matrix exponential function $e^{[A]}$. Thus

$$\sinh([A]) = 0.5.\left(e^{[A]} - e^{-[A]}\right) \tag{C.1}$$

$$\cosh([A]) = 0.5.\left(e^{[A]} + e^{-[A]}\right) \tag{C.2}$$

Taking into consideration the definition of the matrix exponential function (Eqn.5.99) the matrix hyperbolic functions $\sinh([A])$ and $\cosh([A])$ can be defined by the infinite power series

$$\sinh([A]) = \sum_{k=0}^{k=\infty} \frac{[A]^{2k+1}}{(2k+1)!} = [A] + \frac{[A]^3}{3!} + \frac{[A]^5}{5!} + \ldots \tag{C.3}$$

$$\cosh([A]) = \sum_{k=0}^{k=\infty} \frac{[A]^{2k}}{(2k)!} = [1] + \frac{[A]^2}{2!} + \frac{[A]^4}{4!} + \ldots \tag{C.4}$$

It can be seen from the above equations that the matrix hyperbolic functions $\sinh([A])$ and $\cosh([A])$ represent matrix polynomial functions of the form

$$P([A]) = \alpha_0.[1] + \alpha_1.[A] + \alpha_2.[A]^2 + \ldots + \alpha_n.[A]^n \tag{C.5}$$

According to the Hamilton-Cayley theorem, every square matrix [A] satisfies its characteristic equation, i.e.

$$\Delta([A]) = [A]^n - p_1.[A]^{n-1} - p_2.[A]^{n-2} - \ldots - p_{n-1}.[A] - p_n \tag{C.6}$$

From the above equation, the inverse of matrix [A] can be expressed as:

$$[A]^{-1} = \frac{1}{p_n}.\left([A]^{n-1} - p_1.[A]^{n-2} - \ldots p_n\right) \tag{C.7}$$

Using the above equation, it can be concluded that if matrix [A] is a matrix polynomial, its inverse is also a polynomial. Thus, from Eqn.(C.7) it follows that the inverses of $\sinh([A])$ and $\cosh([A])$ are also matrix polynomial functions of the same matrix [A]. It is shown in Ref.[81] that any two polynomial functions of a square matrix commute. According to this property, $\sinh([A])$ and $\cosh([A])$ and their inverses are commutative matrices. This property makes possible the definition of the $\tanh([A])$ and $\cot anh([A])$ matrix hyperbolic functions as

$$\tanh([A]) = \sinh([A]).\left(\cosh([A])\right)^{-1} = \left(\cosh([A])\right)^{-1}.\sinh([A]) \tag{C.8}$$

$$\cot anh([A]) = \cosh([A]).(\sinh([A]))^{-1} = (\sinh([A]))^{-1}.\cosh([A]) \qquad (C.9)$$

Being the product of two matrix polynomials, $\tanh([A])$ and $\cot anh([A])$ with their inverses are themselves matrix polynomial functions.